



Tumour-Stromal Crosstalk in Metastatic Lymph Nodes of Oral Squamous Cell Carcinoma.

Alice Elizabeth Pilborough

A thesis submitted in partial fulfilment of the requirements for the degree of Doctor
of Philosophy

The University of Sheffield
Faculty of Medicine, Dentistry and Health
School of Clinical Dentistry

April 2018

Names of supervisors:

Dr Syed Ali Khurram

Dr Daniel W. Lambert

Acknowledgments

Firstly, I would like to thank my supervisors Dr Dan Lambert and Dr Ali Khurram for giving me the opportunity to pursue this PhD. Thanks for all your advice, support and encouragement over the last few years. I always left our meetings with refreshed enthusiasm and am grateful for all the experience and opportunities I have gained throughout this PhD.

Thank you to Brenka McCabe for technical support and for all your hard work keeping the labs running so smoothly. Also David Thompson for assistance with slide cutting. I would also like to thank my Sheffield Undergraduate Research Experience (SURE) student Katie Bolton who carried out much of the collagen IHC lab work as part of a summer project.

A massive thank you to all the research students, past and present, at the Dental School who have made my PhD experience so enjoyable. Particular thanks must go to Zaki and Mark who have been there throughout my PhD journey and also to Dr Genevieve Melling, Dr Tasnuva Kabir and Dr Sadhvi Nithiananthan for providing training in the lab.

Thank you to The University of Sheffield for funding my PhD.

Thanks to my housemates throughout the last few years – especially Sarah and Prea for great chats and therapeutic squash sessions!

I am thankful to my wonderful boyfriend Alister for his patience and encouragement and for being there for me during all the lows and the highs over the last three years.

Finally, I want to say a huge thank you to my family, especially my parents, for all your financial and loving support throughout my education. I truly could not have got here without you.

Abstract

The prognosis of patients with oral squamous cell carcinoma (OSCC) worsens dramatically when tumours metastasise to neck lymph nodes, particularly when they spread beyond the node capsule (extracapsular spread, ECS). Although the importance of the tumour microenvironment has been well established in OSCC, it is poorly understood in the context of ECS and lymph node metastases. This work aimed to examine the lymph node tumour microenvironment in ECS and to investigate the mechanisms of tumour-stromal crosstalk, which may drive lymph node tumour development.

Stromal and epithelial-mesenchymal transition (EMT) markers in paired primary and lymph node tumours with and without ECS were compared by IHC. It was found that the stroma of ECS-positive lymph nodes and their matched primary tumours have a higher proportion of α SMA-positive myofibroblasts and that microvascular vessel density is also elevated in ECS-positive nodes.

Key stromal cell types including myofibroblasts, senescent fibroblasts, cancer-associated fibroblasts (CAF), vascular and lymphatic endothelial cells were co-cultured with oral cancer cell lines (OCCL), including those derived from lymph node metastases. EMT marker expression was detected in metastatic OCCL, which also showed significantly higher migration capacity, but more work is needed to determine the impact of fibroblasts on these processes. Both primary and metastases-derived OCCL induced tubule formation in lymphatic endothelial cells. OCCL, particularly those derived from lymph node metastases, and were also able to induce IL-6 and CCL2 secretion in normal oral fibroblasts and exposure of endothelial cells to OCCL and fibroblast conditioned media also resulted in a significant increase in expression of the inflammatory mediator IL-6.

The findings of this thesis describe novel data relating to the role of the tumour microenvironment in lymph node metastases and ECS. Increased understanding of this process will aid the development of new biomarkers and treatment options for patients with advanced OSCC.

Contents

Acknowledgments.....	i
Abstract.....	ii
List of Figures	vi
List of Tables.....	x
Abbreviations	xi
Chapter 1: Introduction and literature review	1
1.1. Oral cancer	1
1.1.1. Lymph node metastasis	2
1.2. Extracapsular Spread (ECS).....	3
1.2.1. Lymph node structure	3
1.2.2. ECS development.....	6
1.2.3. Prognostic value of ECS.....	6
1.2.4. ECS detection	8
1.3. Epithelial-mesenchymal transition (EMT), the tumour microenvironment and ECS development.....	9
1.4. Fibroblasts in cancer metastasis	14
1.4.1. Effects of fibroblasts on cancer cells – proliferation, EMT induction and invasion	15
1.4.2. Effects of cancer cells on fibroblasts	19
1.4.3. Cancer-associated fibroblast (CAF) heterogeneity.....	20
1.4.4. Fibroblast reticular cells (FRC)	21
1.5. The extracellular matrix (ECM) and cancer metastasis.....	22
1.6. Lymphatic and vascular cells in cancer metastasis	24
1.6.1. Blood vessels.....	24
1.6.2. Lymphatic vessels	26
1.6.3. Endothelial-mesenchymal transition (EndMT).....	27
1.7. Inflammation in cancer metastasis	28
1.7.1. Tumour-associated macrophages (TAM)	29
1.7.2. Cytokine and chemokine signalling in the tumour microenvironment....	30
1.8. Gaps, issues and impact of current research	33

1.8.1. Targeting the tumour microenvironment in extracapsular spread.....	34
1.9. Aims and Hypothesis	35
Chapter 2: Materials and methods	37
2.1. Immunohistochemistry (IHC)	37
2.1.1. Specimen selection	37
2.1.2. Haematoxylin and eosin staining.....	37
2.1.3. IHC protocol	37
2.1.4. IHC quantification	39
2.2. General tissue culture.....	42
2.2.1. Routine maintenance of cell culture.....	42
2.2.2. Fibroblast differentiation and senescence	43
2.2.3. Preparation of conditioned media.....	44
2.3. Cell migration assay	44
2.4. Cell proliferation assay	47
2.5. Microtubule formation assay	47
2.6. Enzyme linked immunosorbent assay (ELISA).....	50
2.7. SDS-PAGE and Western Blotting	51
2.7.1. Lysate preparation	51
2.7.2. Gel electrophoresis and membrane transfer	51
2.7.3. Immunodetection and development.....	52
2.8. Quantitative real time polymerase chain reaction (qRT-PCR)	53
2.8.1. RNA extraction	53
2.8.2. cDNA generation.....	54
2.8.3. qRT-PCR run and analysis.....	54
2.9. Statistics.....	56
Chapter 3: Investigating stromal and EMT markers in ECS positive and negative matched lymph node tumours.....	57
3.1. Introduction, hypothesis and aims	57
3.2. Results.....	58
3.2.1. Defining the patient cohort	58
3.2.2. Expression of CAF markers in patients with and without ECS.....	60

3.2.3. Comparing vascular and lymphatic density in ECS.....	64
3.2.4. Analysis of tumour-associated macrophage in ECS.....	67
3.2.5. Expression of epithelial-mesenchymal transition (EMT) markers in ECS.	69
3.3. Summary.....	74
Chapter 4: Investigating OCCL-fibroblast crosstalk using an <i>in vitro</i> co-culture system	76
4.1. Introduction, hypothesis and aims.....	76
4.2. Results	77
4.2.1. Generation and characterisation of myofibroblasts, senescent fibroblasts and CAF	77
4.2.2. Effect of myofibroblasts on EMT marker expression in OCCL.....	85
4.2.3. Effect of senescent fibroblasts on EMT marker expression in OCCL.....	90
4.2.4. Effect of CAF on EMT marker expression in H357 cells.....	98
4.2.5. Effect of fibroblasts on migration of OCCL	102
4.2.6. OCCL effect on differentiation and cytokine secretion in fibroblasts	107
4.3. Summary.....	112
Chapter 5: Modulation of vasculature and endothelial cell behaviour	114
5.1. Introduction, hypothesis and aims.....	114
5.2. Results	115
5.2.1. OCCL effect on endothelial cell behaviour <i>in vitro</i>	115
5.2.2. Myofibroblast and senescent fibroblast effect on endothelial cell behaviour <i>in vitro</i>	120
5.2.3. OCCL effect on cytokine secretion by endothelial cells	125
5.2.4. Myofibroblasts and senescent fibroblasts alter cytokine secretion by endothelial cells	130
5.3. Summary.....	136
Chapter 6: Discussion.....	138
6.1. Investigating ECS <i>ex vivo</i>	139
6.1.1. CAF marker expression in ECS	140
6.1.2. Altered vasculature and ECS.....	142
6.1.3. Macrophage in ECS	144
6.1.4. EMT marker expression in ECS	146
6.1.5. Summary of IHC findings	148

6.2. Fibroblasts	148
6.2.1. Myofibroblast generation	149
6.2.2. Senescent fibroblast generation	149
6.2.3. Evaluation of the use of CAF models <i>in vitro</i>	151
6.3. EMT and migration in lymph node metastasis	153
6.3.1. EMT marker expression in oral cancer cell lines (OCCL)	154
6.3.2. Fibroblast effect on EMT marker expression by OCCL	154
6.3.3. Fibroblast effect on migration of OCCL	157
6.4. Vasculature	159
6.4.1. OCCL effect on endothelial cell microtubule formation	159
6.4.2. Fibroblast effect on endothelial cell microtubule formation	160
6.4.3. Investigating endothelial cell behaviour <i>in vitro</i>	161
6.5. Cytokine secretion by OSCC stromal cells	162
6.5.1. OCCL effect on immune signalling by fibroblasts	163
6.5.2. OCCL and CAF effect on immune signalling in endothelial cells	167
6.6. Conclusion and impact	171
6.7. Future work	173
References	175
Appendices	193

List of Figures

Figure 1.1. Structure of the lymph node and infiltration by tumour cells.	5
Figure 1.2. Epithelial-mesenchymal transition (EMT).	12
Figure 1.3. Cells and components of the tumour microenvironment.	13
Figure 2.1. IHC quantification of percentage positive cell number (sections 3.2.2-5).	40
Figure 2.2. IHC quantification of percentage cover of collagen I (section 3.2.2.)	41
Figure 2.3. Migration assay quantification using ImageJ.	46
Figure 2.4. Microtubule assay quantification using ImageJ.	49

Figure 3.1. Immunohistochemical staining of α SMA in ECS+ and ECS- matched primary and lymph node tissue specimens.	62
Figure 3.2. Immunohistochemical staining of collagen I in ECS+ and ECS- matched primary and lymph node tissue specimens.	63
Figure 3.3. Immunohistochemical analysis of microvascular density (MVD) in ECS+ and ECS- matched primary and lymph node tissue specimens.	65
Figure 3.4. Immunohistochemical analysis of lymphatic vessel density (LVD) in ECS+ and ECS- matched primary and lymph node tissue specimens.	66
Figure 3.5. Immunohistochemical expression of the pan macrophage marker CD68 in ECS+ and ECS- matched primary and lymph node tissue specimens.	68
Figure 3.6. Immunohistochemical expression of slug and snail (SNAI1/2) in ECS+ and ECS- matched primary and lymph node tissue specimens.	71
Figure 3.7. Immunohistochemical expression of TWIST1 in ECS+ and ECS- matched primary and lymph node tissue specimens.	72
Figure 3.8. Immunohistochemical expression of ZEB1 in ECS+ and ECS- matched primary and lymph node tissue specimens.	73
Figure 4.1. TGF- β 1 causes increased α SMA expression and altered morphology in oral fibroblasts.	80
Figure 4.2. Generation of senescent fibroblasts by H ₂ O ₂ treatment.....	81
Figure 4.3. Characterisation of replicative senescent fibroblasts.....	82
Figure 4.4. Expression of myofibroblast markers in normal oral fibroblasts (NOF) and cancer-associated fibroblasts (CAF).	83
Figure 4.5. Expression of senescent markers in normal oral fibroblasts (NOF) and cancer-associated fibroblasts (CAF).	84
Figure 4.6. Protein levels of EMT markers in OCCL treated with myofibroblast-conditioned media.	87
Figure 4.7. Protein levels of EMT-inducing transcription factors in OCCL treated with myofibroblast-conditioned media.	88

Figure 4.8. mRNA expression of EMT markers in OCCL treated with myofibroblast-conditioned media.	89
Figure 4.9. Protein levels of EMT markers in OCCL treated with H ₂ O ₂ -induced senescent fibroblast conditioned media.....	92
Figure 4.10. Protein levels of EMT-inducing transcription factors in OCCL treated with H ₂ O ₂ -induced senescent fibroblast conditioned media.....	93
Figure 4.11. mRNA expression of EMT markers in OCCL treated with H ₂ O ₂ -induced senescent fibroblast conditioned media.....	94
Figure 4.12. Protein levels of EMT markers in OCCL treated with replicative senescent fibroblast conditioned media.....	95
Figure 4.13. Protein levels of EMT-inducing transcription factors in OCCL treated with replicative senescent fibroblast conditioned media.....	96
Figure 4.14. mRNA expression of EMT markers in OCCL treated with replicative senescent fibroblast conditioned media.....	97
Figure 4.15. Protein levels of EMT markers in H357 cells treated with NOF and CAF conditioned media for 24, 48 or 72 h.	99
Figure 4.16. Protein levels of EMT-inducing transcription factors in H357 cells treated with NOF and CAF conditioned media for 24, 48 or 72 h.	100
Figure 4.17. mRNA expression of EMT markers in H357 cells treated with NOF and CAF conditioned media for 24, 48 or 72 h.	101
Figure 4.18. Effect of myofibroblast conditioned media on OCCL migration.	104
Figure 4.19. Effect of H ₂ O ₂ -senesced fibroblast conditioned media on OCCL migration.	105
Figure 4.20. Effect of CAF conditioned media on OCCL migration.	106
Figure 4.21. Effect of OCCL conditioned media on α SMA and collagen I mRNA expression by normal oral fibroblasts (NOF).	109
Figure 4.22. Effect of OCCL conditioned media on IL-6 and CCL2 secretion by normal oral fibroblasts (NOF).	110

Figure 4.23. Effect of OCCL conditioned media on IL-6, CCL2 and IL-8 mRNA expression by normal oral fibroblasts (NOF).	111
Figure 5.1. Effect of OCCL conditioned media on microtubule formation by HLEC.	117
Figure 5.2. Effect of OCCL conditioned media on microtubule formation by HMEC.	118
Figure 5.3. Effect of OCCL conditioned media on proliferation of HLEC and HMEC.	119
Figure 5.4. Effect of fibroblast conditioned media on microtubule formation by HLEC.	122
Figure 5.5. Effect of fibroblast conditioned media on microtubule formation by HMEC.....	123
Figure 5.6. Effect of fibroblast conditioned media on proliferation of HLEC and HMEC.....	124
Figure 5.7. Effect of OCCL conditioned media on IL-6 and CCL2 production by HLEC and HMEC.....	127
Figure 5.8. Effect of OCCL conditioned media on immune marker mRNA expression by HLEC.....	128
Figure 5.9. Effect of OCCL conditioned media on immune marker mRNA expression by HMEC.....	129
Figure 5.10. Effect of myofibroblast conditioned media on IL-6 and CCL2 production by HLEC and HMEC.....	132
Figure 5.11. Effect of myofibroblast conditioned media on immune marker mRNA expression by HLEC and HMEC.	133
Figure 5.12. Effect of H ₂ O ₂ -senesced fibroblast conditioned media on IL-6 and CCL2 production by HLEC and HMEC.....	134
Figure 5.13. Effect of H ₂ O ₂ -senesced fibroblast conditioned media on immune marker mRNA expression by HLEC and HMEC.....	135

Appendix Figure A.1. SNAI1/2 antibody immunohistochemical (IHC) blocking control experiment.	193
Appendix Figure B.1. SYBR green primer melt curves.	194
Appendix Figure C.1. Optimisation and use of TWIST1 antibody (Abcam ab50887) for western blot.....	195

List of Tables

Table 2.1. Details of antibodies used for immunohistochemistry.	39
Table 2.2. Details of SDS-PAGE gel constituents.	52
Table 2.3. Details of antibodies used for Western blotting.	53
Table 2.4. Reagents used for cDNA generation.	54
Table 2.5. SYBR green primer sequences.	55
Table 2.6. qRT-PCR primer master mix.	56
Table 2.7. qRT-PCR cycle steps.....	56
Table 3.1. Clinical and pathological characteristics of OSCC patient cohort.	59
Table 3.2. Summary of IHC results comparing ECS+ and ECS- matched tumours.	75
Table 4.1. Summary of fibroblast co-culture experiment results comparing between oral cancer cell lines derived from primary and lymph node tumours.	112
Table 5.1. Summary of endothelial cell microtubule formation and proliferation assays comparing the effect of conditioned media from different OCCL and fibroblast types.....	136
Table 5.2. Summary of chemokine and cytokine response of endothelial cells to conditioned media from different OCCL and fibroblast types.....	137

Abbreviations

α SMA	Alpha-smooth muscle actin
CAF	Cancer-associated fibroblast
CCL2	CC chemokine ligand 2
DMEM	Dulbecco's Modified Eagle's Medium
ECM	Extracellular matrix
ECS	Extracapsular spread
EGF	Epidermal growth factor
ELISA	Enzyme linked immunosorbent assay
EMT	Epithelial-mesenchymal transition
EndMT	Endothelial-mesenchymal transition
FBS	Foetal bovine serum
FRC	Fibroblast reticular cell
HEV	High endothelial venules
HLEC	Human dermal lymphatic endothelial cells
HMEC	Human dermal microvascular endothelial cells
IHC	Immunohistochemistry
IL	Interleukin
LVD	Lymphatic vessel density
MCP-1	Monocyte chemoattractant protein-1
MMP	Matrix metalloprotease
MVD	Microvascular vessel density
NOF	Normal oral fibroblast
OCCL	Oral cancer cell line
OSCC	Oral squamous cell carcinoma
PBS	Phosphate buffered saline
qRT-PCR	Quantitative real time polymerase chain reaction
ROI	Region of interest
ROS	Reactive oxygen species
RT	Room temperature
SASP	Senescence-associated secretory phenotype

SA- β -gal	Senescence-associated β -galactosidase assay
SFM	Serum-free media
SLN	Sentinel lymph node
Slug (SNAI2)	Snail Family Zinc Finger 2
Snail (SNAI1)	Snail Family Zinc Finger 1
TAM	Tumour-associated macrophage
TDLN	Tumour-draining lymph node
TGF- β 1	Transforming growth factor- β 1
TWIST1	Twist Basic Helix-Loop-Helix Transcription Factor 1
VEGF	Vascular endothelial growth factor
ZEB1	Zinc Finger E-Box Binding Homeobox 1

Chapter 1: Introduction and literature review

1.1. Oral cancer

Oral cancer is a significant cause of mortality and morbidity worldwide, ranking as the 13th most common cause of cancer incidence and mortality in the world (Ferlay *et al.*, 2013). In the UK, it accounted for about 6800 cases and 2100 deaths in 2012 (Cancer Research UK, 2014). However, there is a large amount of geographical variation in incidence. In high-risk developing countries such as India and Pakistan oral cancer is the most common cancer in men, contributing up to 25% of all reported cancer cases (Warnakulasuriya, 2009). In Western Europe oral cancer incidence has increased in recent decades, with the UK reporting a 30% increase in the last decade (Cancer Research UK, 2011) and predicting a 25% increase in cases in the next two decades (Mistry *et al.*, 2011). As well as occurring more frequently in men and with increasing age, tobacco, betel quid and alcohol use have been identified as key risk factors. This strong link to lifestyle factors coupled by the additional role now found to be played by human papillomavirus (HPV) infection may help to explain the projected increase in incidence, but to a large extent, the reasons are poorly understood. Despite treatment advances, survival rates remain static at 50%, and mortality rates are projected to increase in the next decade in the UK due to increasing incidence (Olsen, Parkin and Saseini, 2008). Successful treatment of oral cancer is impeded by its propensity to metastasise to locoregional sites such as the cervical lymph nodes and the development of extracapsular spread. In comparison to other common cancers, the molecular landscape of oral cancer is poorly understood, hampering the development of novel treatments and prognosticators informing treatment options.

Oral Squamous Cell Carcinoma (OSCC) originates from the squamous epithelial cells of the oral cavity mucosa and is the most common form of oral cancer. Oral cavity cancer has been identified as distinct from oropharyngeal cancer in terms of both clinicopathological and prognostic characteristics (Shield *et al.*, 2017). The most common sites of origin are the tongue and floor of mouth, with tumours commonly presenting as painless lesions or ulcers in the early stages.

These can develop into large exophytic masses or destructive ulcers with associated muscle impairment and pain due to direct invasion of local structures including muscle and nerves in the connective tissue (Sapp, Eversole and Wysocki, 2004; Soames and Southam, 2005).

1.1.1. Lymph node metastasis

Metastasis of OSCC, usually to the cervical lymph nodes depending upon the site of the primary tumour, worsens prognosis (Myers *et al.*, 2001; Shaw *et al.*, 2010). Initial colonisation of lymph nodes by the metastatic deposit is followed by secondary growth and proliferation. In some instances, the metastatic tumour can grow and infiltrate beyond the capsule of the lymph node resulting in invasion into the surrounding adipose tissue and muscle. This phenomenon is termed extracapsular spread (ECS) and results in a further significant reduction in patient survival and disease-free period (Myers *et al.*, 2001; Greenberg *et al.*, 2003; Woolgar *et al.*, 2003; Wenzel *et al.*, 2004; Larsen *et al.*, 2009; Shaw *et al.*, 2010; Kokemueller *et al.*, 2011; Michikawa *et al.*, 2011; Joo *et al.*, 2013; Maxwell *et al.*, 2013; Prabhu *et al.*, 2014; Shibuya *et al.*, 2014). Occasionally, metastasis to more distant sites may occur, with lungs and liver being the more frequently involved sites (Sapp, Eversole and Wysocki, 2004).

OSCC is most commonly treated by surgery which may be followed up by radiotherapy or chemotherapy (Sapp, Eversole and Wysocki, 2004). The high mortality rate associated with lymph node metastasis means identification of patients with lymph node involvement is essential to guide treatment strategies. Currently, fine needle aspiration, core biopsies, ultrasound or magnetic resonance imaging (MRI) scanning and sentinel node biopsies are used to identify patients with lymph node involvement without the need for complex surgery. However, evidence suggests that these methods are not 100% sensitive (Tandon *et al.*, 2008; Govers *et al.*, 2013) and the risks associated with false negative rate means that a large number of patients undergo elective neck dissections despite being classified as N0 clinically (i.e. negative for metastatic tumour clinically). Approximately 30% of N0 patients undergoing elective neck dissection are found to have lymph node

involvement (D’Cruz *et al.*, 2015). Although the identification and removal of positive nodes confers a survival benefit (D’Cruz *et al.*, 2015), a large number of neck dissections are unnecessary, and patients must deal with the associated morbidity. For those with confirmed node involvement either selective or radical neck dissection is carried out and may be accompanied by post-operative radiotherapy or chemotherapy. Neck dissection may result in neck stiffness and constriction, pain, numbness and damage to the spinal accessory nerve which can impair shoulder function (Inoue *et al.*, 2006).

As with all cancers, early and accurate diagnosis is critical to the success of treatment. This is even more critical in the context of OSCC as many patients present with late stage disease largely due to patient’s delay in consulting a physician (McGurk *et al.*, 2005). The morbidity associated with aggressive treatment means that the need for accurate prognostic tools is crucial to balance its success with maintaining quality of life.

1.2. Extracapsular Spread (ECS)

1.2.1. Lymph node structure

The complex lymph node structure and the cell types contained within it play a key role in the colonisation, growth and local invasion of OSCC tumours. The highly organised structure of a lymph node (Figure 1.1.) facilitates interactions between cells of the immune system and foreign antigens but is also the principal site of metastasis in OSCC. In normal function, lymph fluid drained from surrounding tissues enters the lymph node via the afferent lymph vessels along with circulating antigen-presenting cells (APC). Here the subcapsular sinus prevents fluid entering the lymph node but APC are able to actively cross it along with their antigen cargo and macrophages are capable of sampling antigen for presentation to B lymphocytes (Harwood and Batista, 2010). Fluid containing small antigens and chemokines are transported around the lymph node via collagen conduits formed and covered by fibroblast reticular cells (FRC). Dendritic cells found on these conduits are able to sample antigen directly from the fluid (Rozen daal, Mebius and

Kraal, 2008). The entire lymph node is also surrounded by a fibrocollagenous capsule that supports the lymph node structure.

Lymphocytes within the lymph node are organised into specific compartments in the cortical areas, formed by connecting fibroblast cells. B lymphocytes are localised to B cell follicles in the outer cortex, whereas T lymphocytes are located in the inner paracortical areas. Within the B cell follicles, follicular dendritic cells form a supportive network, and secrete a wide range of immune cell modulators (Allen and Cyster, 2008). Naïve lymphocytes enter from blood vessels via the high endothelial venules in the paracortex. The inner medulla area contains the efferent lymph vessels which drain lymph fluid and lymphocytes from the lymph node (Abbas, Lichtman and Pillai, 2015).

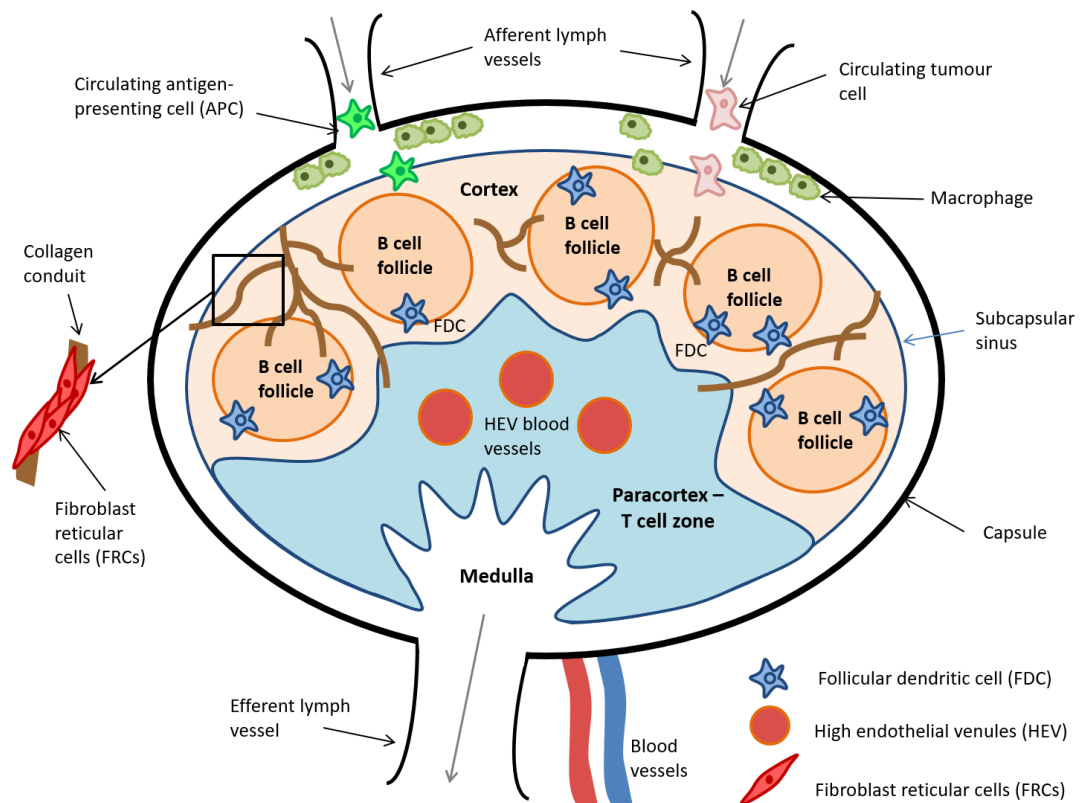


Figure 1.1. Structure of the lymph node and infiltration by tumour cells. Cancer cells enter the lymph node via afferent lymph vessels along with antigen-presenting cells. The subcapsular sinus prevents fluid from entering the cortical areas but allows active cellular transport, including that of cancer cells. Macrophages in the subcapsular sinus are capable of sampling large antigens for presentation to B cells. B cell zones are found in the cortex along with follicular dendritic cells (FDC) with T cells contained with the paracortex. Collagen conduits formed by fibroblastic reticular cells (FRC) carry fluid around the lymph node and blood vessels carrying naïve lymphocytes enter via the high endothelial venules (HEV) in the paracortex. Lymph fluid is drained from the node via the efferent lymph vessels. The whole lymph node structure is surrounded by a fibrocollagenous capsule structure.

1.2.2. ECS development

The routes of lymph node entry used by immune cells are also exploited by tumour cells. This is particularly important for OSCC as oral structures (in particular tongue) have abundant superficial lymphatic vessels allowing tumour cells to adhere and gain access to the lymphatic system. Tumour cells that have invaded into lymphatic vessels follow the path of the natural lymph drainage and enter the lymph node via the afferent lymph vessels and collect at the subcapsular sinus (Nathanson, Shah and Rosso, 2015) (Figure 1.1.). It is thought that complementary chemokine expression by tumour cells and the lymphatic endothelial cells lining the subcapsular sinus facilitates tumour migration into the cortex (Podgrabinska and Skobe, 2014). Once within the cortex, tumour cells proliferate, develop a blood vessel network and, in some cases, generate a supportive stroma. Cancer cells can migrate and invade through lymph node tissue and break out of the capsule surrounding the lymph node into the surrounding adipose and muscle tissue, a process termed ECS. The exact mechanism by which ECS occurs is somewhat controversial, with mechanical disruption of the capsule due to expanding tumour growth and direct invasion into the capsule through collagenase production proposed as possible mechanisms (Michikawa *et al.*, 2018). Nevertheless, the high connectivity of the lymph node to both lymphatic and circulatory systems also means there are multiple routes through which tumour cells can spread to another site (Nathanson, Shah and Rosso, 2015).

1.2.3. Prognostic value of ECS

Multiple studies investigating prognostic factors in OSCC have highlighted ECS as a key indicator of poor survival, increased recurrence and increased rate of distant metastasis (Myers *et al.*, 2001; Greenberg *et al.*, 2003; Woolgar *et al.*, 2003; Wenzel *et al.*, 2004; Liao *et al.*, 2007; Larsen *et al.*, 2009; Shaw *et al.*, 2010; Kokemueller *et al.*, 2011; Michikawa *et al.*, 2011; Joo *et al.*, 2013; Maxwell *et al.*, 2013; Shibuya *et al.*, 2014; Prabhu *et al.*, 2014; Sutton *et al.*, 2017). For example, Shaw *et al.* (2010) reported 5-year survival rates of 65%, 52% and 23% in node negative, node positive ECS negative (ECS-) and node positive ECS positive (ECS+) patients, respectively. By using retrospective data, these studies do not represent

the impact of current treatment strategies; however, they do provide clear evidence that ECS is a crucial indicator of particularly poor prognosis, even in comparison to patients with lymph node involvement. This is further highlighted by the fact that the recent update to TNM classification recommends ECS being taken into account and consideration for the tumour to be up-staged. It must be noted that for some studies this link was only significant in cases of multiple ECS+ nodes (Greenberg *et al.*, 2003) or advanced ECS+ nodes with severely damaged tissue architecture (Prabhu *et al.*, 2014). Additionally, a recent study showed that when ECS was categorised based on the level of invasion out of the lymph node, patients with the highest level of invasion had a significantly poorer survival and recurrence rate (Yamada *et al.*, 2016). Conversely, other studies reported no difference in survival rate when comparing macroscopic versus microscopic ECS (Woolgar *et al.*, 2003; Shaw *et al.*, 2010), or the extent of invasion (Greenberg *et al.*, 2003) and it has also been reported that patients with smaller size ECS+ nodes have a lower survival rate compared to those with large ECS+ nodes (Michikawa *et al.*, 2018). This controversy highlights how little is known about the exact mechanism by which ECS occurs and invites the possibility that the driving mechanism behind it may vary between cases. It also highlights the need for a standardised definition of ECS and suggests that the extent of ECS should be reported to allow for better analysis of clinical outcomes.

A comparative analysis of two large scale clinical trials in locally advanced head and neck cancer identified ECS as one of only two factors for which concurrent postoperative radiation and cisplatin-based chemotherapy conferred a significant survival benefit (Bernier *et al.*, 2005). In addition, follow-up studies have shown that this benefit is long-term (Cooper *et al.*, 2012), but is also associated with significant toxicity. More recently other strategies have been suggested that may confer survival benefit for these patients whilst reducing the treatment toxicity (Mermod *et al.*, 2016). However, these have yet to be validated in the clinic and so the treatment options available to ECS+ patients remain limited.

1.2.4. ECS detection

Currently, the presence of ECS is usually confirmed histologically following lymph node removal as part of a neck dissection. Although there have been some reports of partially successful detection with ^{18}F -fluorodeoxyglucose (FDG) positron emission tomography (PET)/computed tomography (CT) (Joo *et al.*, 2013) and CT scans for central node necrosis (Randall *et al.*, 2015), there is also evidence to suggest that pre-operative imaging techniques currently used for ECS diagnosis, such as CT and MRI scans, do not have the required reliability or sensitivity (Coatesworth and MacLennan, 2002; Woolgar *et al.*, 2003; Shaw *et al.*, 2010; Aiken *et al.*, 2015). A recent meta-analysis revealed that the mean sensitivity or specificity of these methods does not rise above 0.85, meaning that a significant proportion of patients are still being misdiagnosed (Su *et al.*, 2016). Indeed, Coatesworth and MacLennan (2002) and Sutton *et al.* (2017) showed the histological presence of ECS in a subset of patients declared node negative based on scans and physical examination. This false negative reporting could delay the identification of patients requiring more aggressive treatment, such as radio- or chemoradiotherapy, alongside surgery.

There have been some reports investigating gene expression signatures that can predict ECS. The identified signatures included gene copy number aberrations (Michikawa *et al.*, 2011; Peng *et al.*, 2011), epigenetic modifications (Jithesh *et al.*, 2013), as well as specific changes in RNA and protein expression (Zhou *et al.*, 2006; Dhanda *et al.*, 2014; Wang *et al.*, 2015; Mermod *et al.*, 2017) and identified markers such as epidermal growth factor receptor (EGFR), α -smooth muscle actin (α SMA) and the proto-oncogene *MYC*. All of these studies utilised primary tumour samples, which may suggest the genes identified are predictive of more aggressive disease rather than having a direct effect on ECS specifically. On the other hand, predicting ECS from features of the primary tumour samples would aid treatment decisions by identifying patients likely to develop ECS. However, there are currently no molecular biomarkers in clinical use and larger and more wide-ranging clinical studies are needed before translation to the clinic can be considered. In addition,

multiple markers were often required to reach prognostic significance in these studies, which call into question their predictive power.

In order to develop effective diagnostic and therapeutic tools, the process of ECS needs to be understood better, as well as its causes and effects, both within the tumour and in its surrounding environment.

1.3. Epithelial-mesenchymal transition (EMT), the tumour microenvironment and ECS development

The ability of cancer cells to migrate and invade through the microenvironment is central to the development of ECS. It is well known that EMT plays a key role in the acquisition of these abilities in many cancer types including OSCC (Krisanaprakornkit and Iamaroon, 2012). EMT was first studied in the context of embryology, wound healing and tissue regeneration. However, later research showed that it played an important role in cancer metastasis and could be linked to increased recurrence and decreased survival (Krisanaprakornkit and Iamaroon, 2012).

During EMT cell-cell adhesion is lost with epithelial adhesion molecules such as integrins and E-cadherin being replaced with mesenchymal markers such as N-cadherin and vimentin in a process of cadherin switching (Wheelock *et al.*, 2008). This is followed by a loss of baso-apical polarity and remodelling of the cytoskeleton including actin reorganisation and the formation of invadopodia (Takkunen *et al.*, 2010). Finally, the release of extra-cellular matrix (ECM) degrading enzymes, such as matrix metalloproteases (MMPs), leads to a loss of cell-ECM adhesion (Polette *et al.*, 2004). The result of these changes is an increase in the migratory and invasive ability of the cells and, subsequently, an increase in metastatic potential (see Figure 1.2.).

The induction of EMT in cancer cells is complex, involving many cellular and genetic processes. A crucial step is the epigenetic down-regulation of the cell-cell adhesion molecule E-cadherin due to the binding of transcriptional repressors such as slug (Snail Family Zinc Finger 2, SNAI2), snail (Snail Family Zinc Finger 1, SNAI1),

TWIST1 (Twist Basic Helix-Loop-Helix Transcription Factor 1) and ZEB1 (Zinc Finger E-Box Binding Homeobox 1) (Krisanaprakornkit and Iamaroon, 2012). This is known to be triggered by various growth factors including transforming growth factor- β 1 (TGF- β 1) and epidermal growth factor (EGF). Both extrinsic and intrinsic factors have been found to initiate EMT in many different cancers. For example, cell culture media containing secretions from cancer-associated fibroblasts was able to induce EMT in breast cancer cells (Lebret *et al.*, 2007) and mutations affecting the TGF- β 1 signalling pathway induced EMT changes in many cancers including gastric, breast, colon and pancreatic cancer (Levy and Hill, 2006). Genetic mutations, proteolytic cleavage of E-cadherin, micro-RNAs, and cytokine signalling have also been implicated in EMT induction (Krisanaprakornkit and Iamaroon, 2012).

In oral cancer cell lines (OCCL) TGF- β 1 (Qiao, Johnson and Gao, 2010; Richter *et al.*, 2011; Yu *et al.*, 2011), snail cDNA (Takkunen *et al.*, 2006) and AKT activation (Grille *et al.*, 2003) have been used *in vitro* to induce EMT-like changes. Although not always tested, this artificial induction was often accompanied by an increase in invasive ability (Richter *et al.*, 2011; Yu *et al.*, 2011), including in an *in vivo* model (Grille *et al.*, 2003). Additionally, OCCL with low E-cadherin/high snail expression were found to be more invasive (Yokoyama *et al.*, 2001).

The link between EMT and metastasis has also been demonstrated in many cancer types (Voulgari and Pintzas, 2009). There is also evidence linking EMT to metastasis in OSCC. Primary tumour samples with low E-cadherin and high vimentin expression correlated with a higher rate of distant metastasis (Nijkamp *et al.*, 2011) and high N-cadherin and vimentin expression has been linked to increased rate of cervical lymph node metastasis (Ding *et al.*, 2014). In addition, increased expression of several EMT transcription factors including slug, TWIST1 and ZEB1 has been linked to increased lymph node metastasis in OSCC (Wang *et al.*, 2012; Y. Zhou *et al.*, 2015; Yao and Sun, 2017). Through single-cell transcriptome analysis of a cohort of OSCC tumours, Puram *et al.* (2017) identified an EMT expression signature in a subset of the malignant cells. Although this was characterised by the expression of several classical EMT markers, including vimentin and TGF- β 1, cells retained expression of epithelial markers, albeit at a reduced level, and lacked expression of

most of the EMT transcription factors. Nevertheless, this “partial-EMT” expression signature was found to be associated with increased lymph node metastasis and ECS when applied to a large TCGA dataset.

There are few papers reporting on EMT in OSCC lymph node metastases. Lee *et al.* (2014) investigated EMT marker expression in the lymph nodes of ECS+/- patients. They found that EMT was a better predictor of poor survival than ECS alone as ECS+ patients with a high percentage of tumour cells expressing vimentin had a five times worse survival rate compared to ECS- patients. Puram *et al.* (2017) also extended their analysis to a set of matched lymph node metastases and were able to identify their partial-EMT signature in a subset of the metastatic cells. Furthermore, the proportion of malignant cells expressing this partial-EMT signature matched to that seen in the corresponding primary tumour, suggesting that EMT state was maintained at the metastatic site. Histology of OSCC lymph node tumours revealed tumour nests with partial-EMT markers expressed at in cells at the leading edge, surrounded by CAF, suggesting that this altered expression state coupled with stromal cell influence may be involved in invasion at the lymph node site.

However, further work is needed to determine to what extent EMT is important to ECS and whether alternative mechanisms are involved. Furthermore, it is now known that cancers are heavily influenced by the multitudinous cell types present in the tumour microenvironment (Figure 1.3.). Fibroblasts, lymphatic and vascular endothelial cells, and inflammatory immune cells are all key components of the tumour microenvironment and are able to influence cancer development through many complex signalling pathways and through their influence on the extracellular matrix (ECM) structure. When considering the lymph node tumour microenvironment, the role of lymph node specific cells such as FRC and the actions of resident immune cells must also be considered. The current evidence relating to these cell types and their influence on processes linked to ECS, including EMT, will be discussed in subsequent sections.

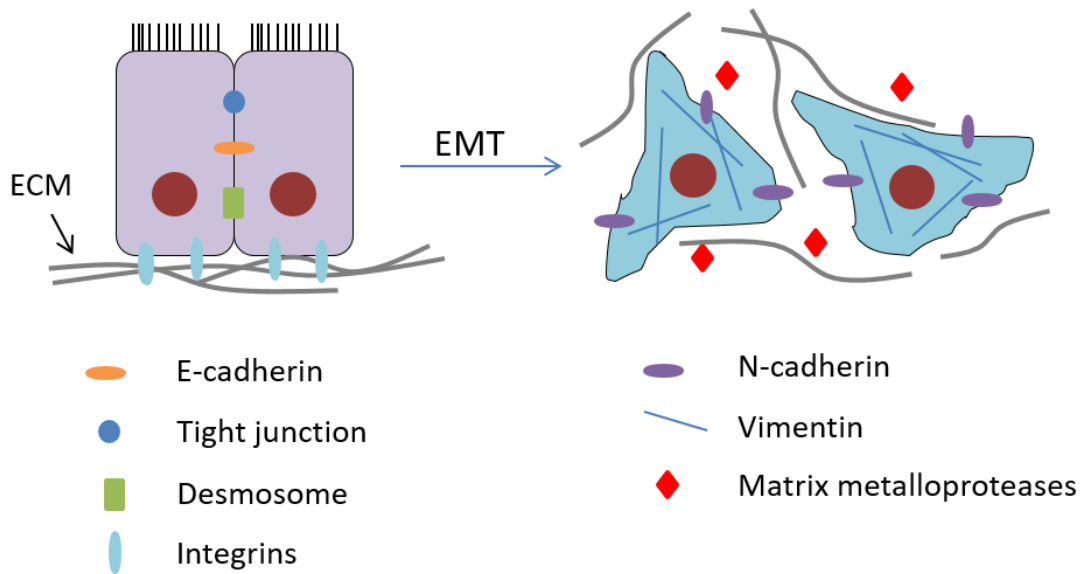


Figure 1.2. Epithelial-mesenchymal transition (EMT). Epithelial cells express cell-cell (including E-cadherin, tight junction, and desmosome components) and cell-extracellular matrix (ECM; including integrins) adhesion molecules. These are lost, along with basal-apical polarity, during epithelial-mesenchymal transition (EMT). After EMT, cells instead express mesenchymal markers such as N-cadherin and vimentin (an intermediate filament protein). They also secrete matrix metalloproteases (MMPs) which degrade the ECM. Together these changes facilitate migration and invasion abilities in cancer cells.

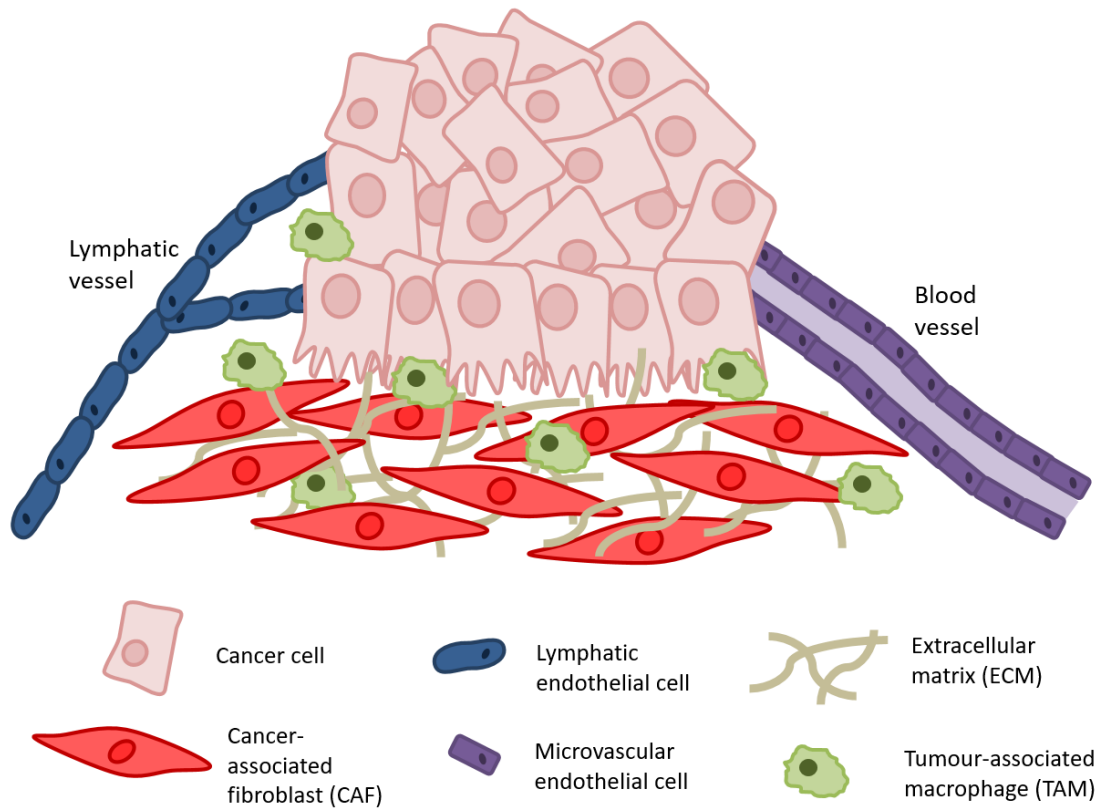


Figure 1.3. Cells and components of the tumour microenvironment. Malignant epithelial cancer cells are supported by several stromal cell types that make up the tumour microenvironment. Cancer associated fibroblasts (CAF) promote tumour development through the secretion of a range of growth factors, proteases and cytokines as well as secreting and remodelling the extracellular matrix (ECM). Blood and lymphatic vessels are important structures in the tumour microenvironment and represent key routes of metastasis. Tumour cells, alongside CAF, recruit inflammatory innate immune cells to the tumour site, such as tumour-associated macrophage (TAM). TAM themselves are able to promote tumour growth, vessel formation and ECM modulation as well as inhibiting anti-tumour immune responses.

1.4. Fibroblasts in cancer metastasis

As well as providing structural support in lymph nodes, fibroblasts have many active roles within healthy lymph nodes as well as other tissues. They are the primary secretors of the ECM and form the connective tissue of all organs. In the wound healing process, fibroblasts are activated to differentiate into myofibroblasts and play a key role in the rebuilding of the tissue structure. However, this activation is reversible and controlled in healthy tissue.

Cancer is often referred to as a dysregulated wound so it is not surprising that fibroblasts are also found in close proximity to tumours. Specifically, the term cancer-associated fibroblast (CAF) refers to fibroblast-like cells surrounding the epithelial tumour islands (particularly towards the invasive front) and contributing to cancer progression through crosstalk with tumour cells. Although this term is often used interchangeably with myofibroblast there is a large amount of evidence showing that the CAF population is in fact very heterogeneous (Madar, Goldstein and Rotter, 2013). The heterogeneity of CAF also means that identifying their origins is difficult. Various sources including recruited mesenchymal stem cells, resident fibroblasts and differentiated epithelial cancer cells have been suggested (Madar, Goldstein and Rotter, 2013). The presence of senescent fibroblasts has also been observed in the stroma of a number of different cancers including prostate, breast and oral cancers. The specific secretory profile of these cells, termed the senescence-associated secretory phenotype (SASP), contains proteases and soluble factors, including chemokines and growth factors such as TGF- β 1. Through this, senescent fibroblasts have been shown to influence cell proliferation, migration and invasion in several cancer types (Coppé *et al.*, 2010). It is now known that this senescence can develop as a result of a variety of cellular stresses including telomeric dysfunction and reactive oxygen species generation. Additionally, external factors including cigarette smoke (Coppe *et al.*, 2008) and cancer chemo- and radiotherapies designed to induce apoptosis through DNA damage may instead promote cellular senescence (Gewirtz, Holt and Elmore, 2008).

Despite this confusion in definition, several “CAF” markers have been suggested and correlated to adverse prognosis and changes to cancer cell

behaviour. In OSCC, expression of the myofibroblast marker α -smooth muscle actin (α SMA) in the tumour stroma has been linked to poor survival and increased recurrence (Kellermann *et al.*, 2007, 2008; Vered, Dobriyan, *et al.*, 2010; Bello *et al.*, 2011; Marsh *et al.*, 2011). Expression of α SMA has also been linked to increased lymph node metastasis and ECS in OSCC (Kellermann *et al.*, 2007; Marsh *et al.*, 2011; Dhanda *et al.*, 2014) which suggests there is a connection between stromal fibroblast presence, poor survival and ECS occurrence. However, the origins and mechanisms by which CAF are generated in the lymph node have yet to be elucidated.

However, the data described so far rely upon deducing links between factors based purely on observed correlations. In order to back up these findings it is necessary to carry out functional studies demonstrating a direct link between the presence of fibroblasts and altered cancer cell behaviour, in the context of ECS.

1.4.1. Effects of fibroblasts on cancer cells – proliferation, EMT induction and invasion

In primary OSCC tumours, there is a large amount of evidence showing that CAF have the ability to promote cancer migration, invasion and metastasis (see 1.4 and individual sections below). Although very few studies have looked at the role of fibroblasts in ECS specifically, information from these primary tumour studies is useful to predict the role that fibroblasts may play in promoting ECS.

Proliferation

Sustained proliferation is crucial for the maintenance and growth of a tumour. Both Kellermann *et al.* (2008) and Sobral *et al.* (2011) showed that media from myofibroblasts enhanced the proliferation of OCCL when compared to normal oral fibroblast media. The origin of these fibroblasts was different in each case. Kellermann *et al.* (2008) used TGF- β 1 to generate myofibroblasts from a culture of primary oral fibroblast and showed that TGF- β 1 itself could not induce the same changes in the OCCL. This differentiation method was also used by Berndt *et al.* (2014) who attributed the increase in proliferation to EGF receptor (EGFR) signalling. In contrast, the myofibroblasts in the Sobral *et al.* (2011) study were

monoclonal cultures derived from individual α SMA and collagen expressing cells isolated from patients' tumour samples. Although this means that induction of myofibroblast differentiation was more "natural", the derivation of monoclonal cultures does limit the heterogeneity of the cell population.

However, aggressive tumours not only display sustained proliferation but also the ability to migrate and invade into surrounding tissue and undergo metastasis. These changes are especially crucial if ECS is to occur.

Migration

Fibroblasts have been shown to influence cancer cell migration in models of OSCC primary tumours. Increased migration of primary tumour OCCL in response to conditioned media from myofibroblasts, senescent fibroblasts and CAF derived from genetically-unstable tumours has been previously demonstrated in our lab (Kabir, 2015; Kabir *et al.*, 2016; Melling *et al.*, 2018). Zhou *et al.* (2014) also showed that α SMA-positive CAF could increase the migration of several OCCL compared to normal healthy fibroblasts. Additionally, Pal *et al.* (2013) showed that OCCL migrated more in response to fibroblasts treated with cigarette smoke condensate which connects to the increased risk of OSCC in smokers. However, none of these studies investigated motility in lymph node tumour cells.

Epithelial-mesenchymal transition (EMT) induction

As previously discussed, the induction of the EMT process in cancer cells enhances their invasive and metastatic ability and so is likely to be important to the ECS process. Using immunohistochemical analysis of OSCC patient samples, Ding *et al.* (2014) found a correlation between high α SMA expression and expression of the mesenchymal markers vimentin and N-cadherin. These three markers were also predictive of lymph node metastasis and higher TMN staging. Puram *et al.* (2017) identified a partial-EMT expression signature in a cohort of OSCC tumours and found that cells positive for this signature localised to the leading edge of tumour islands and were also surrounded by CAF. This was observed in both primary tumours and lymph node metastases and the CAF were also found to be enriched

for EMT-promoting ligands such as TGF- β 1. Together this provides strong *ex vivo* evidence linking EMT and CAF presence.

Berndt *et al.* (2014) showed that myofibroblast-conditioned media caused an upregulation of the mesenchymal marker vimentin. Although this suggests a potential link, it is surprising that no significant correlation with any of the other investigated EMT markers (E-cadherin, N-cadherin and cytokeratin) was found. Using a similar method Sobral *et al.* (2011) reported an upregulation of the ECM-degrading enzymes MMP-2 and -9 coupled with an increase in invasion of OCCL in response to myofibroblast conditioned medium. Use of indirect co-culture through the transfer of conditioned medium allows the transfer of soluble factors. However, as the cells in these assays are not in close proximity it also eliminates contact-dependant signalling and the two-way crosstalk that must occur in a real tumour environment.

A separate study by Dudás, Bitsche, *et al.* (2011) used an alternative method whereby OCCL and fibroblasts are co-cultured separated only by a thin membrane using transwell chambers. Using this technique, they saw an increase in vimentin expression coupled with a decrease in E-cadherin expression in the OCCL when co-cultured with fibroblasts. This alteration of cancer cell expression caused by non-activated fibroblasts could be seen to contradict the studies discussed previously. However, the direct co-culture method allows for simultaneous crosstalk between the two cell types allowing for the alteration of fibroblast phenotype by cancer cells and the authors reported that they were indeed altered into CAF-like cells. Using a similar methodology Zhou *et al.* (2014) showed that CAF cultured in transwells were able to induce a decrease in E-cadherin coupled with an increase in vimentin and fibronectin in OCCL to a greater extent than NOF from the same patient. This was also associated with an increase in migratory ability.

Invasion

The prognostic significance and effect of fibroblasts on EMT marker expression and migration suggest that they may play an important role in invasion and metastasis, processes key to ECS. This has been supported by several studies.

The ability of fibroblasts to promote the invasion of OSCC cells was demonstrated many years ago by Matsumoto *et al.* (1989) who showed that, when cancer cell lines were grown on a collagen matrix, invasion was only seen when this matrix contained fibroblasts or fibroblast conditioned medium. More recent studies quantified this observation, showing that the percentage of cells invading into ECM-like Matrigel matrix coated membranes was significantly increased when myofibroblast, senescent fibroblast or CAF cells or conditioned media were present on the lower side of the membrane (Lewis *et al.*, 2004; Daly, McIlreavey and Irwin, 2008; Marsh *et al.*, 2011; Sobral *et al.*, 2011; Li *et al.*, 2015; Kabir *et al.*, 2016; Lin *et al.*, 2017; Melling *et al.*, 2018). In addition, Costea *et al.* (2006) showed that even dysplastic oral keratinocytes were induced to invade by the presence of fibroblasts highlighting the important role that fibroblasts may play in inducing cancer cell aggression in the early stage of tumour development.

In vitro assays can also provide information on the form of cellular invasion, comprising of single cell or collective invasion. In single cell invasion, individual cells undergo EMT and use their newly acquired motility and ability to degrade the ECM and invade into nearby structures including blood and lymphatic vessels. Collective invasion, in contrast, involves the movement of groups of carcinoma cells that retain their epithelial phenotype facilitated by the ECM degrading properties of myofibroblasts. Most work has focussed on the role of EMT and link of this to invasion, however Gaggioli *et al.* (2007) focussed on the collective invasion process. They observed that fibroblasts were able to enhance the invasion of epithelial cancer cells more than mesenchymal cancer cells. This invasion was collective, with groups of epithelial cells invading through a collagen matrix almost always following a leading fibroblast. Interestingly these tracks alone, without the presence of fibroblasts, were enough to facilitate collective invasion and blocking ECM-degrading and remodelling enzymes prevented invasion. Further to this, work in our lab has demonstrated the ability of cisplatin-senesced fibroblasts to induce invasion of primary tumour-derived OCCL in a 3D de-epithelialised dermis model of oral mucosa and observed the collective invasion of groups of cancer cells into the fibroblast filled dermis (Kabir, 2015; Kabir *et al.*, 2016).

1.4.2. Effects of cancer cells on fibroblasts

A complex crosstalk between multiple cell types occurs throughout the body and therefore is likely to influence tumour progression as well. This includes the ability of cancer cell to manipulate surrounding cells and the suggestion that they may play a role in fibroblast activation. TGF- β 1, an inducer of myofibroblast differentiation, is frequently increased in cancer (Levy and Hill, 2006) which could be explained by an increase in TGF- β 1 secretion by cancer cells and other cells of the tumour microenvironment. Lewis *et al.* (2004) showed that OCCL medium was able to induce myofibroblast differentiation in oral fibroblasts and blocking TGF- β 1 prevented this. Similarly, Dudás, Bitsche, *et al.* (2011) saw an alteration of fibroblasts into CAF when co-cultured with OCCL.

Senescent CAF have also been identified as a key part of the tumour stroma. Hassona *et al.* (2013) showed that medium from genetically unstable cancer cells caused senescence in fibroblasts and, crucially, this equated to the senescent state of the CAF at the original tumour site. This senescence was attributed to oxidative damage and TGF- β 1 signalling.

There are further examples where crosstalk between fibroblasts and cancer cells altered both their behaviours, highlighting the importance of considering other cell types when analysing cancer cell behaviour. For example, Hwang *et al.* (2012) found that insulin-like growth factor-II mRNA- binding protein-3 (IMP-3), which is needed for ECM remodelling activity and functional invadopodia formation, was also required for podoplanin mRNA stabilisation. Loss of either caused a decrease in cancer cell invasion and correlated with decreased lymph node metastasis. TGF- β 1, released by fibroblasts, was found to induce the podoplanin mRNA stabilisation activity of IMP-3. A cytokine array revealed that the cancer cells were releasing interleukin (IL)-1 β , a known TGF- β 1 inducer, indicating a crosstalk between the two cell types. However, IL-1 β depletion experiments were not carried out so it is possible that other cancer cell-secreted factors also play a role.

A further study showed that IL-1 α secretion by OCCL induced CCL7 release by CAF in a co-culture system. CCL7 was able to bind to chemokine receptors on the OCCL to induce increased invasion and migration (Jung *et al.*, 2010). The use of 3D

co-culture systems in this study more closely emulates the *in vivo* situation. These examples highlight many of the cell types and molecules discussed in this thesis and demonstrate the complexity of the tumour microenvironment signalling network and the effect this has on tumour cell behaviour.

1.4.3. Cancer-associated fibroblast (CAF) heterogeneity

A significant complicating factor in the investigation of CAF is the heterogeneity within their population. As mentioned previously, both myofibroblastic and senescent markers have been identified in the CAF population but other studies have indicated that CAF may display phenotypes that are even more diverse. Costea *et al.* (2013) used a gene microarray to compare gene expression levels in CAF, dysplastic fibroblast and normal fibroblast samples from OSCC patients. They identified two distinct CAF subgroups: CAF-N, which were similar to normal fibroblasts, and CAF-D, which were more divergent in expression levels. CAF-N induced the formation of tumours by oral dysplastic keratinocytes faster and to a greater extent than CAF-D when co-injected into mice. CAF-N populations were also more migratory, both intrinsically and in response to TGF- β 1. However, CAF-D populations also played a role in cancer development as they were found to be the major secretors of TGF- β 1.

In a separate set of studies, CAF cell lines derived from genetically stable OSCC (GS-OSCC) were compared to those from genetically unstable OSCC (GU-OSCC; defined as tumours with extensive changes in copy number, loss of heterozygosity and loss of p53 and p16^{INK4A}). Comparing the expression profiles revealed there were extensive differences between the two groups and many of the gene changes in GU-OSCC CAF could be linked to poor prognosis (Lim *et al.*, 2011). They also observed functional differences, for example only conditioned media from GU-OSCC CAF could induce invasion of keratinocytes (Hassona *et al.*, 2013). In addition, GU-OSCC CAF appeared to be more senescent and this could be explained by the presence of oxidative damage and a lack of antioxidant defences (Hassona *et al.*, 2013). In another example of crosstalk, conditioned media from GU-OSCC cells could induce senescence in normal fibroblasts. This could be blocked using

antioxidants or blocking TGF- β 1 suggesting that cancer cells may be playing a role in the generation of oxidative damage in these fibroblasts. Interestingly, this cited study observed a correlation between senescence and α SMA expression. The SASP was also analysed and key molecules involved in invasion were identified including MMP-2 (Hassona *et al.*, 2014).

As stated above, the source and development of CAF and how they contribute to ECS is still largely unknown. However, a recent paper from Puram *et al.* (2017) has provided some insight into the lymph node CAF population by carrying out single-cell transcriptome analysis of a cohort of OSCC primary tumours and five matched lymph node metastases. In the primary tumours, they identified several CAF subsets based on their expression profiles: myofibroblasts, resting fibroblasts, and CAF which displayed expression of receptors, ligands and ECM genes that have been previously associated with CAF, and could be further split into two subsets (CAF1 and CAF2) based on their expression of specific markers. Although all of these fibroblast types were also present in lymph node tumours, myofibroblast and CAF1 cells made up a greater proportion of the population, and showed preferential expression of certain ligands and receptors. This suggests that, although the different CAF subpopulations appear to be maintained at metastatic site, the altered signalling environment of the lymph node site has an effect on the specific phenotype of the CAF.

1.4.4. Fibroblast reticular cells (FRC)

Fibroblast reticular cells (FRC) are a specialised sub-type of fibroblasts found within the lymph node (Figure 1.1). They provide structure and support to the lymph node and are crucial to the establishment and maintenance of distinct B and T cell zones through their expression of homeostatic chemokines (Chang and Turley, 2015). FRC produce complex networks of collagen conduits ensheathed in a basement membrane and remain densely covering the conduits, allowing for the tight control of lymphocyte-antigen interactions. These conduits transport fluid containing chemokines and small antigens through the lymph node to the high endothelial venules (HEVs) where lymphocytes and monocytes enter the lymph

node and can initiate an immune response. Entry into the conduits is tightly controlled based on size, facilitating immune cell-antigen interactions whilst also preventing pathogens from entering the bloodstream (Roozendaal, Mebius and Kraal, 2008).

Very few studies have investigated the FRC response to metastatic cancer and no information is available regarding their role in OSCC specifically. An interesting study by Riedel *et al.* (2016) investigated FRC responses in the tumour draining lymph nodes (TDLN) of a mouse melanoma model. They observed an enlargement of pre-metastatic TDLN, which was partly attributed to an expansion of FRC. Whole genome transcriptome analysis comparing non-draining lymph nodes, early and late stage TDLN revealed many alterations in expression including the expression of FRC activation markers including podoplanin. Most significantly, they observed inflammatory cytokine and chemokine signalling in the late stage nodes, which resulted in a disorganised tissue architecture and alteration to immune cell composition. Alterations to transporter function, remodelling of collagen fibres and changes to cell junction proteins were also found in late stage nodes where conduits were widened. The authors suggested this loss of conduit integrity may aid the delivery of tumour-derived factors, debris and antigens deep into the lymph node to aid subsequent lymph node metastasis. However, the impact of FRC on tumour cells and their development once they reach the lymph node is unknown. There is also some evidence to suggest that down-regulation of podoplanin signalling may lead to FRC elongation and loss of their contractile phenotype allowing the lymph node to expand to facilitate tumour growth (Acton *et al.*, 2014).

1.5. The extracellular matrix (ECM) and cancer metastasis

The extracellular matrix (ECM) forms a scaffold on which all cells reside and provides a supportive structure to all tissues. It is made up of fibrous proteins such as collagen and fibronectin and globular sugars such as glycosaminoglycans which are secreted by fibroblasts (Ziober, Falls and Ziober, 2006). Fibroblasts also secrete

enzymes such as matrix metalloproteinases (MMPs) which cleave the ECM proteins, allowing for remodelling of the structure or the release of bound signalling molecules (Lyons and Jones, 2007). The ECM plays an important role in cancer development and has been shown to influence all of the hallmarks of cancer including the promotion of angiogenesis, inflammation, invasion and metastasis (Pickup, Mouw and Weaver, 2014). Cancer cells must migrate along and invade through this dense matrix if they are to metastasise to other sites. Cells bind directly to the ECM via adhesion molecules called integrins and alteration to the integrin ligands present on the ECM can also influence cancer cell behaviour including the promotion of migration and invasion (Lyons and Jones, 2007). In lymph nodes, FRC are the key secretors of ECM, which is primarily made up of collagen conduits ensheathed in a basement matrix (see section 1.4.4.). Using time-lapse multiphoton intravital microscopy through an optical lymph node window in mice, Pereira *et al.* (2018) observed metastasising tumour cells that had entered the lymph node cortex associating with conduits suggesting that cancer cells may use this ECM matrix to migrate along upon lymph node colonisation.

The relationship between ECM component expression and cancer progression is complex as it is not only changes in expression levels but also alteration to the ECM structure and organisation that affect cancer progression (Ziober, Falls and Ziober, 2006). Overexpression of many ECM proteins has been reported in OSCC primary tumours (Ziober, Falls and Ziober, 2006) and expression signatures made up of ECM proteins including several collagen and laminin isoforms have been proposed as biomarkers for OSCC (Ziober *et al.*, 2006; Chen *et al.*, 2008). However, scarce data are available regarding the response of the lymph node ECM to cancer presence or the effect of CAF presence on ECM deposition in lymph nodes. Rizwan *et al.* (2015) investigated collagen density using a mouse model of metastatic breast cancer and found that lymph nodes containing metastatic deposits had a higher density of collagen I compared to mice with non-metastatic breast cancer or no tumour. They also examined human breast cancer lymph nodes with metastasis and saw an up-regulation of collagen, fibronectin and several types of integrin compared to tumour-free lymph nodes.

Disassembly and reorganisation of ECM proteins is also crucial to the process of invasion. Increased expression of MMP enzymes by tumour cells has been linked to increased nodal metastasis in OSCC (Baker *et al.*, 2006) and MMP-2 expression by CAF has been shown to promote invasion of OCCL *in vitro* (Hassona *et al.*, 2014). Studies in breast cancer have demonstrated an upregulation of these enzymes in metastatic lymph nodes compared to tumour-free lymph nodes (Daniele *et al.*, 2010). MMP-2 and -9 expression has also been identified in OSCC lymph node deposits but the significance of this with regard to ECS is unknown (Zhou *et al.*, 2010).

1.6. Lymphatic and vascular cells in cancer metastasis

Endothelial cells form both blood and lymphatic vessels, both of which are important in facilitating tumour growth as well as providing a route of metastasis (Figure 1.3.). It is widely known that tumours have the ability to induce angiogenesis and that this is crucial to provide oxygen and nutrients as the tumour grows, and also provides a route by which the cancer cells can metastasise. Lymph vessels also provide a metastatic route via the drainage of tissue fluid; however, whether the tumour can induce the formation of new lymph vessels is more uncertain. In OSCC, increased vascular and lymphatic invasion has been linked to increased nodal metastasis and ECS occurrence (Jones *et al.*, 2009; Adel *et al.*, 2015). Adel *et al.* (2015) investigated each vessel type separately and found that only lymphatic invasion was able to predict survival rates in their cohort, highlighting the importance of this metastatic route in OSCC.

1.6.1. Blood vessels

Increased vessel density in OSCC carcinomas compared to normal or dysplastic tissue has been observed in the primary tumour (Li *et al.*, 2005; Shivamallappa *et al.*, 2011) and correlated to increased lymph node metastasis (Miyahara *et al.*, 2007; Bolzoni Villaret *et al.*, 2009). In addition, elevated expression of factors known to promote angiogenesis, including vascular endothelial growth factor (VEGF), have been observed in primary OSCC carcinomas and correlated to

increased lymph node metastasis (Li *et al.*, 2005; Jung *et al.*, 2015; Sales *et al.*, 2016; Kazakydasan *et al.*, 2017).

There have been only few studies focussed on angiogenesis within the lymph node upon metastasis. A mouse model of OSCC found that vessel density was elevated in tumour draining lymph nodes prior to colonisation when metastatic tumour cells were implanted into the tongue but not when non-metastatic cells were used (Mayorca-Guiliani *et al.*, 2012). Conversely, when Naresh, Nerurkar and Borges (2001) double-immunostained for blood vessel and proliferation markers, they found that metastatic lymph nodes did not have an elevated level of neoangiogenesis compared to non-metastatic lymph nodes in the same patient, whereas extensive neoangiogenesis was seen in the corresponding primary tumour. They suggested this was because the rich vessel nature of the lymph node meant that inducing new vessel growth was not necessary for tumour survival. However, this needs to be confirmed in a larger sample size. Another study focussed on blood vessels as a route of metastasis from the lymph node using a mouse model of metastatic squamous cell carcinoma (Pereira *et al.*, 2018). Time-lapse multiphoton intravital microscopy through an optical lymph node window showed that once metastasising tumour cells had entered the lymph node cortex they accumulated around blood vessels as a result of directed migration and were also observed moving inside the vessel lumen. This highlights the importance of considering blood vessels as a metastatic route from lymph node metastasis and the potential role of this in the development of distant metastasis.

The role of fibroblasts in vessel formation is another important consideration as CAF are known to secrete factors which promote vessel formation (Coppé *et al.*, 2010; Cirri and Chiarugi, 2012). Increased α SMA expression and a higher blood vessel density have been correlated in primary OSCC tumours and, in a mouse model, OSCC cells co-injected with CAF showed elevated blood vessel density compared to OSCC cells injected alone or with NOF (Lin *et al.*, 2017). Furthermore, in a mouse breast cancer model epithelial tumours co-injected with senescent fibroblasts displayed increased tumour vascularisation compared to pre-

senescent fibroblasts (Coppé *et al.*, 2006). However, this has yet to be demonstrated in the context of lymph node metastases.

In the lymph node, specialised blood vessels called high endothelial venules (HEV) are found in the lymph node paracortex, formed of cuboidal endothelial cells surrounded by FRC (Figure 1.1). In OSCC lymph nodes with metastatic deposits, an increased density of HEVs has been observed and correlated to poor prognosis (Lee *et al.*, 2012). However, HEV density has also been found to be elevated during lymph node enlargement prior to metastatic colonisation (Shen *et al.*, 2014) and elevation of HEV density has been reported in sentinel lymph nodes (SLN) regardless of metastatic status compared to non-SLNs (Chung *et al.*, 2012). Moreover, Shen *et al.* (2014) observed tumour deposits adjacent to HEVs suggesting this may be an alternative route for lymph node metastasis.

1.6.2. Lymphatic vessels

In primary OSCC, high lymph vessel density (LVD) and elevated levels of the pro-lymphangiogenic factor VEGF-C have been associated with increased risk of lymph node metastasis and decreased survival (Kyzas *et al.*, 2005; Zhao *et al.*, 2008; Abdul-Aziz *et al.*, 2017). In addition, co-expression of proliferation and lymph vessel markers indicated that neolymphangiogenesis was occurring within the tumour (Kyzas *et al.*, 2005; Zhao *et al.*, 2008). This is backed up by the observation in these studies that vessels within the tumour were smaller and potentially more immature than those surrounding the tumour. However, these studies used only primary tumour samples so whether neolymphangiogenesis occurs in metastatic tumours in lymph nodes is less clear. Chung *et al.* (2012) reported an increase in LVD in sentinel lymph nodes (SLNs) regardless of metastasis status compared to non-SLN, whereas Wakisaka *et al.* (2015) found that LVD was significantly higher in SLN with metastatic deposits compared to tumour-free SLN. Neither report compared metastatic tumours in lymph nodes with and without ECS.

Additionally, functional *in vitro* studies have shown that metastatic cancer cell lines can increase vessel formation and alter gene expression of human lymphatic endothelial cells (HLEC) compared to HLEC grown with non-metastatic

cancer cell lines. These alterations included expression of VEGF-A and -C and increased expression of chemokines known to be involved in attracting cancer cells to invade into lymph vessels (Zhuang *et al.*, 2010). This implies that, as with fibroblasts, there may be a crosstalk of signals between endothelial and tumour cells that alter the behaviour of both cell types. However, validation of these findings in a broader range of cell lines is needed to confirm this and link it to the lymph node setting.

In addition, there is evidence that fibroblasts play a role in influencing lymphatic endothelial cell behaviour. A correlation between α SMA expression and a higher LVD in primary OSCC tumours has been found and correlated with higher TMN stage (Ding *et al.*, 2014; Lin *et al.*, 2017). This implicates myofibroblasts in vessel formation in OSCC. Furthermore, there is evidence that senescent fibroblasts can induce endothelial cell migration and invasion through the secretion of VEGF and other chemo-attractants (Coppé *et al.*, 2010).

There are limited data relating to the role of lymph vessel formation in lymph nodes and its role in ECS. However, given the crucial role played by lymph vessels in the metastasis of cancer, it is likely that their presence is important in the process of ECS.

1.6.3. Endothelial-mesenchymal transition (EndMT)

As with EMT, EndMT was first investigated in the context of embryonic development but it emerged that this phenotypic transformation also plays a role in pathological conditions including cancer and fibrosis. During EndMT, endothelial cells lining vessel walls delaminate from their cell layer, acquire a mesenchymal phenotype and invade into the surrounding tissue. Endothelial cells may be a significant source of CAF. Zeisberg *et al.* (2007) demonstrated that up to 40% of CAF displayed endothelial markers in two mouse models of cancer. In head and neck cancer it has been shown that TWIST1 expression can induce EndMT (Chen *et al.*, 2014) and it is thought that EMT and EndMT share many of the same signalling mechanisms. Furthermore, EndMT is suspected to play a role in the promotion of angiogenesis: firstly as a source of tip cells which lead the growth of sprouting blood

vessels but also as a source of supporting cells such as pericytes and smooth muscle cells (Welch-Reardon, Wu and Hughes, 2014). However, the exact role of EndMT in OSCC tumours has not been investigated.

1.7. Inflammation in cancer metastasis

Although the immune system plays a key role in cancer prevention, it is now known that chronic inflammation increases cancer risk and that the generation of an inflammatory microenvironment is a crucial driver of tumour progression. Most, if not all, solid tumours generate an inflammatory microenvironment due to the secretion of cytokines and chemokines by both cancer cells and stromal cells, including CAF. The innate immune cells crucial to this inflammatory response, including macrophages, neutrophils and mast cells, have multitudinous effects on the tumour and its microenvironment through their secretion of cytokines, chemokines, prostaglandins, growth factors and reactive oxygen and nitrogen species (Grivennikov, Greten and Karin, 2010).

Inflammation is an important factor to consider when investigating the causes of invasion and metastasis. Innate immune cells secrete factors that induce angiogenesis, increase vascular permeability and promote EMT, all factors that facilitate the metastasis of tumour cells (Grivennikov, Greten and Karin, 2010). Lymph nodes are a central part of the immune system and so the response of both native and recruited immune cells to the presence of tumour cells within the lymph node is an important consideration and may influence ECS development. Aberrant chemokine and cytokine signalling by lymph node FRC (see section 1.4.4.) in response to the presence of cancer in a mouse metastatic melanoma model has been shown to result a disorganised tissue architecture and alteration to immune cell composition (Riedel *et al.*, 2016).

The importance of inflammation to cancer progression also provides another potential avenue of treatment options. It is thought that combining traditional cell-killing chemotherapies with anti-inflammatory drugs may enhance treatment

responses and early clinical trials have shown promise in preventing tumour progression (Mantovani *et al.*, 2008).

As the most common inflammatory cell type found in the tumour microenvironment macrophages are particularly important in the context of OSCC development both at the primary and lymph node sites.

1.7.1. Tumour-associated macrophages (TAM)

Macrophages are derived from blood monocytes, which are recruited to the tumour in response to a variety of signals secreted by tumour and stromal cells, such as the chemokine CCL2 (MCP-1) and the pro-angiogenic factor VEGF. Aberrant chemokine signalling in FRC in response to the presence of cancer has been shown to cause an increase in the presence of macrophages in a mouse model of metastatic melanoma cancer (Riedel *et al.*, 2016). Macrophages can be polarised to two phenotypes: M1 classically activated macrophages which secrete pro-inflammatory cytokines and contribute to anti-pathogenic and anti-tumour activity, and M2 alternatively activated macrophages which are anti-inflammatory and promote tissue remodelling and repair (Sica *et al.*, 2008). Tumour-associated macrophages (TAM) are usually of the M2 phenotype and are able to aid tumour progression through the stimulation of proliferation, secretion of pro-angiogenic factors, suppression of anti-tumour immunity and remodelling of the ECM to aid invasion and metastasis (Takeya and Komohara, 2016).

In primary OSCC tumours, high macrophage numbers (determined by staining specimens for the pan-macrophage marker CD68 by IHC) have been linked to poor prognosis and an increase in lymph node metastasis (Costa *et al.*, 2013; Weber *et al.*, 2014; Ni *et al.*, 2015; Yamagata *et al.*, 2017). However, there is some disagreement as to whether macrophage densities in the tumour, invasive edge or stroma were significant. In addition, in some cases an association with lower survival was only found when looking specifically at M2 macrophages using the CD163 marker (Fujii *et al.*, 2012; He *et al.*, 2014).

Only one study has investigated macrophage presence in metastatic lymph nodes of oral cancer (Wehrhan *et al.*, 2014). However, this focussed on whether

macrophage numbers or polarisation in the lymph node sinus could predict primary tumour invasion and grading parameters, with results varying widely depending on which macrophage marker ratio was used. Although macrophages were quantified in both the tumour and invasive front this was not commented on. Furthermore, none of the papers referenced investigated a potential link to ECS occurrence.

Macrophages are known to influence a number of processes important to invasion and therefore potentially ECS, including EMT. Hu *et al.* (2016) reported that OSCC tumours with high numbers of M2 macrophages also had a lack of E-cadherin staining coupled with high vimentin positivity. Furthermore, when they added conditioned media from the THP-1 macrophage cell line (induced to become an M2 phenotype) to OSCC cells they saw a decrease in E-cadherin and increase in vimentin protein expression respectively, indicating EMT may have occurred. This was also accompanied by an increase in migration and invasion ability.

Furthermore, macrophages are known to have the ability to induce angio- and lymphangiogenesis, which aid metastasis. In OSCC, high macrophage numbers have been linked to a higher microvascular density (El-Rouby, 2010) and lymph vessel density (Yamagata *et al.*, 2017) *ex vivo*. There is also evidence that OSCC cells can induce expression of M2-macrophage markers in monocytes, including a significant increase in VEGF expression (Essa *et al.*, 2016) and macrophages co-expressing M2 markers and VEGF-C have been observed surrounding invading tumour nests in OSCC tissues (Yamagata *et al.*, 2017).

1.7.2. Cytokine and chemokine signalling in the tumour microenvironment

Cytokines are the key immune signalling molecules that are released by immune, tumour and stromal cells in order to alter their microenvironment. Chemokines are cytokines that act as chemoattractants to direct the movement of immune cells. There are multitudinous cytokines and chemokines that have been shown to facilitate the formation of a pro-tumour immune response and promote tumour development, and many have been highlighted as potential biomarkers and treatment targets. CAF are known to secrete a wide variety of these molecules which have diverse effects on immune cell recruitment and tumour cell behaviour

(Turley, Cremasco and Astarita, 2015). In addition, endothelial cells are now being recognised as playing an active role in the immune response to tumour presence (Young, 2012; Turley, Cremasco and Astarita, 2015), but this remains an understudied topic in OSCC.

As previously discussed in section 1.7.1., the ability to recruit macrophages to the tumour microenvironment facilitates tumour development. The chemokine CCL2 (also known as monocyte chemoattractant protein-1, MCP-1) is a potent chemoattractant of macrophages and is secreted by both tumour and stromal cells. CCL2 expression has been observed in OSCC and was reported to be increased in lymph nodes with metastatic deposits (Ferreira *et al.*, 2008). Elevated CCL2 secretion and mRNA expression has also been observed in senesced oral fibroblasts and in CAF from genetically-unstable OSCC tumours (Kabir, 2015; Kabir *et al.*, 2016). In addition, Li *et al.* (2014) showed that when oral cancer cells were co-cultured with CAF, CCL2 levels were significantly elevated and this could be attributed to the CAF. Stromal CCL2 production has also been shown to be important for the promotion of cancer cell migration and invasion. Migration of oral cancer cells and invasion in a 3D model was promoted by the presence of senescent fibroblasts or their conditioned media but this was ablated by the addition of an anti-CCL2 antibody (Kabir, 2015; Kabir *et al.*, 2016). Similarly, Li *et al.* (2014) found that reducing CCL2 expression levels with siRNA significantly decreased the invasive and migratory capacity of the cancer cells. This suggests that CCL2 signalling may have multiple roles with the tumour microenvironment of OSCC and influence processes crucial to ECS.

Increased expression of certain cytokine molecules are strongly linked to cancer progression. One of these is the pro-inflammatory cytokine IL-6, which is upregulated in most cancers. Produced by fibroblasts, endothelial cells, immune cells and tumour cells, increased IL-6 levels lead to the activation of multitudinous signalling pathways that influence tumour survival, invasion, proliferation and angiogenesis (Ataie-Kachoie, Pourgholami and Morris, 2013). Elevated IL-6 serum levels have been observed in OSCC and are associated with an increased incidence of lymph node metastasis and poor survival (Shinriki *et al.*, 2011; Goda *et al.*, 2017).

IL-6 is a known component of the SASP and elevated IL-6 secretion and mRNA expression has been identified in senescent fibroblasts and CAF from genetically-unstable OSCC tumours (Kabir, 2015; Kabir *et al.*, 2016). *In vitro* OSCC studies also showed that co-culture of primary tumour-derived OCCL and fibroblasts leads to an up-regulation of IL-6 mRNA expression (Dudás, Fullár, *et al.*, 2011; Qin *et al.*, 2018). Furthermore, IL-6 has been shown to promote MMP production in oral cancer cells *in vitro* facilitating the invasion process (Sundelin *et al.*, 2005). In addition, IL-6 has also been shown to up-regulate the production of both VEGF and VEGF-C *in vitro* and blocking IL-6 inhibited angio- and lymphangiogenesis in a mouse xenograft model (Shinriki *et al.*, 2009, 2011).

Elevated salivary IL-8 (CXCL8) levels have also been identified as a potential biomarker for OSCC (Punyani and Sathawane, 2013) and elevated IL-8 in serum and OSCC tumour tissues has been linked to poor prognosis (Fujita *et al.*, 2014). This negative effect may be explained not just through the neutrophil attracting chemokine activity of IL-8, which promotes inflammation, but also through its many downstream signalling pathways. These have been shown to stimulate cancer cell survival, migration and also promote angiogenesis and stimulate growth factor release by macrophage (Waugh and Wilson, 2008). There is also significant interest in IL-1 antagonism as a potential treatment strategy for solid tumours including OSCC (Wu *et al.*, 2016; Mantovani, Barajon and Garlanda, 2018), due to its central role in initiating inflammatory reactions and link to the promotion of metastasis. Wu *et al.* (2016) observed elevated IL-1 β expression in OSCC tissues and saw that siRNA knockdown of IL-1 β or use of an IL-1 receptor 1 (IL-1R1) antagonist reduced oral cancer growth *in vitro* and in an *in vivo* rat model. Studies linking these cytokines to stromal cell signalling are scarce but co-culture of OCCL and NOF has been shown to induce increased IL-1 β mRNA expression (Dudás, Bitsche, *et al.*, 2011) and IL-6/8 mRNA expression has been shown to be up-regulated in endothelial cells as a result of co-culture with OCCL (Neiva *et al.*, 2009).

Cytokines represent a promising area for the identification of novel biomarkers and treatment targets for OSCC and research into this area continues to

reveal multiple mechanisms by which stromal cells can exert their influence on the tumour microenvironment.

1.8. Gaps, issues and impact of current research

This literature review has detailed the current information regarding the response of the lymph node tumour microenvironment to tumour metastasis but has also highlighted the lack of specific information related to ECS induction, despite its prognostic significance. There is mounting evidence that stromal cells have the ability to induce invasion and metastasis of primary tumour OSCC. However, direct evidence and specific mechanisms of action with regards to ECS are lacking. Moreover, many questions remain unanswered including the source of lymph node CAF and the response of the many resident immune cells to the presence of metastatic deposits.

As well as their role in cancer, the source of CAF in ECS is also under debate. Whether CAF are recruited by the invading tumour cells or travel with the tumour from the primary site is also unknown. Vered, Dayan, *et al.* (2010) noted that the EMT marker and α SMA expression profiles of primary and lymph node tumours matched and these correlations were not seen in fibroblasts from a benign lymph node. Puram *et al.* (2017) also identified the same CAF subpopulations in matched primary OSCC and lymph node metastasis tumours but observed an alteration in the proportion of different subsets and changes to expression of specific markers including increased IL-1R1 expression. This suggests that there is a link between the nature of cancer-stromal behaviour at both sites but does not explain whether the stromal cells are altered in response to the presence of the tumour or if the CAF metastasise with the tumour cells. Our experience of histological examination of small initial metastatic deposits suggests that these initial tumour foci are devoid of surrounding stroma. This suggests that metastatic deposits might be undergoing a second EMT and/or inducing new stroma within the lymph node environment.

1.8.1. Targeting the tumour microenvironment in extracapsular spread

Given the importance now placed on the tumour microenvironment in promoting many of the processes involved in ECS and the correlation with survival, it is not surprising that therapeutic targeting of many of the stromal cell types is seen as a promising approach. The greater genetic stability and influence CAF, TAM, FRC and endothelial cells have on the ECM, which is often a barrier for the delivery of drugs to solid tumours, makes them even more attractive. This could be particularly effective if used alongside cancer cell-killing drugs to target both sides of the crosstalk events as described above.

For example, Meng *et al.* (2014) used a computer algorithm to model the interactions of proteins which display altered expression levels in both CAF and OSCC cells. They identified a loss of TGF β receptor III (TGF β RIII) as a common occurrence in both cell types. They showed that administration of TGF β RIII slowed tumour growth, increased E-cadherin expression and decreased metastasis in an *in vivo* mouse model and that this was more effective if it was administered to both the tumour and the stromal fibroblasts. Furthermore, therapies targeted solely at cells of the tumour microenvironment, given alongside existing therapies, could also have a positive influence on patient survival. Antagonists of the pro-inflammatory cytokine IL-6 are currently being trialled as an anti-cancer therapy (Kumari *et al.*, 2016) and there is enormous potential for the use of anti-inflammatory drugs, especially in combination with cancer cell-killing drugs. However, the potential side effects of inhibiting normal cell function, particularly the wound healing role of myofibroblasts and anti-tumour immune activity must be considered when investigating new tumour microenvironment-targeted therapies.

Given the difficulties faced in the detection of ECS pre-surgery, the tumour microenvironment also represents a promising area for the identification of novel prognostic biomarkers for use in either primary tumour samples or lymph node biopsies.

It is hoped that understanding the ECS process, the mechanisms underpinning it and the role played by stromal cells will lead to better detection methods and even improved treatment strategies. This could have a significant

impact on prognostic and therapeutic tools available to clinicians treating OSCC patients.

1.9. Aims and Hypothesis

It is now known that the tumour microenvironment plays a key role in the promotion of invasion and metastasis in primary OSCC tumours as well as many other cancer types. However, tumour-stromal crosstalk has not been fully explored in metastatic lymph nodes to date. In addition, little is known about the nature and origins of the lymph node stroma and how this differs from that in primary OSCC. However, it seems likely that tumour-stroma crosstalk accelerates the development of lymph node tumours. Given the poor prognosis and aggressive nature of ECS positive tumours, this study hypothesises that these lymph node tumours have a heightened ability to induce a myofibroblastic and vessel rich stroma, which promotes tumour growth and the induction of ECS, in part through the induction of EMT.

The specific aims of this project are:

1. To compare markers of stroma, vascularity and epithelial-mesenchymal transition (EMT) in ECS positive and negative tumour sections. Paired primary site and lymph node tumour sections will be used to enable multiple comparisons to be made, with the aim to determine if the stroma is altered in ECS positive tumours and if this equates to what is seen at the primary tumour site.

2. To generate myofibroblasts and senescent fibroblasts from primary normal oral fibroblasts and compare key markers to primary OSCC CAF.

3. To examine the effect of myofibroblast and senescent fibroblast conditioned media on EMT marker expression and migration of oral cancer cell lines, including those derived from lymph node tumours. EMT has been shown to promote invasion and metastasis in many cancer types and so it was hypothesised that it may play a role in promoting ECS.

4. To examine the effect of conditioned media from oral cancer cells, myofibroblasts and senescent fibroblasts on lymphatic and vascular endothelial cells. Both lymph and blood vessels are potential metastatic routes for OSCC and new vessel growth facilitates tumour progression in primary OSCC. Therefore, this part of the study aims to find out if metastatic tumour cells can alter the vessel formation ability and growth of endothelial cells in an *in vitro* co-culture system.

5. To examine the effect of co-culture of oral cancer cells, fibroblasts and endothelial cells on immune modulation. Inflammation is an important driver of cancer progression, including invasion and metastasis. Lymph nodes play a central role in immune reactions so it was hypothesised that inflammation also plays a role in the progression of OSCC lymph node metastases. This part of the study aims to investigate this by assessing pro-inflammatory signalling molecules released by stromal cells whilst in a co-culture system.

Overall, this project aims to improve our understanding of the nature of the lymph node tumour microenvironment in OSCC and how this relates to ECS induction. Understanding this important clinical process is crucial to advance the treatment options available to patients with advanced OSCC.

Chapter 2: Materials and methods

2.1. Immunohistochemistry (IHC)

2.1.1. Specimen selection

The case cohort was selected using the local pathology database and retrieved from the archive including tongue and floor of mouth OSCCs with matched metastatic lymph nodes with and without ECS (n=40, 10 in each group). Immunohistochemistry was then carried out on 4 µm formalin fixed paraffin embedded (FFPE) tissue sections (South Sheffield Ethics Approval Committee Ref: 07/H1309/105). One FFPE block from the primary tumour and one from a lymph node metastasis were used from each case for subsequent staining and analysis.

2.1.2. Haematoxylin and eosin staining

Sections were dewaxed in xylene followed by incubation in graded ethanol. Haematoxylin and eosin (H&E) staining in tissue sections was carried out using a Leica ST4040 automated stainer in accordance with the manufacturer's instructions before dehydrating and mounting using DPX and coverslips. Clinicopathological characteristics were determined by a registered pathologist.

2.1.3. IHC protocol

Sections were dewaxed by placing in xylene for 2 x 5 min followed by 5 min each in absolute ethanol and 95% (v/v) ethanol. Endogenous peroxidases were blocked by placing sections in 3% (v/v) hydrogen peroxide in methanol for 20 min before rinsing briefly in phosphate buffered saline (PBS). Antigen retrieval was achieved by pressure cooking (using the Retriever 2100, Aptum Biologics Ltd.) for 20 min followed by 20 min of cooling in 0.01 M sodium citrate buffer (pH 6) or Tris-EDTA buffer (10 mM Tris base, 1 mM ethylenediaminetetraacetic acid (EDTA), pH 9) before transferring to PBS. Non-specific protein binding sites were blocked using 100% serum (horse serum for antibodies raised in mouse; goat serum for antibodies raised in rabbit) for 30 min at room temperature (RT). Primary antibodies (see Table 2.1.) were diluted in 100% serum and added to slides overnight at 4°C.

After washing twice for 5 min in PBS, slides were incubated for 30 min at RT with secondary antibody in accordance with the manufacturer's instructions (VECTASTAIN Elite ABC kit, PK-6101/2, 1 drop in 10 ml PBS). Following two further 5 min washes in PBS, Avidin Biotin Complex (ABC) solution was prepared and added at RT in accordance with the manufacturer's instructions (VECTASTAIN Elite ABC kit, two drops solution A, two drops solution B per 5 ml PBS, incubated at RT for 30 min before use). Slides were then washed twice for 5 min in PBS. Colour development was achieved using a DAB substrate kit (Vector Laboratories, SK-4100) for 10 min or until colour developed before transferring the slides to distilled water to stop the reaction. Sections were counterstained in haematoxylin before dehydrating and mounting using DPX and coverslips.

Optimisation of primary antibody concentration was carried out by testing a range of dilutions based on guidance from the manufacturer's data sheet. Negative controls (incubated with 100% serum only, with no primary antibody) were included in each optimisation experiment and during subsequent staining of clinical specimens. Positive controls (previously optimised antibodies with the same host species) were also utilised in optimisation experiments to enable troubleshooting in cases with no positive staining. Negative control slides were checked for the absence of DAB positive staining and were scanned to allow consideration in quantification analysis. In addition, for the SNAI1/2 antibody it was possible to obtain the peptide from which it was raised, enabling peptide blocking control experiments to be conducted (see Appendix A).

Table 2.1. Details of antibodies used for immunohistochemistry.

Target	Host species	Concentration and buffer used	Manufacturer
α -SMA	Mouse mAb	1/100; SC	Dako M0851
CD34	Mouse mAb	1/200; SC	Dako M7165
D2-40	Mouse mAb	1/100; TE	Dako M361901-2
TWIST1	Mouse mAb	1/100; SC	Abcam ab50887
Snail and slug (SNAI1/2)	Rabbit pAb	1/800; SC	Abcam ab85936
ZEB1	Rabbit pAb	1/500; SC	Santa Cruz H102 sc-25388
Collagen I	Rabbit mAb	1/2000; TE	Abcam ab138492
CD68	Mouse mAb	1/500; SC	Dako M0814

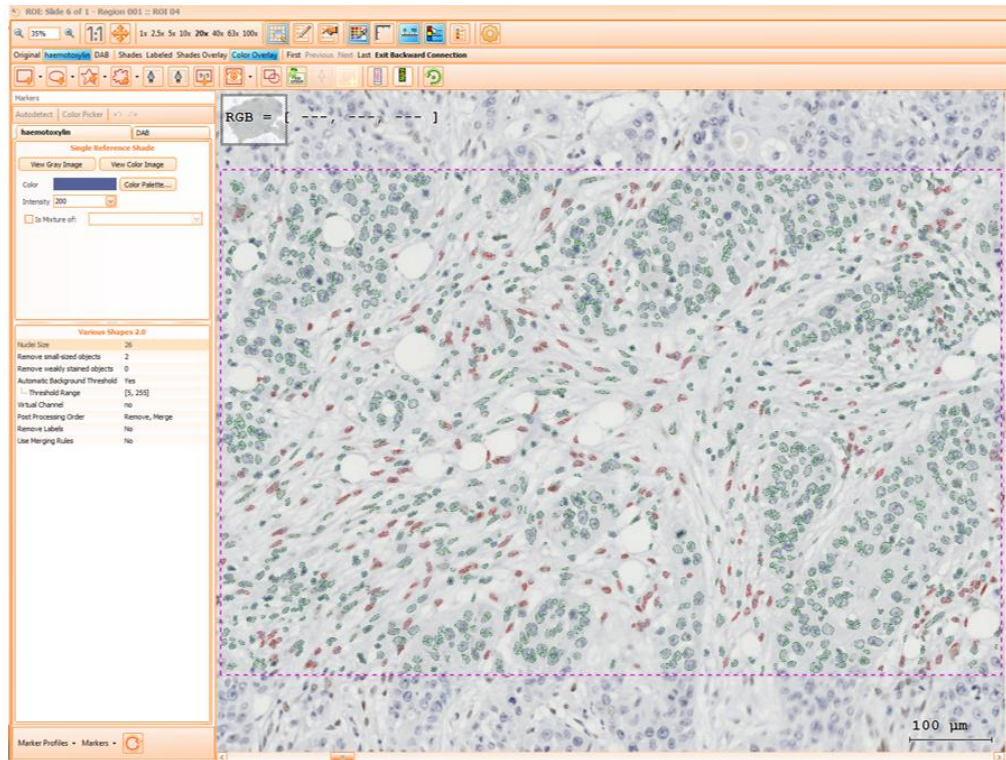
mAb: monoclonal; pAb: polyclonal; SC: Sodium citrate; TE: Tris-EDTA

2.1.4. IHC quantification

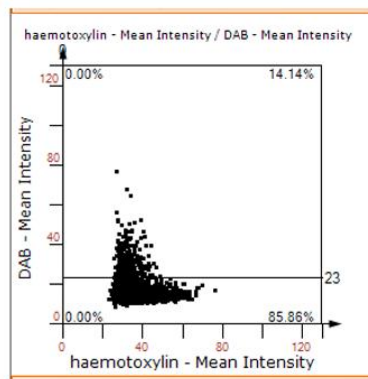
Quantitative analysis was performed using the HistoQuest software system (TissueGnostics, version 4.0.4). Six regions of interest (ROIs) per slide of equal size were selected covering a total area of 3.3 mm². The percentage positive cells were calculated by the software based on a threshold of DAB intensity level set by the user (Figure 2.1.). Negative control slides for each marker were also analysed to ensure selected thresholds resulted in < 0.5% percentage positivity for these slides.

For collagen I analysis percentage coverage per ROI was calculated (Figure 2.2.) and for vessel density the number of vessels was counted by hand and density calculated based on the size of ROI. All analysis was carried out blinded to the slide identity. Mean results for each specimen were calculated and analysed using ANOVA with $p < 0.05$ considered significant. For some specimens analysis of all markers was not possible due to tissue damage or because tumour tissue was no longer present on the section. All final n numbers are detailed in individual figure legends.

A)



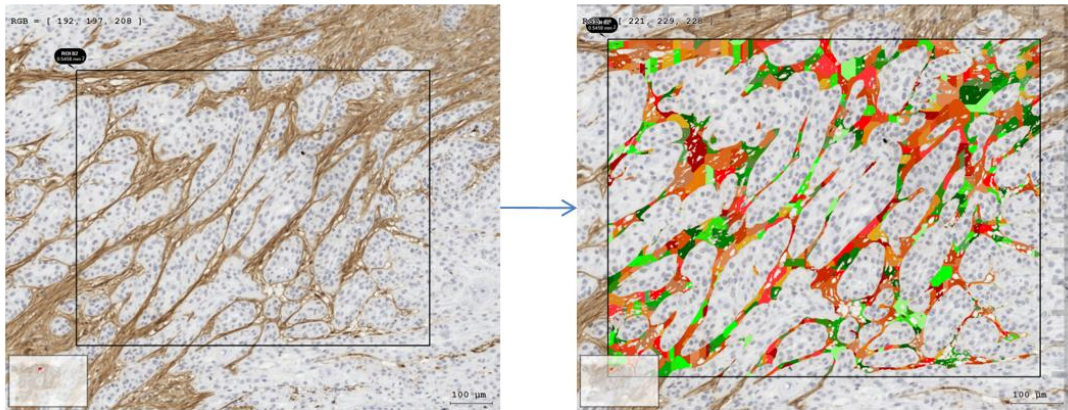
B)



C)

Global Measurements	
Parameter	Value
Area	0.58 mm ²
Perimeter	3.12mm
Number of cells	1874
DAB - Mean Intensity-Positive Cells	265

Figure 2.1. IHC quantification of percentage positive cell number (sections 3.2.2-5). (A) Screen shot showing HistoQuest (TissueGnostics, version 4.0.4) analysis interface with selected region of interest (ROI) with cell nuclei denoted by individual outlines. Scale bar 100 μ m. Red outlined nuclei are positive and green outlined nuclei are negative based on a threshold of DAB intensity set by the user (B). Cytoplasmic or nuclei staining setting could be selected. The number of DAB positive cells is then generated and the percentage of positive cells can be calculated by comparing to the total number of cells in the ROI (C).



$$\frac{\text{Collagen area } (\mu\text{m}^2)}{\text{area of ROI } (\mu\text{m}^2)} \times 100 = \% \text{ cover}$$

Figure 2.2. IHC quantification of percentage cover of collagen I (section 3.2.2.). Example regions of interest (ROIs) of original (left) and analysed (right) images from HistoQuest software (TissueGnostics, version 4.0.4). Shaded areas on the analysed image are “positive” for collagen I. Both total area of the ROIs and the collagen I “positive” area were calculated by the software and used to calculate percentage cover using the equation stated above. Scale bars 100 µm.

2.2. General tissue culture

2.2.1. Routine maintenance of cell culture

A panel of oral cancer cell lines (OCCL) was chosen to represent the successive stages of OSCC. H357 represents a non-metastatic primary tumour (site = tongue, Stage I, well differentiated, node negative, 74 year old male) and H376 a metastatic primary tumour (site = floor of mouth, Stage III, well differentiated, node positive, 40 year old female) (Prime *et al.*, 1990; Prime, Game, *et al.*, 1994; Prime, Matthews, *et al.*, 1994). Two lymph node tumour derived cell lines were included to investigate whether these tumours behave similarly to primary tumours: BICR22 (neck node derived, primary site tongue (Edington *et al.*, 1995)) and TR146 (neck node derived, primary site buccal mucosa, well differentiated (Rupniak *et al.*, 1985)).

H357 and H376 cell lines were grown in Dulbecco's Modified Eagle's Medium (DMEM) with 10% (v/v) foetal bovine serum (FBS), 1% (v/v) L-glutamine (LG) and 1% (v/v) Penicillin/Streptomycin (P/S). BICR22 and TR146 cell lines were cultured in keratinocyte growth media (KGM) media comprising a 3:1 ratio of DMEM and Ham's F12 supplemented with 10% (v/v) FBS, 1% (v/v) P/S, 1% (v/v) LG, 1% (v/v) amphotericin B, 1.8×10^{-4} M adenine, 0.5 $\mu\text{g/ml}$ hydrocortisone, 10^{-10} M cholera toxin, 5 $\mu\text{g/ml}$ insulin and 10 ng/ml epidermal growth factor (EGF).

Cells were passaged by washing twice with PBS, adding trypsin/EDTA and incubating at 37°C until cells were detached. Trypsin/EDTA was neutralised by adding culture medium containing serum and cells were pelleted by centrifuging at 1000 x *g* for 5 min. Pellets were resuspended in the appropriate media before being plated out at the densities stated.

Primary normal oral fibroblasts (NOF) were obtained from healthy oral mucosa from patients undergoing routine dental procedures with informed, written consent (ethics code: 09/H1308/66). Cancer associated fibroblasts (CAF) were obtained from OSCC patient tissues removed at the time of surgery (ethics reference: 13/NS/0120, STH17021; kindly provided by Amy Harding). Cells were isolated using selective trypsinisation, collagen digested (as described in Hearnden

et al., 2009) and used within passage 3-10 unless otherwise stated. Cells were routinely cultured in DMEM with 10% (v/v) FBS, 1% (v/v) LG and 1% (v/v) P/S and passaged as described above.

Primary human dermal lymphatic endothelial cells (HLEC) were obtained from Promocell (Heidelberg, Germany, Catalogue number C-12216) and used within passage 2-10. Human dermal microvascular endothelial cells (HMEC) were also obtained from Promocell (Heidelberg, Germany, Catalogue number C-12210). Both cell types were cultured in MV media (Promocell) and passaged as described above.

All cells were grown at 37°C in a humidified 5% CO₂ in air atmosphere.

2.2.2. Fibroblast differentiation and senescence

NOF were seeded at 1×10^6 cells/T175 flask. They were serum starved in serum free DMEM + 1% (v/v) LG + 1% (v/v) P/S for 24 h, followed by the addition of 5 ng/ml recombinant TGF- β 1 (R&D Systems) in DMEM with 0.5% (v/v) FBS and 1% (v/v) LG + 1% (v/v) P/S for 72 h, by which point cells reached 80-90% confluency. Myofibroblast differentiation was confirmed by western blot and qRT-PCR to verify an increase in α SMA expression.

Senescent fibroblasts were generated by seeding NOF at 1×10^6 cells/T175 flask and leaving overnight to attach. Senescence was induced by adding 500 μ M H₂O₂ in serum free DMEM + 1% (v/v) LG + 1% (v/v) P/S for 2 h. Serum-containing DMEM was then replaced and cells cultured for a further 10 days. NOF derived from the same source and cultured in parallel but without the addition of H₂O₂, were used as controls. The senescence-associated β -galactosidase (SA- β -gal) assay kit (Abcam, ab65351) was used according to instructions with 20,000 cells seeded per well of a 12-well plate in duplicate. The percentage of positively stained cells was calculated based on four images per well taken at x 10 magnification and was quantified using the ImageJ “Cell Counter” plug-in (version 1.49, NIH, USA).

Replicative senescent fibroblasts were generated from NOF by prolonged culturing. At each passage, 350,000 cells were seeded per T175 flask and grown to 90% confluence. Senescence was assessed at each passage using a SA- β -gal assay as

described above. NOF from the same source but at a passage <10 were used as controls.

2.2.3. Preparation of conditioned media

Conditioned media was generated from fibroblasts and oral cancer cell lines by incubating them with serum-free DMEM (+ 1% (v/v) LG + 1% (v/v) P/S) for 24 h. Volumes of media added were 6 ml per T175 flask, 3 ml per T75 flask and 1 ml per T25 flask. Upon collection, cells were counted and the volume of media used was normalised to the lowest cell count in each experiment so that all conditioned media samples were generated from the same number of cells. Conditioned media samples were topped up with serum-free DMEM to the lowest equal volume for all cell types. Conditioned media was passed through a 0.22 µm sterile filter before being added to recipient cells. OCCL were serum starved for 24 h before addition of conditioned media. However, primary fibroblasts, HLEC and HMEC were not serum starved due to their intolerance to pre-longed serum starvation. Incubation times with conditioned media and their subsequent use in experiments is detailed in each results chapter and described in methods 2.3-2.6.

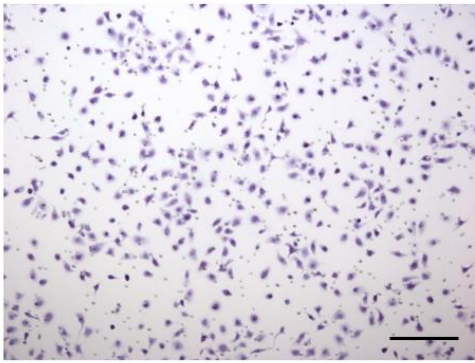
2.3. Cell migration assay

Conditioned media generated from myofibroblasts, senescent fibroblasts or patient-derived CAF and NOF control fibroblasts was collected, passed through a 0.22 µm sterile filter, and normalised for cell number. Conditioned media (500 µl/well) was added to wells of 24 well, notched companion plates (Falcon, 353504) in triplicate per OCCL used and mitomycin C added to a concentration of 1 µg/ml. OCCL (serum starved in DMEM for 24 h before experiment) were resuspended in DMEM + 1% (v/v) LG + 0.1% (w/v) BSA at a concentration of 10×10^4 /ml. Transwell inserts (Falcon, 353097, 8.0 µm pore, PET membrane) were placed in each well containing conditioned media and 200 µl of the OCCL cell suspension was added per well (in triplicate per conditioned media type) resulting in 20,000 cells per insert. Cells were left to migrate at 37°C for 16 h.

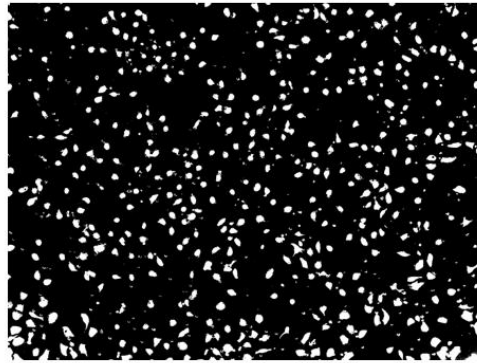
After 16 h the inserts were washed briefly in PBS before being fixed in methanol for 20 min. Membranes were stained by placing them in 0.1% (w/v) crystal violet (in 10% (v/v) methanol, 0.22 μm filtered before use) for 20 min, followed by two washes in distilled water. Once dry membranes were cut out and mounted on glass slides using DPX mountant.

Four images at x 10 magnification were taken per membrane for quantification. Images were converted to binary form and the number of cells counted using the ImageJ “Analyse Particles” function (version 1.49, NIH, USA; Figure 2.3.).

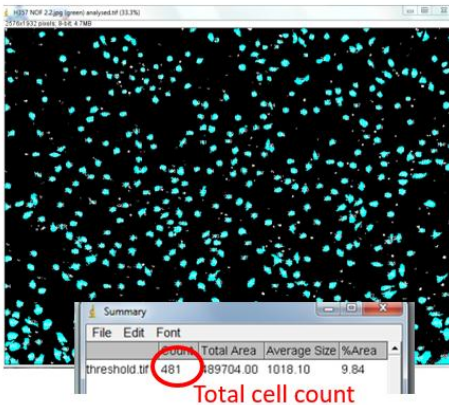
A) Original image



B) Binary image



C) "Analyze Particles" result



Detailed view (example of excluded membrane pores circled)

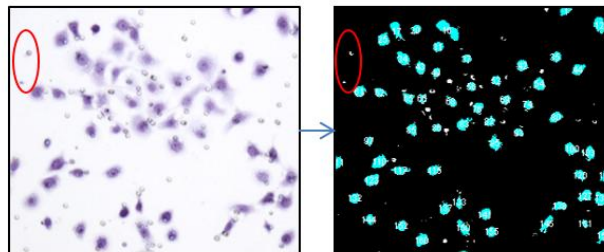


Figure 2.3. Migration assay quantification using ImageJ. Images of crystal violet stained cells from migration assays (A, scale bar 200 μm) were converted to binary images by splitting the image channels, selecting the green channel image and adjusting the brightness and contrast and image threshold to select cells only (B). The "Analyze Particles" function was used quantify the number of cells per image with identified particles labelled blue (C). By setting a minimum particle size of 250 pixels² membrane pores and other debris were excluded from the cell count (example of excluded pores circled in red in detailed view). Analysis carried out using ImageJ, version 1.49, NIH, USA.

2.4. Cell proliferation assay

HMEC or HLEC cells were seeded at a density of 5000 cells/well in a 96 well plate. After 24 hrs, cells were washed twice with PBS before the addition of conditioned media generated from fibroblasts or OCCL (see section 2.2.3. but containing 0.1% (v/v) FBS; 200 µl/well in triplicate) and were then incubated at 37 °C for 16 h. DMEM + 1% (v/v) LG + 1% (v/v) P/S + 0.1% (v/v) FBS previously incubated at 37°C for 24 h was used as a negative control. VEGF-A (for HMEC, Thermo PHC9394, 200 ng/ml) and VEGF-C (for HLEC, Peprotech 100-20CB, 100ng/ml) diluted in DMEM + 1% (v/v) LG + 1% (v/v) P/S + 0.1% (v/v) FBS previously incubated at 37°C for 24 h were used as positive controls.

A standard curve of HLEC or HMEC was generated by plating out 40000 cells subsequently diluted 1:2 seven times (in duplicate) and leaving them to attach at 37 °C for 1 h. All wells were washed x2 with PBS before adding 100 µl SFM followed by 20 µl MTS reagent (Cell Titer 96® Aqueous One Solution Cell Proliferation Assay reagent, Promega G3580). Plates were incubated in the dark at 37 °C for 1 h before reading at absorbance 492 nm. Cell numbers for each condition were estimated by extrapolating from the standard curve.

2.5. Microtubule formation assay

Conditioned media containing 0.1% (v/v) FBS was collected, filtered and normalised for cell number as described in section 2.2.3. DMEM + 1% (v/v) LG + 1% (v/v) P/S + 0.1% (v/v) FBS previously incubated at 37°C for 24 h was used as a negative control. VEGF-A (for HMEC, Thermo PHC9394, 200 ng/ml) and VEGF-C (for HLEC, Peprotech 100-20CB, 100ng/ml) diluted in DMEM + 1% (v/v) LG + 1% (v/v) P/S + 0.1% (v/v) FBS previously incubated at 37°C for 24 h were used as positive controls.

Growth factor-reduced Matrigel (Corning, 356230) was thawed on ice and 40 µl added per well of a 96-well plate. Plates were incubated at 37°C for 1 h to allow the Matrigel to set. HMEC and HLEC cells were resuspended in each media

type and 200 μ l of cell suspension added in triplicate to the Matrigel coated plates to give final densities of 20,000 cells/well of HMEC and 25,000 cells/well of HLEC.

Plates were incubated at 37°C for 16 h before being imaged at x 10 magnification using a light microscope. One image per well was skeletonised by tracing over tubules. The number of junctions was then quantified by counting using the ImageJ “Cell Counter” plug-in (version 1.49, NIH, USA). See Figure 2.4 for more details.

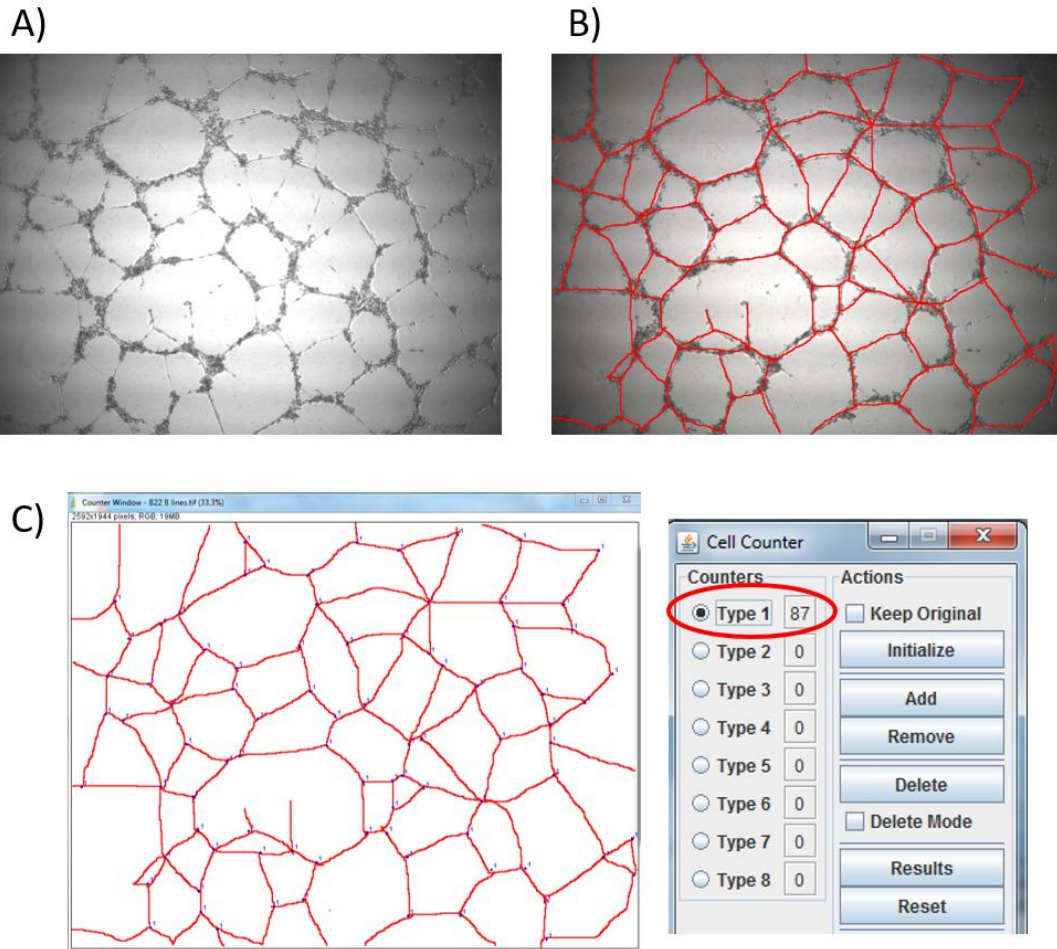


Figure 2.4. Microtubule assay quantification using ImageJ. Images from microtubule assays (A) were skeletonised by tracing over visible tubules using GNU Image Manipulation Program software (version 2.8.18) (B). The traced layer was extracted and placed on a white background for clarity and the number of junctions quantified using ImageJ (version 1.49, NIH, USA) “Cell Counter” plug-in (C). Blue dots on image indicate junctions and the red circle shows the total number counted.

2.6. Enzyme linked immunosorbent assay (ELISA)

To generate conditioned media for ELISA analysis conditioned media was collected from OCCL or fibroblasts (after 24 h) as described in section 2.2.3. and added to NOF, HMEC or HLEC as stated in the text. After 24 h cells were washed x2 with PBS and serum-free DMEM (+ 1% (v/v) LG + 1% (v/v) P/S) added for a further 24 h before being collected, normalised for cell number, and used in subsequent ELISAs. All experiments involving HMEC or HLEC were carried out using DMEM containing 1% (v/v) FBS due to their intolerance to serum starvation.

ELISAs were performed using BD OptEIA™ kits according to the provided instructions (BD Biosciences, IL-6: C555220, CCL2: 555179). Capture antibodies diluted 1:250 in 0.1 M sodium carbonate, pH 9.5, were added to 96-well ELISA plates (100 µl/well) and incubated overnight at 4°C.

Plates were washed three times with PBS 0.05% Tween-20 (PBST) before blocking with 200 µl/well assay diluent (PBS + 10% (v/v) FBS) for 1 h at RT.

Recombinant IL-6 and CCL2 were diluted to 300 pg/ml and 500 pg/ml, respectively, in assay diluent and serial dilutions (1:2) performed to yield seven standard curve solutions. If required, conditioned media was diluted in assay diluent to ensure results remained in the standard curve range. After three washes in PBST, 100 µl of each standard (in duplicate), conditioned media samples (in triplicate) and assay diluent alone were added to the plate and incubated at RT for 2 h.

Working detector solutions were prepared for each kit by diluting biotinylated detection antibodies (IL-6 1:250, MCP-1 1:1000) and streptavidin-horseradish peroxidase conjugate (1:250) in assay diluent. After five washes in PBST, 100 µl of this solution was added per well and plates were incubated for 1 h at RT.

Plates were washed seven times in PBST, leaving to soak for 30 sec to 1 min each time. 100 µl TMB substrate solution (0.1 mg/ml 3,3',5,5'-tetramethylbenzidine dihydrochloride (TMB) in 0.05 M phosphate-citrate buffer with 2 µl 30% (v/v) H₂O₂ per 10ml added immediately before use) was added per well and incubated for 30

min (IL-6) or 45 min (CCL2) at RT in the dark. The reaction was stopped by addition of 50 μ l 2 M H₂SO₄ per well. Plates were scanned at 450 nm and 570 nm.

ELISA results were analysed by subtracting 570 nm absorbance values from those measured at 450 nm. Conditioned media absorbance values were converted into concentrations by interpolating from the standard curve.

2.7. SDS-PAGE and Western Blotting

2.7.1. Lysate preparation

Cells were lysed using radioimmunoprecipitation (RIPA) buffer with protease inhibitors (completeULTRA tablets, Roche, 1 per 10 ml) and left on ice for 30 min. Cell debris was then removed by centrifuging at 15000 x *g* for 10 min. Protein concentrations were determined using a BCA protein assay kit (Pierce, 23227). Samples (10 μ l of each, diluted in distilled water) in duplicate and a standard curve of BSA protein standards were added to a 96 well plate. BCA assay reagent (200 μ l) was added to all wells and after 30 min incubation at 37°C absorbance was measured at 570 nm.

2.7.2. Gel electrophoresis and membrane transfer

Samples (20 μ g of each, normalised in concentration using distilled water) were mixed 1:5 with protein loading buffer (National Diagnostics). Each mixture was heated at 95°C for 5 min before loading. Sodium dodecyl sulphate polyacrylamide gel electrophoresis (SDS-PAGE) gels prepared according to Table 2.2. were placed in running buffer (12 g Tris, 57.5 g glycine, 4 g SDS, to 1 L with H₂O) with 500 μ l antioxidant before loading samples, 20 μ g/lane. EZrun protein ladder (5 μ l, FisherScientific, BP36031) was added to one well per gel. Gels were run at 150 V for 1 h or until samples reached the bottom of the gel.

Gels were transferred onto 0.2 μ m nitrocellulose membranes using either the iBLOT (ThermoScientific) or Trans-Blot Turbo (Bio-Rad) dry transfer systems. Success of transfer was confirmed using Ponceau staining.

Table 2.2. Details of SDS-PAGE gel constituents.

	12% Resolving gel	5% stacking gel
Acrylamide	3 ml	0.975 ml
Tris	2.5 ml	2.1 ml
H₂O	4.725 ml	4.725 ml
5% APS	350 μ l	17 μ l
TEMED	5 μ l	100 μ l

TEMED: tetramethylethylenediamine, APS: ammonium persulphate

2.7.3. Immunodetection and development

Non-specific antibody binding sites were blocked for 1 h before adding primary antibody diluted in blocking buffer (see Table 2.3. for details of blocking buffer and antibody dilutions) at 4°C overnight on a rocker. Membranes were then washed x 3 in Tris-Buffered Saline with 0.5% (v/v) Tween-20 (TBST) for 5 min on the rocker at RT. Secondary antibody (see Table 2.3.) was then added to the membranes diluted in blocking buffer as before and incubated at RT on a rocker for 1 h. Membranes were washed again x 3 in TBST for 5 min on a rocker at RT. Before March 2017, membranes were developed using enhanced chemiluminescence (ECL, Pierce, 32109) western blotting substrate and x-ray films. From March 2017, membranes were analysed using the LI-COR C-Digit blot scanner following incubation with ECL for 5 min. This is indicated in individual figure legends.

Membranes were stripped using Restore Western Blot Stripping Buffer (Thermo Scientific, 21059) before blocking and labelling as above.

Protein expression was normalised relative to β -actin or glyceraldehyde-3-phosphate dehydrogenase (GAPDH). Prior to March 2017 ImageJ software (Java, v1.48) was used to calculate the band density, however, after March 2017 LI-COR Image Studio Lite was used to analyse scanned membranes from the blot scanner (this is indicated in individual figure legends).

Table 2.3. Details of antibodies used for Western blotting.

Target	Host species/label	Concentration	Manufacturer
Slug (SNAI2)	Rabbit mAb	1/500 in 5% (w/v) BSA	Cell Signalling, 9585
Snail (SNAI1)	Rabbit pAb	1/500 in 5% (w/v) milk	Thermo, PA5-11923
TWIST1	Mouse mAb	1/50 in 5% (w/v) BSA	Abcam, ab50887
ZEB1	Rabbit pAb	1/200 in 5% (w/v) milk	Santa Cruz, H102
E-cadherin	Rabbit mAb	1/20000 in 5% (w/v) milk	Abcam, ab40772
Vimentin	Mouse mAb	1/2000 in 5% (w/v) milk	Abcam, ab8978
αSMA	Mouse mAb	1/1000 in 5% (w/v) milk 3% (w/v) BSA	SIGMA, A5228
β-actin	Mouse mAb	1/10000 in 5% (w/v) milk	SIGMA, A1978
GAPDH	Rabbit mAb	1/5000 in 5% (w/v) BSA	Abcam, ab185059
<i>Mouse IgG</i>	<i>Horse, HRP labelled</i>	<i>1:3000</i>	<i>Cell signalling, #7076</i>
<i>Rabbit IgG</i>	<i>Goat, HRP labelled</i>	<i>1:3000</i>	<i>Cell Signalling, #7074</i>

BSA: bovine serum albumin, HRP: horse radish peroxidase; pAb = polyclonal antibody, mAb = monoclonal antibody; antibodies in italics are secondary antibodies

2.8. Quantitative real time polymerase chain reaction (qRT-PCR)

2.8.1. RNA extraction

RNA was extracted using the RNeasy mini kit (QIAGEN 74104). Cell lysates were collected by scraping cells into RLT buffer containing 10 μ l/ml β -mercaptoethanol (350 μ l per well of a 6-well plate). An equal volume of 70% (v/v) ethanol was added to the lysate and mixed. The mixture was transferred to a spin column and centrifuged at $\geq 8000 \times g$ for 15 sec, after which the flow-through was discarded. RW1 buffer (700 μ l) was added, tubes centrifuged at $\geq 8000 \times g$ for 15 sec and flow through discarded. RPE buffer (500 μ l) was added, tubes centrifuged at $\geq 8000 \times g$ for 15 sec and flow through discarded. This was then repeated but with a 2 min centrifuge step before replacing the collection tube. RNase-free water (30 μ l)

was added and tubes centrifuged at $\geq 8000 \times g$ for 1 min. The eluted solution was collected and RNA concentration determined using the Nanodrop 1000 spectrophotometer (version 3.7.0.).

2.8.2. cDNA generation

RNA (500 ng) was diluted to a volume of 10 μ l in RNase-free water for each sample. Reverse transcriptase (RevT) master mix was prepared using the High Capacity cDNA Reverse Transcription kit (Applied Biosystems, 4368813) by multiplying volumes shown in Table 2.4. by the number of samples. A RevT negative (without reverse transcriptase) master mix was also prepared per sample (see Table 2.4.) as a negative control.

Each RNA sample (10 μ l) was mixed with 10 μ l master mix in PCR tubes, briefly centrifuged and then placed in the cDNA thermocycler (BioRad). This was repeated using the RevT negative master mix. cDNA was generated by incubation at 25°C for 10 min, 37°C for 120 min and 85°C for 5 min.

Table 2.4. Reagents used for cDNA generation.

	Volume (μ l)	
	RevT positive	RevT negative
10x RT buffer	2	2
25x dNTP mix (100 mM)	0.8	0.8
10x RT random primers	2	2
Reverse transcriptase	1	0
Nuclease free H₂O	3.2	4.2
Total per reaction	10	10

2.8.3. qRT-PCR run and analysis

For SYBR green primers (α SMA, p16^{INK4a}, p21/cip1 and U6 reference gene; primer sequences listed in Table 2.5.; melt curves included in Appendix B) master mixes were prepared for each primer for each sample in triplicate by multiplying volumes shown in Table 2.6. For Taqman probe/primers (ThermoFisher: slug

(SNAI2), Hs00950344_m1; snail (SNAI1), Hs00195591_m1; TWIST1, Hs01675818_s1; ZEB1, H200232783_m1; IL-6, Hs00985639_m1; CCL2/MCP-1, Hs00234140_m1; IL-1 α , Hs00174092_m1; IL-1 β , Hs00174097_m1; IL-8, Hs00174103_m1; Col1A1, Hs00164004_m1) master mixes were prepared for each target gene in triplicate per sample by multiplying volumes shown in Table 2.6. Beta-2-microglobulin (B2M) reference gene (Applied Biosystems, 4325797) was included in the same mixture per sample (see Table 2.6.).

qRT-PCR was carried out using the Rotor-Gene Q real-time PCR cycler (QIAGEN). SYBR primer or Taqman primer/probe master mix (9 μ l) was added to PCR tubes along with 1 μ l cDNA (in triplicate). Cycle temperatures and times are detailed in Table 2.7.

CT values were calculated using Rotor-Gene analysis software to set a threshold. Δ CT values were calculated from the average difference in CT values between the target and the reference gene for each triplicate sample. $\Delta\Delta$ CT values were then calculated relative to the control sample for each cell line to normalise the expression levels using the Livak method (Livak and Schmittgen, 2001) and data were analysed using a paired t-test or one-way ANOVA. P values <0.05 were considered as statistically significant.

Table 2.5. SYBR green primer sequences.

Gene	Forward primer	Reverse Primer
α SMA	5' GAAGAAGAGGACAGCACTG 3'	5' TCCCATTCACCATCAA 3'
p16 ^{INK4a}	5' AATAACCTTCGGCTGACTGGCTG 3'	5' TTATTCGCCTCCAGCAGCGCCCG 3'
p21/cip1	5' AATAATGCCGCCGCTCTTC 3'	5' TTATTGTTCCATCGCTCACG 3'
U6	5' CTCGCTTCGGCAGCACA 3'	5' AACGTTACGAATTTGCGT 3'

Table 2.6. qRT-PCR primer master mix.

Taqman	SYBR green
5µl master mix (Applied Biosystems 4369016)	5µl master mix (Applied Biosystems 4367659)
0.5µl target primer/probe	0.5µl forward primer
0.5µl reference gene primer/probe	0.5µl reverse primer
3µl RNase-free H ₂ O	3µl RNase-free H ₂ O
Per well: 9µl	Per well: 9µl (ref and target primers prepared separately and included in separate wells)

Table 2.7. qRT-PCR cycle steps.

Stages	SYBR		Taqman	
	Temperature (°C)	Time	Temperature (°C)	Time (min)
Hold	95	10 min	95	10 min
Cycle (x40)	95	10 sec	95	10 sec
	60*	45 sec	60	15 sec
			72*	20 sec

* fluorescence data acquired at this step for every cycle

2.9. Statistics

All statistical analysis was carried out using GraphPad Prism software (version 7.02, La Jolla, California, USA). Student's t-test or one-way ANOVA were used to compare between pairs/groups of results. Fisher's exact test and the chi-squared test for trend were used to test for differences in clinical and pathological characteristics between the ECS positive and negative groups. Correlation was used to analyse paired IHC specimens. In all cases p values <0.05 were considered significant.

Chapter 3: Investigating stromal and EMT markers in ECS positive and negative matched lymph node tumours

3.1. Introduction, hypothesis and aims

To date few studies have looked in detail at the morphology of OSCC lymph node tumour development, the expression of relevant markers, both in the tumour and stroma, and how this relates to ECS development. The majority of studies which identify markers predictive of ECS have done so only by quantifying their presence in the primary tumour (Michikawa *et al.*, 2011; Wang *et al.*, 2015). Although this is useful for early identification of patients at risk of developing more aggressive disease, the inclusion of lymph node metastases in this work provides a more in depth view of how this relates to tumour development within lymph nodes themselves.

As previously discussed in sections 1.3-7, cancer-associated fibroblasts, endothelial cells and inflammatory immune cells have been shown to play a role in promoting tumour development and have been linked to poor prognosis in OSCC. However, in this study the aim was to compare their abundance in metastatic lymph node tumours with and without ECS to elucidate their potential role in ECS development. Matched primary tumours were included to investigate the predictive power of the abundance of these cell types in the primary tumour and allow comparisons to be made between the two sites. Due to the important and now established role of epithelial-mesenchymal transition (EMT) in OSCC invasion and metastatic spread, markers for EMT were also included in the analysis.

Given the poor prognosis and aggressive nature of ECS positive tumours, this study hypothesises that lymph node tumour deposits have the ability to induce a myofibroblastic, inflammatory and vessel rich stroma that promotes disease aggression, metastasis and the induction of ECS.

Specific Aims:

1. To assess the clinical and pathological characteristics of OSCC patients with ECS negative (ECS-) and ECS positive (ECS+) lymph node metastases.

2. To quantify and compare stromal markers in ECS+ and ECS- lymph node metastases and their paired primary tumours using immunohistochemistry. Markers to be investigated are:
 - α -smooth muscle actin (α SMA, for myofibroblasts)
 - Collagen I (extracellular matrix protein)
 - CD34 to assess microvascular density (MVD)
 - D2-40 to assess lymphatic vessel density (LVD)
 - Macrophage density at the invasive front using CD68
3. To quantify and compare markers of epithelial-mesenchymal transition (EMT) in tumour and stromal cells in ECS+ and ECS- lymph node metastases and their paired primary tumours using immunohistochemistry. Markers to be investigated are the EMT-inducing transcription factors slug (SNAI2), snail (SNAI1), TWIST1 and ZEB1.

3.2. Results

3.2.1. Defining the patient cohort

Cases with neck dissections were identified over a 10-year period using the local pathology database. From the metastatic cases, the first 20 patients who had undergone a primary OSCC excision with a neck dissection were selected to ensure paired primary-metastatic tumour tissue availability for both ECS+ and ECS- groups (20 ECS+ and 20 ECS-). Within the 20 patients in each group, equal distribution between tongue and floor of mouth (n=10 each) was ensured for the primary tumour as these are the two most common sites for OSCC. A detailed analysis was then undertaken using IHC for the markers described above using one primary tumour and one lymph node metastasis FFPE block from each case (South Sheffield Ethics Approval Committee Ref: 07/H1309/105).

The clinical and pathological characteristics of our cohort are detailed in Table 3.1. Sex ratios and age were roughly equivalent between the groups. A higher number of patients in the ECS+ group had poorly graded tumours (70% vs. 40%) but

this was not significantly different using Fisher's exact test. Primary tumour size was significantly larger in the ECS+ group with nine tumours ≥ 40 mm in diameter compared to only two in the ECS- group ($p < 0.01$, chi-squared test). No significant difference in the depth of primary tumour invasion was seen and, although the ECS+ group had higher levels of lymphovascular invasion (40% vs. 25%) and perineural invasion (40% vs. 30%), this was not significant between the two groups using Fisher's exact test.

Table 3.1. Clinical and pathological characteristics of OSCC patient cohort.

Clinical factor	Number of patients (%)		p value
	pN+ ECS-	pN+ ECS+	
Total number of patients	20	20	/
Primary tumour site			
Tongue	10 (50)	10 (50)	/
Floor of mouth	10 (50)	10 (50)	
Sex			
Male	12 (60)	13 (65)	p>0.999
Female	8 (40)	7 (35)	
Age: median [range]	58 [43-81]	61 [48-81]	/
Grade			
Well	3 (15)	2 (10)	p = 0.116
Moderate	9 (45)	4 (20)	
Poor	8 (40)	14 (70)	
Primary tumour size (mm)			
0-19	10 (50)	4 (20)	p = 0.009
20-39	8 (40)	7 (35)	
40-59	1 (5)	4 (20)	
≥ 60	1 (5)	5 (25)	

Primary tumour depth (mm)			
0-7	10 (50)	9 (45)	
7.1-15	6 (30)	8 (40)	p>0.999
15.1-22	3 (15)	2 (10)	
>22	1 (5)	1 (5)	
Lymphovascular invasion			
Yes	5 (25)	8 (40)	p = 0.501
No	15 (75)	12 (60)	
Perineural invasion			
Yes	6 (30)	8 (40)	p = 0.741
No	14 (70)	12 (60)	

3.2.2. Expression of CAF markers in patients with and without ECS

The importance of cancer-associated fibroblasts (CAF) in OSCC development is well established, as detailed in section 1.4. Elevated expression of the myofibroblast marker α -smooth muscle actin (α SMA) is found in CAF and has been linked to poor prognosis in OSCC (Kellermann *et al.*, 2007; Marsh *et al.*, 2011). Fibroblasts are also key secretors and re-modellers of the extracellular matrix (ECM), the structure, physical properties and abundance of which has been highlighted as a key factor in OSCC development (Ziober, Falls and Ziober, 2006). Therefore, α SMA expression and the abundance of the extracellular matrix component collagen I were assessed in our cohort.

All specimens were stained for the myofibroblast marker α SMA and the percentage of positive cells within six regions of interest (ROIs) in the tumour-adjacent stroma was quantified in all sections (for details on quantification method see Figure 2.1.). All 20 ECS+ lymph nodes contained abundant associated stroma whereas less stroma was seen in ECS- lymph nodes with four nodes lacking any associated stroma. The sections without stroma were excluded from the analysis to avoid bias. Staining patterns were variable and ranged from scattered focal staining, thin ribbons running through tumour areas, thick bands surrounding tumour islands and larger solid areas of positive stroma observed in both groups. Larger areas of

staining were more common in the ECS+ group and in ECS+ lymph nodes positive staining was often located towards the periphery of the metastatic tumour or surrounding invading islands of tumour cells. This strong staining surrounding invasive tumour islands was also observed in some primary tumours in both groups.

Quantification of staining revealed that ECS+ lymph nodes had a significantly higher proportion of α SMA positive cells compared to ECS- lymph nodes ($p < 0.05$, Figure 3.1. A&C). Matched primary tumours from the ECS+ group also had higher α SMA percentage positive cell number compared to primary tumours from the ECS- group ($p < 0.01$, Figure 3.1. A&B). Nevertheless, there was a broad range of percentage positive cell numbers, particularly in the ECS+ primary tumour and all lymph node specimens. However, levels of percentage expression did not correlate directly between the matched pairs ($R^2 = 0.097$, $p = 0.069$).

Collagen I is a key component of the extracellular matrix secreted by fibroblasts and has been shown to be elevated in OSCC compared to normal mucosa (Ziober, Falls and Ziober, 2006). Staining for collagen I was observed to some degree in all specimens, either in thin bands throughout the tumour or forming a dense mesh covering the tumour area. Positive staining surrounding tumour-associated stromal and immune cells was often observed but dense immune cell areas in lymph node specimens did not stain positively (Figure 3.2. A).

Because collagen is extra-cellular, the use of percentage positive cell number was not appropriate. Therefore, the "Total Area Measurements" analysis tool on the HistoQuest software was used to first define all colour shades attributable to DAB positive staining and then calculate the area within each ROI covered by DAB positive staining. From this the percentage collagen I coverage in six ROIs placed in representative areas within the tumour site was calculated for all specimens (for more details on quantification method see Figure 2.2.). No significant differences in percentage coverage between the ECS+ and ECS- groups in either lymph node or primary tumours were observed (Figure 3.2. B&C). Additionally, percentage coverage of collagen I did not significantly correlate between matched primary and lymph node tumours or to α SMA percentage positivity.

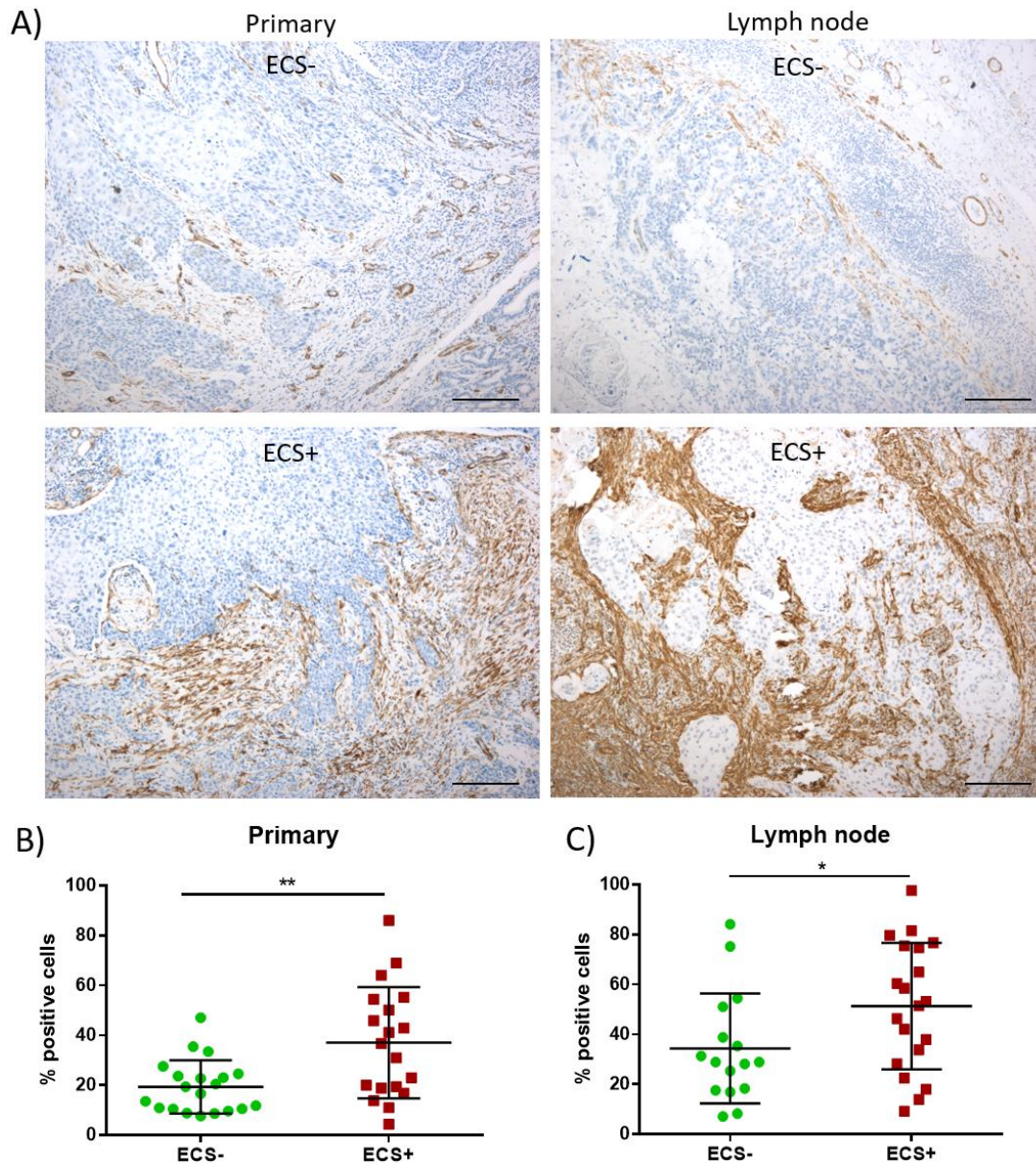


Figure 3.1. Immunohistochemical staining of α SMA in ECS+ and ECS- matched primary and lymph node tissue specimens. (A) Representative photomicrographs of α SMA immunohistochemical staining in ECS+ and ECS- primary and lymph node tumour specimens. x 10 magnification, scale bars 200 μ m. (B) Quantification data from matched primary and lymph node tumours. Data points represent mean percentage positive cells from six representative ROIs per sample taken from within the tumour-associated stroma. Four ECS- lymph nodes were not included due to the absence of tumour-associated stroma. Primary tumour: ECS- n=20, ECS+ n=19; lymph node: ECS- n=16, ECS+ n=20. Graphs show overall mean \pm SD, analysed by student's t-test, *p<0.05, **p<0.01.

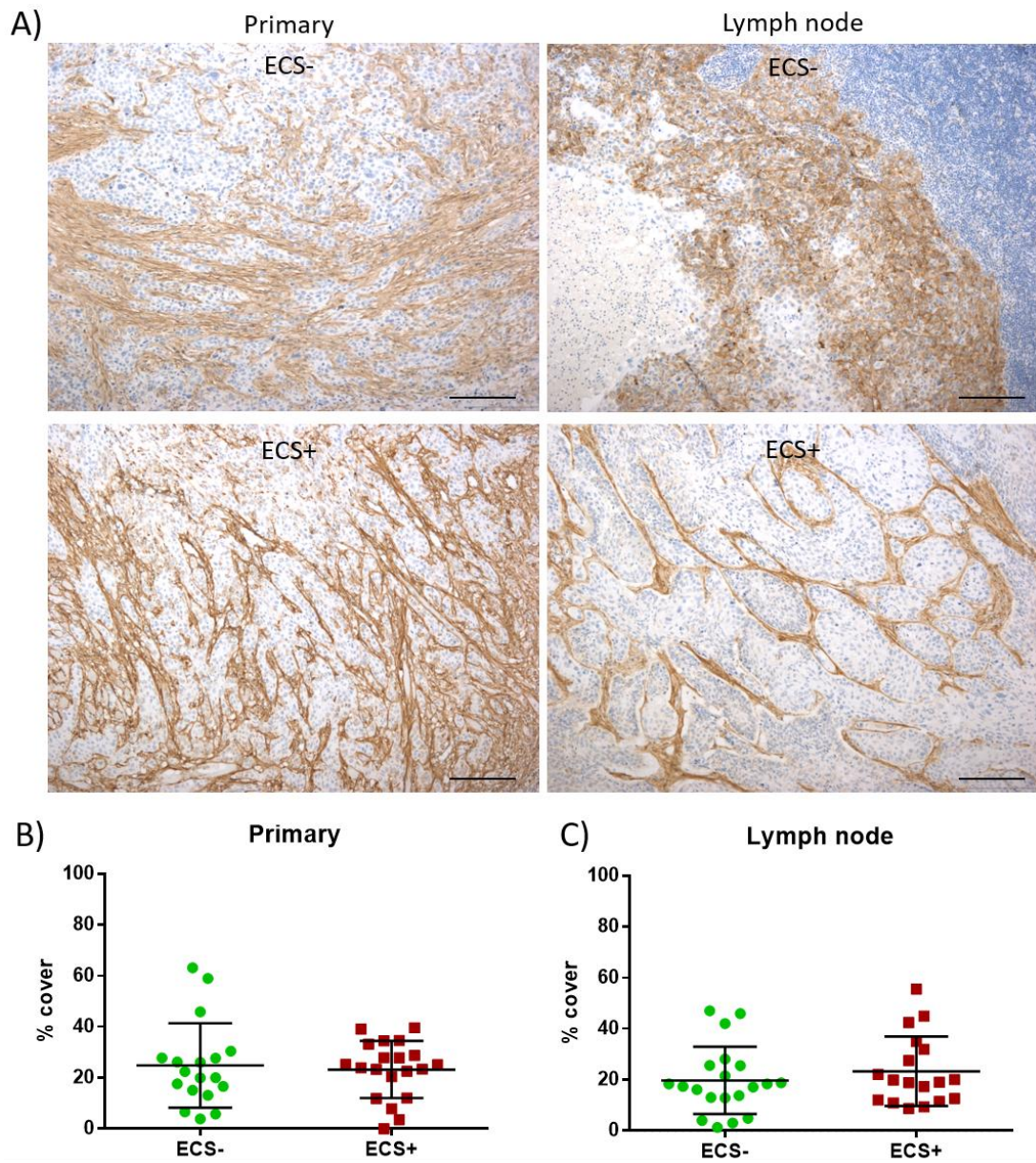


Figure 3.2. Immunohistochemical staining of collagen I in ECS+ and ECS- matched primary and lymph node tissue specimens. (A) Representative photomicrographs of collagen I immunohistochemical staining in ECS+ and ECS- primary and lymph node tumour specimens. x 10 magnification, scale bars 200 μ m. (B) Quantification data from matched primary and lymph node tumours. Data points represent mean percentage area covered by DAB positive staining in six representative ROIs per sample taken from within the tumour area. Primary tumour: ECS- n=18, ECS+ n=20; lymph node: ECS- n=20, ECS+ n=18. Graphs show overall mean \pm SD, analysed by student's t-test.

3.2.3. Comparing vascular and lymphatic density in ECS

The presence of vascular and lymphatic vessels is important for the development of tumours and also provides a potential route for metastasis. Although elevated vascular and lymphatic vessel density has been observed in primary OSCC and correlated to increased rate of lymph node metastasis (Kyzas *et al.*, 2005; Li *et al.*, 2005; Zhao *et al.*, 2008) there are few studies investigating vessel density in lymph nodes or relating it to ECS.

Vascular density was assessed by staining specimens for the vascular endothelial cell marker CD34 (Figure 3.3. A). The number of vessels in six ROIs placed in representative areas within the tumour area was used to calculate the microvascular vessel density (MVD). It was found that the MVD was significantly elevated in ECS+ lymph node tumours compared to ECS- ($p < 0.05$, Figure 3.3. C) but there was no significant difference in primary tumour MVD between the two groups (Figure 3.3. B). The range of MVD values was similar when comparing primary and metastatic tumours and there was no correlation between the matched primary and lymph node specimens or with α SMA percentage positivity.

Lymphatic vessel density (LVD) was also calculated by staining sections for the lymphatic endothelial cell specific marker D2-40 (also known as podoplanin, Figure 3.4. A). Interestingly, strong podoplanin staining was observed in some tumours particularly at the invasive edge making vessel identification difficult. Therefore, six ROIs were placed in the tumour periphery, vessels counted and LVD calculated for each specimen. No significant difference in LVD was observed between ECS+ or ECS- patients in primary or lymph node tumours (Figure 3.4. B&C). Moreover, there was no significant correlation in LVD between matched primary and metastatic specimens or with α SMA percentage positivity.

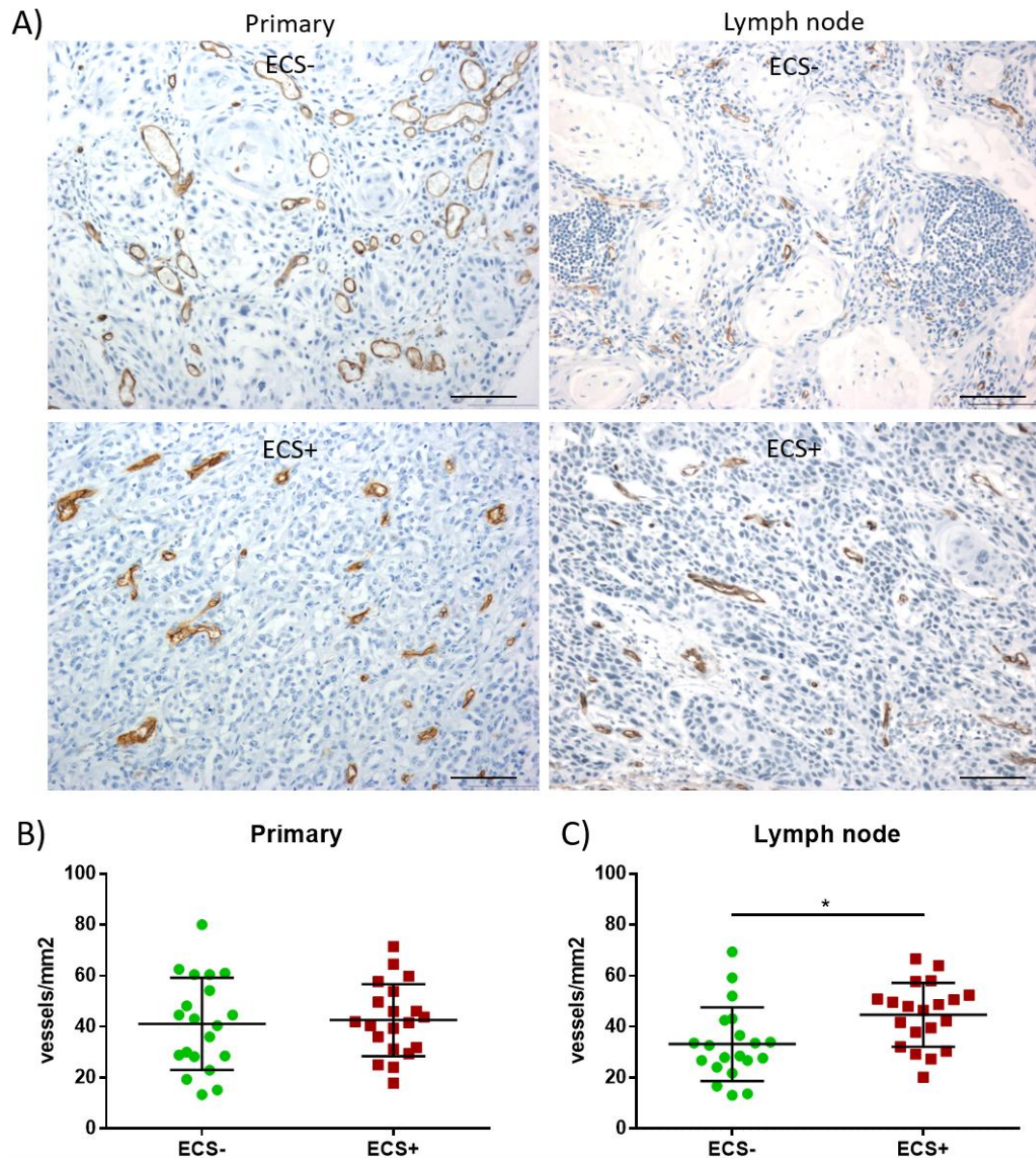


Figure 3.3. Immunohistochemical analysis of microvascular density (MVD) in ECS+ and ECS- matched primary and lymph node tissue specimens. (A) Representative photomicrographs showing CD34 immunohistochemical staining in ECS+ and ECS- primary and lymph node tumour specimens. x 20 magnification, scale bars 100 μ m. (B) Quantification data from matched primary and lymph node tumours. Data points represent mean vessels/mm² from six representative ROIs per specimen taken from within the tumour area. Primary tumour: ECS- n=20, ECS+ n=20; lymph node: ECS- n=20, ECS+ n=20. Graphs show overall mean \pm SD, analysed by student's t-test, *p<0.05.

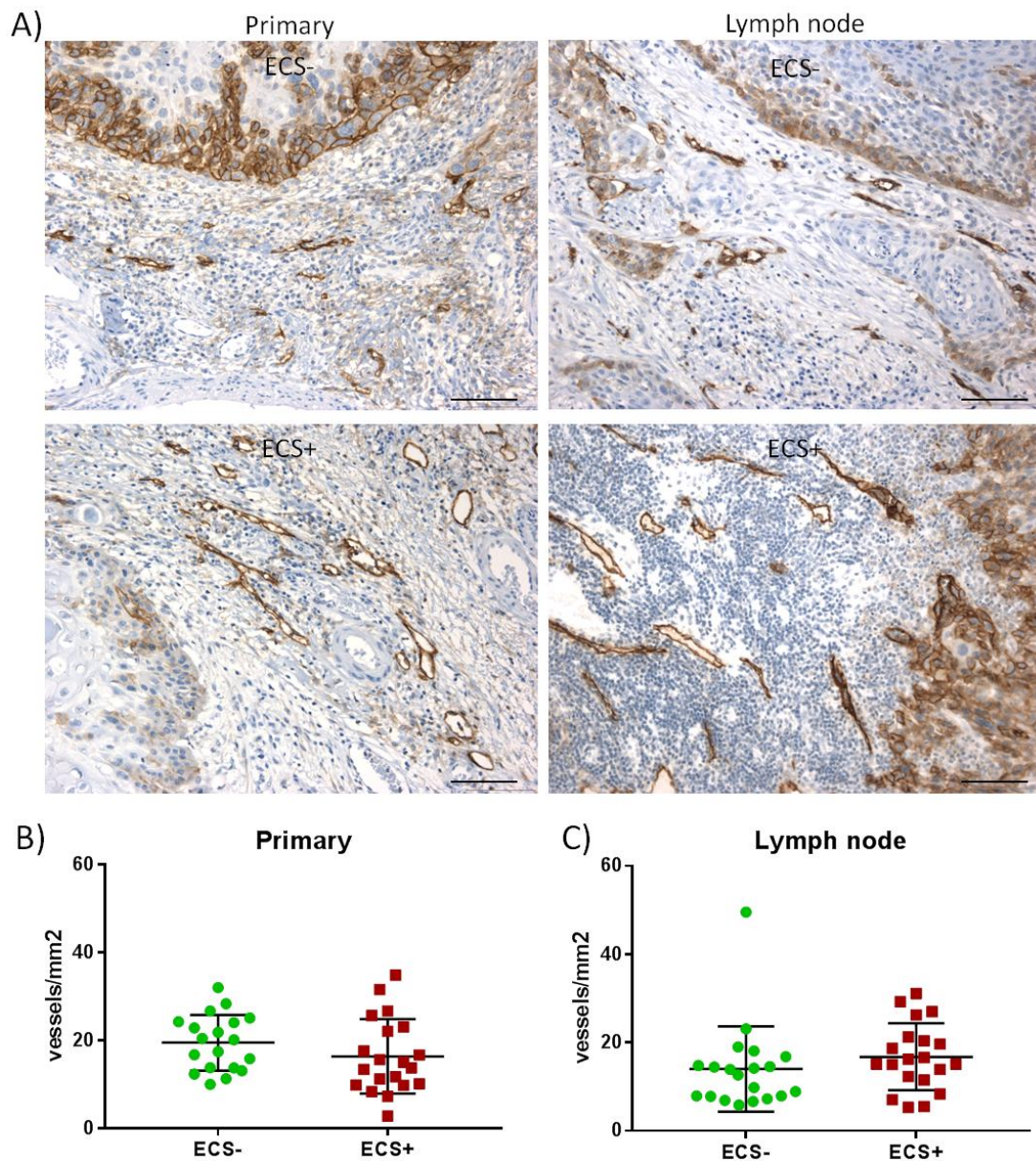


Figure 3.4. Immunohistochemical analysis of lymphatic vessel density (LVD) in ECS+ and ECS- matched primary and lymph node tissue specimens. (A) Representative photomicrographs of D2-40 immunohistochemical staining in ECS+ and ECS- primary and lymph node tumour specimens. x 20 magnification, scale bars 100 μ m. **(B)** Quantification data from matched primary and lymph node tumours. Data points represent mean vessels/mm² from six representative ROIs per sample taken from the tumour periphery. Primary tumour: ECS- n=19, ECS+ n=20; lymph node: ECS- n=20, ECS+ n=20. Graphs show overall mean \pm SD, analysed by student's t-test.

3.2.4. Analysis of tumour-associated macrophage in ECS

Tumour-associated macrophages (TAM) are a key members of the tumour microenvironment and have diverse effects on tumour progression, including the promotion of cancer cell survival and proliferation, as well as modifying the tumour microenvironment by the secretion of pro-angiogenic factors and remodelling of the ECM (Takeya and Komohara, 2016). Elevated macrophage abundance, quantified using the pan-macrophage marker CD68, has been linked to lymph node metastasis and poor survival in OSCC (Ni *et al.*, 2015; Weber *et al.*, 2016; Yamagata *et al.*, 2017). However, TAM and their influence on the progression of tumours within the lymph node have been scarcely reported on. Therefore, the aim of this part of the study was to assess macrophage density within the paired cohort of OSCC specimens using the CD68 marker.

Macrophages were most commonly found within the stroma, often along the invasive edge or surrounding invading tumour islands and accompanied by fibroblasts or in groups of immune cells. However, there was also evidence of macrophages scattered within the tumour islands to varying degrees. These staining patterns were similar in both lymph node and primary tumour sites (Figure 3.5. A). Macrophage density was assessed by calculating the percentage of CD68 positive cells within six ROIs placed in the stroma alongside the tumour invasive edge (for details on quantification method see Figure 2.1.). This location was picked due to the potential importance of these macrophages in inducing invasion and because the majority of macrophages are found here. There was no significant difference in the mean percentage of positive cells when comparing the ECS- and ECS+ groups in either the lymph nodes or corresponding primary tumours. However, when the results were separated based on primary tumour site a significant increase in macrophage density was observed in the tongue ECS+ group compared the tongue ECS- group whereas conversely the floor of mouth ECS+ group showed a lower density compared to the floor of mouth ECS- group. This was significant in both cases for the primary tumour specimens whereas for lymph nodes only the tongue data were significant ($p < 0.05$, Figure 3.5. B&C). Reflecting this converse trend the paired specimens correlated significantly with each other ($R^2 = 0.305$, $p < 0.001$).

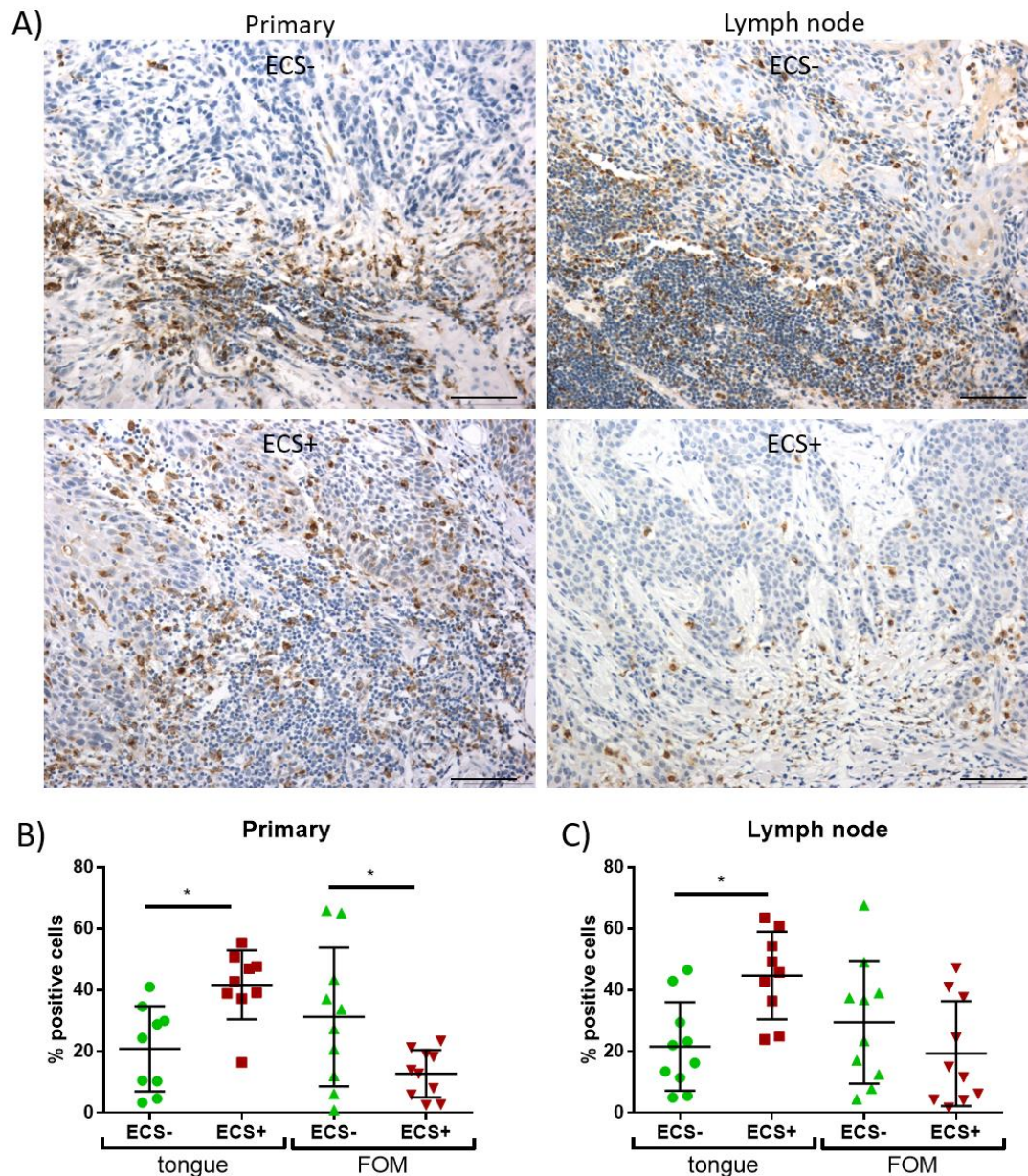


Figure 3.5. Immunohistochemical expression of the pan macrophage marker CD68 in ECS+ and ECS- matched primary and lymph node tissue specimens. (A) Representative photomicrographs of CD68 immunohistochemical staining in ECS+ and ECS- primary and lymph node tumour specimens. x 20 magnification, scale bars 100 μ m. **(B)** Quantification data from matched primary and lymph node tumours. Data points represent mean percentage positive cells from six representative ROIs per sample taken from stroma adjacent to the tumour invasive edge. Primary tumour: ECS- n=19, ECS+ n=19; lymph node: ECS- n=20, ECS+ n=20. Graphs show overall mean \pm SD, analysed by one-way ANOVA, * p <0.05.

3.2.5. Expression of epithelial-mesenchymal transition (EMT) markers in ECS

The ability to migrate and invade is central to ECS and it is well known that EMT is an important process by which cells can gain this ability (Krisanaprakornkit and Iamroon, 2012). The first crucial step in this process is the down-regulation of the cell-cell adhesion molecule E-cadherin due to the action of transcriptional repressors such as slug (SNAI2), snail (SNAI1), TWIST1 and ZEB1 (Krisanaprakornkit and Iamroon, 2012). Decreased expression of E-cadherin and increase in the mesenchymal markers N-cadherin and vimentin in primary OSCC has been linked to increased metastasis (Nijkamp *et al.*, 2011; Ding *et al.*, 2014). Additionally, expression of vimentin at the invasive edge of ECS+ lymph node tumours has been linked to particularly poor survival and increased distant metastasis rate (Lee *et al.*, 2014). However, expression of EMT markers, specifically the EMT-inducing transcription factors, in ECS+ and ECS- tumours has not been compared.

Firstly, expression of the snail family of transcription factors was assessed in the patient cohort using an antibody reactive with both snail (SNAI1) and slug (SNAI2). Nuclear staining was observed in both tumour and stromal cells (Figure 3.6.) with some cytoplasmic background staining observed in tumour cells. The percentage positive cells in six ROIs (three within the tumour area, three within the tumour-associated stroma) were quantified for each sample (for details on quantification method see Figure 2.1.). Specimens without a tumour-associated stroma (four of the ECS- lymph node specimens) were included in the tumour analysis only. Quantification of staining showed a significant decrease in percentage positive cell number in ECS+ lymph nodes and the matched primary tumour group. This was the case for both tumour and stroma ($p < 0.01$, Figure 3.6. A&B). However, there was a large range in percentage positive cell numbers, particularly in the ECS+ cases (primary tumour: ECS- 40-98% vs. ECS+ 15-97%; lymph node tumour: ECS- 64-98% vs. ECS+ 35-98%; primary stroma: ECS- 29-90% vs. ECS+ 5-73%; lymph node stroma: ECS- 44-89% vs. ECS+ 5-87%). Percentage positivity did not correlate between the matched primary and lymph node tumour cells in samples but stromal percentage positivity in the primary tumour did show a weak but significant positive correlation with α SMA primary tumour percentage positivity ($R^2 = 0.174$, $p < 0.05$).

Peptide blocking control experiments confirmed that when pre-incubated with the peptide by which the antibody was raised, no staining was observed (see Appendix A).

Nuclear staining of TWIST1 and ZEB1 was also observed in both tumour and stromal cells (Figure 3.7. A, Figure 3.8. A). The majority of positive cells were stromal and had elongated nuclei suggestive of fibroblasts but areas of positive tumour cell staining were also observed. Using the same method (mean percentage positively stained cells) expression of each marker was quantified from three ROIs within the tumour and three in the tumour stroma per specimen (for details on quantification method see Figure 2.1.). Specimens without a tumour-associated stroma (four of the ECS- lymph node specimens) were included in the tumour analysis only. No significant difference in TWIST1 percentage positivity was observed between the groups within the tumour or stroma (Figure 3.7. B&C). However, percentage positive cell numbers did significantly correlate between the matched primary and lymph node pairs in tumour ($R^2 = 0.455$, $p < 0.0001$) and stromal sites ($R^2 = 0.321$, $p < 0.001$). Quantification of ZEB1 percentage positivity also revealed no significant differences between ECS+ and ECS- groups at either site (Figure 3.8. B&C). However, again percentage positivity had a weak but significant correlation between the primary and lymph node pairs at tumour ($R^2 = 0.112$, $p < 0.05$) and stromal sites ($R^2 = 0.290$, $p < 0.001$). No correlation was observed between α SMA and TWIST1 or ZEB1 percentage positivity.

No correlation between percentage positive cell numbers for the EMT markers and blood or lymphatic vessel density were found, with the exception of ZEB1 whose percentage positivity in the tumour and stroma of lymph node specimens correlated weakly with lymph node MVD (tumour: $R^2 = 0.185$, $p < 0.01$, stroma: $R^2 = 0.109$, $p < 0.05$) and SNA11/2 percentage positivity which correlated weakly with primary tumour lymphatic vessel density in the primary tumour and stroma (tumour: $R^2 = 0.139$, $p < 0.05$, stroma: $R^2 = 0.106$, $p < 0.05$).

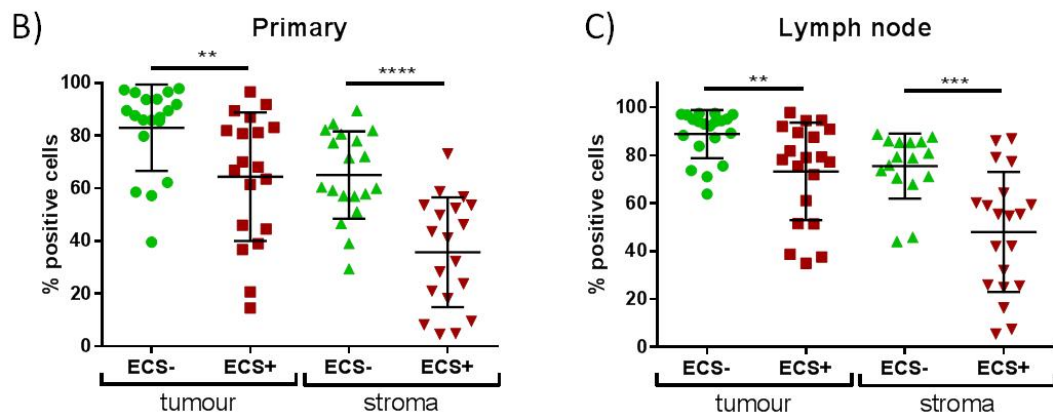
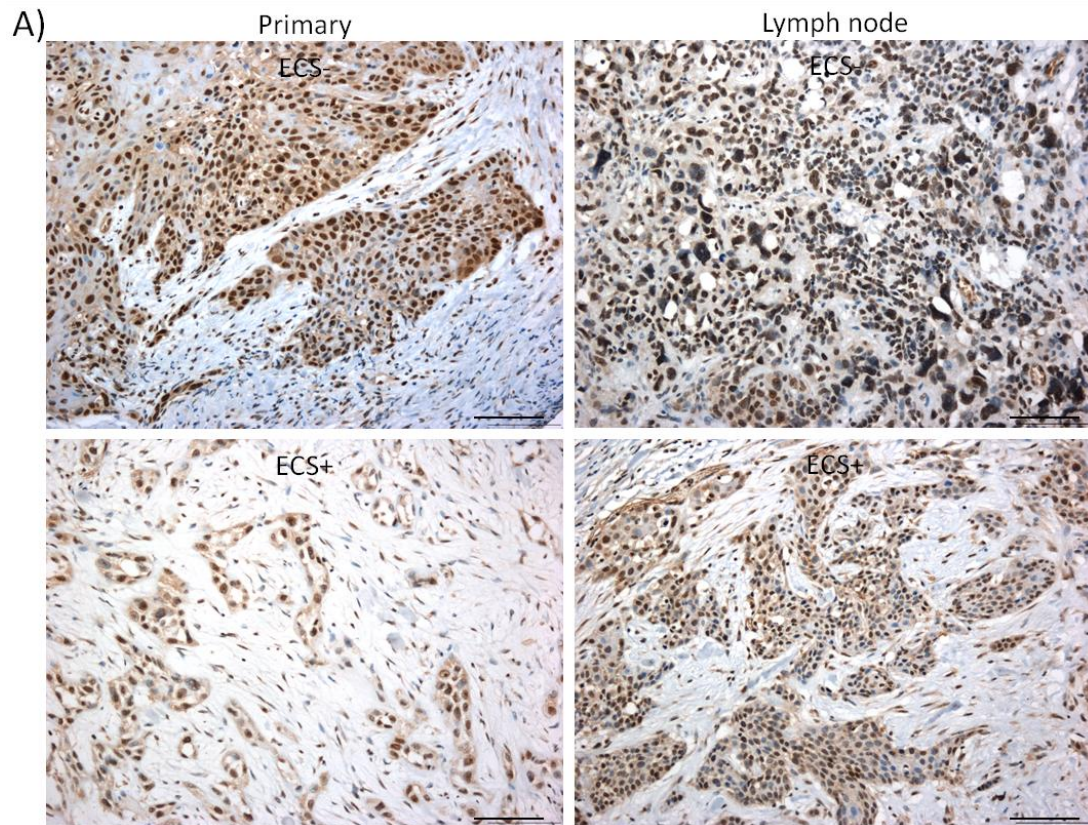


Figure 3.6. Immunohistochemical expression of slug and snail (SNAI1/2) in ECS+ and ECS- matched primary and lymph node tissue specimens. (A) Representative photomicrographs showing SNAI1/2 immunohistochemical staining in ECS+ and ECS- primary and lymph node tumour specimens. x 20 magnification, scale bars 100 μ m. (B) Quantification data from matched primary and lymph node tumours. Data points represent mean percentage positive cells from three representative ROIs, from either within the tumour or the surrounding stroma. Primary tumour: ECS- n=19, ECS+ n=19; lymph node: ECS- n=20, ECS+ n=20. Graphs show overall mean \pm SD, analysed by student's t-test between tumour or stroma pairs, **p<0.01, ***p<0.001, ****p<0.0001

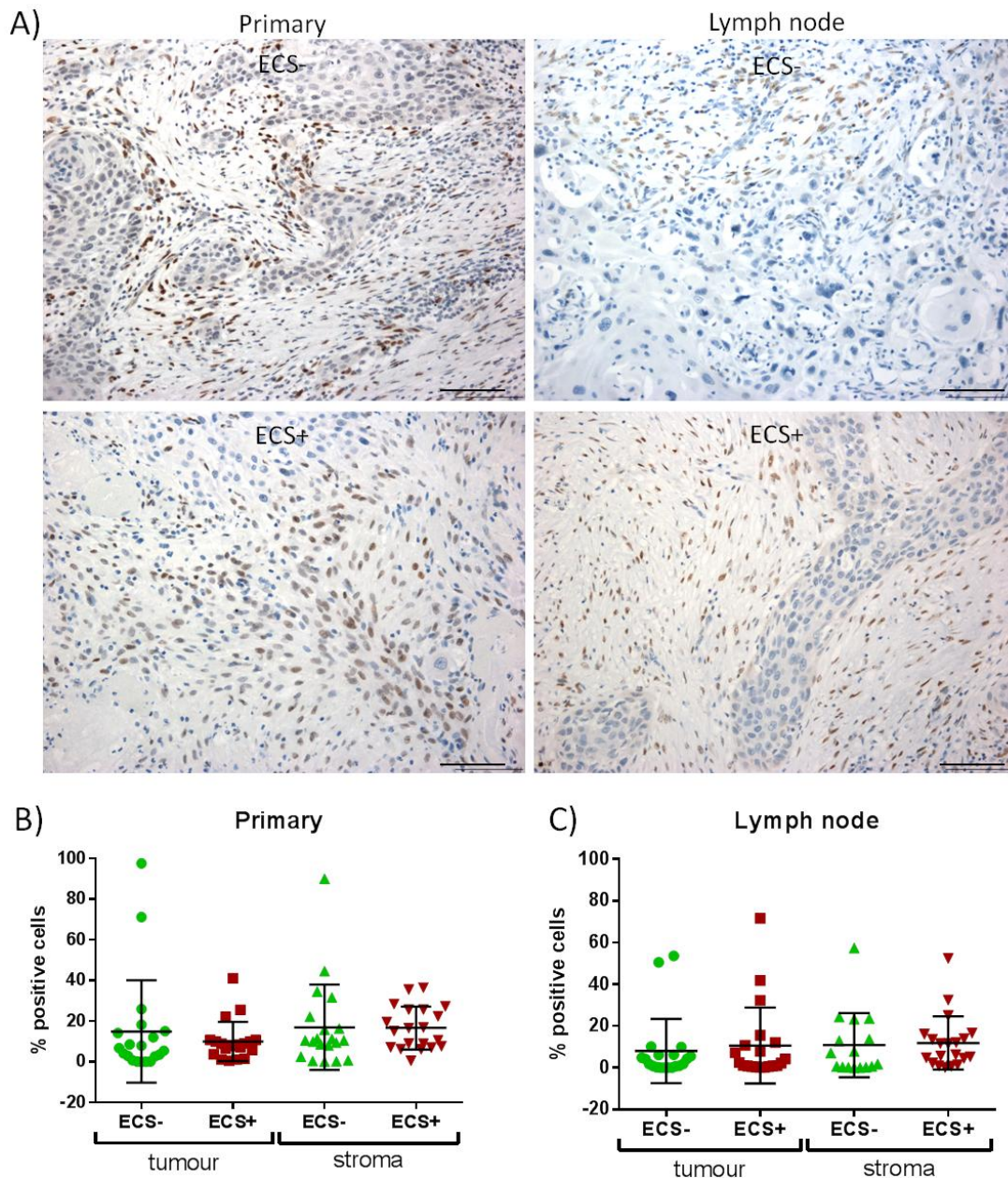


Figure 3.7. Immunohistochemical expression of TWIST1 in ECS+ and ECS- matched primary and lymph node tissue specimens. (A) Representative photomicrographs showing TWIST1 immunohistochemical staining in ECS+ and ECS- primary and lymph node tumour specimens. x 20 magnification, scale bars 100 μ m. (B) Quantification data from matched primary and lymph node tumours. Data points represent mean percentage positive cells from three representative ROIs, from either within the tumour or the surrounding stroma. Primary tumour: ECS- n=20, ECS+ n=20; lymph node: ECS- n=20, ECS+ n=20. Graphs show overall mean \pm SD, analysed by student's t-test between tumour or stroma pairs.

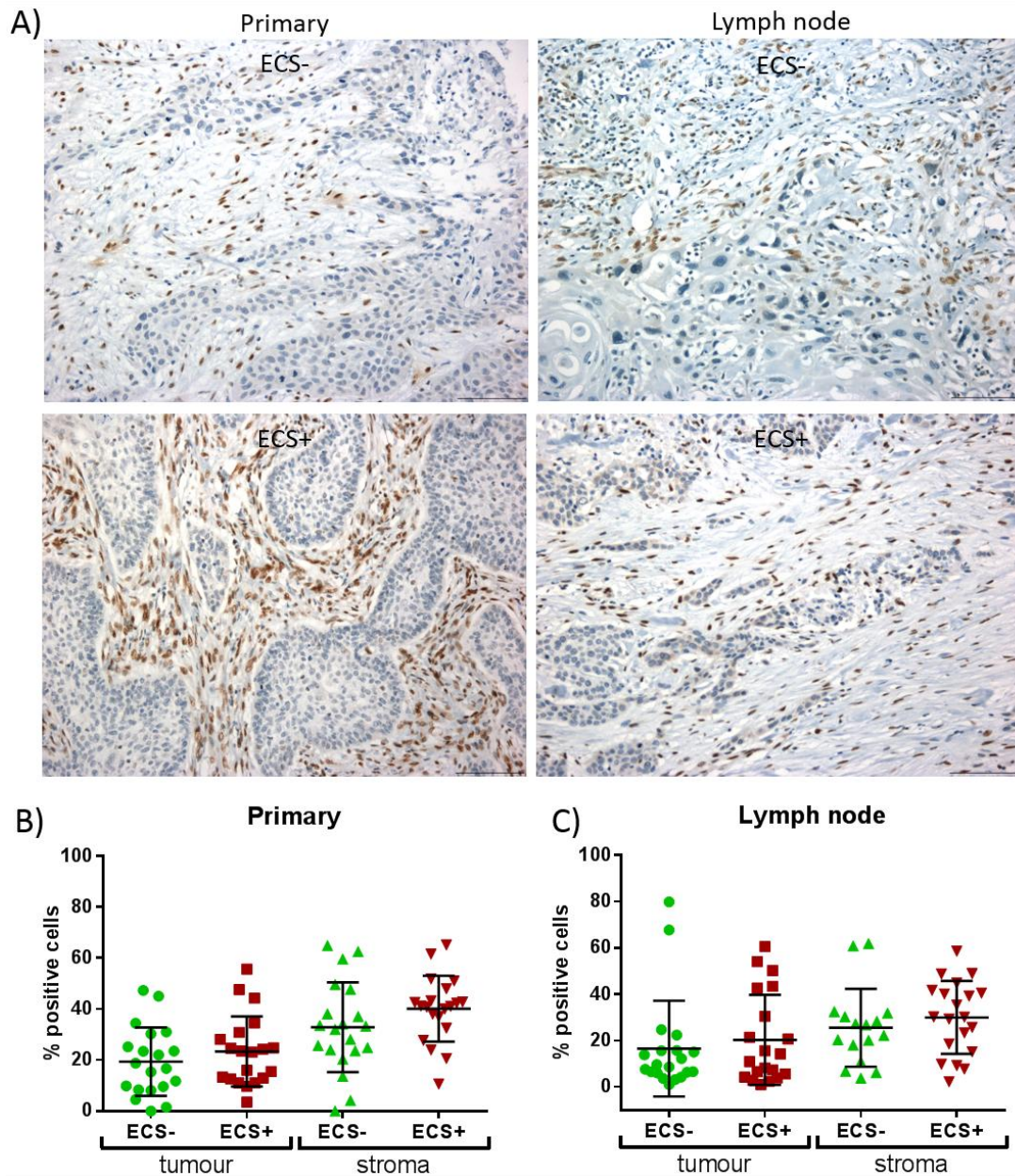


Figure 3.8. Immunohistochemical expression of ZEB1 in ECS+ and ECS- matched primary and lymph node tissue specimens. (A) Representative photomicrographs showing ZEB1 immunohistochemical staining in ECS+ and ECS- primary and lymph node tumour specimens. x 20 magnification, scale bars 100 μ m. **(B)** Quantification data from matched primary and lymph node tumours. Data points represent mean percentage positive cells from three representative ROIs, from either within the tumour or the surrounding stroma. Primary tumour: ECS- n=20, ECS+ n=20; lymph node: ECS- n=20, ECS+ n=20. Graphs show overall mean \pm SD, analysed by student's t-test between tumour or stroma pairs.

3.3. Summary

This chapter describes the results of an immunohistochemical study of metastatic OSCC lymph node tumours, with and without ECS, and their matched primary tumours. Stromal, vascular, immunological and EMT related markers were investigated. A summary of the results for each marker can be found in Table 3.2. A significant increase in α SMA positive stroma in both primary and lymph node tumours was observed but collagen I coverage did not differ between the groups. Additionally, a significant increase in vascular density in ECS+ lymph nodes was observed but lymphatic vessel density was not altered in ECS+ tumours compared to ECS-. Quantification of macrophage density revealed contrasting trends in percentage positivity between tongue and floor of the mouth specimens, with an increase seen in the tongue ECS+ group but a decrease in the floor of mouth ECS+ group when comparing to the corresponding ECS- group. Antibodies for the snail family of EMT inducing transcription factors showed a decrease in percentage positivity in ECS+ tumour and stromal areas. However, no difference in TWIST1 or ZEB1 markers was observed.

Both macrophage density and percentage positivity of the majority of EMT markers correlated between the matched primary tumour and lymph node pairs. In addition, EMT marker percentage positivity correlated with α SMA percentage positivity in some cases.

Table 3.2. Summary of IHC results comparing ECS+ and ECS- matched tumours.

	Increased or decreased in ECS?	
	Primary tumour	Lymph node
α -smooth muscle actin (α SMA)	↑ Significantly increased (p<0.01)	↑ Significantly increased (p<0.05)
Collagen I	NSD	NSD
Blood vessel density (CD34)	NSD	↑ Significantly increased (p<0.05)
Lymphatic vessel density (D2-40)	NSD	NSD
Macrophages (CD68)	NSD (↑ in tongue site group, ↓ in floor of mouth group, both significant: p<0.05)	NSD (↑ in tongue site group, significant: p<0.05)
Slug and snail (SNAI1/2)	↓ Decreased (in tumour and stroma, both significant: p<0.01)	↓ Decreased (in tumour and stroma, both significant: p<0.01)
TWIST1	NSD	NSD
ZEB1	NSD	NSD

Key: NSD (no significant difference)

Chapter 4: Investigating OCCL-fibroblast crosstalk using an *in vitro* co-culture system

4.1. Introduction, hypothesis and aims

The presence and importance of cancer-associated fibroblasts (CAF) in cancer development and progression is now well established. Previous work has shown that both myofibroblasts and senescent fibroblasts are present in CAF populations in OSCC (Prime *et al.*, 2016) and are capable of influencing cancer cell behaviour through the secretion of a complex mix of proteases, growth factors and cytokines. Interestingly, although normal lymph nodes have minimal fibroblasts, abundant CAF are present in association with metastatic deposits in lymph nodes. Furthermore, data from section 3.2.2. suggest that not only is α SMA expression elevated in ECS positive nodes but also that elevated α SMA expression in the primary tumour is predictive of ECS. Therefore, the aim of this part of the study was to generate both myofibroblasts and senescent fibroblasts to model the CAF phenotype experimentally and compare this to patient-derived CAF.

The influence of CAF is known to extend to many of the hallmarks of cancer first described by Hanahan and Weinberg (Hanahan and Weinberg, 2011) including the promotion of proliferation, evasion of apoptosis, induction of angiogenesis and promotion of invasion and metastasis (Pietras and Ostman, 2010). Given the focus of this study on metastatic tumours in lymph nodes and ECS, the effect of CAF on mechanisms associated with migration and invasion of oral cancer cells derived from both primary and metastatic lymph node tumours was investigated. Of particular interest was the ability of CAF to induce epithelial-mesenchymal transition (EMT), due to the importance of this process in the attainment of a migratory ability in cancer cells.

The hypothesis behind this part of the study was that exposure of cancer cell lines to experimentally and patient-derived CAF conditioned media results in functional and gene expression changes suggestive of a more migratory and invasive phenotype. More specifically, it was hypothesised that CAF are capable of increasing the migratory capacity of metastatic cancer cells and that this is, in part, through the induction of EMT. It was also hypothesised that oral cancer cells from

primary and lymph node tumours can promote the activation and pro-tumour activities of normal oral fibroblasts.

Specific Aims:

1. To generate CAF-like phenotypes in primary normal oral fibroblasts (NOF) by inducing myofibroblast differentiation and senescence, characterise these phenotypes and compare them to patient-derived CAF.
2. To investigate the ability of experimentally-derived myofibroblast and senescent fibroblast conditioned media to influence EMT expression in a panel of primary tumour and lymph node metastases-derived oral cancer cell lines (OCCL).
3. To assess the migration ability of the OCCL panel using experimentally-derived myofibroblast and senescent fibroblast conditioned media as a chemoattractant.
4. To compare the EMT expression and migration data obtained using experimentally-derived CAF to experiments using patient-derived CAF.
5. To assess the effect of OCCL conditioned media on the expression of differentiation markers and inflammatory cytokines by NOF.

4.2. Results

4.2.1. Generation and characterisation of myofibroblasts, senescent fibroblasts and CAF

Myofibroblasts and senescent fibroblasts were generated from normal oral fibroblasts (NOF) derived from healthy mucosa (ethics ref: 09/H1308/66) by exposing them to factors present in the tumour microenvironment that are known to induce differentiation to a CAF-like state.

Incubation of NOF with transforming growth factor- β 1 (TGF- β 1) causes them to differentiate into a myofibroblast-like state. This has been previously characterised by our lab (Elmusrati *et al.*, 2017; Melling *et al.*, 2018). Following

incubation with 5 ng/ml human recombinant TGF- β 1 for 72 h, fibroblasts appeared more spindle shaped (Figure 4.1 A). Alpha-smooth muscle actin (α SMA) is a well-defined marker of myofibroblast activation and TGF- β 1 treated cells expressed significantly higher levels of α SMA at both the mRNA ($p < 0.05$, Figure 4.1 B) and protein levels ($p < 0.001$, Figure 4.1 C).

Senescent fibroblast presence in the cancer stroma has been observed in OSCC, particularly in genetically unstable tumours where CAF senescence has been attributed to reactive oxygen species (ROS) production by cancer cells (Hassona *et al.*, 2013). ROS-induced DNA damage causes cells to undergo irreversible growth arrest and obtain a senescence-associated secretory phenotype (SASP).

To model the effect of ROS on fibroblasts, NOF were treated with hydrogen peroxide (H_2O_2) using a treatment protocol previously optimised within our lab (Kabir, 2015; Kabir *et al.*, 2016). After a 2 h treatment with 500 μ M H_2O_2 followed by 10 days of continued culturing, cells appear enlarged, granular, and displayed some multi-nucleation (Figure 4.2. A). Senescence levels were quantified using a senescence associated- β -galactosidase (SA- β -gal) assay in which senescent cells develop a blue perinuclear precipitate due to augmented expression of lysosomal β -galactosidase at pH 6.0 (Dimri *et al.*, 1995). H_2O_2 - treated cells had significantly higher levels of SA- β -gal positive cells compared to untreated control NOF ($p < 0.0001$, Figure 4.2 A&B) with an average of 76% positive cells (compared to 13% in control NOF) over seven independent experiments. In addition, the expression of the cell cycle arrest markers p16^{INK4a} (p16) and p21/cip-1 (p21) was elevated in H_2O_2 -treated cells compared to control fibroblasts although this varied between experiments and did not reach significance following three biological repeats ($p = 0.24$ (p16); $p = 0.14$ (p21); Figure 4.2. C&D). More detailed characterisation by our lab has demonstrated that H_2O_2 -induced senescent fibroblasts show reduced proliferation capacity (in the absence of increased apoptosis or necrosis levels) compared to non-senescent controls with formation of heterochromatin in nuclei shown by immunofluorescence DAPI staining (Kabir, 2015).

In addition to inducing senescence directly, replicative senescent fibroblasts were also generated through prolonged culturing of NOF. The normal culturing

range for NOF is a maximum of 10 passages but, for this aim, passage numbers in excess of 30 were attained. As for H₂O₂-treated NOF, replicative senescent fibroblasts appeared enlarged, granular and displayed multi-nucleation (Figure 4.3 A). Results from SA-β-gal assay for senescence showed significant elevation of SA-β-gal positive cells compared to NOF at passage number below 10 ($p < 0.001$, Figure 4.3 A&B) with average senescent levels of 84% compared to 10% in control NOF over three independent experiments. In addition, the expression of the cell cycle arrest markers p16 and p21 were elevated in replicative senescent fibroblasts compared to control fibroblasts, with both reaching significance across three independent samples ($p < 0.05$, Figure 4.3. C&D).

Primary patient-derived CAF were also used to generate conditioned media and to provide a comparison by which to judge how well the experimentally derived CAF represent the true CAF population. Morphologically CAF appear similar to NOF with elongated cell processes (Figure 4.4 A). CAF displayed a fold change in αSMA protein and mRNA expression of 1.3 ± 0.5 and 1.8 ± 0.5 respectively, which did not reach significance over three independent analyses (Figure 4.4 B&C). Senescence levels were also assessed using SA-β-gal assay which showed that CAF had significant more SA-β-gal positive cells than NOF across four independent tests ($p < 0.05$, Figure 4.5 A&B). However, senescence levels in the third test were considerably higher than the remaining tests, which may have affected the overall result. To validate the senescence profile of CAF compared to NOF, the mRNA expression of the cell cycle arrest markers p16 and p21 was validated by qRT-PCR. CAF showed significantly elevated expression of p21 ($p < 0.0001$) but there was no significant change in p16 expression (Figure 4.5. C&D).

In summary, this section of work has demonstrated the generation of CAF-like cells from NOF, representing both myofibroblastic and senescent phenotypes known to be present in the CAF population. Conditioned media from these cells will be used in subsequent sections of this chapter to evaluate the influence of cellular secretions on oral cancer cell EMT marker expression and migratory behaviour.

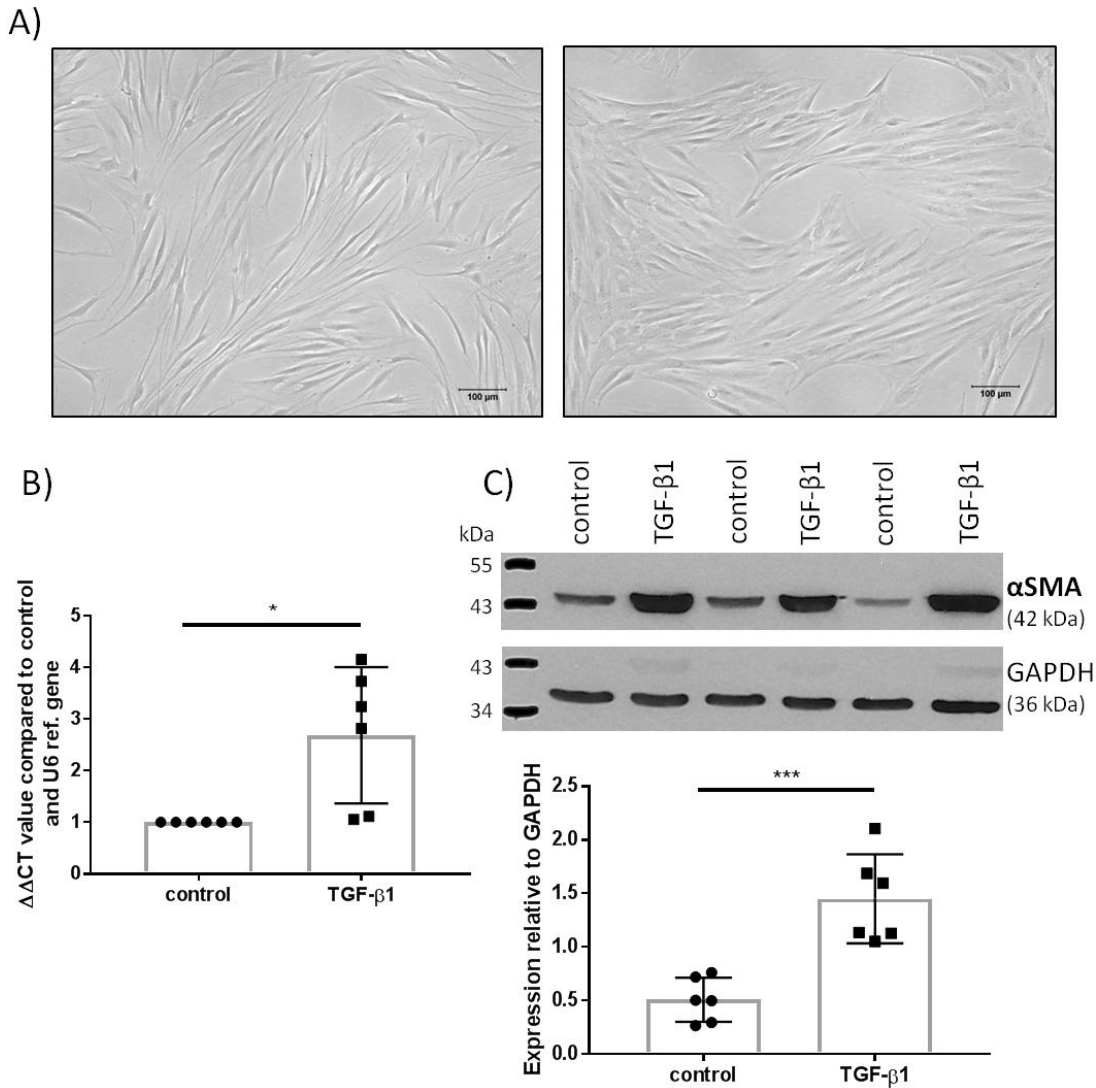


Figure 4.1. TGF-β1 causes increased αSMA expression and altered morphology in oral fibroblasts. αSMA protein levels increase in normal oral fibroblasts (NOF) as a result of TGF-β1 treatment. (A) Representative images of NOF treated with 5 ng/ml TGF-β1 in DMEM for 72 h or DMEM only (control). x 10 magnification, scale bars 200 μm. (B) qRT-PCR and (C) representative western blots (developed by x-ray) for αSMA show significantly increased αSMA mRNA and protein expression levels in TGF-β1 treated NOF compared to untreated controls. qRT-PCR results displayed as ΔΔCT values comparing to control and U6 as a reference gene. Western blot relative band densitometry compared to GAPDH loading control and analysed using ImageJ. Graphs display mean ± SD from six separate experiments, analysed using student's t-test, *p<0.05, ***p<0.001.

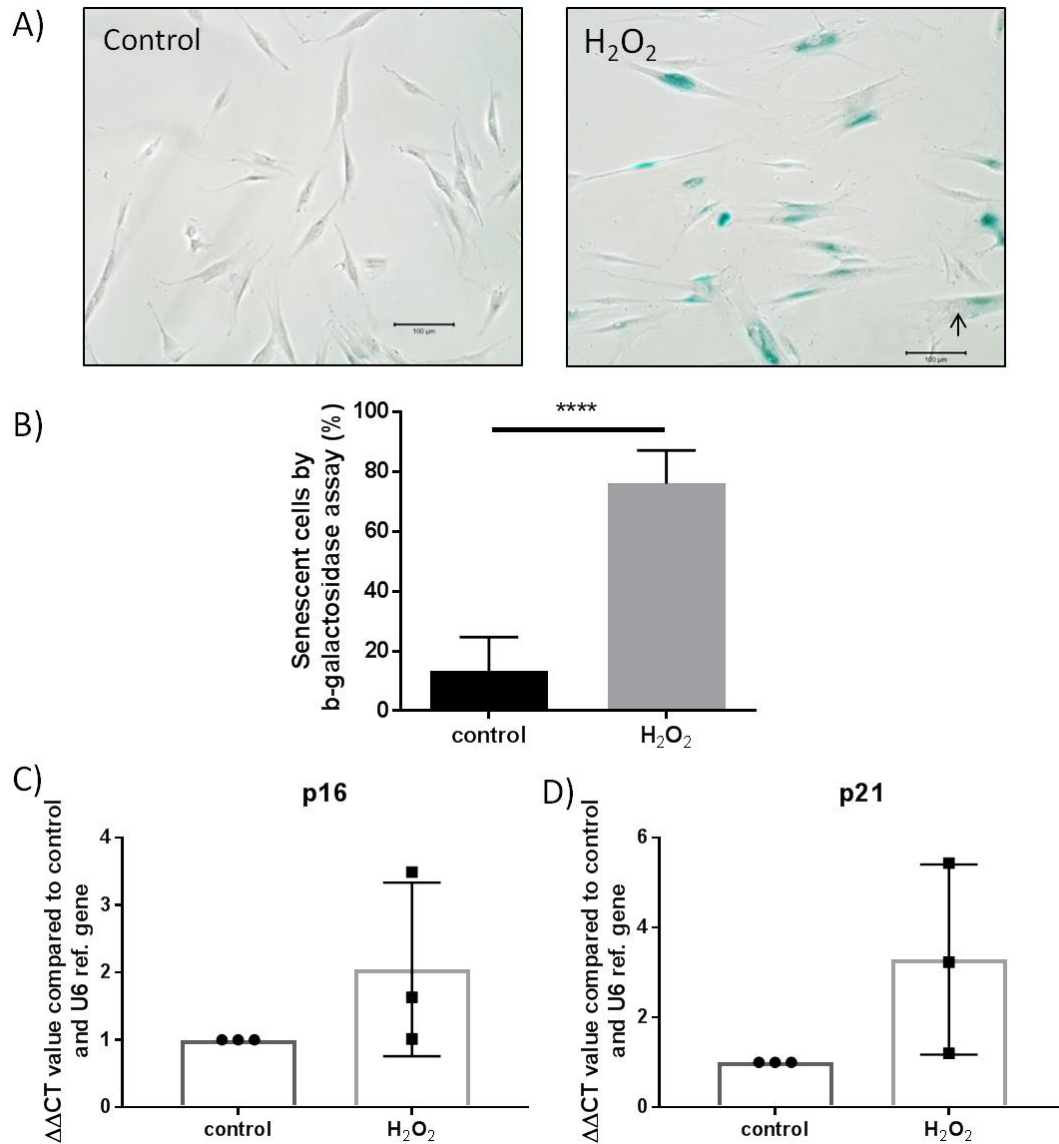


Figure 4.2. Generation of senescent fibroblasts by H₂O₂ treatment. (A) Representative images of untreated normal oral fibroblast controls and senescent fibroblasts (induced using 500 μ M H₂O₂ for 2 h followed by 10 days culture) from senescence-associated β -galactosidase assay (SA- β -gal, Abcam) with blue indicating a senescent cell and arrows indicating multinucleation. x 10 magnification, scale bar 100 μ m. (B) Quantification of percentage SA- β -gal positive cells. Mean of seven separate experiments, each calculated from eight images at x 10 magnification per condition. (C,D) mRNA expression of p16 and p21 cell cycle arrest markers in control and H₂O₂-treated fibroblasts as determined by qRT-PCR. Results from three independent experiments and displayed as $\Delta\Delta$ CT values comparing to control and B2M as a reference gene. Graphs display mean \pm SD, analysed by student's t-test, ****p<0.0001

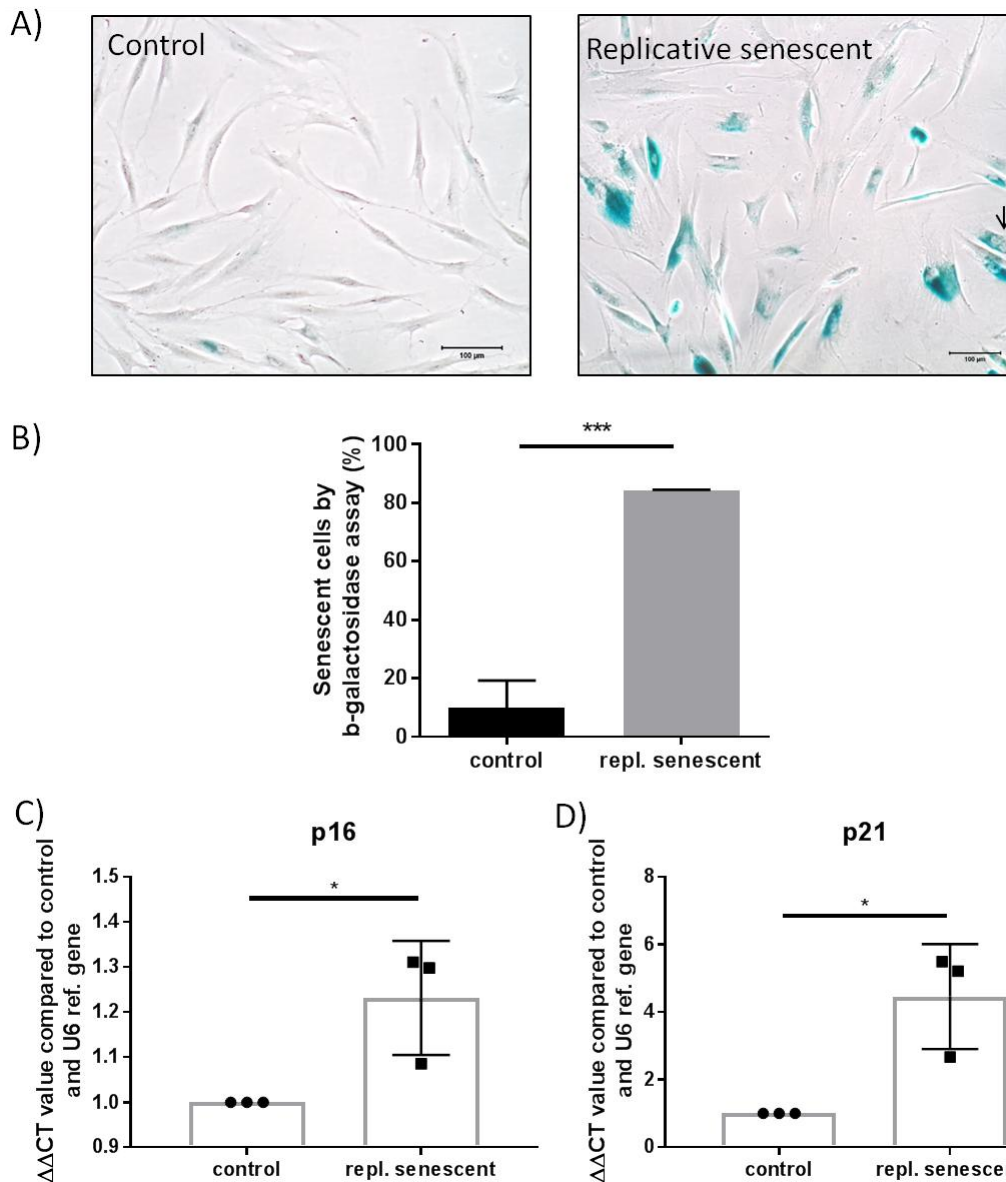


Figure 4.3. Characterisation of replicative senescent fibroblasts. (A) Representative images of normal oral fibroblast controls (passage <10) and replicative senescent fibroblasts from senescence-associated β -galactosidase assay (SA- β -gal, Abcam) with blue indicating a senescent cell and arrows indicating multinucleation. x 10 magnification, scale bars 100 μ m. (B) Quantification of percentage SA- β -gal positive cells. Average of three independent experiments, each calculated from eight images at x 10 magnification. (C,D) mRNA expression of p16 and p21 cell cycle arrest markers in control and replicative senescent fibroblasts as determined by qRT-PCR. Results from three independent experiments and displayed as $\Delta\Delta$ CT values comparing to control and B2M as a reference gene. Graphs display mean \pm SD, analysed by student's t-test, * p <0.05, *** p <0.001.

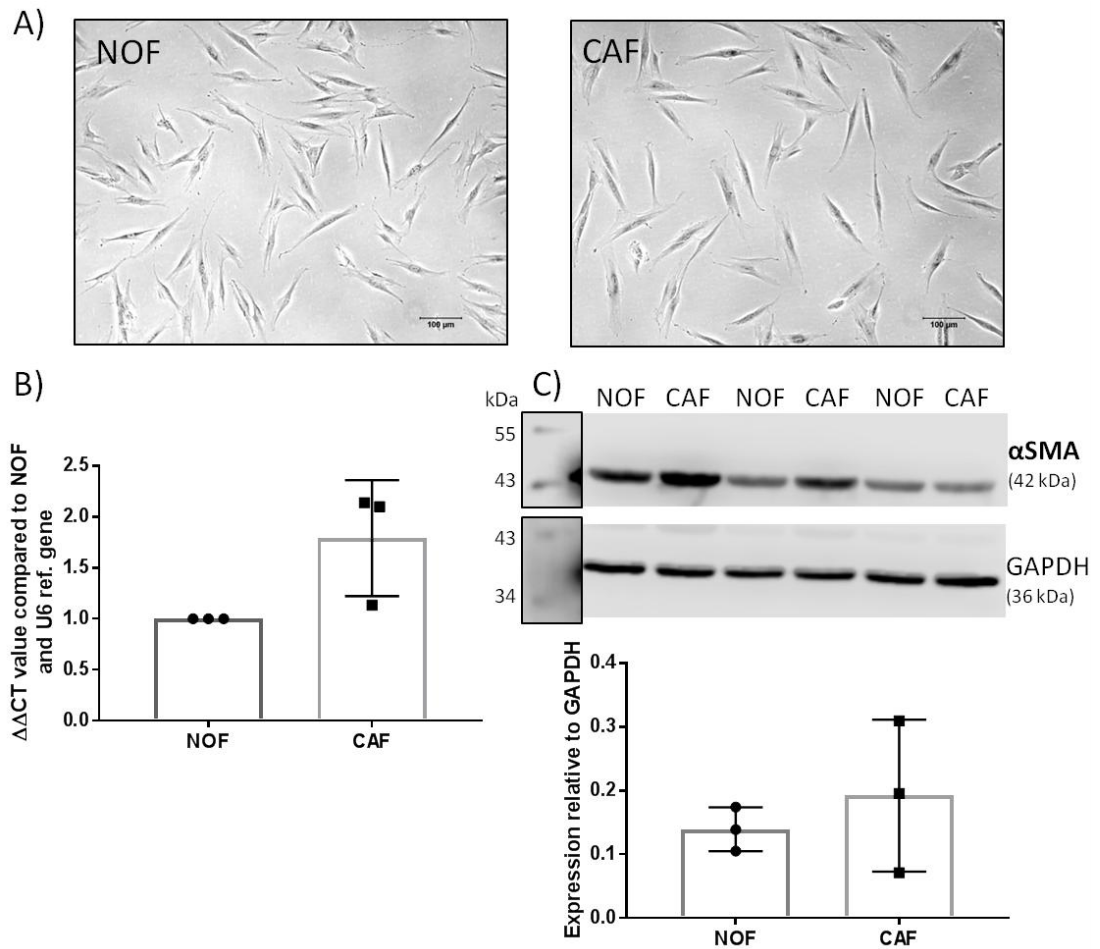


Figure 4.4. Expression of myofibroblast markers in normal oral fibroblasts (NOF) and cancer-associated fibroblasts (CAF). Fibroblasts isolated from healthy and cancer patient samples were analysed for myofibroblast markers. (A) Representative images of NOF and CAF cells. x 10 magnification, scale bars 100 μm. (B) αSMA levels assessed by qRT-PCR displayed as $\Delta\Delta\text{CT}$ values comparing to control and B2M as a reference gene. (C) Western blot and relative band densitometry for αSMA protein levels. GAPDH was included as a loading control (developed and analysed using LI-COR scanner and software, inserted ladder images shown at high contrast to allow visualisation). Graphs display mean \pm SD from three separate experiments, analysed by student's t-test.

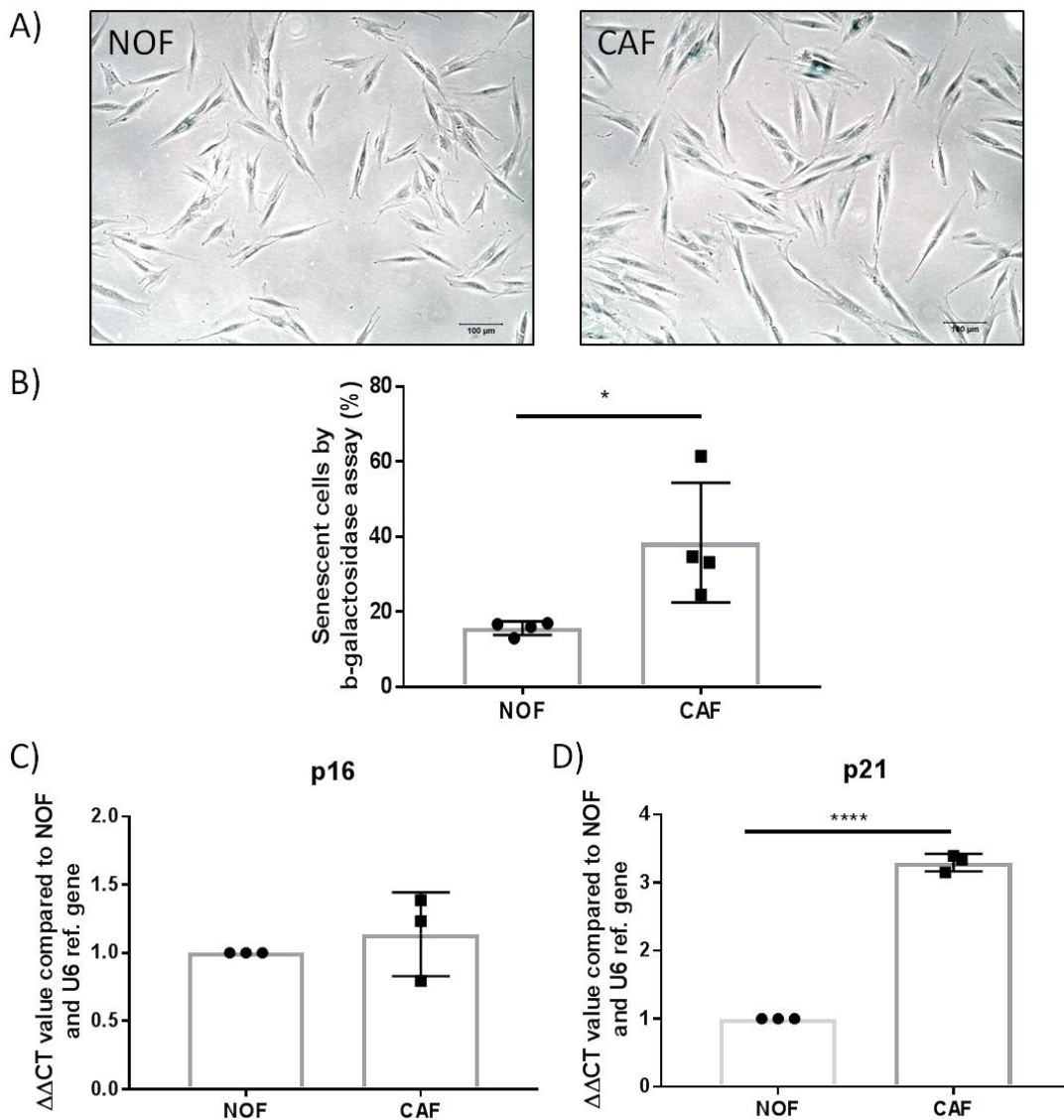


Figure 4.5. Expression of senescent markers in normal oral fibroblasts (NOF) and cancer-associated fibroblasts (CAF). Fibroblasts isolated from healthy and cancer patient samples were analysed for senescence markers. (A) Representative images from senescence associated-β-galactosidase assay (SA-β-gal) for cellular senescence (Abcam) with blue indicating a senescent cell. x 10 magnification, scale bars 100 μm. (B) Quantification of SA-β-gal assay results from four separate experiments with percentage of SA-β-gal positive cells calculated from eight images at x 10 magnification. (C) mRNA expression of p16 and p21 cell cycle arrest markers in NOF and CAF as determined by qRT-PCR. Results from three independent experiments displayed as ΔΔCT values comparing to NOF control and B2M as a reference gene. Graphs display mean ± SD, analysed by student's t-test, *p < 0.05, ****p < 0.0001.

4.2.2. Effect of myofibroblasts on EMT marker expression in OCCL

Epithelial-mesenchymal transition (EMT) is a key mechanism by which cancer cells gain the ability to migrate and invade. Although it is hypothesised that primary OSCC tumour metastasis occurs as a result of cancer cells undergoing EMT, it is unknown what happens upon their arrival at the metastatic lymph node site. The majority of metastatic OSCCs in lymph nodes appear epithelial in morphology, raising the question of whether these metastatic deposits undergo mesenchymal-epithelial transition (MET) once within the lymph node, and also whether a second cycle of EMT is required for ECS to occur considering the stromal desmoplasia seen in ECS. This section of the study aimed to determine if media from the experimentally derived CAF-like cells described in section 4.2.1. could affect EMT marker expression in oral cancer cell lines (OCCL) and if this effect differed between primary OSCC and lymph-node metastases derived cells.

A panel of OCCL were selected to represent the different stages of disease and allow comparison with previous work. The cell lines used were H357 (tongue, Stage I, well differentiated, node negative), H376 (floor of mouth, Stage III, well differentiated, node positive), BICR22 (neck node derived metastatic, primary site tongue), and TR146 (neck node derived metastatic, primary site buccal mucosa, well differentiated). Conditioned media from myofibroblasts was prepared as detailed in section 2.2.3. and incubated with OCCL for 48 h. Media conditioned by untreated NOF cultured in parallel was used as a control.

Western blots for the epithelial marker E-cadherin and mesenchymal marker vimentin revealed that both H376 and BICR22 already display a mesenchymal signature with TR146 showing weak expression of both markers (Figure 4.6.). The non-metastatic primary tumour derived cell line H357 had strong E-cadherin expression and a lack of vimentin in keeping with an epithelial phenotype and this did not appear to be altered by conditioned media treatment. Protein expression of the EMT-inducing transcription factors slug (SNAI2), snail (SNAI1) and ZEB1 was also assessed by western blot. It was planned to include TWIST1 protein expression analysis but despite optimisation experiments indicating that BICR22 and TR146 cells express TWIST1, no specific bands were observed when experimental samples

were used (see Appendix C for details). Expression of all three remaining transcription factors was evident in the majority of cell lines including those with a mesenchymal phenotype; however, the H357 non-metastatic primary tumour derived cell line lacked ZEB1 expression. An increase in slug protein expression in response to myofibroblast conditioned media treatment was seen but this was not significant over three separate experiments ($p=0.37$, Figure 4.7.).

Expression of slug, snail, TWIST1 and ZEB1 were also analysed by qRT-PCR. Expression of snail and ZEB1 in H357 cells could only just be detected (cycle numbers >35) so these markers were not used for further analysis for this cell line. Although small increases were observed for most markers, these did not reach significance in most cases with the exception of slug and ZEB1, which increased in TR146 and BICR22 cell lines, respectively, as a result of treatment with myofibroblast conditioned media ($p<0.05$, Figure 4.8.).

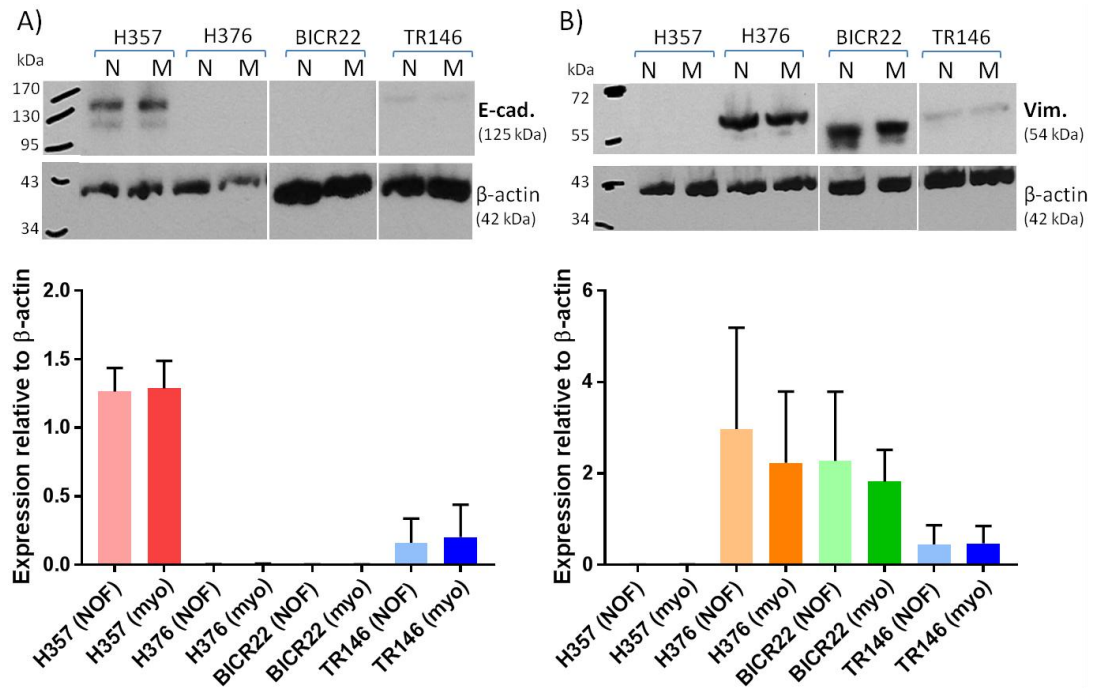


Figure 4.6. Protein levels of EMT markers in OCCL treated with myofibroblast-conditioned media. Cell lysates collected from OCCL treated with conditioned media from untreated normal oral fibroblasts (NOF, N) or myofibroblasts (myo, M) and analysed by western blot for (A) E-cadherin (E-cad.) and (B) vimentin (Vim.), (developed by x-ray). For each marker a representative blot is shown and below densitometry graphs (analysed using ImageJ) showing mean relative expression of blots from three separate experiments. β -actin was included as a loading control for each blot. Graphs display mean \pm SD, analysed by student's t-test between pairs.

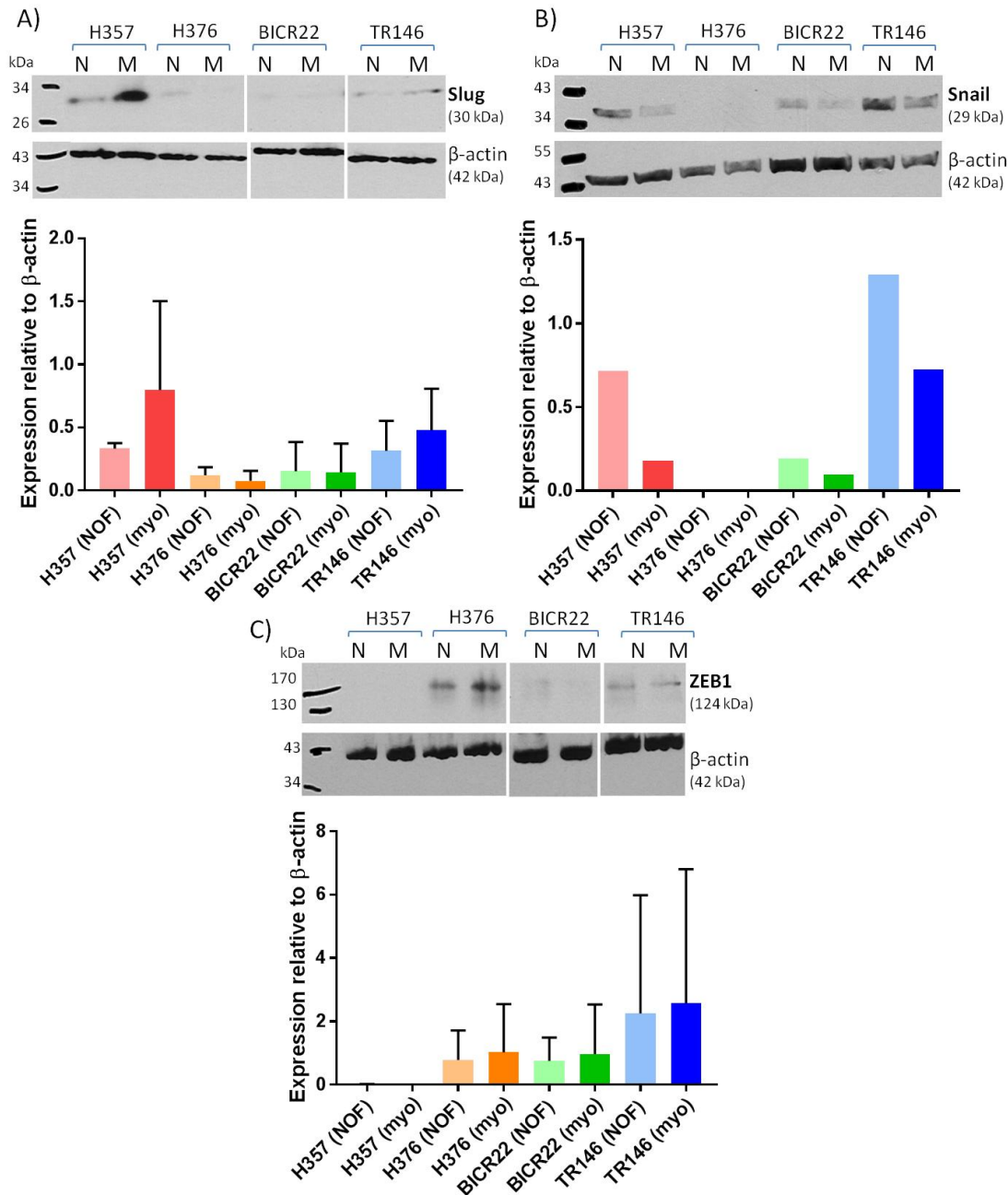


Figure 4.7. Protein levels of EMT-inducing transcription factors in OCCL treated with myfibroblast-conditioned media. Cell lysates collected from OCCL treated with conditioned media from untreated normal oral fibroblasts (NOF, N) or myfibroblasts (myo, M) and analysed by western blot for (A) slug, (B) snail and (C) ZEB1 (developed by x-ray). For each marker a representative blot is shown and below densitometry graphs (analysed using ImageJ) showing mean relative expression of blots from three separate experiments (n=1 for snail). β-actin was included as a loading control for each blot. Graphs display mean ± SD, analysed by student's t-test between pairs.

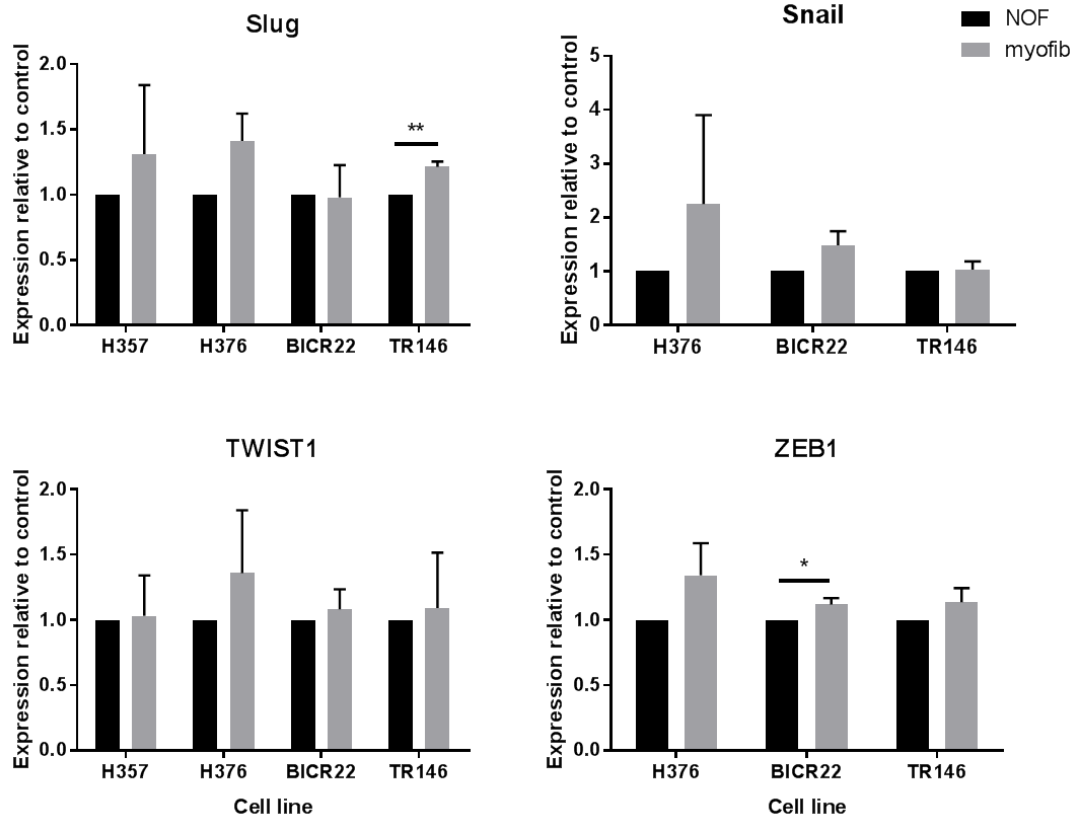


Figure 4.8. mRNA expression of EMT markers in OCCL treated with myofibroblast-conditioned media. Cell lysates collected from OCCL treated with conditioned media from untreated normal oral fibroblasts (NOF) or myofibroblasts (myofib). mRNA levels of EMT markers slug, snail, TWIST1 and ZEB1 were measured by qRT-PCR using Taqman probes. H357 produced very high Δ CT values (>35) for snail and ZEB1 so were not included in the analysis. Δ CT values plotted relative to control cells of each type and B2M reference gene. Controls normalised to 1 in each case but basal expression was not equal in each cell line. Graphs display mean \pm SD from three separate experiments, analysed by student's t-test between pairs, *p<0.05, **p<0.01.

4.2.3. Effect of senescent fibroblasts on EMT marker expression in OCCL

Senescent fibroblasts are also a key component of the tumour stroma, contributing to the large array of secreted molecules in the tumour microenvironment. The same OCCL as used in myofibroblast experiments (section 4.2.2.) were incubated with conditioned media (generated as described in section 2.2.3.) from either H₂O₂-induced or replicative senescent fibroblasts for 48 h.

Western blots for the epithelial marker E-cadherin and mesenchymal marker vimentin confirmed earlier results showing that H376, BICR22 and TR146 already express mesenchymal markers (Figure 4.9.). Despite this, EMT-inducing transcription factor protein expression was observed in all cell lines although there was variation between the different markers. H357 cells expressed higher levels of slug and snail markers and lower levels of ZEB1 as was seen for myofibroblast experiments. However, no significant increases in expression as a result of H₂O₂-induced senescent fibroblast conditioned media treatment was observed after three experiments despite a large increase in slug expression in one repeat (Figure 4.10.).

mRNA analysis of H₂O₂-induced senescent fibroblast conditioned media treated OCCL revealed small increases in expression of each of the EMT-inducing transcription factors. However, as seen previously there was a large variation between the samples. Only snail expression in H376 and ZEB1 expression in TR146 significantly increased ($p < 0.05$, Figure 4.11.). There was no obvious difference between the primary and metastatic cell lines and the significant increases seen did not match those observed in myofibroblast conditioned media experiments. As stated previously, expression of snail and ZEB1 in H357 cells could only just be detected (cycle numbers > 35) so these markers were not used for further analysis for this cell line.

OCCL incubated with conditioned media from replicative senescent fibroblasts were compared to those incubated with normal oral fibroblasts of the same origin but at passage numbers below 10. The same pattern of E-cadherin and vimentin expression was seen as observed previously (Figure 4.12.). Protein levels of EMT transcription factors were also compared and, as observed previously, H357

cells expressed higher levels of slug and snail than ZEB1. However, no significant change in any of the markers assessed was found following conditioned media treatment.

There was a large variation in the response of cell lines in terms of mRNA expression. Significant decreases in snail, slug and ZEB1 mRNA levels were observed in the TR146 cell line as a result of treatment with replicative senescent fibroblast conditioned media ($p < 0.01$, Figure 4.14.) but no other significant changes were observed.

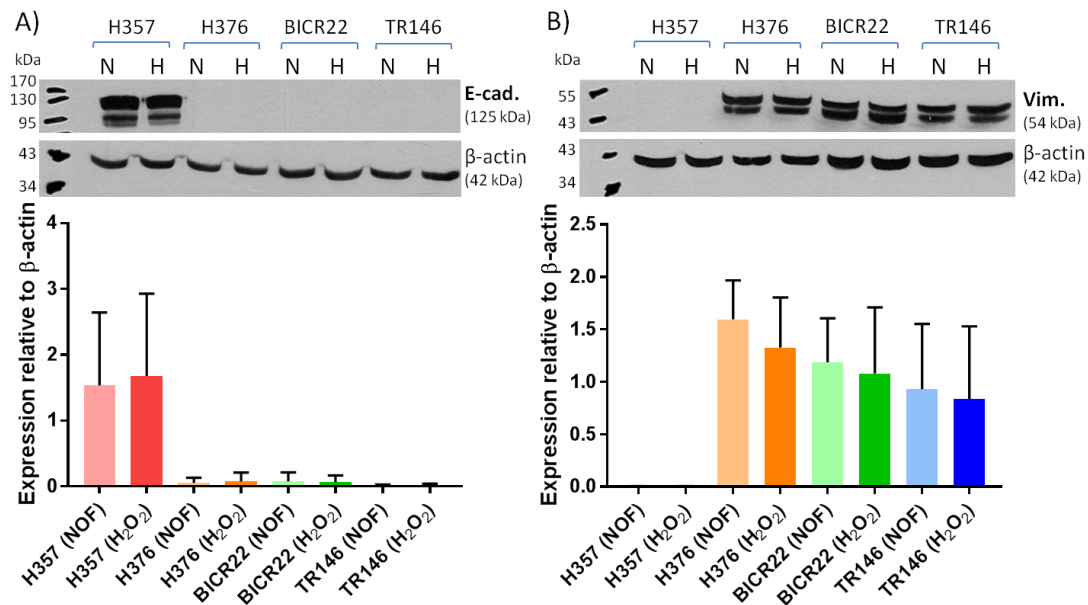


Figure 4.9. Protein levels of EMT markers in OCCL treated with H₂O₂-induced senescent fibroblast conditioned media. Cell lysates collected from OCCL treated with conditioned media from untreated normal oral fibroblasts (NOF, N) or H₂O₂-induced senescent fibroblasts (H₂O₂, H). OCCL lysates analysed by western blot for (A) E-cadherin (E-cad.) and (B) vimentin (Vim.), (developed by x-ray). For each marker a representative blot is shown and below densitometry graphs (analysed using ImageJ) showing relative expression as a mean of blots from three separate experiments. β -actin was included as a loading control for each blot. Graphs display mean \pm SD, analysed by student's t-test between pairs.

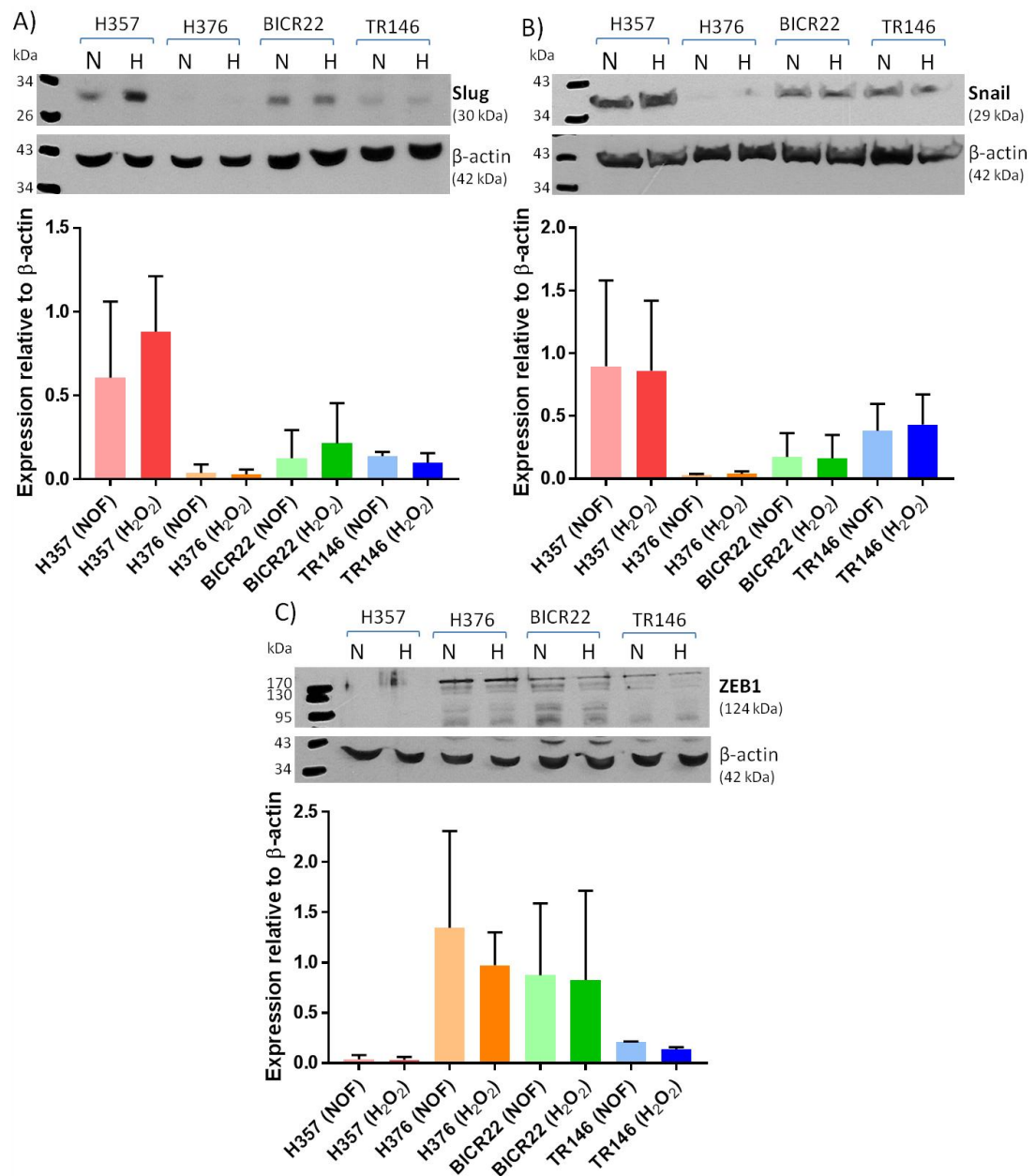


Figure 4.10. Protein levels of EMT-inducing transcription factors in OCCL treated with H₂O₂-induced senescent fibroblast conditioned media. Cell lysates collected from OCCL treated with conditioned media from untreated normal oral fibroblasts (NOF, N) or H₂O₂-induced senescent fibroblasts (H₂O₂, H). OCCL lysates analysed by western blot for (A) slug, (B) snail and (C) ZEB1 (developed by x-ray). For each marker a representative blot is shown and below densitometry graphs (analysed using ImageJ) showing relative expression as a mean of blots from three separate experiments. β -actin was included as a loading control for each blot. Graphs display mean \pm SD, analysed by student's t-test between pairs.

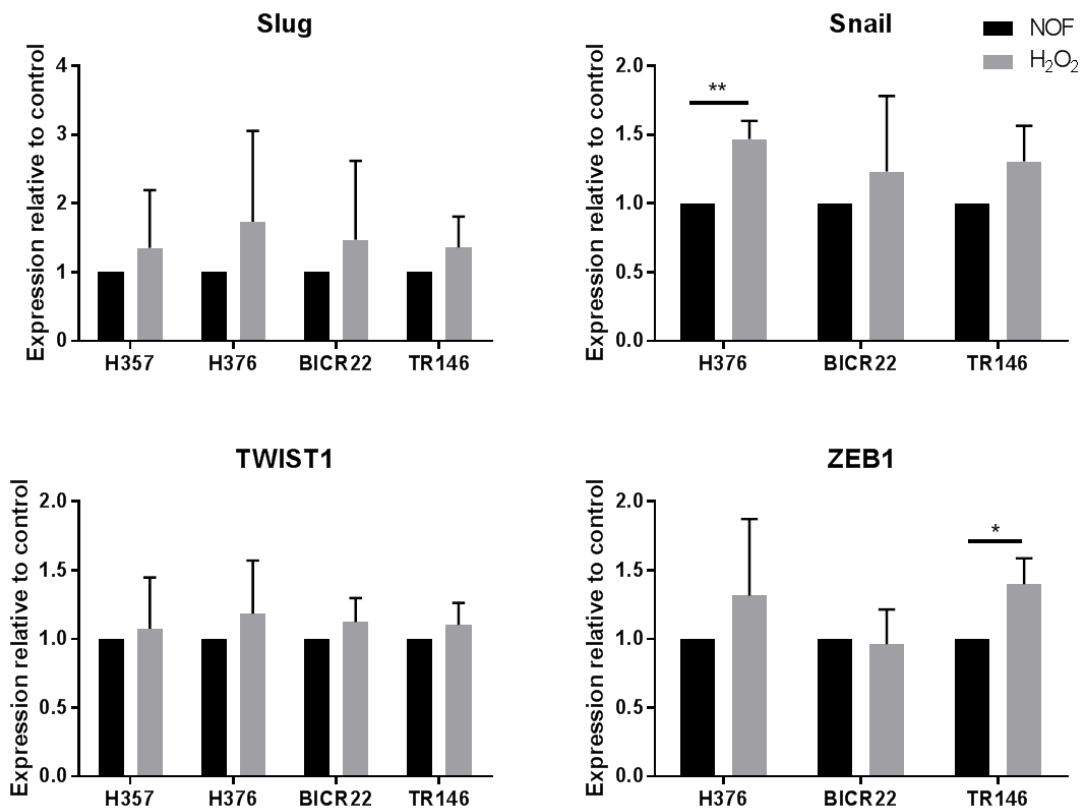


Figure 4.11. mRNA expression of EMT markers in OCCL treated with H₂O₂-induced senescent fibroblast conditioned media. Cell lysates collected from OCCL treated with conditioned media from untreated normal oral fibroblasts (NOF) or H₂O₂-induced senescent fibroblasts (H₂O₂). mRNA levels of EMT markers slug, snail, TWIST1 and ZEB1 measured by qRT-PCR using Taqman probes. H357 produced very high Δ CT values (>35) for snail and ZEB1 so were not included in the analysis. Δ CT values plotted relative to control cells of each type and B2M reference gene. Controls normalised to 1 in each case but basal expression was not equal in each cell line. Graphs display mean \pm SD from four separate experiments, analysed by student's t-test between pairs, * p <0.05, ** p <0.01.

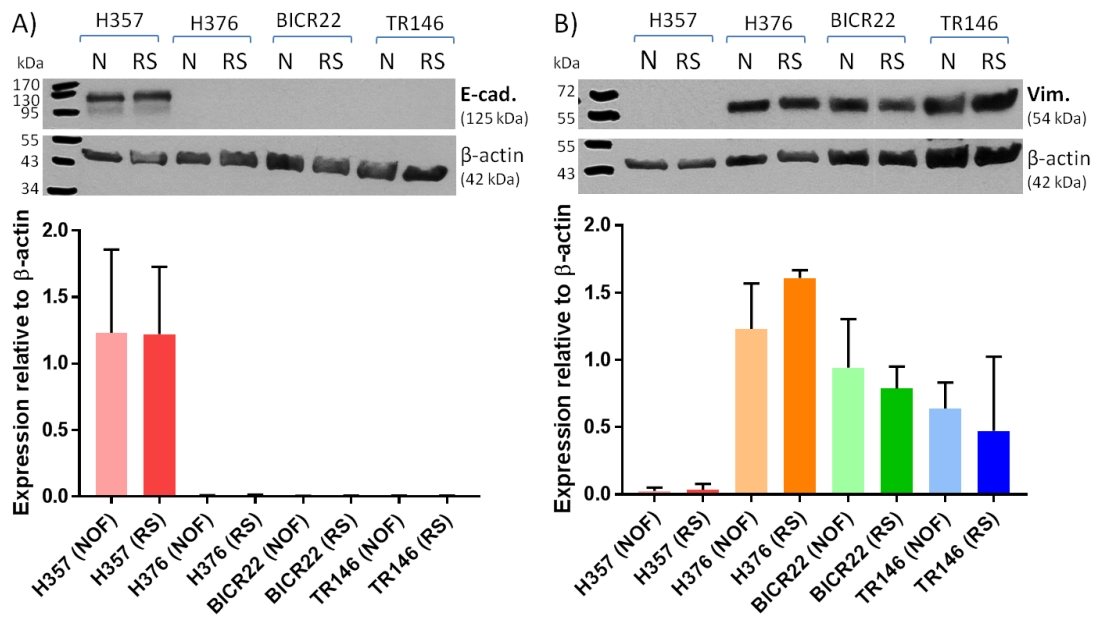


Figure 4.12. Protein levels of EMT markers in OCCL treated with replicative senescent fibroblast conditioned media. Cell lysates collected from OCCL treated with conditioned media from untreated normal oral fibroblasts (NOF, N) or replicative senescent fibroblasts (RS). OCCL lysates analysed by western blot for (A) E-cadherin (E-cad.) and (B) vimentin (Vim.), (developed by x-ray). For each marker a representative blot is shown and below densitometry graphs (analysed using ImageJ) showing relative expression as a mean of blots from three separate experiments. β -actin was included as a loading control for each blot. Graphs display mean \pm SD, analysed by student's t-test between pairs.

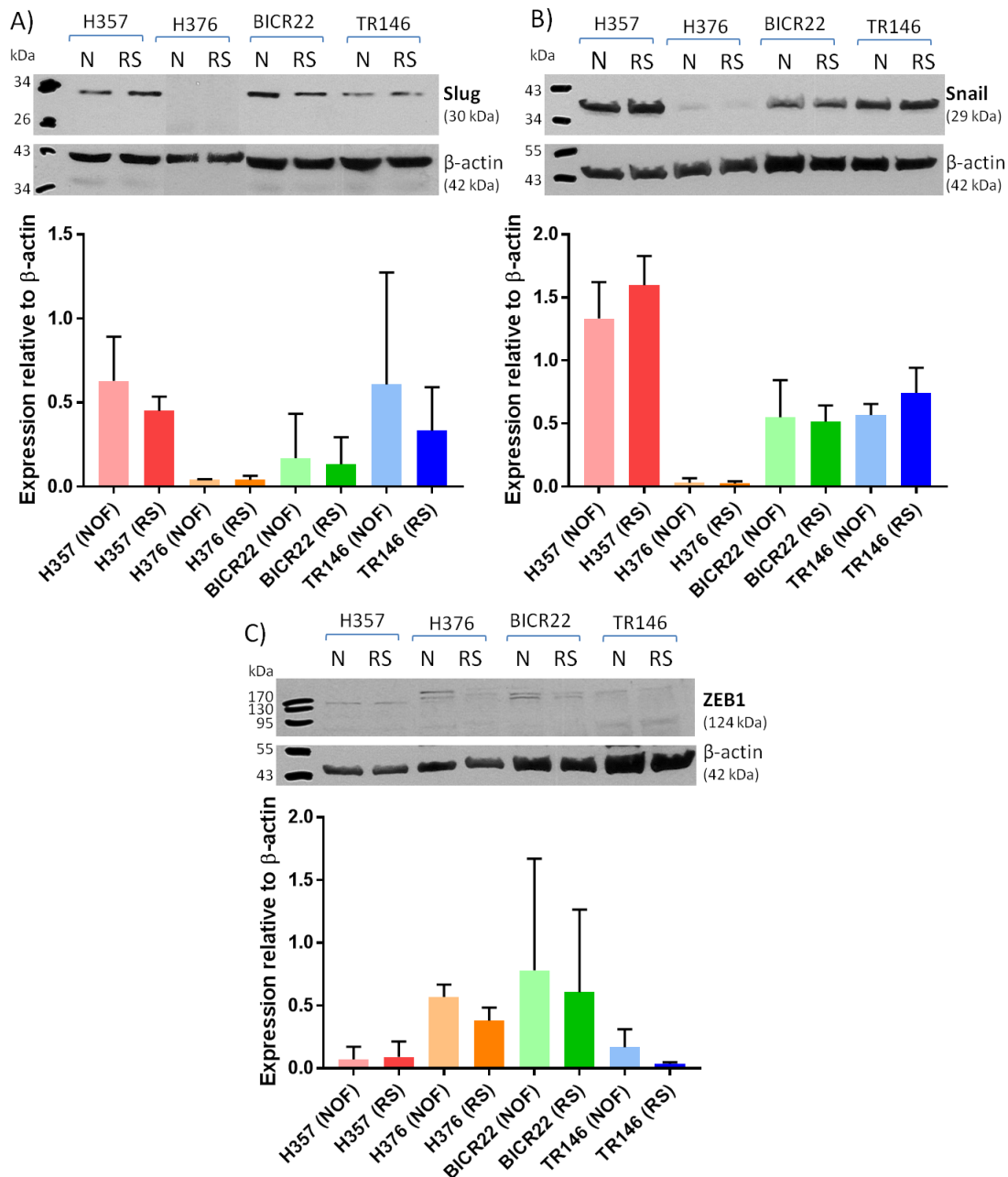


Figure 4.13. Protein levels of EMT-inducing transcription factors in OCCL treated with replicative senescent fibroblast conditioned media. Cell lysates collected from OCCL treated with conditioned media from untreated normal oral fibroblasts (NOF, N) or replicative senescent fibroblasts (RS). OCCL lysates analysed by western blot for (A) slug, (B) snail, and (C) ZEB1 (developed by x-ray). For each marker a representative blot is shown and below densitometry graphs (analysed using ImageJ) showing relative expression as a mean of blots from three separate experiments (n=2 for snail). β-actin was included as a loading control for each blot. Graphs display mean ± SD, analysed by student's t-test between pairs.

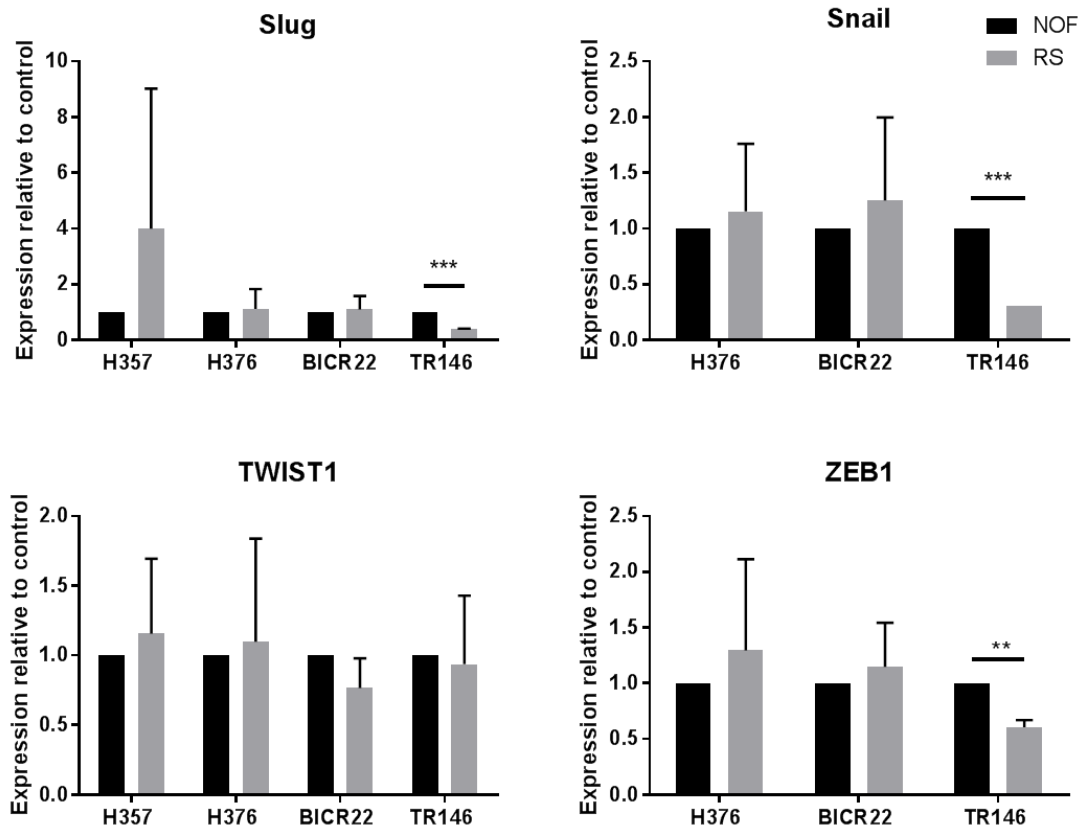


Figure 4.14. mRNA expression of EMT markers in OCCL treated with replicative senescent fibroblast conditioned media. Cell lysates collected from OCCL treated with conditioned media from untreated normal oral fibroblasts (NOF) or replicative senescent fibroblasts (RS). mRNA levels of EMT markers slug, snail, TWIST1 and ZEB1 measured by qRT-PCR using Taqman probes. H357 produced very high Δ CT values (>35) for snail and ZEB1 so were not included in the analysis. $\Delta\Delta$ CT values plotted relative to control cells of each type and B2M reference gene. Controls normalised to 1 in each case but basal expression was not equal in each cell line. Graphs display mean \pm SD from three separate experiments ($n=2$ for TR146), analysed by student t-test between pairs, ** $p<0.01$, *** $p<0.001$.

4.2.4. Effect of CAF on EMT marker expression in H357 cells

Previous experiments in this chapter have demonstrated that although all cell lines express EMT-inducing transcription factors to some extent, only H357 cells display an epithelial phenotype as determined by high E-cadherin expression and low vimentin expression. Therefore, the H357 non-metastatic primary tumour derived cell line was treated with conditioned media from primary patient derived CAF (prepared as detailed in section 2.2.3.). H357 cells were collected after incubation with conditioned media for 24, 48 and 72 h for protein and mRNA analysis. H357 treated with conditioned media from NOF or SFM only were included as controls for comparison.

As for previous experiments, E-cadherin expression was evident in all samples as well as an absence of vimentin staining and across three repeats levels were not significantly altered (Figure 4.15.). Protein expression of the EMT-inducing transcription factors slug, snail and ZEB1 was also observed for all treatment types at all the time points. There was no significant change in expression between any of the conditions used (Figure 4.16.). As for previous experiments, only slug and TWIST1 showed mRNA expression but statistical analysis did not reveal any significant differences between the treatment conditions compared to the SFM control (Figure 4.17.).

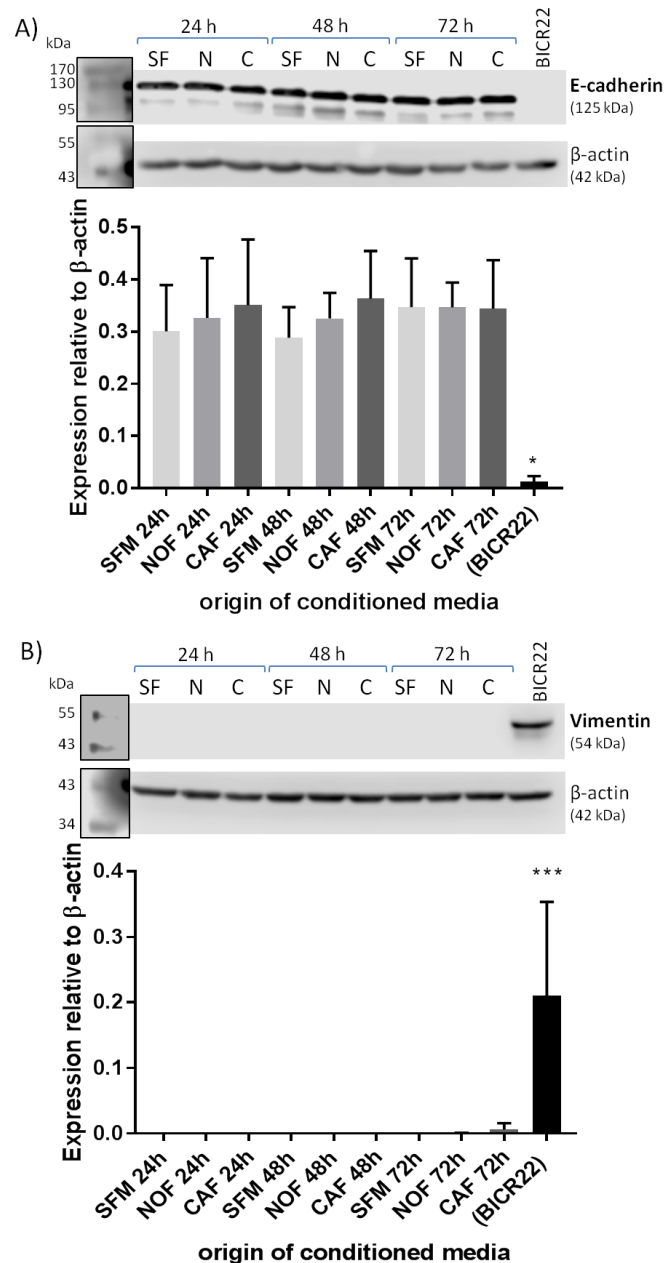


Figure 4.15. Protein levels of EMT markers in H357 cells treated with NOF and CAF conditioned media for 24, 48 or 72 h. Cell lysates from H357 cells treated with conditioned media from untreated normal oral fibroblasts (NOF, N), cancer-associated fibroblasts (CAF, C) or serum-free media as a control (SFM, SF). Lysates analysed by western blot for (A) E-cadherin and (B) vimentin. For each marker a representative blot is shown and, below, densitometry graphs showing relative expression as a mean of blots from three separate experiments (developed and analysed using LI-COR scanner and software, inserted ladder images shown at high contrast to allow visualisation). β -actin included as a loading control plus untreated BICR22 lysates as a positive control for mesenchymal markers. Graphs display mean \pm SD, analysed by one-way ANOVA, * $p < 0.05$, *** $p < 0.001$ (BICR22 compared to all H357 cell results).

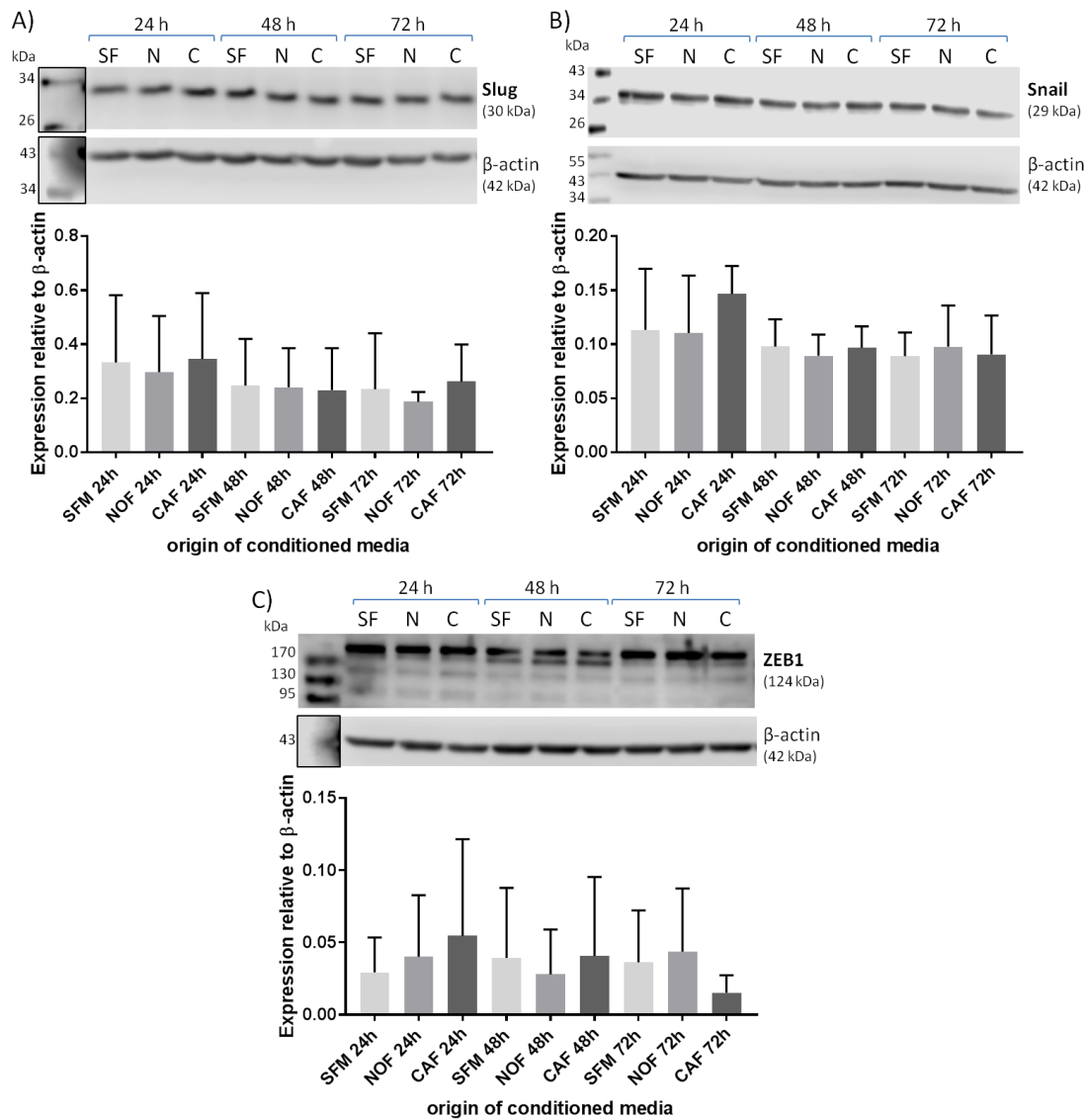


Figure 4.16. Protein levels of EMT-inducing transcription factors in H357 cells treated with NOF and CAF conditioned media for 24, 48 or 72 h. Cell lysates collected from H357 cells treated with conditioned media from untreated normal oral fibroblasts (NOF, N), cancer-associated fibroblasts (CAF, C) or serum-free media as a control (SFM, SF). Lysates analysed by western blot for (A) slug, (B) snail and (C) ZEB1. For each marker a representative blot is shown and below densitometry graphs showing relative expression as a mean of blots from three separate experiments (developed and analysed using LI-COR scanner and software, inserted ladder images shown at high contrast to allow visualisation). β-actin was included as a loading control for each blot. Graphs display mean ± SD analysed by one-way ANOVA.

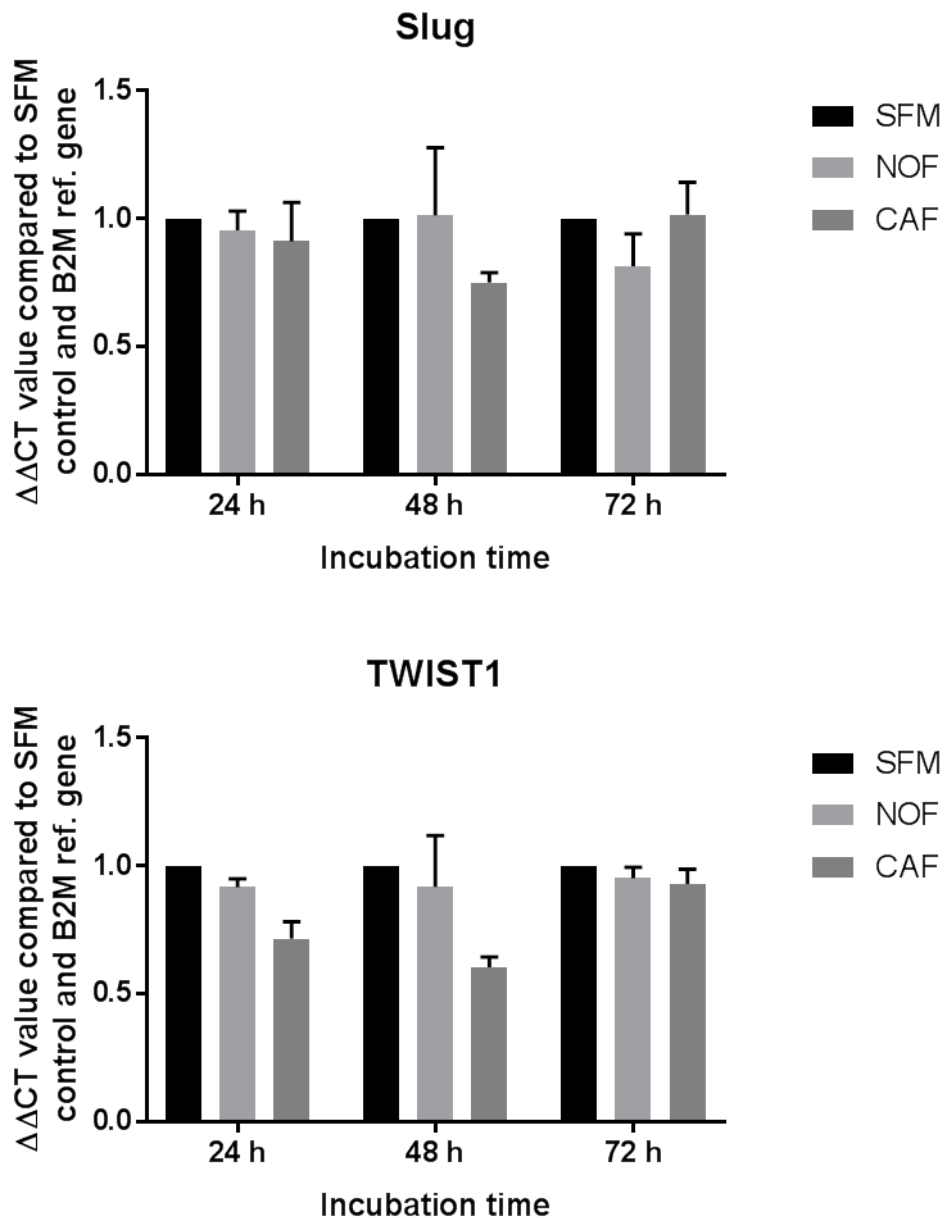


Figure 4.17. mRNA expression of EMT markers in H357 cells treated with NOF and CAF conditioned media for 24, 48 or 72 h. Cell lysates collected from H357 cells treated with conditioned media from untreated normal oral fibroblasts (NOF) or cancer-associated fibroblasts (CAF) or serum-free media as a control (SFM). mRNA levels of EMT markers slug and TWIST1 measured by qRT-PCR using Taqman probes. $\Delta\Delta\text{CT}$ values plotted relative to control cells of each type and B2M reference gene. Controls normalised to 1 in each case. Graphs display mean \pm SD from three separate experiments, analysed by two-way ANOVA.

4.2.5. Effect of fibroblasts on migration of OCCL

Having investigated EMT as a possible mechanism by which CAF induce migration of oral cancer cells both in the primary and lymph node sites, this study aimed to look at the functional effect of fibroblasts on the migration of OCCL. There is already some evidence to suggest that oral fibroblasts can induce OCCL migration (Zhou *et al.*, 2014) including senescent fibroblasts (Kabir *et al.*, 2016). Therefore, the aim was to investigate whether myofibroblasts, senescent fibroblasts and CAF could induce migration in our cell line panel and to what extent this differed between the primary tumour and lymph node metastases-derived cell lines.

Preliminary experiments were carried out with conditioned media (prepared as detailed in section 2.2.3.) from normal oral fibroblasts (NOF), experimentally-derived myofibroblasts, H₂O₂-senesced fibroblasts and patient-derived CAF, which was added to wells of a 24 well plate. Serum-starved OCCL were then added to transwell inserts containing an 8.0 µm pore PET membrane and placed in the conditioned media wells. One experimental repeat of each condition treatment was carried out in triplicate, comparing to NOF controls in each experiment for all fibroblasts types. After 16 h, OCCL on the membrane were fixed, non-migrated cells swabbed from the upper side of the membrane and the remaining cells stained using crystal violet before being mounted on slides. Four images at x 10 magnification were taken per membrane for quantification by converting them to binary images and counting the number of cells using the ImageJ “Analyse Particles” function (See Figure 2.3. for details).

Firstly, the effect of conditioned media from experimentally-derived myofibroblasts was compared to NOF conditioned media. Both lymph node-derived metastatic OCCL (BICR22 and TR146) displayed significantly higher migration compared to the primary tumour derived OCCL (H357 and H376, $p < 0.0001$, Figure 4.18.). However, there was no significant difference between the number of migrated cells in the presence of myofibroblast and NOF conditioned media for any of the OCCL used.

A slightly different pattern was observed when comparing the response to conditioned media from NOF and H₂O₂-senesced fibroblasts. The metastatic

primary tumour cell line H376 and both lymph node tumour-derived cell lines (BICR22 and TR146) had significantly higher numbers of migrated cells compared to the non-metastatic primary cell line H357 ($p < 0.0001$, Figure 4.19.) which also had markedly lower numbers of migrated cells compared to the myofibroblast experiment. A significant increase in the number of migrated cells in response to the H_2O_2 -senesced fibroblast conditioned media compared to NOF-conditioned media was seen for both the H357 (primary, $p < 0.0001$) and BICR22 (metastatic, $p < 0.05$) cell lines (Figure 4.19. B).

The H357 cell line also had significantly lower number of migrated cells compared to the other OCCL ($p < 0.0001$ comparing to H376, BICR22 or TR146) in experiments comparing the effect of NOF and patient-derived CAF conditioned media. However, no significant difference in migration level was observed in CAF-conditioned media treated cells compared to those incubated with NOF conditioned media (Figure 4.20.).

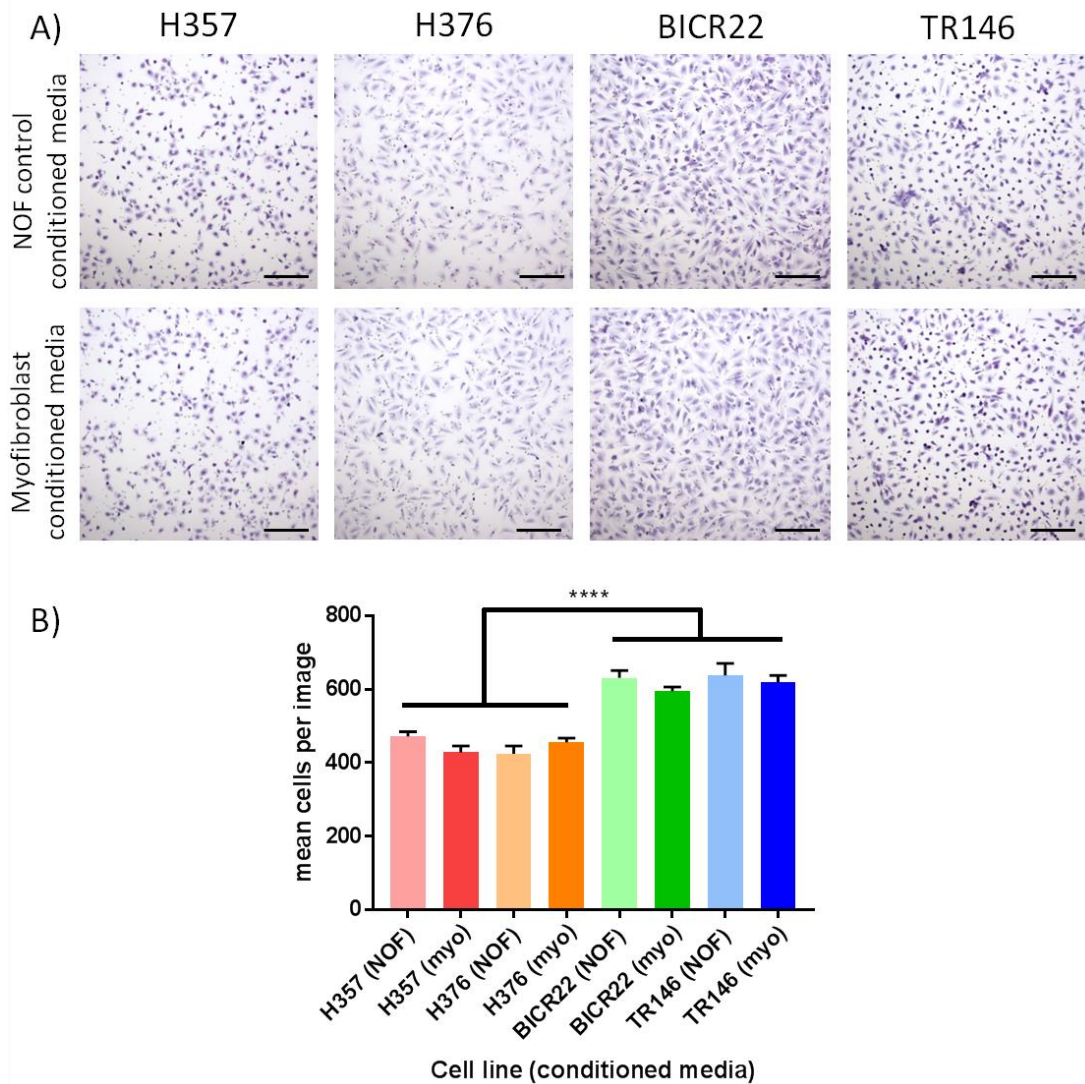


Figure 4.18. Effect of myofibroblast conditioned media on OCCL migration. (A) Representative photomicrographs of migrated OCCL on the underside of a transwell insert membrane in wells containing conditioned media from either normal oral fibroblast control (NOF) or myofibroblasts (myo). Cells stained with crystal violet. x 10 magnification, scale bars 200 μ m. (B) Mean number of migrated cells from four x 10 images per membrane calculated using ImageJ “Analyze particles” function. Graph shows mean of three membranes from one experimental repeat, analysed by one-way ANOVA. **** p <0.0001

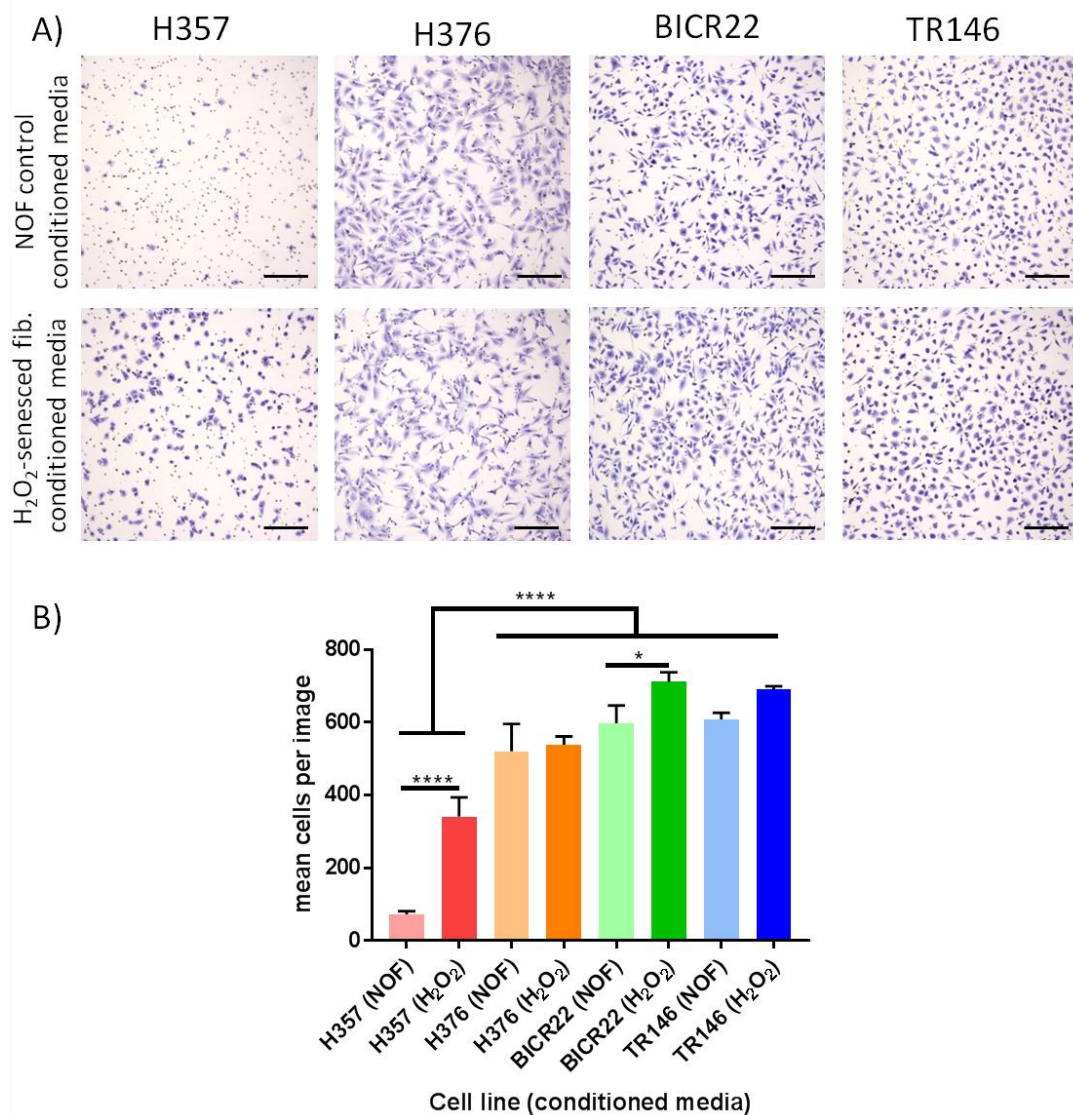


Figure 4.19. Effect of H₂O₂-senesced fibroblast conditioned media on OCCL migration. (A) Representative photomicrographs of migrated OCCL on the underside of a transwell insert membrane in wells containing conditioned media from either normal oral fibroblast control (NOF) or H₂O₂-senesced fibroblasts (H₂O₂). Cells stained with crystal violet. x 10 magnification, scale bars 200 μm. (B) Mean number of migrated cells from four x 10 images per membrane calculated using ImageJ “Analyze particles” function. Graph shows mean of three membranes from one experimental repeat, analysed by one-way ANOVA, *p<0.05, ****p<0.0001.

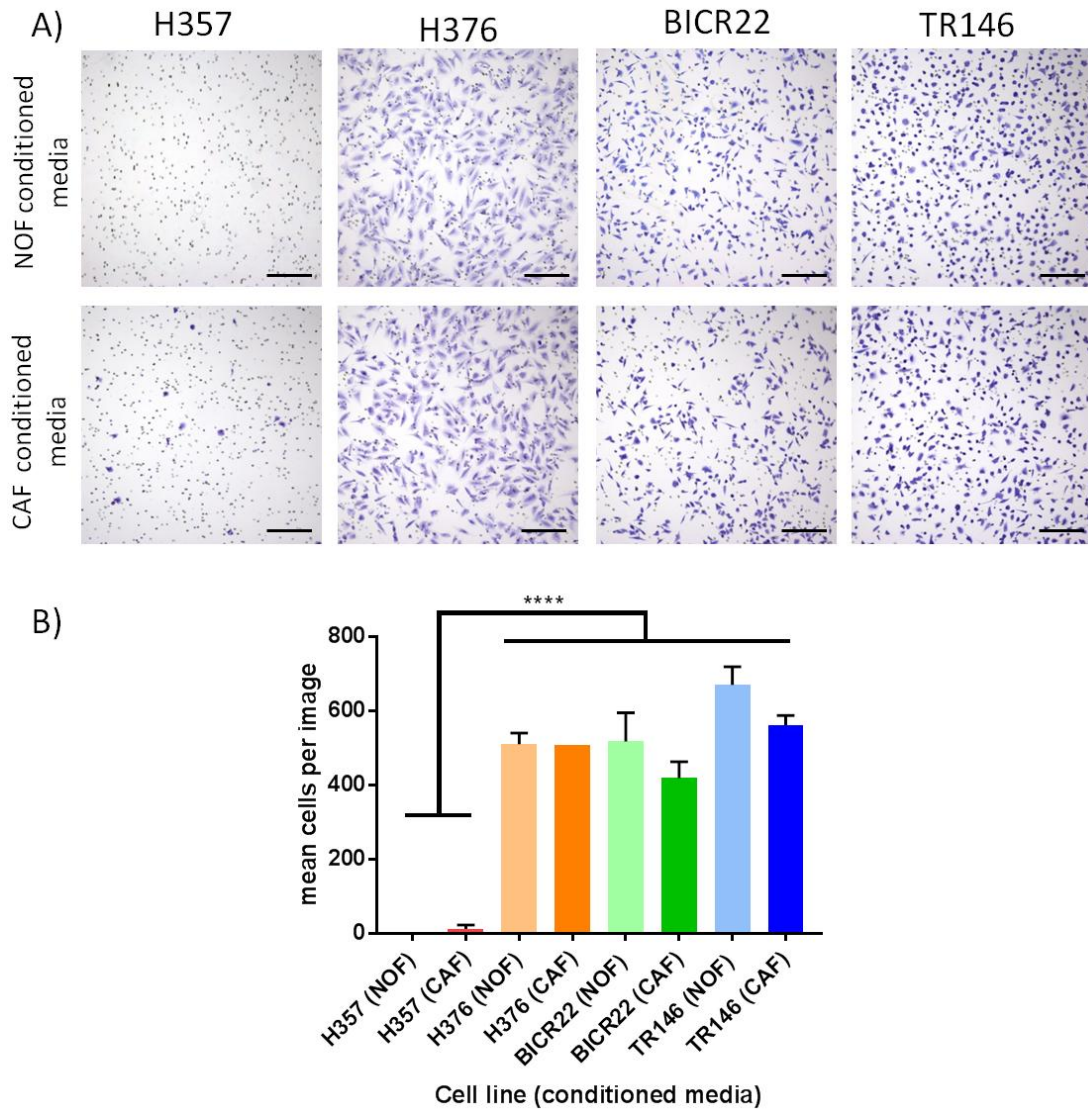


Figure 4.20. Effect of CAF conditioned media on OCCL migration. (A) Representative photomicrographs of migrated OCCL on the underside of a transwell insert membrane in wells containing either conditioned media from normal oral fibroblasts (NOF) or primary CAF. Cells stained with crystal violet. x 10 magnification, scale bars 200 μm . (B) Mean number of migrated cells from four x 10 images per membrane calculated using ImageJ “Analyze particles” function. Graph shows mean of three membranes from one experimental repeat (H376 (CAF) from one membrane due to lack of migration on further two membranes), analysed by one-way ANOVA, **** $p < 0.0001$.

4.2.6. OCCL effect on differentiation and cytokine secretion in fibroblasts

Cancer cells are thought to be able to generate a CAF-rich stroma through the secretion of a variety of growth factors including TGF- β 1, which is often elevated in the tumour microenvironment. However, in oral cancer lymph node metastasis the source of CAF has not been established.

Therefore, the aim was to determine if conditioned media from the OCCL panel used previously could affect CAF marker expression in NOF (conditioned media prepared as detailed in section 2.2.3.). NOF were incubated with conditioned media for 24 h before being collected for mRNA analysis by qRT-PCR. Only conditioned media from the non-metastatic primary tumour cell line (H357) caused a significant increase in α SMA expression ($p < 0.01$, Figure 4.21. A). However, collagen I mRNA expression was not affected by incubation with conditioned media from any of the OCCL (Figure 4.21. B).

Fibroblasts have also been implicated in aiding the generation of a tumour-promoting inflammatory microenvironment. They are capable of secreting a variety of cytokines and chemokines that recruit inflammatory immune cells to the tumour site. These cells are in turn capable of promoting tumour survival, angiogenesis, metastasis and genomic instability. However, the role of immune cells and related signalling mechanisms in oral cancer lymph node tumours has not been elucidated. Therefore, the aim of this part of the project was to investigate how cytokine signalling by NOF was affected due to exposure to OCCL conditioned media.

Secretion of IL-6 and CCL2 (MCP-1) was analysed by ELISA. OCCL conditioned media (prepared as detailed in section 2.2.3.) was added to NOF for 24 h. Fresh serum free media (SFM) was then replaced for a further 24 h before being collected for analysis. Conditioned media was normalised to cell number in each case. IL-6 concentration was significantly increased as a result of incubation with conditioned media from all of the cell lines with the exception of H376 compared to the SFM control ($p < 0.05$, Figure 4.22. A). CCL2 secretion was only significantly increased after incubation with conditioned media from the lymph node metastases-derived cell lines BICR22 and TR146 ($p < 0.05$, Figure 4.22. B). The increases in secreted protein

levels were particularly great after exposure to TR146 conditioned media ($p < 0.0001$, Figure 4.22. A&B).

Cell lysates were also collected to allow for analysis of mRNA expression levels. Only TR146 conditioned media elicited a significant increase in IL-6 and CCL2 mRNA expression ($p < 0.05$, Figure 4.23. A&B). BICR22 showed a slight increase in CCL2 expression but this was not significant. mRNA expression of the cytokines IL-1 α , IL-1 β and IL-8 was also assessed but expression of either IL-1 isoforms could not be detected. A large increase in IL-8 expression as a result of TR146 conditioned media treatment was also seen ($p < 0.05$, Figure 4.23. C), with mean fold change levels reaching 480 times higher than the SFM control.

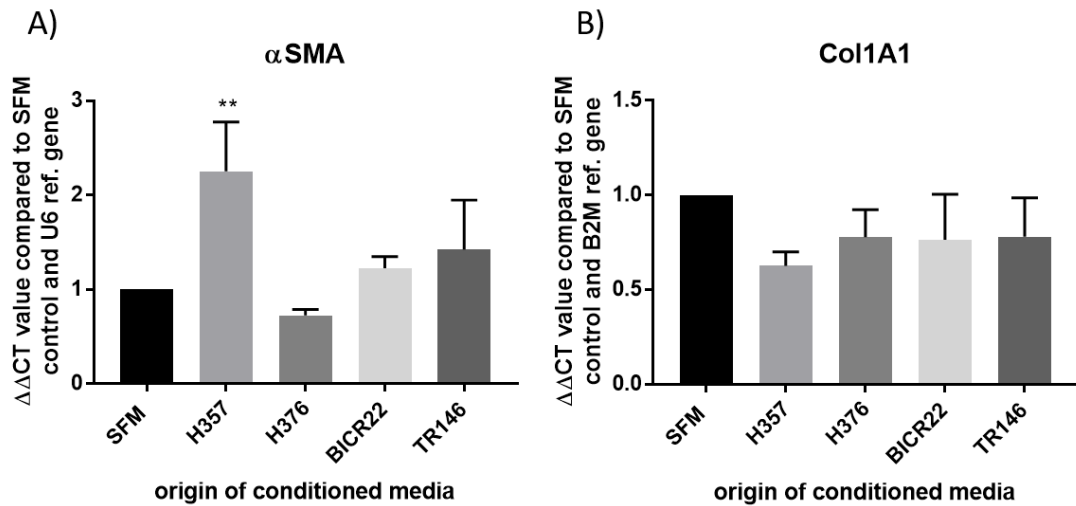


Figure 4.21. Effect of OCCL conditioned media on α SMA and collagen I mRNA expression by normal oral fibroblasts (NOF). mRNA expression of α SMA and collagen I (Col1A1) by NOF after 24 h treatment with cancer cell line (H357, H376, BICR22 and TR146) conditioned media as determined by qRT-PCR. Bars display the mean of three independent experiments \pm SD. Results are displayed as $\Delta\Delta$ CT values comparing to SFM control and B2M as a reference gene. Results were analysed using one-way ANOVA comparing each cell line to the SFM control, ** $p < 0.01$.

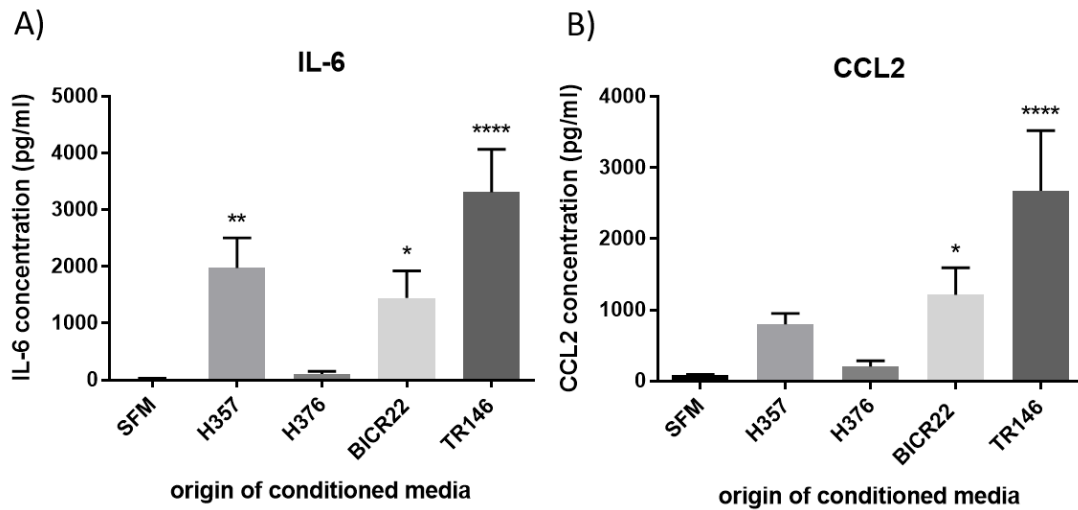


Figure 4.22. Effect of OCCL conditioned media on IL-6 and CCL2 secretion by normal oral fibroblasts (NOF). IL-6 and CCL2 concentration in NOF conditioned media after 24 h pre-treatment with cancer cell line (H357, H376, BICR22 and TR146) conditioned media or serum-free DMEM only (SFM), as determined by ELISA. Bars display the mean of three independent experiments \pm SD. Results were analysed using one-way ANOVA comparing each cell line to the SFM control, * $p < 0.05$, ** $p < 0.01$, **** $p < 0.0001$.

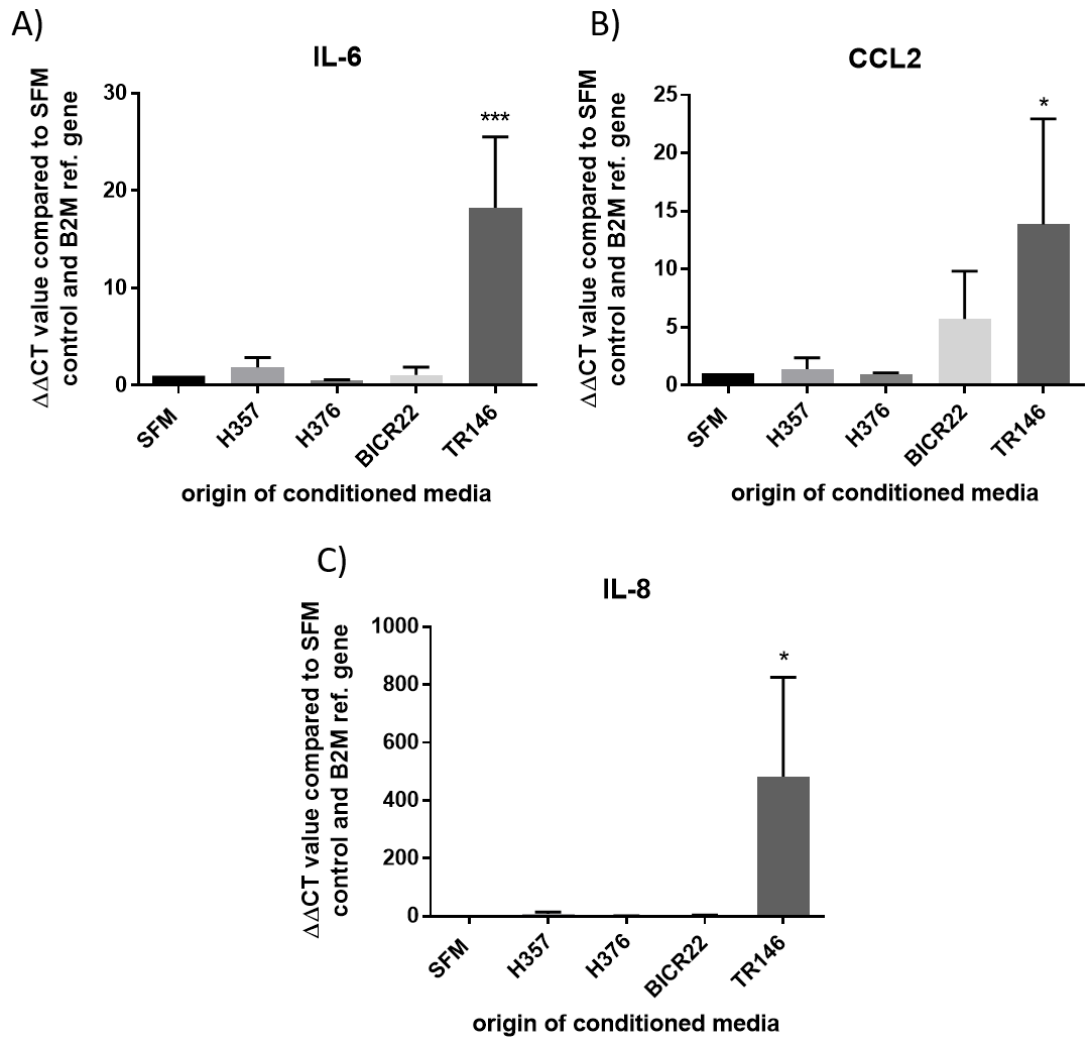


Figure 4.23. Effect of OCCL conditioned media on IL-6, CCL2 and IL-8 mRNA expression by normal oral fibroblasts (NOF). mRNA expression of IL-6, CCL2 and IL-8 by NOF after 24 h treatment with cancer cell line (H357, H376, BICR22 and TR146) conditioned media as determined by qRT-PCR. Bars display the mean of three independent experiments \pm SD. Results are displayed as $\Delta\Delta$ CT values comparing to SFM control and B2M as a reference gene. Results were analysed using one-way ANOVA comparing each cell line to the SFM control, * $p < 0.05$, *** $p < 0.001$.

4.3. Summary

This chapter has described experiments investigating the relationship between oral cancer cells and fibroblasts in the cancer stroma using *in vitro* cell co-culture. Firstly, the ability to generate fibroblasts with myofibroblastic and senescent characteristics and marker expression from normal oral fibroblasts was demonstrated. Patient-derived CAF displayed expression of these same markers but often to a lesser extent. A panel of oral cancer cell lines derived from primary (metastatic and non-metastatic) and lymph node oral cancer tumours was used to allow a comparison of their responses to co-culture with experimentally and patient-derived CAF. A comparison of the results for each of the cell lines can be seen in Table 4.1.

Although little effect of experimentally or patient-derived CAF conditioned media on EMT marker expression or migration was seen, both the metastatic primary tumour-derived and lymph node tumour-derived cell lines expressed mesenchymal markers and elevated migration ability. Lymph node tumour-derived cell lines, particularly the TR146 cell line, were also able to induce a robust chemokine and cytokine response in normal oral fibroblasts, above that induced by the primary tumour-derived cell lines.

Table 4.1. Summary of fibroblast co-culture experiment results comparing between oral cancer cell lines derived from primary and lymph node tumours.

	H357 (non-metastatic primary tumour derived)	H376 (metastatic primary tumour derived)	BICR22 and TR146 (lymph node metastases derived)
Epithelial/mesenchymal marker expression	High E-cadherin/lack vimentin expression	High vimentin/lack E-cadherin expression	High vimentin/lack or low E-cadherin expression
EMT transcription factor expression	Elevated slug/snail and lowered ZEB1 protein expression, lack snail/ZEB1 mRNA expression	Low protein expression (some ZEB1 elevated)	Variable protein expression but often lowered

Influence of myofibroblast and senescent fibroblast conditioned media on EMT marker expression	No effect seen	Sig. increase in snail mRNA in response to H ₂ O ₂ -senesced fibroblast CM	Sig. increase in ZEB1 and slug mRNA in BICR22 and TR146, respectively, in response to myofib. CM; ZEB1 mRNA sig. increased in TR146 in response to H ₂ O ₂ -senesced fib. CM but replicative senescent fib. CM caused a decrease in slug, snail and ZEB1 mRNA in TR146
Effect of CAF conditioned media on EMT marker expression	No effect seen	/	/
Migration ability	Lower compared to other OCCL. Sig. increased in response to H ₂ O ₂ -senesced fib. CM	Response either equal or elevated compared to H357; no response to CM observed	Both elevated compared to H357 and possibly H376; BICR22 sig. increased in response to H ₂ O ₂ -senesced fib. CM
Effect on fibroblast differentiation markers	Sig. increased α SMA but not collagen I mRNA expression	No effect	No effect
Effect on fibroblast cytokine/chemokine production	Sig. increased IL-6 secretion only	No effect	Both sig. increased IL-6 and CCL2 secretion. TR146 sig. increased mRNA expression of IL-6, IL-8 and CCL2

Key: CM (conditioned media); sig. (significant(ly)); fib. (fibroblast)

Chapter 5: Modulation of vasculature and endothelial cell behaviour

5.1. Introduction, hypothesis and aims

Endothelial cells are a key component of the tumour microenvironment, lining blood and lymphatic vessels that are crucial to the growth of tumours as well as providing a route of metastasis. Higher blood and lymphatic vessel densities have been reported in primary OSCC tumours and linked to increased lymph node metastasis (Zhao *et al.*, 2008; Shivamallappa *et al.*, 2011). Additionally, data from other cancer types have provided evidence linking the presence of both inflammatory immune cells and CAF to increased vessel formation (Coppé *et al.*, 2006; Ding *et al.*, 2014; Yamagata *et al.*, 2017). Data from section 3.2.3. suggested that blood vessel densities are elevated in ECS+ lymph nodes, although no significant difference in lymphatic vessel density was observed, but there are currently little *in vitro* data to mechanistically underpin these findings. Therefore, the aim was to investigate the tubule forming ability of endothelial cells to model vessel formation *in vitro* in the presence of CAF and our panel of OCCL.

Endothelial cells also contribute to the signalling milieu of the tumour microenvironment, interacting with CAF and immune cells as well as tumour cells themselves. The ability of endothelial cells to recruit inflammatory immune cells is also important as it facilitates the formation of an inflammatory microenvironment, which is conducive to tumour development. However, the role and behaviour of endothelial cells in the lymph node tumour microenvironment is less clear. Therefore, this part of the study aimed to investigate the inflammatory response of endothelial cells to the presence of tumour cells from primary and lymph node OSCC tumours and CAF *in vitro*.

The hypothesis behind this part of the study was that both cancer cells and CAF have the ability to induce vessel formation by endothelial cells and that this is true of both primary and lymph node-derived oral cancer cell lines. It was also hypothesised that exposure to media conditioned by cancer cells and CAF induces chemokine and cytokine expression in endothelial cells, contributing to the generation of an inflammatory microenvironment.

Specific Aims

1. To assess the effect of oral cancer cell line (OCCL) conditioned media on microtubule formation ability and proliferation of lymphatic and microvascular endothelial cells, and to compare the relative effect of primary tumour and lymph node tumour-derived OCCL
2. To assess the effect of conditioned media from experimentally-derived CAF (both myofibroblasts and senescent fibroblasts, see section 4.2.1.) on microtubule formation and proliferation of lymphatic and microvascular endothelial cells.
3. To measure the secretion and mRNA expression of key cytokines and chemokines by lymphatic and microvascular endothelial cells in response to incubation with conditioned media from primary tumour and lymph node-derived OCCL and experimentally-derived CAF (both myofibroblasts and senescent fibroblasts, see section 4.2.1.).

5.2. Results

5.2.1. OCCL effect on endothelial cell behaviour *in vitro*

Although there is some *ex vivo* evidence linking increased vessel formation to metastasis (Zhao *et al.*, 2008; Shivamallappa *et al.*, 2011), there are limited data from *in vitro* functional studies or using lymph-node derived cells or tissues. Therefore, the ability of our OCCL panel to alter microtubule formation by endothelial cells *in vitro* was assessed to allow a comparison of primary and lymph node-derived OCCL.

Primary human dermal lymphatic endothelial cells (HLEC) and human dermal microvascular endothelial cells (HMEC) were resuspended in OCCL conditioned media (generated as described in section 2.2.3. but with the addition of 0.1% (v/v) FBS due to the intolerance of HLEC and HMEC to serum starvation) and added to wells of a 96-well plate containing growth factor-reduced Matrigel. HMEC/HLEC were also resuspended in DMEM + 0.1% (v/v) FBS only as a negative control and

DMEM + 0.1% (v/v) FBS containing VEGF-A (for HMEC) or VEGF-C (for HLEC) as a positive control. All conditions were performed in triplicate and after 16 h, tubules were observed to form spontaneously. One image per well was taken, tubules skeletonised and the number of junctions quantified (see Figure 2.4.).

Significantly higher numbers of tubule junctions were found when HLEC were incubated with DMEM containing VEGF-C or conditioned media from any of the OCCL used compared to DMEM alone ($p < 0.05$, Figure 5.1.) with the exception of TR146 ($p = 0.07$). However, there was no significant difference in the number of tubule junctions in HMEC experiments under any of the conditions used (Figure 5.2.). To control for differences in cell proliferation rate HLEC and HMEC were seeded at equal density and incubated with the same conditioned and control media as for microtubule assays in a 96-well plate without Matrigel. After 16 h, cell numbers were quantified using an MTS assay and comparing to a standard curve. Although there was a trend towards increased cell number in HLEC, this was not significant across three independent experiments (Figure 5.3. A). There was also no significant difference in the number of HMEC between the conditions (Figure 5.3. B).

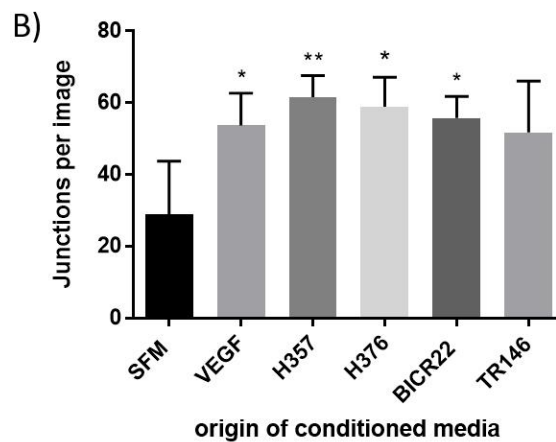
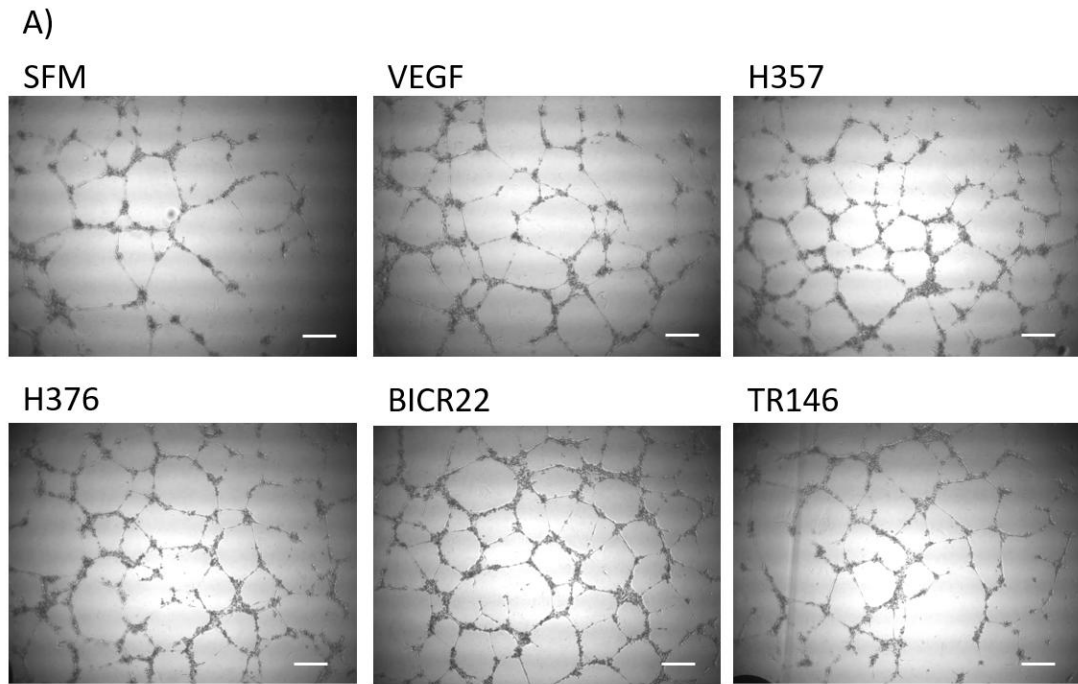


Figure 5.1. Effect of OCCL conditioned media on microtubule formation by HLEC.
 (A) Representative images of microtubules formed by HLEC after 16 h incubation with conditioned media from the stated cell type, serum-free DMEM only (SFM, negative control) or DMEM containing VEGF-C (positive control). 0.1 % (v/v) FBS was included in all conditions to prevent cell death. x 10 magnification, scale bars 100 μ m. (B) Quantification of tubule formation. One image from each well was skeletonised and the number of junctions counted. Graphs display mean \pm SD from three independent experiments, analysed by one-way ANOVA comparing to SFM control, * $p < 0.05$, ** $p < 0.01$.

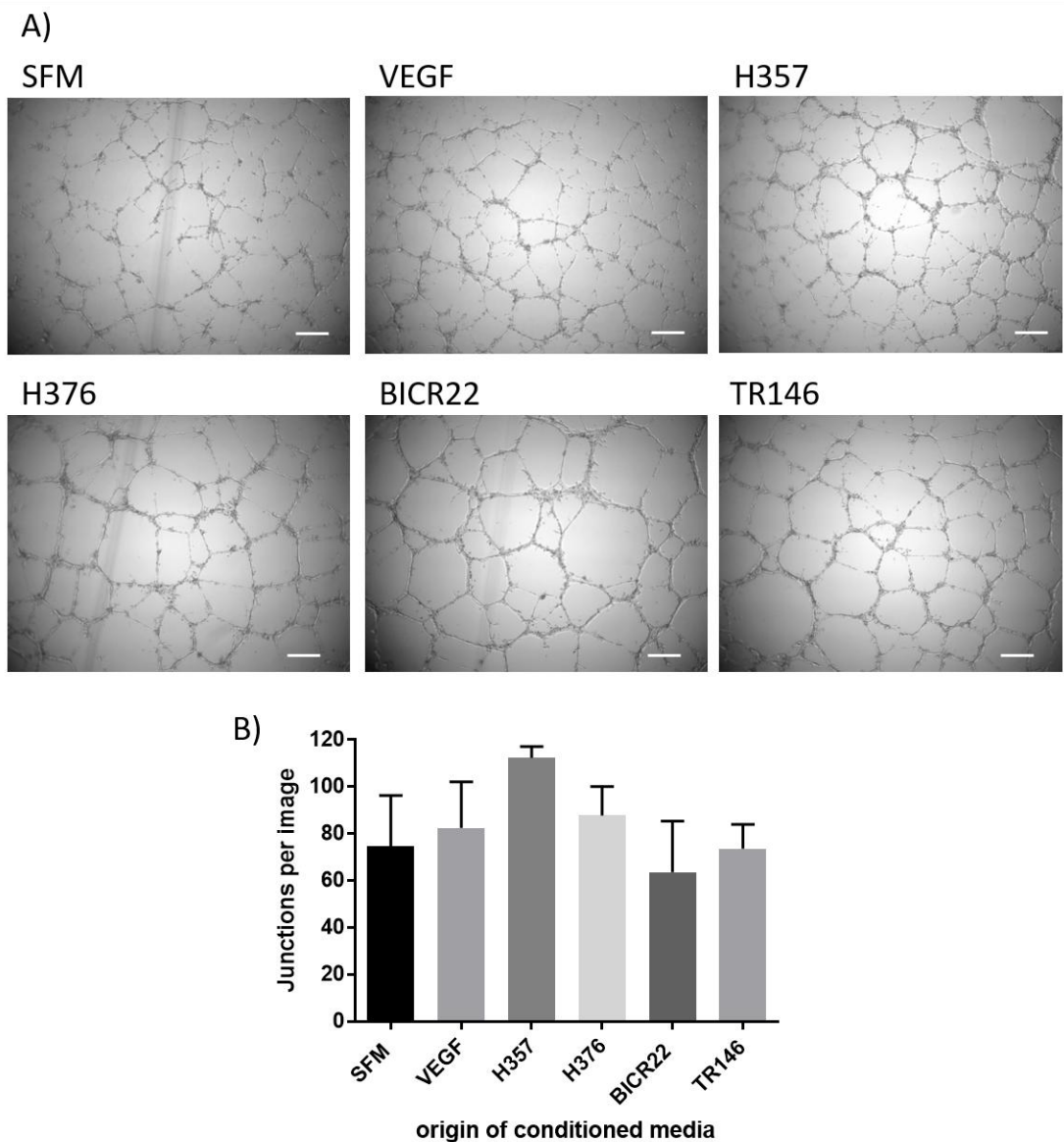


Figure 5.2. Effect of OCCL conditioned media on microtubule formation by HMEC.

(A) Representative images of microtubules formed by HMEC after 16 h incubation with conditioned media from the stated cell type, serum-free DMEM media only (SFM, negative control) or DMEM containing VEGF-A (positive control). 0.1 % (v/v) FBS was included in all conditions to prevent cell death. x 10 magnification, scale bars 100 μ m. (B) Quantification of tubule formation. One image from each well was skeletonised and the number of junctions counted. Graphs display mean \pm SD from three independent experiments, analysed by one-way ANOVA comparing to SFM control, * $p < 0.05$, ** $p < 0.01$.

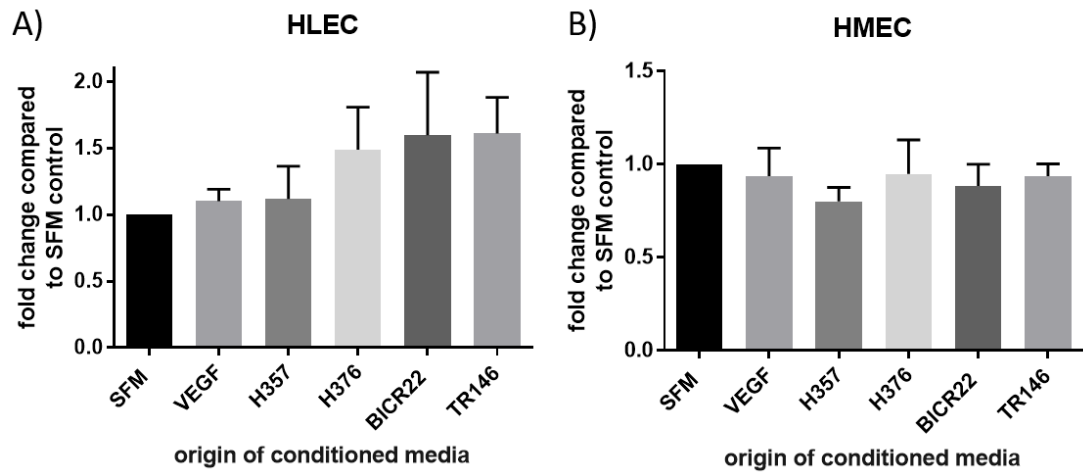


Figure 5.3. Effect of OCCL conditioned media on proliferation of HLEC and HMEC. MTS assay results from (A) HLEC and (B) HMEC after 16 h incubation with conditioned media from OCCL, serum-free DMEM media (SFM, negative control) or DMEM containing VEGF (positive control). 0.1 % (v/v) FBS was included in all conditions to prevent cell death. Cell numbers calculated in each experiment by comparing absorbances to a standard curve. Graphs represent the mean fold change in cell number \pm SD from three separate experiments analysed by one-way ANOVA comparing to the SFM control.

5.2.2. Myofibroblast and senescent fibroblast effect on endothelial cell behaviour *in vitro*

Research in other cancer types suggests that CAF are capable of altering endothelial cell behaviour and promoting vessel formation both *in vitro* and *in vivo* (Coppé *et al.*, 2006; Ding *et al.*, 2014). However, there is relatively little evidence connecting CAF to the promotion of vessel formation in OSCC. Therefore, the effect of conditioned media from experimentally derived-CAF, both myofibroblastic and senescent (as described in section 4.2.1.), on microtubule formation by HLEC and HMEC was assessed.

Microtubule assays were carried out using the same experimental protocol and controls as for OCCL (section 5.2.1.) but with conditioned media from myofibroblasts generated through TGF- β 1-treatment of normal oral fibroblasts (NOF) or senescent fibroblasts generated through H₂O₂-treatment of NOF (see section 4.2.1.). NOF conditioned media was included in all experiments for comparison. All conditions were performed in triplicate and after 16 h one image per well was taken for quantification as described previously (see Figure 2.4.).

Although there appeared to be a slight upward trend, there was no significant difference in the number of tubule junctions found when HLEC were incubated with myofibroblast conditioned media although large variation in the SFM control was observed (Figure 5.4. A&B). Additionally, incubation with conditioned media from H₂O₂-senesced fibroblasts did not significantly affect the number of tubule junctions formed by HLEC (Figure 5.4. A&C). Quantification of the number of tubule junctions formed by HMEC incubated with myofibroblast conditioned media also suggested an upwards trend but did not reveal any statistically significant differences (Figure 5.5. A&B). However, the number of tubule junctions was significantly increased on incubation of HMEC with conditioned media from H₂O₂-senesced fibroblasts compared to the SFM control ($p < 0.05$, Figure 5.5. A&C).

The effect of fibroblast conditioned media on proliferation of HLEC and HMEC was also assessed by MTS assay using the same experimental protocol and controls as for OCCL (section 5.2.1.). Both control NOF and myofibroblast

conditioned media caused a significant increase in HLEC cell number compared to the SFM control ($p < 0.01$, Figure 5.6. A). However, neither H_2O_2 -senesced fibroblasts nor their corresponding control NOF caused a significant change in cell number although an upwards trend was observed (Figure 5.6. C). No effect on HMEC cell number as a result of incubation with any of the fibroblast conditioned medias was seen (Figure 5.6. B&D).

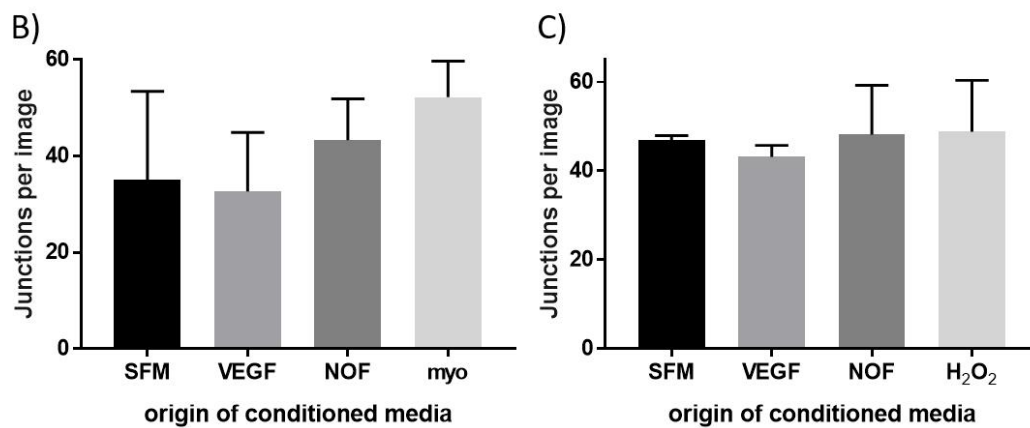
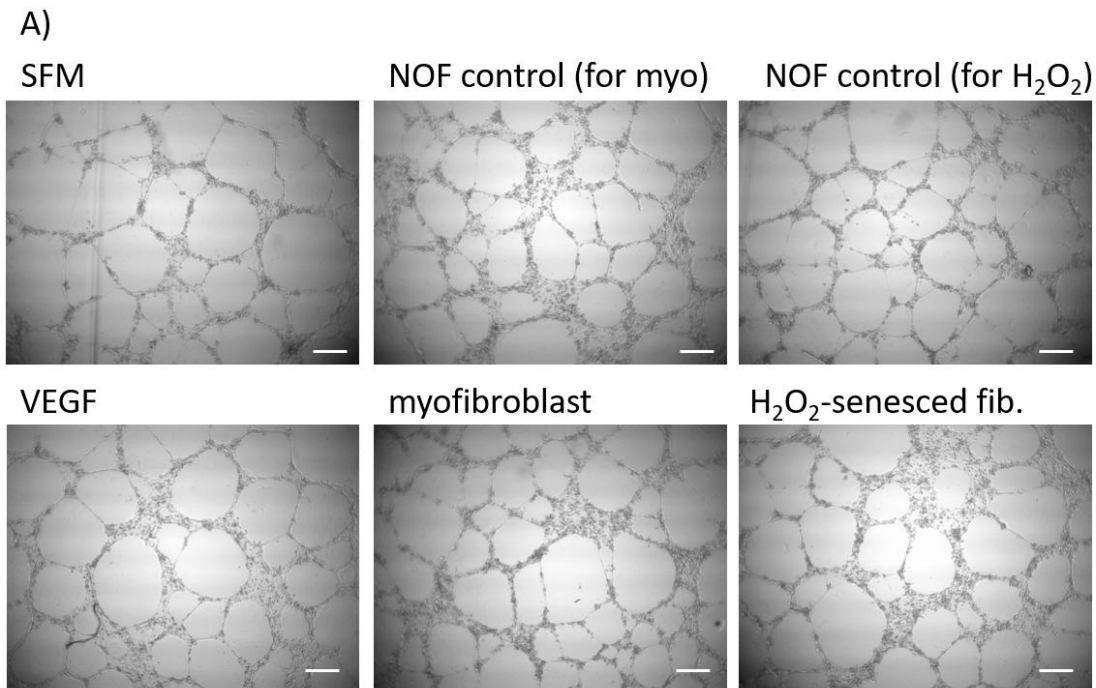


Figure 5.4. Effect of fibroblast conditioned media on microtubule formation by HLEC. (A) Representative images of microtubules formed by HLEC after 16 h incubation with conditioned media from normal oral fibroblasts (NOF), myofibroblasts (myo), H₂O₂-senesced fibroblasts (H₂O₂), serum-free DMEM media only (SFM, negative control) or DMEM containing VEGF-C (positive control). 0.1 % (v/v) FBS was included in all conditions to prevent cell death. x 10 magnification, scale bars 100 μ m. (B,C) Quantification of tubule formation. One image from each well was skeletonised and the number of junctions counted. Graphs display mean \pm SD from (B) three or (C) two independent experiments, analysed by one-way ANOVA comparing to SFM control.

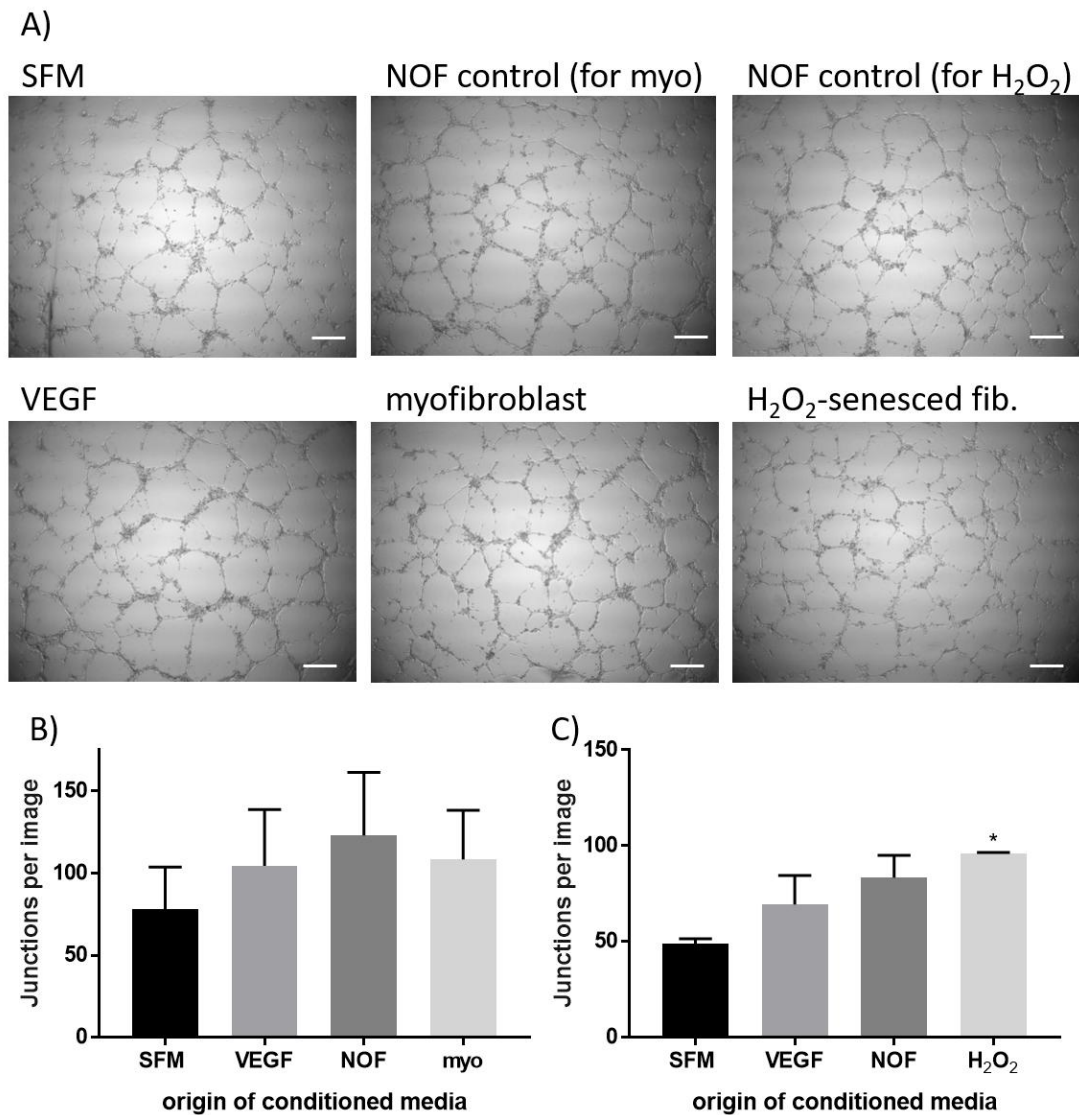


Figure 5.5. Effect of fibroblast conditioned media on microtubule formation by HMEC. (A) Representative images of microtubules formed by HMEC after 16 h incubation with conditioned media from normal oral fibroblasts (NOF), myofibroblasts (myo), H₂O₂-senesced fibroblasts (H₂O₂), serum-free DMEM media only (SFM, negative control) or DMEM containing VEGF-A (positive control). 0.1 % (v/v) FBS was included in all conditions to prevent cell death. x 10 magnification, scale bars 100 μ m. (B,C) Quantification of tubule formation. One image from each well was skeletonised and the number of junctions counted. Graphs display mean \pm SD from (B) three or (C) two independent experiments, analysed by one-way ANOVA comparing to SFM control, * p <0.05.

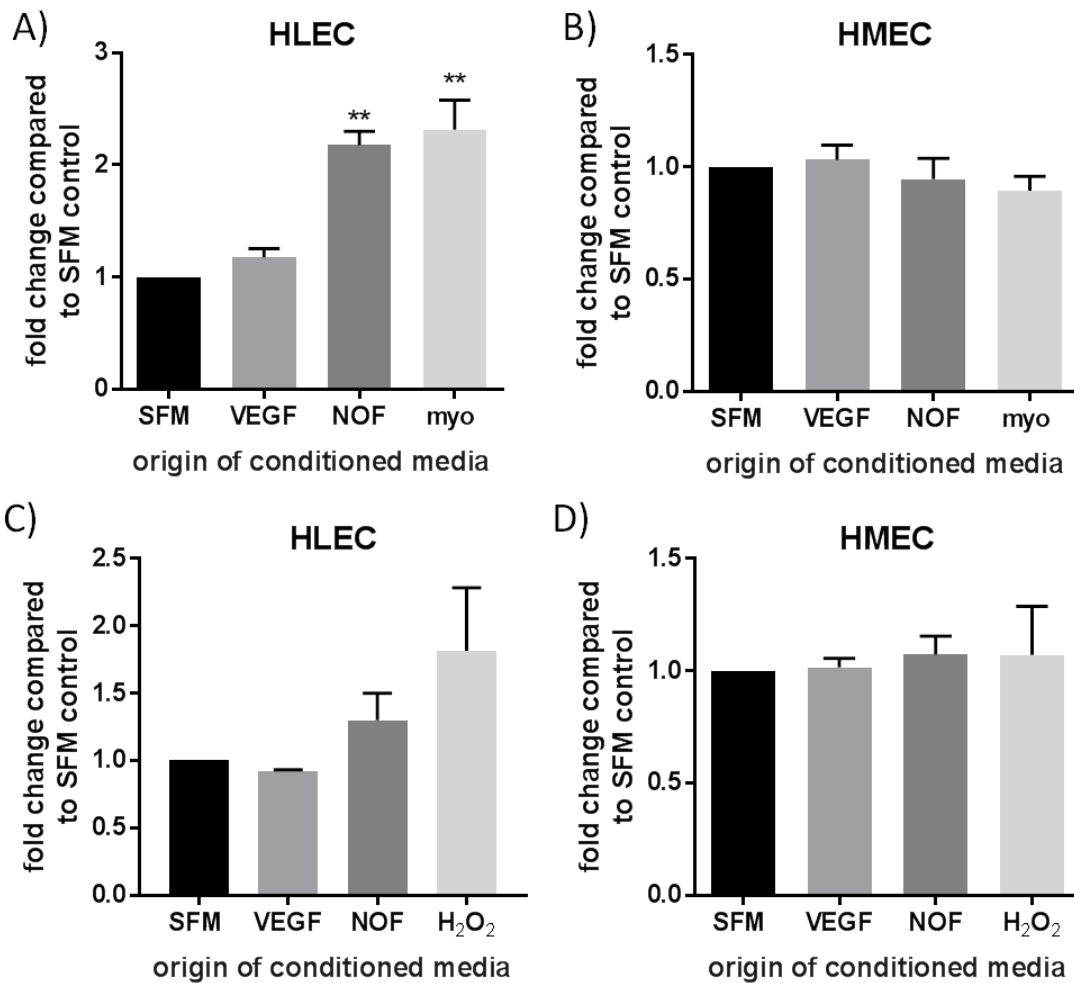


Figure 5.6. Effect of fibroblast conditioned media on proliferation of HLEC and HMEC. MTS assay results from HLEC (A,C) and HMEC (B,D) after 16 h incubation with conditioned media from normal oral fibroblasts (NOF) and either myofibroblasts (myo; A,B) or H₂O₂-senesced fibroblasts (H₂O₂; C,D) plus serum-free DMEM media (SFM, negative control) or DMEM containing VEGF (positive control). 0.1 % (v/v) FBS was included in all conditions to prevent cell death. Cell numbers calculated in each experiment by comparing absorbances to a standard curve. Graphs represent the mean fold change in cell number \pm SD from (A,B) three or (C,D) two separate experiments analysed by one-way ANOVA comparing to the SFM control, **p<0.01.

5.2.3. OCCL effect on cytokine secretion by endothelial cells

As well as forming vessel structures, endothelial cells are an important part of the tumour microenvironment signalling network, communicating with CAF, immune and tumour cells. The formation of an inflammatory microenvironment and recruitment of inflammatory immune cells is now known to be very important to tumour development and endothelial cells are capable of secreting a variety of cytokines and chemokines that promote this (Young, 2012). However, the role of endothelial cells in this capacity in OSCC and particularly within the lymph node is not well defined. Therefore, the effect of OCCL conditioned media on the secretion and expression of selected cytokines and chemokines by HLEC and HMEC was investigated.

Secretion of IL-6 and CCL2 (MCP-1) by HLEC and HMEC was analysed by ELISA. OCCL conditioned media (produced as described in section 2.2.3. but with the addition of 1% (v/v) FBS due to the intolerance of HLEC and HMEC to serum starvation) was added to HLEC and HMEC for 24 h. Fresh serum free media (SFM, also with the addition of 1% (v/v) FBS) was then replaced for a further 24 h before being collected for analysis. Conditioned media was normalised to cell number in each case.

There was a large variation in secretion levels of IL-6 by HLEC and HMEC in response to OCCL conditioned media. Although the mean concentration level was increased in all cases in response to OCCL conditioned media compared to the SFM control this was only significant in the case of H357 (for HLEC and HMEC, $p < 0.05$, Figure 5.7. A&B) and BICR22 (for HLEC only, $p < 0.05$, Figure 5.7. A). Media collected from HLEC and HMEC contained very high concentrations of CCL2 compared to that observed previously from NOF even under SFM control conditions (mean concentration 35 ng/ml for HLEC and 3 ng/ml for HMEC vs. 0.081 ng/ml in NOF control, see section 4.2.6 and Figure 4.22.). However, there was no significant change in CCL2 concentration following treatment with any of the OCCL conditioned medias when compared to the SFM control (Figure 5.7. C&D).

Cell lysates were also collected for analysis of mRNA expression levels. There was little change in expression levels of IL-6 or CCL2 as a result of conditioned

media treatment from any of the OCCL used by HLEC (Figure 5.8. A&B) or HMEC (Figure 5.9. A&B). Only TR146 conditioned media elicited a significant increase in CCL2 mRNA expression in HLEC but the fold change was small (1.3-fold increase, $p < 0.05$, Figure 5.8. B). HMEC IL-6 mRNA expression was also only significantly elevated due to BICR22 conditioned media exposure ($p < 0.01$, Figure 5.9. A). mRNA expression of the cytokines IL-1 α , IL-1 β and IL-8 was also assessed. Unlike NOF (see section 4.2.6.), both HLEC and HMEC displayed mRNA expression of both IL-1 α and IL-1 β but no significant change in expression levels was seen following conditioned media treatment (Figure 5.8. C&D; Figure 5.9. C&D). The largest mRNA response was seen for IL-8 with significant increases in expression by HLEC in response to both lymph node-derived cell lines (BICR22 and TR146, $p < 0.01$, Figure 5.8. E). Mean fold change values for above 2 for IL-8 were also seen for BICR22 and TR146 conditioned media-treated HMEC but these were not significant across three independent experiments (Figure 5.9.E).

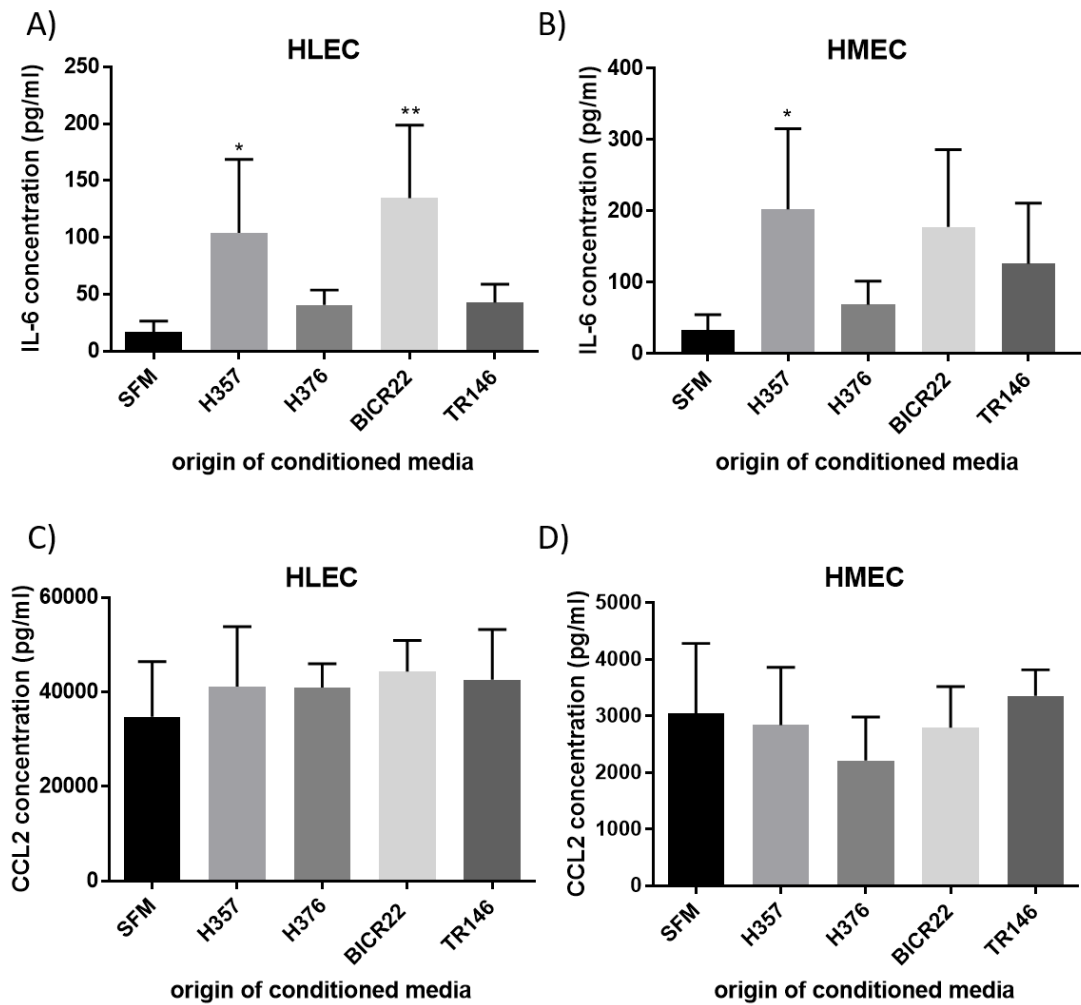


Figure 5.7. Effect of OCCL conditioned media on IL-6 and CCL2 production by HLEC and HMEC. Concentration of IL-6 (A,B) and CCL2 (C,D) in HLEC (A,C) or HMEC (B,D) conditioned media after 24 h pre-treatment with cancer cell line (H357, H376, BICR22 and TR146) conditioned media or serum-free DMEM only (SFM), as determined by ELISA. 1% (v/v) FBS was included in all conditions to prevent cell death. Graphs display the mean of four independent experiments \pm SD, analysed by one-way ANOVA comparing to SFM control, * $p < 0.05$, ** $p < 0.01$.

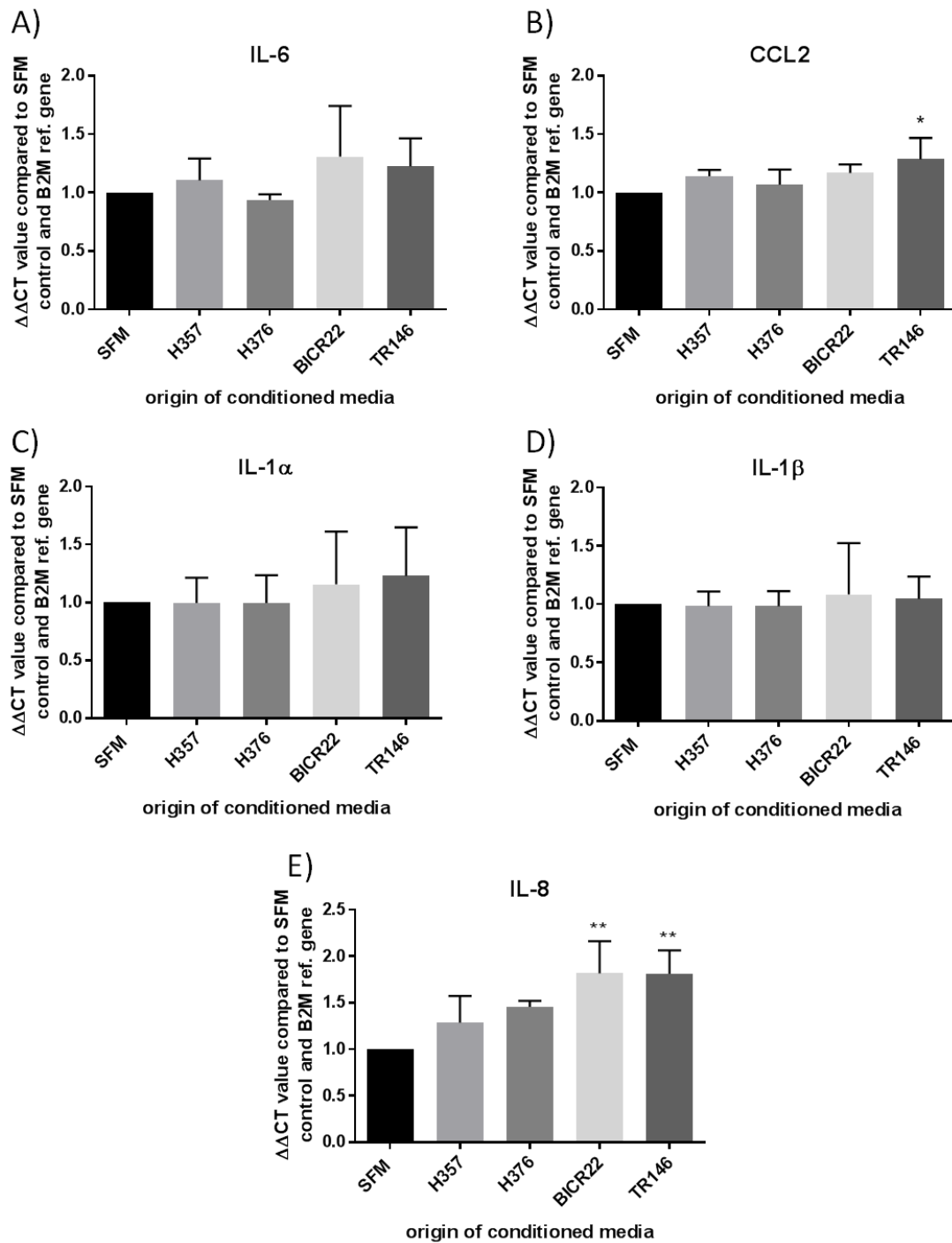


Figure 5.8. Effect of OCCL conditioned media on immune marker mRNA expression by HLEC. mRNA expression of (A) IL-6, (B) CCL2, (C) IL-1 α , (D) IL-1 β and (E) IL-8 by HLEC after 24 h pre-treatment with oral cancer cell line (H357, H376, BICR22 and TR146) conditioned media or serum-free DMEM only (SFM), as determined by qRT-PCR. 1% (v/v) FBS was included in all conditions to prevent cell death. Bars display the mean of three independent experiments \pm SD. Results are displayed as $\Delta\Delta\text{CT}$ values comparing to SFM control and B2M reference gene, analysed by one-way ANOVA comparing to SFM control, * $p < 0.05$, ** $p < 0.01$.

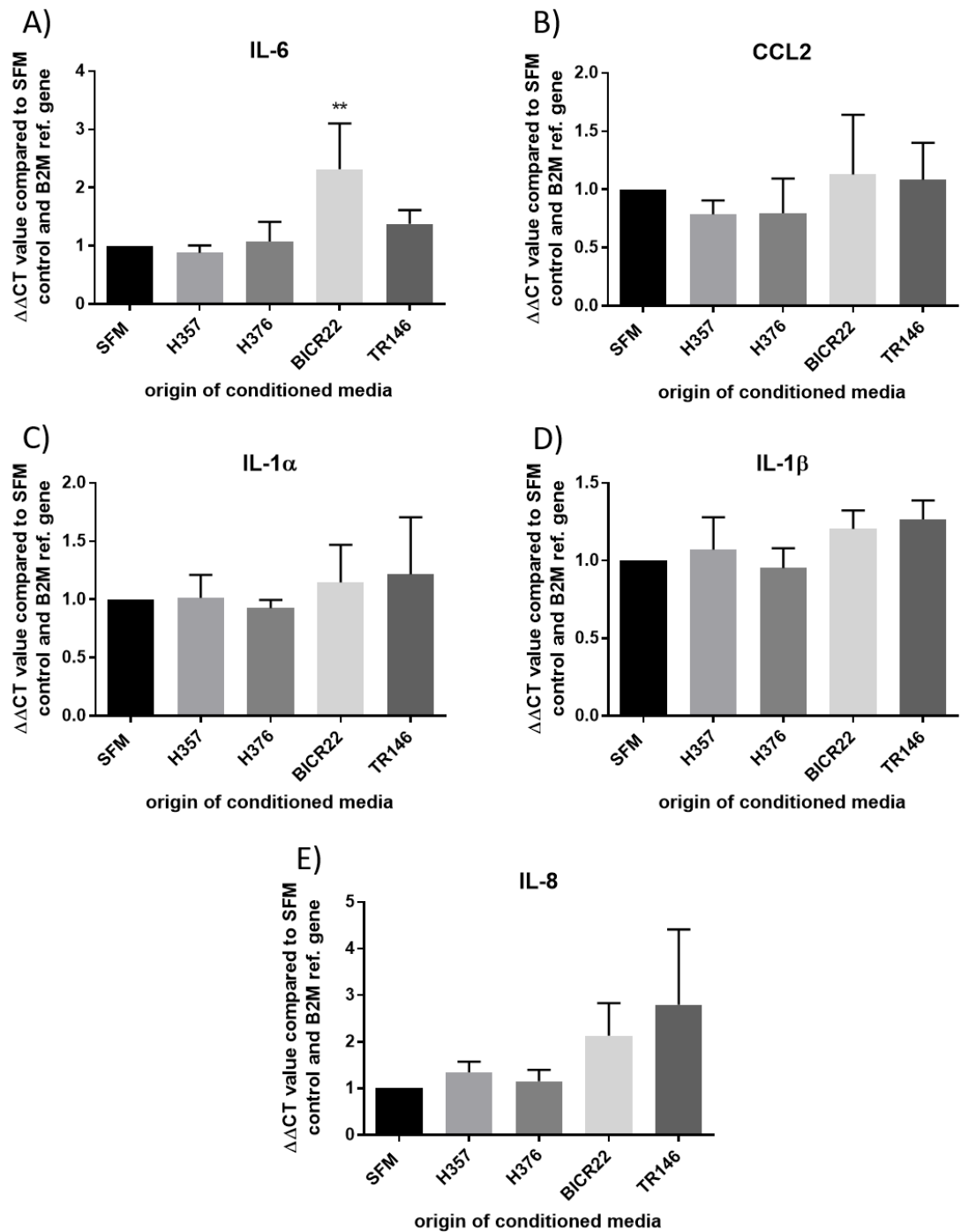


Figure 5.9. Effect of OCCL conditioned media on immune marker mRNA expression by HMEC. mRNA expression of (A) IL-6, (B) CCL2, (C) IL-1 α , (D) IL-1 β and (E) IL-8 by HMEC after 24 h pre-treatment with cancer cell line (H357, H376, BICR22 and TR146) conditioned media or serum-free DMEM only (SFM), as determined by qRT-PCR. 1% (v/v) FBS was included in all conditions to prevent cell death. Bars display the mean of three independent experiments \pm SD. Results are displayed as $\Delta\Delta\text{CT}$ values comparing to SFM control and B2M reference gene, analysed by one-way ANOVA comparing to SFM control, ** $p < 0.01$.

5.2.4. Myofibroblasts and senescent fibroblasts alter cytokine secretion by endothelial cells

Endothelial cells are exposed to signals from a diverse range of cell types present in the tumour microenvironment, including CAF. Given that CAF are capable of both producing and responding to inflammatory signals, it is possible they also communicate with endothelial cells to promote the formation of an inflammatory microenvironment. However, this has not been investigated in OSCC. Therefore, the effect of conditioned media from experimentally derived-CAF, both myofibroblastic and senescent (as described in section 4.2.1.), on the secretion and expression of selected cytokines and chemokines by HLEC and HMEC was investigated.

Secretion of IL-6 and CCL2 (MCP-1) was analysed by ELISA using the same experimental protocol as for OCCL (section 5.2.3.) but with conditioned media from myofibroblasts generated through TGF- β 1-treatment of NOF or senescent fibroblasts generated through H₂O₂-treatment of NOF (see section 4.2.1.). NOF conditioned media was included in all experiments for comparison, as well as a serum-free media (SFM) control. mRNA analysis of the same cytokine and chemokine markers used in section 5.2.3. was also carried out.

Myofibroblast, but not NOF, conditioned media caused a significant increase in IL-6 concentration in media collected from HLEC compared to the SFM control ($p < 0.01$, Figure 5.10. A). Although mean IL-6 concentration was increased in HMEC media in response to incubation with myofibroblast conditioned media the change was not significant when compared to the SFM control (Figure 5.10. B). As observed in section 5.2.3., CCL2 secretion levels were extremely high for both HLEC and HMEC and no significant change in expression was observed as a result of myofibroblast conditioned media treatment (Figure 5.10. C&D).

Analysis of IL-6 and CCL2 mRNA expression did not reveal any significant changes in expression in either HLEC or HMEC due to myofibroblast conditioned media treatment compared to the SFM control (Figure 5.11. A&B). The same was true when IL-1 α and IL-1 β were analysed although myofibroblast conditioned media treated HMEC had significantly higher expression of IL-1 α compared to NOF treated HMEC ($p < 0.05$, Figure 5.11. C&D). IL-8 mRNA expression levels were raised as a

result of myofibroblast conditioned media treatment for both cell types but this was not significant (Figure 5.11. E).

No significant effect of H₂O₂-senesced fibroblast conditioned media on IL-6 or CCL2 secretion was observed although there was a large variation in the concentration measured (Figure 5.12.). Furthermore, no significant change in IL-6 mRNA expression was seen in either HMEC or HLEC as a result of conditioned media treatment (Figure 5.13. A). However, CCL2 mRNA levels were significantly elevated in H₂O₂-senesced fibroblast conditioned media treated HLEC compared to either the SFM or NOF conditioned media treated controls but the mean fold change was small (1.3-fold increase compared to SFM or NOF, p<0.05, Figure 5.13. B). Although HLEC displayed no significant change in IL-1 α expression, there was a mean 2-fold increase in IL-1 β expression in cells treated with H₂O₂-senesced fibroblast conditioned media although this was not significant compared to the SFM control (Figure 5.13. C&D). In addition, IL-8 expression by HLEC was significantly increased following incubation with conditioned media from H₂O₂-senesced fibroblasts (p<0.01, Figure 5.13. E). There was no significant change in IL-1 α , IL-1 β or IL-8 mRNA expression in HMEC cells although large variation was seen between repeats (Figure 5.13. C,D,E).

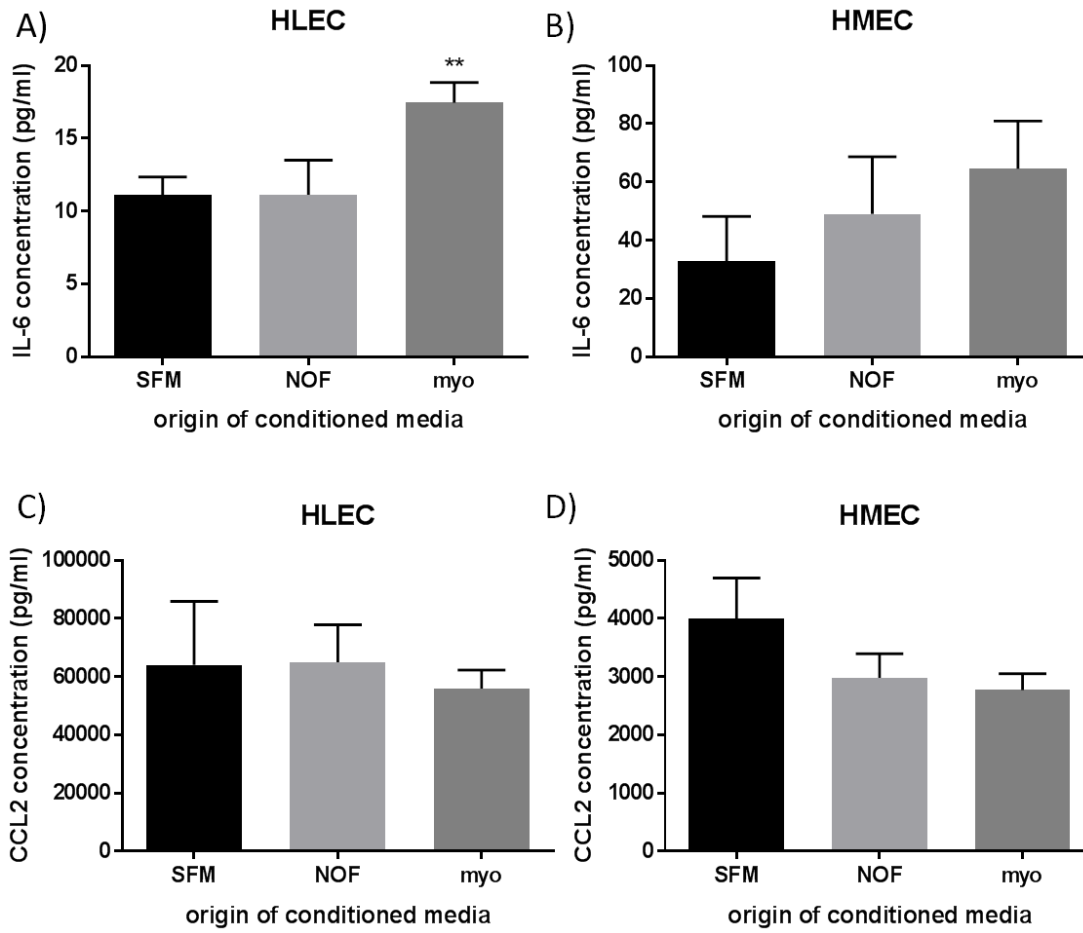


Figure 5.10. Effect of myofibroblast conditioned media on IL-6 and CCL2 production by HLEC and HMEC. Concentration of IL-6 (A,B) and CCL2 (C,D) in HLEC (A,C) or HMEC (B,D) conditioned media after 24 h pre-treatment with normal oral fibroblast (NOF) or myofibroblast (myo) conditioned media or serum-free DMEM only (SFM) as determined by ELISA. 1% (v/v) FBS was included in all conditions to prevent cell death. Graphs display the mean of three independent experiments \pm SD, analysed by one-way ANOVA comparing to SFM control, ** $p < 0.01$.

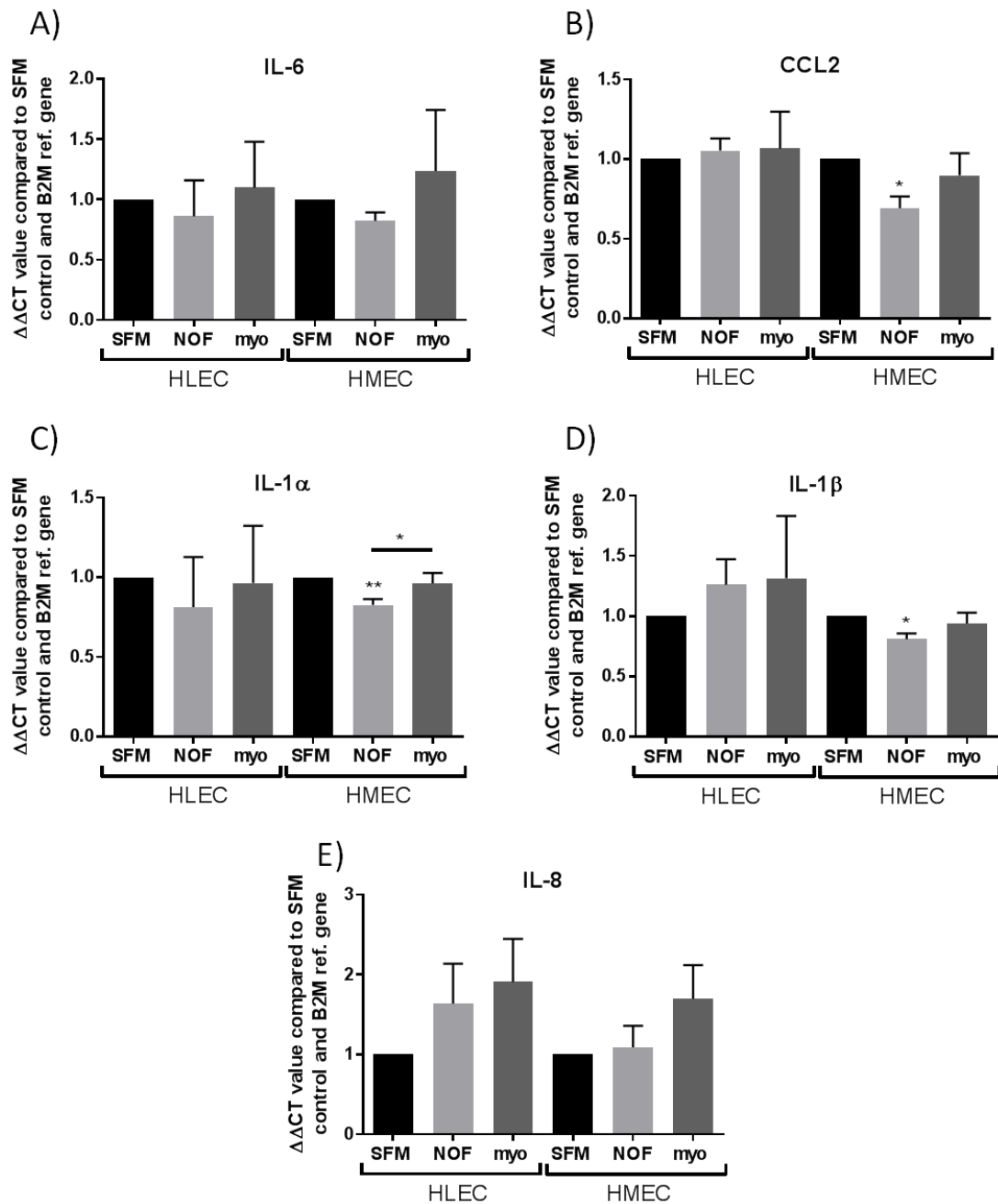


Figure 5.11. Effect of myofibroblast conditioned media on immune marker mRNA expression by HLEC and HMEC. mRNA expression of (A) IL-6, (B) CCL2, (C) IL-1 α , (D) IL-1 β and (E) IL-8 by HLEC and HMEC after 24 h pre-treatment with normal oral fibroblast (NOF) or myofibroblast (myo) conditioned media or serum-free DMEM only (SFM) as determined by qRT-PCR. 1% (v/v) FBS was included in all conditions to prevent cell death. Bars display the mean of three independent experiments \pm SD. Results are displayed as $\Delta\Delta\text{CT}$ values comparing to SFM control and B2M as a reference gene, analysed by one-way ANOVA comparing to respective SFM control (or to control NOF as indicated), * $p < 0.05$, ** $p < 0.01$.

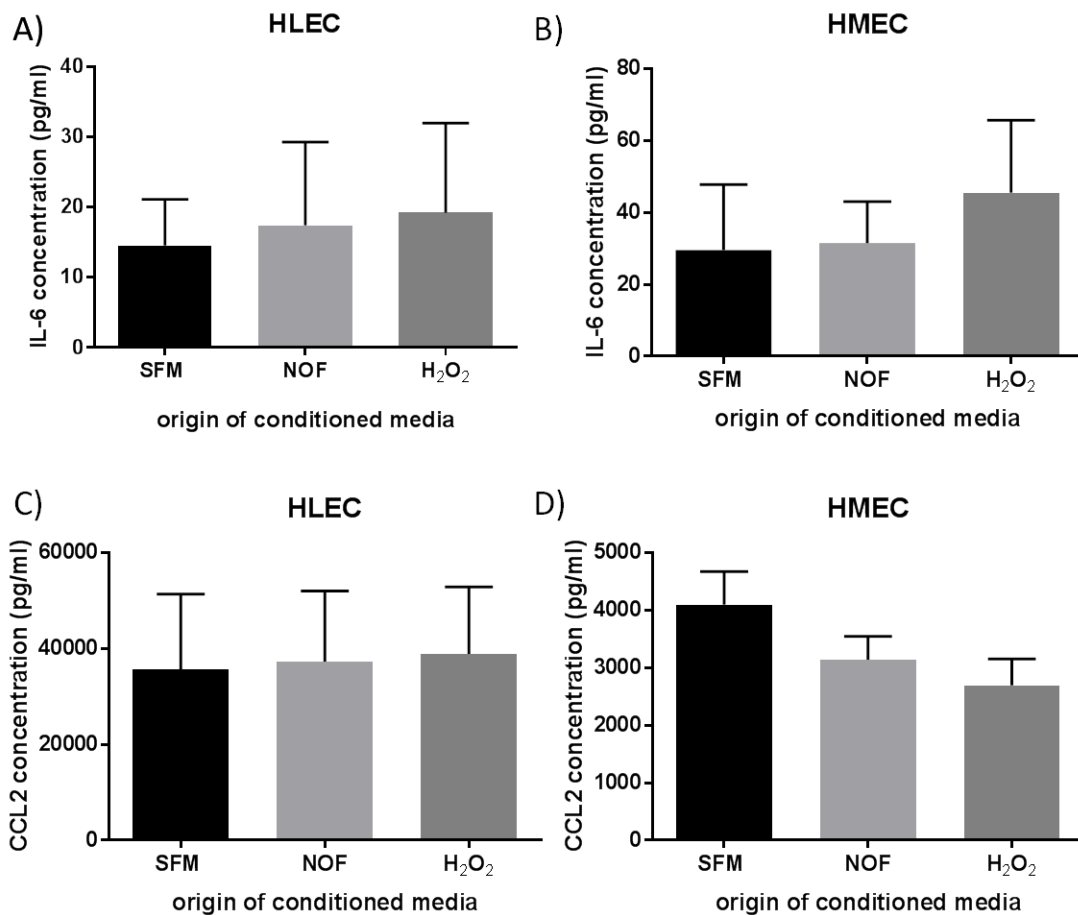


Figure 5.12. Effect of H₂O₂-senesced fibroblast conditioned media on IL-6 and CCL2 production by HLEC and HMEC. Concentration of IL-6 (A,B) and CCL2 (C,D) in HLEC (A,C) or HMEC (B,D) conditioned media after 24 h pre-treatment with normal oral fibroblast (NOF) or H₂O₂-senesced (H₂O₂) fibroblast conditioned media or serum-free DMEM only (SFM) as determined by ELISA. 1% (v/v) FBS was included in all conditions to prevent cell death. Graphs display the mean of three independent experiments \pm SD (HLEC IL-6 n=2 only due to anomalous result in 3rd experiment), analysed by one-way ANOVA comparing to SFM control.

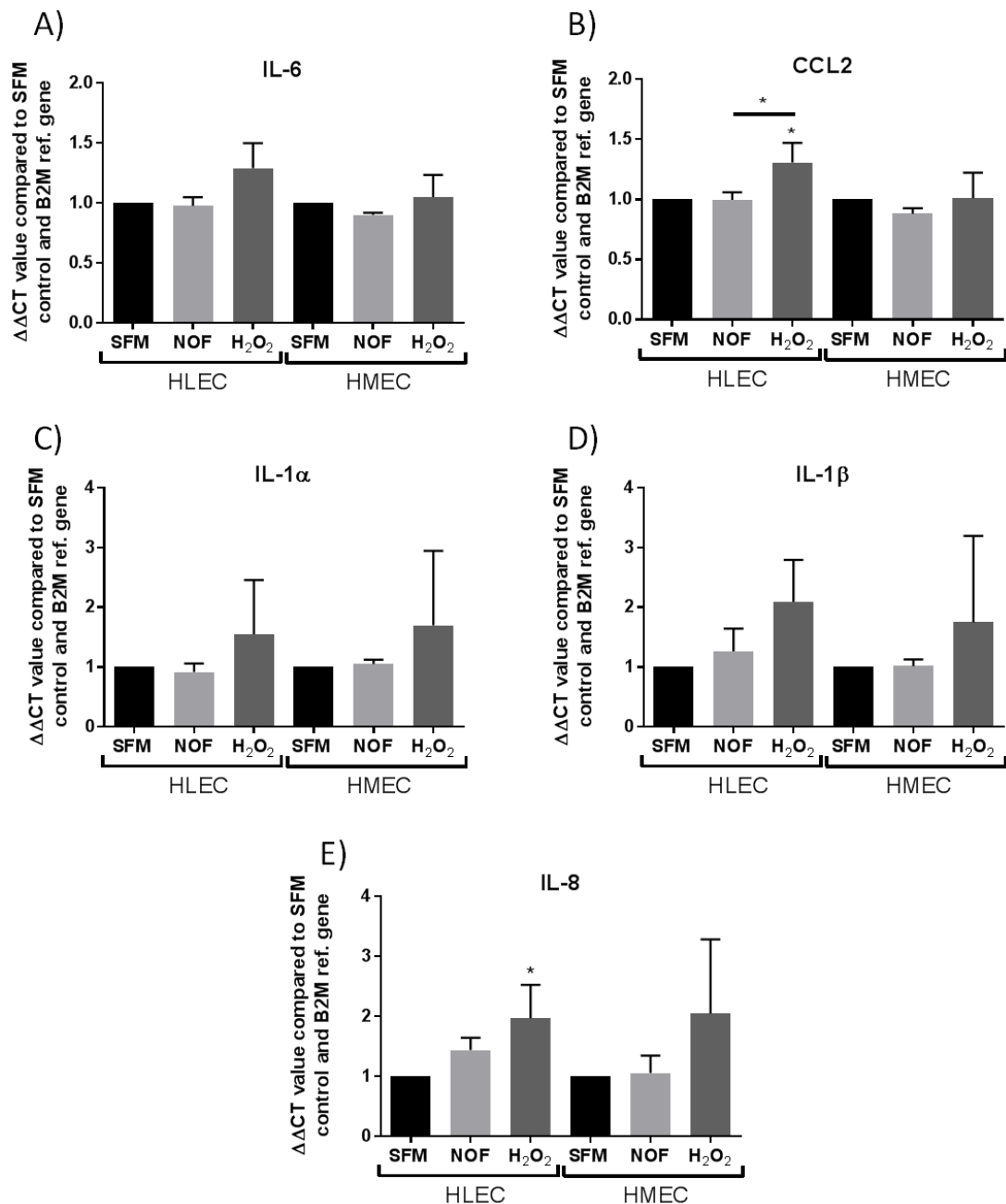


Figure 5.13. Effect of H₂O₂-senesced fibroblast conditioned media on immune marker mRNA expression by HLEC and HMEC. mRNA expression of (A) IL-6, (B) CCL2, (C) IL-1α, (D) IL-1β and (E) IL-8 by HLEC and HMEC after 24 h pre-treatment with normal oral fibroblast (NOF) or H₂O₂-senesced (H₂O₂) fibroblast conditioned media or serum-free DMEM only (SFM) as determined by qRT-PCR. 1% (v/v) FBS was included in all conditions to prevent cell death. Bars display the mean of three independent experiments ± SD. Results are displayed as ΔΔCT values comparing to SFM control and B2M as a reference gene, analysed by one-way ANOVA comparing to respective SFM control (or NOF control, as indicated), *p<0.05.

5.3. Summary

This chapter has described experiments investigating the effect of oral cancer cells and CAF on endothelial cell behaviour and immune marker expression *in vitro*. Firstly, assays related to vessel formation were carried out using both microvascular and lymphatic endothelial cells to test the hypothesis that primary tumour and lymph node metastases-derived OCCL and CAF can induce endothelial vessel formation. Tubule formation and proliferation assays were used and results are summarised in Table 5.1. OCCL conditioned media increased tubule formation in HLEC but only H₂O₂-senescent fibroblast conditioned media caused an increase in HMEC tubule formation. Proliferation rates were unchanged in both endothelial cell types with the exception of myofibroblast conditioned media-treated HLEC where an increase in cell number was observed.

Secondly, the hypothesis that OCCL and CAF conditioned media can induce inflammatory cytokine and chemokine expression in endothelial cells was tested. The secretion and mRNA expression of selected inflammatory cytokines and chemokines by HLEC and HMEC after conditioned media treatment was assessed and the results are summarised in Table 5.2. OCCL and experimentally derived-CAF conditioned media treatment resulted in some increases in IL-6 secretion and mRNA expression. Further mRNA analysis also revealed IL-8 expression was often elevated as a result of conditioned media treatment. This was true for both HLEC and HMEC.

Table 5.1. Summary of endothelial cell microtubule formation and proliferation assays comparing the effect of conditioned media from different OCCL and fibroblast types.

	Lymphatic endothelial cells (HLEC)	Vascular endothelial cells (HMEC)
OCCL induction of tubule formation	Significant increase due to conditioned media from all OCCL except TR146	<i>No significant effect</i>
OCCL effect on proliferation	<i>No significant effect</i>	<i>No significant effect</i>

Myofibroblast induction of tubule formation	<i>No significant effect</i>	<i>No significant effect</i>
Myofibroblasts effect on proliferation	Significant increase due to conditioned media from myofibroblasts and NOF	<i>No significant effect</i>
Senescent fibroblast induction of tubule formation	<i>No significant effect</i>	Significant increase due to conditioned media from H ₂ O ₂ -senescent fibroblasts
Senescent fibroblasts effect on proliferation	<i>No significant effect</i>	<i>No significant effect</i>

Table 5.2. Summary of chemokine and cytokine response of endothelial cells to conditioned media from different OCCL and fibroblast types.

	Lymphatic endothelial cells (HLEC)	Microvascular endothelial cells (HMEC)
OCCL effect on IL-6 and CCL2 secretion	Some increase in IL-6 (H357 and BICR22 significantly)	Some increase in IL-6 (H357 significantly)
OCCL effect on immune marker mRNA expression	Significant increase in IL-8 expression due to BICR22 and TR146 conditioned media <i>No other significant expression changes</i>	Significant increase in IL-6 expression due to BICR22 conditioned media Fold change >2 in IL-8 due to BICR22 and TR146 conditioned media but not significant <i>No other significant expression changes</i>
Myofibroblast effect on IL-6 and CCL2 secretion	Significant increase in IL-6 due to myofibroblast conditioned media.	<i>No significant effect</i>
Myofibroblast effect on immune marker mRNA expression	<i>No significant effect</i>	<i>No significant effect</i>
Senescent fibroblast effect on IL-6 and CCL2 secretion	<i>No significant effect</i>	<i>No significant effect</i>
Senescent fibroblast effect on immune marker mRNA expression	H ₂ O ₂ -senesced fibroblast conditioned media significantly increased CCL2 and IL-8 expression <i>No significant effect for remaining markers</i>	<i>No significant effect</i>

Chapter 6: Discussion

Lymph node involvement is the most important prognostic indicator in OSCC. Tumour presence in the lymph nodes results in a marked reduction in prognosis and survival rate and this is significantly worsened if tumours grow and infiltrate beyond the lymph node capsule into the surrounding neck tissue in a process called extracapsular spread (ECS) (Shaw *et al.*, 2010). The prognostic significance of these processes make development of lymph node metastases and ECS important areas of study but the mechanisms underlying them are poorly understood.

The role of the tumour microenvironment in promoting tumour development and metastasis is well established in OSCC and many other cancers. Cancer-associated fibroblasts (CAF) have been shown to play a particularly prominent role in promoting tumour development through the secretion of a variety of growth factors, cytokines and proteases and through their role in the maintenance of the extracellular matrix (ECM) (Madar, Goldstein and Rotter, 2013). The interaction of both CAF and tumour cells with endothelial cells and the immune system is also important, allowing the growth of new vessels and the formation of an inflammatory microenvironment. However, little is known about the nature and origins of the lymph node stroma and how it differs from the primary OSCC tumour stroma. Although there is growing evidence that tumour-stromal crosstalk promotes invasion, metastasis and EMT in primary OSCC, there is limited evidence for a role of the tumour microenvironment in promoting the growth and development of metastatic deposits in lymph nodes and particularly on ECS development.

This is the first study to comprehensively examine stromal and EMT marker expression in OSCC lymph node metastases and their paired primary tumours, and to compare those findings between ECS+ and ECS- patients. In addition, the inclusion of primary and lymph node-derived oral cancer cells in co-culture with fibroblasts and endothelial cells in a range of functional and expression based assays provides a novel insight into the similarities and differences between these two distinct tumour sites.

The specific aims of this project were:

1. To compare markers of stroma, vascularity and EMT in paired ECS positive (ECS+) and negative (ECS-) tumour tissue sections.
2. To generate myofibroblast and senescent fibroblasts from primary normal oral fibroblasts (NOF) and compare key markers to primary OSCC CAF.
3. To examine the effect of myofibroblast and senescent fibroblast conditioned media on EMT marker expression and migration of oral cancer cell lines (OCCL), including those derived from lymph node metastases.
4. To examine the effect of conditioned media from OCCL, myofibroblasts and senescent fibroblasts on lymphatic and vascular endothelial cell vessel formation and growth.
5. To examine the effect of co-culture of oral cancer cells, fibroblasts and endothelial cells on pro-inflammatory signalling.

6.1. Investigating ECS *ex vivo*

Despite their clinical significance, there is a lack of prognostic and diagnostic tools that can accurately predict lymph node metastasis (section 1.1.1.) and ECS occurrence (section 1.2.4.). As a result, many patients undergo elective neck dissection, which in many cases is unnecessary and results in significant morbidity. Using primary tumour clinicopathological data from the patient cohort used in this study it was not possible to predict ECS with the exception of primary tumour size, which was increased in ECS+ cases (section 3.2.1.). Other studies with much larger cohort sizes also do not report a direct link between primary tumour clinicopathological prognostic indicators and ECS (Wenzel *et al.*, 2004; Michikawa *et al.*, 2011) suggesting that likelihood of developing ECS is more complex than can be predicted from primary tumour pathology alone. It also highlights the need for investigation into more specific markers that can be used to predict ECS likelihood from primary tumours and explain its occurrence in lymph nodes. Due to its growing prominence in the cancer field, this project focussed on the tumour

microenvironment as well as the invasion-promoting EMT process by staining ECS+/- lymph nodes and their matched primary tumours for a range of markers.

6.1.1. CAF marker expression in ECS

This study found that percentage expression of the myofibroblast marker α SMA is enhanced in ECS+ lymph nodes and their paired primary tumours compared to ECS- specimens (section 3.2.2.). This agrees with and extends upon previous studies that identified elevated α SMA expression in primary OSCC tumours as a predictor of ECS (Kellermann *et al.*, 2007; Marsh *et al.*, 2011). Both of these previous studies carried out quantification by sorting primary tumour specimens into two or three categories based on the level of staining. In contrast, in this thesis percentage positive expression levels were calculated, reducing the subjectivity of the data collection. Nevertheless, the cohort size used here is smaller than these previous studies so validation of this finding in a larger sample size would give greater weight to this evidence. Increased α SMA expression in primary OSCC tumours has also been linked to increased recurrence and poor survival (Kellermann *et al.*, 2007, 2008; Vered, Dobriyan, *et al.*, 2010; Bello *et al.*, 2011; Marsh *et al.*, 2011) but our novel finding that myofibroblast presence is elevated in ECS+ lymph nodes suggests they may also play a role in promoting lymph node tumour development and ECS. In addition, stroma was absent in four of the 20 ECS- lymph nodes whereas all of the ECS+ had an identifiable stroma which suggests that the presence of stroma may play a role in facilitating ECS development.

Although these data provide strong evidence that a myofibroblast-rich stroma is important to the development of ECS there is also evidence that the CAF population is very heterogeneous and other CAF-characteristics may have significant prognostic implications. Of particular interest is the senescent CAF phenotype as this results in the secretion of many factors which influence cancer cell migration and invasion (Coppé *et al.*, 2008). However, identification of a senescence marker for use in IHC is difficult. The best-characterised marker for senescence, senescence-associated β -galactosidase (SA- β -gal), can only be detected in fresh or frozen tissue and is not suitable for formalin-fixed paraffin embedded

(FFPE) tissue. Most other proposed senescence markers either detect growth arrest rather than senescence specifically (e.g. cell cycle arrest or DNA damage markers) or cannot be measured in fixed tissue (e.g. telomere length). Sudan Black-B, a histochemical stain of lipofuscin (an aggregate of oxidised proteins) has been proposed as a novel method of senescence detection in FFPE tissue (Georgakopoulou *et al.*, 2013) but use of this stain has not been widely reported so requires independent validation to confirm its specificity. Nevertheless, if suitable markers can be identified, quantification of the senescent CAF population in these tumour specimens may yield interesting results.

Myofibroblasts are key secretors and remodellers of the ECM, of which the main structural protein is collagen I. However, no significant difference in the presence of collagen I between ECS+ and ECS- specimens was seen in this study (section 3.2.2.). There are limited data related to collagen presence in metastatic OSCC lymph nodes but evidence from a breast cancer study using metastatic mouse models and human lymph node tissue samples showed that collagen I density was increased in lymph nodes with metastatic deposits compared to tumour-free nodes (Rizwan *et al.*, 2015). This is backed up by research in other cancer types which linked increased collagen density and stiffness to a poor prognosis and the promotion of tumour invasion (Egeblad, Rasch and Weaver, 2010). However, there is currently limited evidence linking increased collagen deposition to OSCC progression (Ziober, Falls and Ziober, 2006; Salo *et al.*, 2014) and research suggests that ECM deposition and structure is very heterogeneous between cancer types and even between patients (Pickup, Mouw and Weaver, 2014). Investigation into alternative collagen isoforms and ECM components may therefore be necessary to elucidate any prognostic link in this case.

Additionally, ECM structure remodelling within metastatic lymph nodes may be an important and interesting avenue of research. Using a metastatic melanoma mouse model Riedel *et al.* (2016) found that collagen fibres were remodelled in late stage metastatic lymph nodes and that conduits were wider. Indeed there is a wealth of evidence to suggest that the structural organisation of collagen fibres and action of ECM-remodelling enzymes such as matrix metalloproteinases (MMPs),

impacts heavily on tumour behaviour (Egeblad, Rasch and Weaver, 2010). Elevated expression of MMPs in metastatic lymph nodes of breast cancer compared to tumour-free nodes has been reported (Daniele *et al.*, 2010) and MMP-2 and -9 expression has also been identified in OSCC lymph node deposits (Zhou *et al.*, 2010) but the significance of this with regards to ECS is unknown.

6.1.2. Altered vasculature and ECS

This study also found an increase in microvascular density (MVD) in ECS+ lymph nodes compared to ECS- nodes but found no significant difference in MVD in the primary tumours of the two groups (section 3.2.3). Several previous studies in OSCC have linked high primary tumour blood vessel density to increased lymph node metastasis (Miyahara *et al.*, 2007; Bolzoni Villaret *et al.*, 2009) and deeper local invasion (Li *et al.*, 2005), but did not report on the ability of primary tumour MVD to predict ECS. The only study looking in detail at blood vessel growth in OSCC lymph nodes found no difference in the number of vessels that co-stained with the proliferation marker ki67 when comparing nodes with and without metastatic deposits whereas extensive proliferating vessels were seen in the corresponding primary tumours (Naresh, Nerurkar and Borges, 2001). Surprisingly they also found that MVD was elevated in non-metastatic lymph nodes compared to metastatic nodes. However, this work was carried out in a very small cohort (n=9 OSCC cases), also included cases of laryngeal cancer and limited visual or quantification data were provided. Additionally, evidence from an *in vivo* mouse model of OSCC found that MVD is elevated in pre-metastatic tumour draining lymph nodes in response to implantation of metastatic cancer cells in the tongue compared to non-metastatic tumour cells (Mayorca-Guiliani *et al.*, 2012). This suggests that MVD is increased in lymph nodes in preparation for colonisation by tumour cells. However, no comparison to ECS was carried out in either study so these data remain the first to suggest MVD is increased in ECS.

Established systemic blood vessel markers were used in this study to allow a comparison with primary tumour MVD; however, several studies have instead focussed on the density of the lymph node-specific high endothelial venule blood

vessels (HEV). As for MVD, conflicting evidence has been reported showing that HEV density is elevated in lymph nodes with metastatic deposits (Lee *et al.*, 2012) but also conversely that HEV density is increased in sentinel lymph nodes (SLN) prior to lymph node colonisation (Chung *et al.*, 2012; Shen *et al.*, 2014). However, the correlation between HEV density and ECS was not reported in either of these studies and so a comparison of blood vessel and HEV density in our cohort would be an interesting extension to this work.

In contrast, this study found no significant difference in lymphatic vessel density (LVD) between the ECS+ and ECS- groups at either primary or lymph node sites (section 3.2.3.). Increased LVD has been linked to increased invasion and lymph node metastasis (Kyzas *et al.*, 2005; Zhao *et al.*, 2008) but available evidence on lymph node LVD changes are more conflicting. Increased LVD in SLN with metastatic deposits compared to those without has been previously reported (Wakisaka *et al.*, 2015). However, LVD has also been reported to be elevated in all SLN regardless of metastatic status compared to non-SLN (Chung *et al.*, 2012) and metastatic tumour cells have been shown to elevate LVD in pre-metastatic tumour draining lymph nodes to a greater extent than non-metastatic tumour cells implanted in to the tongue of mice (Mayorca-Guiliani *et al.*, 2012). This suggests that, as for MVD, LVD is elevated in lymph nodes and that this promotes colonisation. However, it is unclear if further changes occur following metastasis and, as this study is the first to compare lymph nodes with and without ECS, there is currently no evidence to support the theory that lymph vessel density or growth is important to ECS.

Another factor that may be as important as vessel density is the ability of tumour cells to invade into vessels. Clinicopathological data for this cohort found that higher numbers of ECS+ cases had primary tumour lymphovascular invasion compared to ECS- (40% vs. 25%) but this was not significant (section 3.2.1.). In contrast, other studies have found a link between lymphovascular invasion at the primary site and increased rate of lymph node metastasis and ECS (Jones *et al.*, 2009; Adel *et al.*, 2015). Adel *et al.* (2015) used a comparatively large cohort of 571 and found that when lymphatic and vascular invasion were considered as

independent factors only lymphatic invasion was a significant predictor of metastasis and ECS. This suggests that the ability of cancer cells to invade into vessels may be a better predictor of tumour metastasis than simply the presence of vessel structures. Pereira *et al.* (2018) examined the lymph nodes of head & neck cancer patients and observed isolated tumour cells at the leading edge of tumour masses in close association with blood vessels and, in a third of the samples, inside the vessel lumen. However, a correlation with clinical outcome or ECS was not reported.

6.1.3. Macrophage in ECS

When macrophage numbers were quantified contrasting results were seen depending on the primary tumour site, with an increase in macrophage density seen in ECS+ tongue specimens but a decrease seen for ECS+ floor of mouth specimens compared to their corresponding ECS- groups. This pattern was the same for lymph node and primary tumour sites (section 3.2.4.). The reason for this discrepancy is unknown but may be due to differences in environment found at each primary tumour site determining the level of macrophage recruitment. There was a large range in percentage positive cell numbers so it may also be that macrophage presence does not promote ECS directly but that the ability of primary tumours to attract macrophage to the tumour site may be reflected in their metastatic deposits. This is supported by the fact that macrophage percentage positivity correlated significantly between matched primary and lymph node tumour pairs. Most data relating to macrophages and OSCC development focus on the primary tumour where high macrophage numbers (using the CD68 marker as for this study) have been linked to higher rates of lymph node metastasis and poor prognosis (Weber *et al.*, 2014; Ni *et al.*, 2015; Yamagata *et al.*, 2017). This supports the hypothesis that macrophages promote tumour development but as this is the first study to report on macrophage levels in patients with and without ECS, it is hard to draw definite conclusions.

An important point raised by these studies is their disagreement as to the most appropriate microlocalisation to quantify macrophage numbers. Although the

majority of studies found macrophage density in the stroma adjacent to the invasive edge (as used in this study) had prognostic value (Fujii *et al.*, 2012; Ni *et al.*, 2015; Hu *et al.*, 2016; Yamagata *et al.*, 2017), others reported correlations to prognostic factors when quantifying macrophages within the tumour itself (Weber *et al.*, 2014; Hu *et al.*, 2016). Quantification of macrophage within different tumour microlocalisations would provide an interesting extension to this study.

Another important consideration to take into account is not only the numbers but also the polarisation of the macrophages present. As explained in section 1.7.1., macrophages may be one of two phenotypes: M1 (anti-inflammatory and anti-tumour) or M2 (pro-inflammatory and pro-tumour). The CD68 marker used here stains macrophages of both types. However, several studies either have focussed entirely on M2 macrophages using markers such as CD163, or have measured both M1 and M2 macrophages in order to calculate the degree of polarisation. Despite the emphasis on the importance of M2 macrophages with regards to cancer progression (Takeya and Komohara, 2016), the majority of OSCC studies found prognostic value in both total macrophage and M2 macrophage densities (Fujii *et al.*, 2012; He *et al.*, 2014; Weber *et al.*, 2014; Hu *et al.*, 2016; Yamagata *et al.*, 2017). This could be explained by the observation that the majority of macrophages found in the vicinity of tumours are of the M2 phenotype, so both quantification methods may simply highlight the importance of macrophage recruitment to tumour progression.

Nevertheless, determining the relative numbers of M1 and M2 macrophages in ECS+ and ECS- metastatic tumours would be an interesting avenue of research especially given the high numbers of native macrophages present in lymph nodes, which may therefore influence the lymph node response to tumour metastasis. The only paper to report on macrophages in the metastatic lymph nodes of OSCC patients, focussed on macrophages found in the lymph node sinus and how their polarisation correlated with clinical parameters in the primary tumour related to increased invasion and metastasis (Wehrhan *et al.*, 2014). Interestingly, they observed no difference in the polarisation of these macrophages between tumour-free and metastasis-containing nodes and hypothesised that changes to

macrophages in the primary tumour alter the phenotype of sinus macrophages to dampen the immune response of the lymph node *prior* to tumour colonisation. However, they did not look at tumour-associated macrophages or compare polarisation or density in ECS+ and ECS- lymph nodes. Determining if macrophage numbers or the degree of polarisation is altered due to ECS occurrence would clarify how effective anti-inflammatory treatments may be for preventing metastasis development in OSCC.

6.1.4. EMT marker expression in ECS

Expression of the EMT-inducing transcription factors slug, snail, TWIST1 and ZEB1 was observed in tumour and stromal cells at both lymph node and primary sites (section 3.2.5.). Antibodies for the snail family of EMT-inducing transcription factors showed a decrease in percentage positive expression in ECS+ tumour and stromal areas compared to ECS-. However, no difference in percentage positive expression of the TWIST1 or ZEB1 markers was observed.

Although there is evidence that elevated expression of these EMT transcription factors is linked to increased lymph node metastasis and poor prognosis in primary tumour OSCC (Wang *et al.*, 2012; Y. Zhou *et al.*, 2015; Yao and Sun, 2017), their prognostic impact in OSCC metastatic lymph nodes has not been reported. However, other studies on snail expression have found few associations with adverse clinicopathological factors and no correlation with increased lymph node metastasis (Franz *et al.*, 2009; Zhao *et al.*, 2012), so the link of these factors to tumour development is not certain. Snail expression has been previously observed in OSCC lymph nodes (Schwock *et al.*, 2010) but the significance of the depletion observed here is unknown.

In a recent seminal paper, which carried out single-cell transcriptome analysis of a cohort of primary and matched metastatic OSCC tumours, expression of these transcription factors at both primary and lymph node sites was found to be lacking, with only slug expression detected (Puram *et al.*, 2017). In addition, expression of epithelial markers persisted in the population but an expression signature of other EMT markers was identified, including podoplanin, vimentin and

TGF- β 1, which could differentiate between the different tumours used. The authors suggested this represented a state of partial EMT (p-EMT) and demonstrated that high expression of this p-EMT signature was maintained in the matched lymph node metastases. High levels of the p-EMT expression signature in a TCGA dataset were also significantly correlated with ECS and other adverse clinicopathological factors. It may be that detecting differences in the levels of classical E-cadherin repressing transcription factors was not possible in this study due to the transient nature of EMT, or because the primary tumour EMT status is maintained in lymph node metastasis regardless of their ECS status. There is little other information available on the EMT status of OSCC lymph node tumours with regards to ECS. Lee *et al.* (2014) found that high vimentin, low E-cadherin expression in lymph node OSCC tumours was a better predictor of recurrence and distant metastasis than ECS status alone. In fact, these EMT marker expressing patients who were also ECS+ had a five times worse survival rate than ECS- patients. This agrees with the findings of Puram *et al.* (2017) and implicates EMT, but not specifically EMT transcription factor expression, in ECS occurrence.

Interestingly, although there was no significant difference between the groups, levels of percentage expression correlated between the primary and lymph node sites for TWIST1 and ZEB1. This agrees with the findings of Vered, Dayan, *et al.* (2010), who found a positive correlation between lymph node and primary tumour expression levels of several EMT markers including TWIST1. Puram *et al.* (2017) also noted that the p-EMT signatures of paired primary and lymph node tumours matched using single cell transcriptome analysis, although some variability was evident. Overall, this suggests that expression of these EMT transcription factors in tumours is maintained at the lymph node site but that they may not be directly useful as prognostic markers for ECS.

This study observed expression of all four transcription factors in stromal cells as well as within the tumour and quantified stromal expression separately although this yielded similar results to tumour areas. TWIST1 and ZEB1 positive cells particularly were observed more commonly in stromal areas. The cause and effect of stromal cell expression of these markers is not clear. Snail and slug expression

has been associated with myofibroblast activation (Francí *et al.*, 2006) and co-expression of snail and α SMA in the stromal invasive front has been previously reported in OSCC (Franz *et al.*, 2009). A weak positive correlation was seen between snail/slug expression and α SMA expression in this study but, as for Franz *et al.* (2009), only α SMA was able to predict adverse clinical outcome. More investigation into the relationship between EMT transcription factor expression and fibroblast activation is needed to fully understand this phenomenon.

6.1.5. Summary of IHC findings

The IHC investigations reported here provide a novel insight into the tumour microenvironment of OSCC lymph nodes and how alterations to this may aid ECS development. They also highlight specific cell types that were altered in ECS+ nodes and therefore are potentially important to lymph node tumour development, notably CAF, endothelial cells and TAM. To follow on from this work, *in vitro* analysis of these cell types in relation to lymph node metastasis-derived oral cancer cell lines (OCCL) was carried out.

6.2. Fibroblasts

There is growing evidence in OSCC and other cancers that cancer-associated fibroblasts (CAF) can have a profound effect on many cancer processes including proliferation, migration, invasion and metastasis. Despite this CAF are still not well defined in terms of CAF-specific cell markers and also their origins (Madar, Goldstein and Rotter, 2013). The origin of CAF within the lymph node is also disputed, as although normal lymph nodes have minimal fibroblasts, abundant CAF are often present in association with metastatic deposits in lymph nodes. To study the interaction of CAF with lymph node and primary tumour OSCC cells *in vitro*, both myofibroblasts and senescent fibroblasts were generated to model the CAF phenotype and were then compared to primary patient-derived CAF.

6.2.1. Myofibroblast generation

This study found a significant elevation in α SMA-positive myofibroblast presence in ECS+ lymph nodes and their matched primary tumours, which supports previous research that has linked myofibroblast presence to altered tumour behaviour (section 3.2.2. and discussion 6.1.1.). To investigate this relationship *in vitro* myofibroblasts were generated from normal oral fibroblasts (NOF) by treating them with TGF- β 1. This resulted in a significant up-regulation of α SMA protein and mRNA levels (section 4.2.1.). The use of TGF- β 1 to induce myofibroblast differentiation has been previously demonstrated successfully in primary oral fibroblast cultures in this lab and by others (Lewis *et al.*, 2004; Kellermann *et al.*, 2008; Berndt *et al.*, 2014; Elmusrati *et al.*, 2017; Melling *et al.*, 2018). TGF- β 1 levels have also been found to be elevated in cancer, making this model physiologically relevant to the cancer setting (Levy and Hill, 2006). Nevertheless, it does represent a simplification of the *in vivo* tumour-stroma signalling situation and alternative methods have been proposed, such as the use of OCCL conditioned media (Lewis *et al.*, 2004; Dudás, Bitsche, *et al.*, 2011). However, in this study exposure of NOF to OCCL conditioned media for 24 h did not induce expression of myofibroblast markers (section 4.2.6.). Alteration to the experimental protocol and extension of incubation time could be used to fully investigate the relative effect of the OCCL panel on NOF differentiation. However, as the aim of generating these fibroblasts was to see how their conditioned media affected the signalling and behaviour of a panel of different OCCL, inducing differentiation using conditioned media would have added more unknown variables to the experimental design. Furthermore, Lewis *et al.* (2004) showed that blocking TGF- β 1 prevented this conditioned media effect, which supports the use of TGF- β 1 as an inducer in this study.

6.2.2. Senescent fibroblast generation

Senescent fibroblasts have also been identified as an important CAF phenotype in OSCC and other cancer types. The senescence-associated secretory phenotype (SASP) results in the secretion of proteases, chemokines, growth factors and other signalling molecules, many of which have been implicated in the promotion of cancer growth and invasion (Coppé *et al.*, 2010). Therefore,

senescence was induced in primary NOF cultures using two different methods to serve as another model of CAF for use in further experiments. Firstly, senescence was induced using hydrogen peroxide (H_2O_2) and, secondly, replicative senescent cells were generated by prolonged culturing.

NOF were exposed to H_2O_2 for 2 h and then cultured for a further 10 days to allow senescence to develop. At this time point over 75% of the cells were senescent according to results from a senescence-associated β -galactosidase (SA- β -gal) assay. Use of H_2O_2 to induce senescence has been previously reported by this lab and others (Hassona *et al.*, 2013; Kabir, 2015; Kabir *et al.*, 2016). Furthermore, the use of hydrogen peroxide is physiologically relevant as reactive oxygen species (ROS) are known to be produced by both tumour cells and CAF (Costa, Scholer-Dahirel and Mechta-Grigoriou, 2014). Hassona *et al.* (2013) showed that conditioned media produced by OSCC cells from a genetically unstable tumour contained ROS and could induce senescence in fibroblasts. The corresponding primary CAF were senescent, and displayed oxidative damage and a lack of antioxidant defences. Indeed there is growing evidence to suggest that the presence of ROS not only activates CAF but also affects their ability to crosstalk with cancer cells (Costa, Scholer-Dahirel and Mechta-Grigoriou, 2014).

Replicative senescence occurs naturally as a result of telomere shortening due to prolonged culturing (Hayflick and Moorhead, 1961). SA- β -gal assays on NOF cultured to passage >30 to cause replicative senescence indicated over 80% of the cells were senescent. Given the link of OSCC with old age, this method is particularly relevant to this study.

Nevertheless, alternative methods of senescence induction such as irradiation or treatment with the chemotherapeutic drug cisplatin could also have been utilised. These methods would be relevant to this study as they represent the potential impact of common OSCC treatments on the remaining CAF population. Cisplatin-induced fibroblast senescence has been previously studied in our lab and was shown to induce morphological and gene expression changes analogous to that seen in H_2O_2 -senesced and replicative senescent fibroblasts, including high SA- β -gal positivity and increased p16 and p21 mRNA expression (Kabir, 2015; Kabir *et al.*,

2016). This work went on to show that cisplatin-senesced oral fibroblast could promote the migration and invasion of primary OCCL, and that this was due, in part, to their elevated secretion of the pro-inflammatory cytokine CCL2.

The main indicator of senescence used here was the SA- β -gal assay. This was first proposed by Dimri *et al.* (1995), who demonstrated, using primary human fibroblast cultures, that senescent cells display augmented expression of lysosomal β -galactosidase at pH 6.0. They reported an absence of positive SA- β -gal staining in quiescent cells generated through serum starvation and confluency of cell cultures. However, others have reported some false positive staining, particularly in over-confluent or stressed cultures (Yang and Hu, 2005). To negate this, fibroblasts were seeded at low density and incubated in full serum media overnight before SA- β -gal assays were carried out. Other markers for senescence have been proposed including DNA damage and cell cycle arrest markers (such p21 and p16 used in this study) and heterochromatin formation (Matjusaitis *et al.*, 2016). However, the large majority of these are not senescence specific and may also be expressed by quiescent cells or cells undergoing cellular stress so must be used with caution, and in combination, to avoid false positive results.

6.2.3. Evaluation of the use of CAF models *in vitro*

Primary CAF cultures were also used in this study to provide a better representation of the OSCC tumour stroma. OSCC-derived CAF have many advantages, particularly as they represent the true heterogeneity of the CAF population (Lim *et al.*, 2011; Costea *et al.*, 2013; Hassona *et al.*, 2013; Madar, Goldstein and Rotter, 2013). Myofibroblast and senescent fibroblast markers were measured to allow a comparison to the experimentally-derived CAF discussed above. CAF displayed some increase in α SMA expression at the protein and mRNA level but this was not significant. CAF also expressed some markers of senescence although the percentage of SA- β -gal positive cells did not reach levels recorded for either H₂O₂-induced or replicative senescent fibroblasts (section 4.2.1.). This suggests that experimentally inducing myofibroblast differentiation or senescence produces cells with a more robust expression of commonly used markers for each

phenotype. However, it also highlights the heterogeneity of CAF as these results could be explained by the existence of multiple sub-types of fibroblast within the CAF population and/or the presence of CAF that are both senescent and α SMA-positive. Hassona *et al.* (2013) found a correlation between senescence and α SMA expression in their panel of primary CAF cultures and also reported that prolonged TGF- β 1 stimulation induced both α SMA and senescence marker expression in NOF. This supports data from our lab which showed that senescence induction in NOF using H₂O₂ or cisplatin is accompanied by an increase in α SMA expression although replicative senescent fibroblasts showed decreased α SMA expression compared to NOF (Kabir, 2015; Kabir *et al.*, 2016). This complexity makes it hard to define the characteristics of a CAF population based on whole population samples. One method to mitigate this heterogeneity is the isolation and clonal expansion of specific cells within the primary CAF population as demonstrated by Sobral *et al.* (2011). However, when using this method, careful selection criteria must be employed to ensure that the cloned population is representative of the CAF population as a whole.

Although primary CAF provide a more accurate representation of the *in vivo* situation, there are some advantages to the use of the experimentally-derived CAF models described above. Firstly, they are easier to source meaning more experiments can be carried out over a set period. They also allow both the control fibroblasts and “CAF” to be derived from the same patient source. This eliminates patient-patient variability as a source of difference in response, making the results more comparable. Although “normal” fibroblasts could be sourced from cancer patients, there is evidence that histologically normal cells in the vicinity of tumours may still exhibit genetic alterations analogous to those seen in malignant cells due to field cancerisation from prolonged carcinogen exposure (Rema *et al.*, 2015). Additionally, this would increase the burden on the OSCC patients and so may not be possible if ethical approval or surgical support is not in place.

There are competing theories as to the origins of lymph node CAF (Madar, Goldstein and Rotter, 2013). The theory that primary CAF travel with tumours to the secondary site and then aid the development of lymph node tumours supports the

use of primary tumour derived CAF as described here. However, if CAF are generated *in situ* due to cancer-derived signals then this may be less directly relevant to the lymph node situation. Characterisation of patient-derived primary tumour and lymph node metastases-associated CAF would allow for a more detailed comparison, especially if derived from the same patient. However, lymph node CAF are difficult to source without compromising the diagnostic pathology process for the patient. The predominant fibroblast population in the lymph node are fibroblast reticular cells (FRC, section 1.4.4.) and so investigation into their response to cancer cell signalling, particularly TGF- β 1 signals, would be a useful next step. However, currently human FRC cultured cells are not available so primary tumour CAF provide the closest equivalent. Endothelial cells have also been cited as a source of CAF, with some reports stating that up to 40% of CAF display endothelial markers (Zeisberg *et al.*, 2007) so their ability to transform into CAF could also be investigated.

Having generated and sourced CAF for use *in vitro*, this study went on to investigate their influence on OSCC cancer cell line signalling and behaviours that relate to lymph node metastasis and ECS.

6.3. EMT and migration in lymph node metastasis

Epithelial-mesenchymal transition (EMT) is a key mechanism by which cancer cells gain the ability to migrate and invade into the surrounding tissues. EMT allows epithelial-like cells to lose their cell-cell adhesion contacts, remodel their cytoskeleton, and form invadopodia, allowing for individual cell movement (Figure 1.2.). A crucial step in the EMT process is the down-regulation of E-cadherin due to the binding of transcriptional repressors such as slug, snail, TWIST1 and ZEB1 (Krisanaprakornkit and Iamaroon, 2012).

There are many known triggers of EMT, both intrinsic and extrinsic. Growth factors such as TGF- β 1 and epidermal growth factor (EGF) have been identified as key initiators of EMT in cancer and have been used in OSCC to induce EMT *in vitro* (Qiao, Johnson and Gao, 2010; Richter *et al.*, 2011; Yu *et al.*, 2011). Fibroblasts, as

key growth factor secretors within the tumour microenvironment, are consequently an interesting avenue of study in relation to EMT. Therefore, co-culture of fibroblasts and oral cancer cells was employed to investigate this.

6.3.1. EMT marker expression in oral cancer cell lines (OCCL)

Evidence of EMT transcription factor expression was found in our primary and lymph node metastasis OSCC specimens although no clear difference was seen between ECS+ and ECS- patients (section 3.2.5. and discussion 6.1.4.). Nevertheless, elevated expression of EMT transcription factors and mesenchymal markers in the primary tumour has been linked to poor prognosis and higher rates of metastasis (Nijkamp *et al.*, 2011; Wang *et al.*, 2012; Ding *et al.*, 2014; Y. Zhou *et al.*, 2015; Yao and Sun, 2017). In concordance with this, in this study both the primary metastatic tumour (H376) and lymph node tumour derived (BICR22 and TR146) OCCL displayed expression of the mesenchymal marker vimentin and lacked expression of the epithelial marker E-cadherin. This was in contrast to the non-metastatic primary tumour-derived cell line H357 that showed strong E-cadherin expression and a lack of mesenchymal markers. Evaluation of EMT marker expression in a larger range of OCCL would be interesting to determine if marker expression is similar in other lymph node-derived cell lines compared to that observed here.

6.3.2. Fibroblast effect on EMT marker expression by OCCL

Conditioned media from myofibroblasts and senescent fibroblasts was added to the panel of OCCL outlined above in order to assess if there was any response in terms of EMT marker expression. In response to myofibroblast conditioned media, very few EMT-related protein and mRNA changes were observed with the only significant increases seen in mRNA expression of ZEB1 and slug in BICR22 and TR146 cell lines, respectively (section 4.2.2.). This is surprising given the reported link between myofibroblasts and EMT induction (Cirri and Chiarugi, 2011, 2012) but may be partly explained by the predominantly mesenchymal nature of the majority of the cell lines used here. As stated above, determining the EMT status of a wider range of lymph node-derived cell lines may

identify OCCL more susceptible to EMT induction *in vitro*. Nevertheless, Berndt *et al.* (2014), who used a similar experimental design to that employed here, reported only an upregulation of vimentin with no change in E-cadherin and no alteration to the mesenchymal markers N-cadherin and cytokeratin in the OCCL used. This suggests that, additionally, exposure of OCCL to myofibroblast conditioned media may not be sufficient to induce a full EMT transition within this time period.

This study also reported very few changes to OCCL EMT marker expression in response to either H₂O₂-senesced or replicative senescent conditioned media (section 4.2.3.); with only slight alteration to mRNA expression of some of the EMT transcription factors observed. There are limited data relating directly to the ability of senescent fibroblasts to induce EMT in OSCC but some evidence from other cancer systems suggests senescent fibroblasts can induce EMT. For example, Taddei *et al.* (2014) incubated prostate cancer cells with conditioned media from replicative senescent and H₂O₂-induced senescent fibroblasts. They observed a significant up-regulation of ZEB1, ZEB2 and vimentin expression corresponding with a decrease in E-cadherin. Similar results using replicative senescent fibroblast conditioned media have been obtained in breast cancer (Coppé *et al.*, 2008) and using epidermal keratinocytes (Malaquin *et al.*, 2013) and these changes were also accompanied by an increase in invasive ability.

In this study, CAF conditioned media also had no effect on the expression of EMT markers by the epithelial OCCL H357. This is in contrast to a previous study that demonstrated the ability of OSCC CAF conditioned media to induce decreased E-cadherin and increased vimentin expression in a panel of OCCL (Zhou *et al.*, 2014). However, in that study, conditioned media was incubated with the OCCL for 2 weeks and different cell lines were used which may explain this difference. This and other previously cited studies (Coppé *et al.*, 2008; Malaquin *et al.*, 2013) suggest that perhaps a longer incubation period is necessary, particularly for the development of phenotypical changes such as the loss of E-cadherin expression. Berdiel-Acer *et al.* (2011) investigated the timing of EMT in more detail by performing a time course analysis of EMT marker expression in colorectal cancer cells incubated with conditioned media from primary CAF. They showed that most

markers increase sequentially over time with some, such as slug, not showing up-regulation until 72 h. Soon *et al.* (2013) measured vimentin and E-cadherin expression in breast cancer cell lines treated with CAF conditioned media after 6 and 10 days of incubation. Although vimentin was upregulated by day 6, E-cadherin did not decrease until day 10 suggesting a longer incubation period may be needed. Nevertheless, several previous studies including those cited above used 24-48 h incubation periods and reported expression changes including E-cadherin and vimentin (Shintani *et al.*, 2013; Taddei *et al.*, 2014; Yu *et al.*, 2014).

As well as alterations to experimental timing and enlargement of the OCCL panel, alternative experimental set-ups could be employed, particularly to determine if direct cell contact is needed for EMT induction by fibroblasts. Alteration to EMT marker expression due to direct co-culture of cancer cells and fibroblasts has been demonstrated in other cancers (Gao *et al.*, 2010) with one study in lung cancer reporting that the changes were more pronounced under direct co-culture conditions (Choe *et al.*, 2013). However, care must be taken to ensure mesenchymal cancer cells and fibroblast cells can be separated at the end of the experimental period, for example by fluorescent cell tagging and separation by fluorescence-activated cell sorting (FACS) (Gao *et al.*, 2010; Choe *et al.*, 2013).

Moreover, the use of 3D models would increase the complexity of co-culture and may better represent the interaction between tumour and stromal cells, as well as allowing the incorporation of an ECM. *In vitro* 3D models of oral mucosa and early invasive OSCC have been developed which include both epithelial/cancer cells and fibroblasts as well as an ECM (Colley *et al.*, 2011) and have also been generated using TR146 cells (Moharamzadeh *et al.*, 2008) and with the use of de-epithelialised dermis with H357 cells (Kabir, 2015; Kabir *et al.*, 2016). This could be used to look at the effect of including myofibroblasts, senescent fibroblasts or primary CAF on the expression of EMT markers by OCCL as well as their invasion pattern (see discussion 6.3.3.). Increases in some EMT transcription factors in H357 cells due to the presence of some subsets of CAF has been demonstrated in preliminary experiments using 3D models in our lab (Kabir, 2015) but further data are needed to confirm and extend this result. Additionally, these models are designed to mimic

the oral mucosa environment through their use of an air-liquid interface and a distinct epidermal and dermal layer so are less relevant to the development of the lymph node metastatic tumour. Instead, the use of multicellular tumour spheroids could be employed (Stadler *et al.*, 2015).

6.3.3. Fibroblast effect on migration of OCCL

The migratory ability of the panel of OCCL in response to fibroblast conditioned media was assessed using transwell assays (section 4.2.5.). This revealed that higher numbers of the lymph node metastases-derived cell lines BICR22 and TR146 migrated to the lower side of the membrane than the non-metastatic primary tumour derived cell line H357. In two experiments the metastatic primary tumour derived cell line H376 displayed migrated cell numbers that were similar to BICR22 and TR146 but levels similar to the H357 cell line were observed in a further experiment using myofibroblast conditioned media. This highlights the variability of cell-based assays and the need for further repeats to fully draw conclusions from this work. The higher migratory ability of the H376, BICR22 and TR146 cell lines makes sense because these cell lines showed expression of mesenchymal markers, which is associated with an increase in migratory ability (section 4.2.2-3.). This matches to previous research showing OCCL with low E-cadherin expression show greater levels of migration in a transwell assay (Yokoyama *et al.*, 2001). In addition, when a primary and lymph node tumour cell line derived from the same patient were compared the metastatic cell line had a higher migratory and invasive capacity (Fujinaga *et al.*, 2014). Although the authors did not report on EMT markers specifically, a microarray revealed an upregulation of the E-cadherin repressor snail in the metastatic cell lines, suggesting the metastatic cells may have been more mesenchymal in nature.

The ability of myofibroblast, senescent fibroblast and CAF-derived conditioned media to induce OCCL migration compared to NOF was also assessed. Only H₂O₂-induced senescent fibroblast conditioned media caused a significant increase in migration (in H357 and BICR22 cells only). This agrees with and extends on previous research in our lab which also found that H₂O₂-induced senescent

fibroblast conditioned media significantly increased the migration of H357 cells using a similar experimental design to that employed here (Kabir, 2015; Kabir *et al.*, 2016). This previous work also reported that CAF conditioned media could increase the migration of H357 cells, in contrast to the preliminary findings here. However, only CAF derived from genetically unstable tumours (which were more senescent) caused a significant increase in migration, with CAF derived from genetically stable tumours inducing a response similar to the NOF control. This suggests that the factors secreted due to senescence induction may be important to the CAF ability to induce migration as both the genetically stable and unstable tumour-derived CAF displayed elevated expression of the α SMA myofibroblast marker. However, myofibroblast conditioned media has been shown to induce migration of H357 cells greater than the corresponding NOF (Melling *et al.*, 2018) and a further study demonstrated that a panel of α SMA expressing CAF could increase the migration of several different OCCL significantly more than low α SMA expressing NOF (Zhou *et al.*, 2014). However, they did not report on the senescent status of the CAF cultures or their genetic background. Together this highlights the inherent heterogeneity between different CAF cultures, meaning multiple samples are needed to determine which CAF characteristics and secreted factors are most associated with stimulation of migration.

Furthermore, an interesting extension to these studies would be the inclusion of an ECM layer to assess the invasive ability of the different cell lines used here and their responses to conditioned media from the different fibroblast types. There is some existing evidence to suggest that myofibroblasts (Daly, McIlreavey and Irwin, 2008; Marsh *et al.*, 2011; Melling *et al.*, 2018), senescent fibroblasts (Kabir, 2015; Kabir *et al.*, 2016) and primary CAF (Li *et al.*, 2015; Lin *et al.*, 2017) are able to increase invasion of OCCL in a transwell assay. However, assessing the relative response of the panel of OCCL used here would be an interesting extension to these previous findings. Furthermore, the use of multicellular 3D models would provide a more detailed insight into the invasion pattern and direct influence of CAF presence (see also 6.3.2. discussion). The enhanced ability of senescent fibroblasts and CAF to induce invasion of H357 cells compared to NOF in 3D de-epithelialised

dermis models of oral mucosa has been demonstrated previously in our lab (Kabir, 2015; Kabir *et al.*, 2016) and demonstrated with further OCCL in a 3D biomatrix model by others (Costea *et al.*, 2013). However, a confirmation of this result and comparison with the remaining cell types on this panel would provide an interesting extension to this work. As stated above, the use of tumour spheroids or a more relevant model to the lymph node microenvironment may also be needed to investigate lymph node metastases invasion more appropriately.

6.4. Vasculature

The ability of tumours to induce the formation of vascular and lymphatic vessels is important not only for the facilitation of tumour growth but also to provide a potential route of metastasis. Elevated vessel densities have been reported in the primary tumour and linked to increased invasion and lymph node metastasis (Miyahara *et al.*, 2007; Zhao *et al.*, 2008). However, the behaviour of endothelial cells in the lymph node tumour microenvironment and the extent to which new vessel growth occurs following tumour colonisation is less clear. This study found that blood vessel densities are elevated in ECS+ lymph nodes but no significant difference in lymphatic vessel density was observed (section 3.2.3. and discussion 6.1.2.). To extend this work, the effect of conditioned media from a panel of primary and lymph node metastases-derived OCCL (as used previously) on the tubule formation ability and proliferation of lymphatic and vascular endothelial cells was assessed.

6.4.1. OCCL effect on endothelial cell microtubule formation

Microtubule formation by human dermal lymphatic endothelial cells (HLEC) was significantly increased in the presence of conditioned media from all OCCL used compared to the media only control with the exception of TR146. This effect could not be attributed to proliferation, as there was no significant difference in cell number after the same time period, as assessed by MTS assay (section 5.2.1.). The ability of OCCL to induce tubule formation in HLEC has been previously demonstrated which supports this result (Zhuang *et al.*, 2010). However, they found

that metastatic OCCL induced HLEC tubule formation to a greater extent than non-metastatic cells which does not match to the finding here of no difference between non-metastatic and metastatic OCCL. However, in contrast, this previous study compared a metastatic OCCL generated through repeated *in vivo* selection for lymph node metastasis in mice to its human parental cell line rather than from a human metastatic tumour. They also carried out the tubule formation assays with fibronectin coated wells rather than using Matrigel and no images were provided to demonstrate the successful formation of tubules. Aside from this study, there is a lack of *in vitro* evidence in OSCC to supporting the finding here that cells derived directly from lymph node metastasis are capable of inducing lymphatic vessel formation equal to that of primary tumour cells. Nevertheless, some *ex vivo* evidence exists that suggests metastatic deposits alter lymphatic vasculature following colonisation (as discussed in section 6.1.2.).

In contrast, microtubule assays carried out using human dermal microvascular endothelial cells (HMEC) found no difference in tubule formation in the presence of OCCL conditioned media compared to the media only control (section 5.2.1.). As for HLEC, there was no significant difference in cell number after the same time period under any of the media conditions used as determined by MTS assay. *In vitro* evidence of OCCL induction of microvascular tubule formation is lacking but co-expression of vascular and proliferative markers has been identified *ex vivo* in the primary tumour (Naresh, Nerurkar and Borges, 2001).

6.4.2. Fibroblast effect on endothelial cell microtubule formation

Ex vivo data have linked higher myofibroblast presence to elevated vascular and lymphatic vessel density in OSCC primary tumours (Ding *et al.*, 2014; Lin *et al.*, 2017). However, this study found no direct correlation between percentage positive cell expression of α SMA and lymphatic or vascular vessel density in the primary and lymph node metastasis specimens used (section 3.2.3.). Nevertheless, there is no doubt that CAF and endothelial cells interact in the tumour microenvironment and that CAF are capable of secreting factors which promote vessel formation (Coppé *et al.*, 2006; Cirri and Chiarugi, 2012). Incubation of HLEC or HMEC with conditioned

media from myofibroblasts or senescent fibroblasts did not result in any significant change in tubule formation with the exception of HMEC treated with H₂O₂-senescent fibroblast conditioned media, which caused increased tubule formation compared to the media only control. However, this was based on two experimental repeats and the increase was not significant compared to NOF conditioned media (section 5.2.2.).

There are little previous experimental data related to OSCC with which to compare these results. The ability of CAF-conditioned media to induce tubule formation in human umbilical vein endothelial cells (HUVEC) to a great extent that that of NOF has been shown in a Matrigel based tubule formation assay (B. Zhou *et al.*, 2015). Myofibroblast (generated through tumour necrosis factor- α (TNF α) stimulation rather than TGF- β 1) conditioned media also increased tubule formation compared to NOF by HUVEC in the same study.

To extend these investigations, primary CAF conditioned media could be used. In addition, conditioned media from CAF co-cultured with different OCCL may better represent how the crosstalk between these two cell types can influence vessel formation and link this work back to lymph node metastasis development. Moreover, FRC have been identified as the principal VEGF secretors in the lymph node (Chyou *et al.*, 2008) so their inclusion in a co-culture model may provide an important tool for the study of lymph node angiogenesis induction.

6.4.3. Investigating endothelial cell behaviour *in vitro*

Microtubule formation assays are a useful and well-used tool for investigating vessel formation *in vitro*. They provide a cheap, quick, and simple method that allows the assessment of attachment, migration and tubule formation processes of angiogenesis in one assay (Arnaoutova and Kleinman, 2010). However, they also have some limitations, which must be taken into consideration when drawing conclusions from this work. One of these is the use of Matrigel to represent the ECM. Matrigel is derived from mouse Engelbreth-Holm-Swarm (EHS) sarcoma, which was found to contain many of the same components as ECM basement membrane found in humans. However, as well as being derived from a mouse

rather than human tumour, it has also been reported that the composition and protein isoforms present may not be equivalent to that seen *in vivo* (Rowe and Weiss, 2008). Other problems such as batch-to-batch variability in protein and growth factor composition were controlled for here by minimising the number of batches used and using growth factor-reduced Matrigel.

As well as alterations to the current method, alternative ways to investigate the relationship between endothelial cells, cancer cells and CAF could be employed. These include comparing the ability of different cell lines to adhere to endothelial cells using fluorescent cell labelling. Analysis of selected secreted factors by CAF and OCCL both in monoculture and co-culture could also be investigated, such as the expression of different VEGF isoforms. Increased secretion of VEGF-A and -C by metastatic OCCL has been demonstrated *in vitro* (Zhuang *et al.*, 2010; Yanase *et al.*, 2014; Morita *et al.*, 2015). In addition, it is known that myofibroblasts and senescent fibroblasts are capable of VEGF secretion (Coppé *et al.*, 2006; Cirri and Chiarugi, 2012), but the relative effect of OCCL with different metastatic potential and origins on secretion levels of these factors by fibroblasts would provide an extra insight into this relationship. This would also link to *ex vivo* studies that found a link between high VEGF-A and -C expression, invasion pattern and lymph node metastasis using immunohistochemical and PCR methodology (Siriwardena *et al.*, 2008; Sales *et al.*, 2016; Abdul-Aziz *et al.*, 2017). To link this work to the development of lymph node metastatic tumours, VEGF secretion by FRC could be investigated with and without the presence of metastatic lymph node-derived OCCL.

6.5. Cytokine secretion by OSCC stromal cells

The generation of an inflammatory microenvironment and the presence of inflammatory immune cells, including macrophage, is known to be an important driver of tumour progression. Inflammatory cytokines and chemokines released by tumour and stromal cells drive this process and have wide-ranging effects on immune cell recruitment, vessel formation, ECM reorganisation and tumour

behaviour (Grivennikov, Greten and Karin, 2010). However, the importance of these molecules in the colonisation, development and invasive ability of lymph node metastases is less well studied, despite the stark difference in native cell population compared to the primary tumour site.

The presence of macrophages within and surrounding tumour islands in primary and lymph node metastases was identified in this study (section 3.2.4. and discussion 6.1.3.) and it is clear from the literature that macrophages are important to tumour progression and promote invasion and metastasis (Takeya and Komohara, 2016). Therefore, secretion of the macrophage-attracting chemokine CCL2 alongside other key inflammatory cytokine molecules that have been previously implicated in the promotion of tumour invasion and metastasis (Mishra, Banerjee and Ben-Baruch, 2011; Voronov *et al.*, 2013; Kabir *et al.*, 2016), were investigated by co-culturing OCCL with stromal cells.

6.5.1. OCCL effect on immune signalling by fibroblasts

CAF play a key role in the modulation of the immune response to tumour presence. They are capable of secreting a wide range of cytokines and chemokines which affect immune cell recruitment, polarisation and function (Turley, Cremasco and Astarita, 2015). Signalling from cancer cells to fibroblasts can result in fibroblast activation, thereby promoting the formation of a pro-inflammatory, pro-tumour immune response in the tumour microenvironment. Although CAF have been shown to modulate immune function in many cancer models, their role in oral cancer development and particularly the development of lymph node metastasis is less well established. Therefore, this study looked at the effect of conditioned media from a panel of OCCL on cytokine and chemokine secretion by normal oral fibroblasts (NOF).

CCL2

Secretion and mRNA expression of CCL2, a potent macrophage attracting chemokine, was assessed because of the interest in the role of macrophage in oral cancer progression (see discussion 6.1.3.). Incubation of NOF with OCCL conditioned media for 24 h resulted in a significant increase in CCL2 secretion by NOF in the case

of the lymph node metastasis-derived OCCL (BICR22 and TR146) conditioned media only. This effect was particularly pronounced with TR146 conditioned media and this was matched by a significant increase in CCL2 mRNA levels in NOF, with a non-significant increase seen for BICR22 conditioned media too (section 4.2.6.). This suggests that tumour cells at metastatic sites are more capable of activating fibroblasts to produce CCL2 than primary tumour cells. Whilst this is the first study to make this comparison *in vitro*, there is *ex vivo* evidence of CCL2 expression in OSCC metastatic lymph nodes although this has primarily focussed on immune cells rather than CAF. One study reported that the percentage of CCL2 positive immune cells was significantly higher in lymph nodes with metastatic deposits compared to tumour-free nodes but reported no difference between N0 and N+ primary tumours (Ferreira *et al.*, 2008). Another reported that all sentinel lymph nodes had CCL2 positive neutrophil regardless of metastatic status whereas they were present in only some primary tumours (Fujita and Ikeda, 2017). Although these results suggest that CCL2 may be important to tumour development in the lymph node, it remains unclear at what stage this occurs and what the role of fibroblast secretion is. Furthermore, these studies used very high-powered field for quantification (x 40 to x 100 magnification) increasing the risk of subjective bias and either used a very low sample size (<10 per group) (Ferreira *et al.*, 2008) or did not carry out any quantification (Fujita and Ikeda, 2017). Therefore, a novel extension to this study would be the quantification of CCL2-expressing cells in lymph nodes, either using the ECS+/- cohort from this study and/or comparing to tumour free nodes.

This is the first study to report on the effect of OCCL on NOF secretion of CCL2, and to compare primary and lymph node metastases-derived OCCL. However, increased CCL2 secretion by CAF as a result of co-culture with OCCL has been previously demonstrated (Li *et al.*, 2014). This previous study also showed that CCL2 production could promote OCCL migration and invasion and that this could be ablated using siRNA knockdown of CCL2. Additionally, previous work in our lab has shown CCL2 secretion is elevated in CAF from genetically-unstable tumours and upon senescence induction in NOF and that antibody blockage of secreted CCL2 diminishes their pro-invasive effect on H357 cells (Kabir, 2015; Kabir *et al.*, 2016).

This suggests that CCL2 secretion by fibroblasts has effects ranging beyond macrophage recruitment. An extension of this study to look at the relative ability of primary and metastatic OCCL to induce CCL2 secretion in CAF and a comparison between secretion levels of CAF derived from primary tumour and lymph node metastasis would extend upon this and previous work.

IL-6

There has been considerable focus on the link between oral cancer progression and IL-6 secretion. Elevated IL-6 has been linked to the promotion of tumour survival, invasion, proliferation and angiogenesis in multiple cancer types (Ataie-Kachoe, Pourgholami and Morris, 2013). Elevated serum and tissue IL-6 mRNA levels have been observed in OSCC and have been associated with increased incidence of lymph node metastasis and poor survival (Shinriki *et al.*, 2011; Goda *et al.*, 2017; Qin *et al.*, 2018), making IL-6 a potentially useful prognostic biomarker. IL-6 secretion by NOF was significantly increased following incubation with all OCCL conditioned medias except for media from the metastatic primary tumour OCCL H376. As for CCL2, this was particularly pronounced with TR146 conditioned media, which also resulted in significantly higher mRNA expression by NOF (section 4.2.6.). This suggests that both lymph node and primary tumour derived cell lines can induce IL-6 secretion by fibroblasts but that the level of induction varies more by cell line rather than by site. The inability of the metastatic primary tumour OCCL H376 to induce induction compared to the non-metastatic primary tumour OCCL H357 is surprising given the link between IL-6 and the induction of invasion (Qin *et al.*, 2018). However, it maybe that H376 cells do not rely on this signalling mechanism to gain invasive ability and, given the multitudinous effects of IL-6, H357 cells may gain other advantages from stimulating its production.

Comparable studies are scarce but the ability of primary tumour-derived OCCL to induce IL-6 mRNA expression by fibroblasts when in co-culture has been reported (Dudás, Fullár, *et al.*, 2011; Qin *et al.*, 2018). This differs slightly to our results which found only TR146 conditioned media could induce increased IL-6 mRNA expression in NOF whereas primary tumour-derived OCCL had no significant effect. This may be explained by the fact that these previous studies co-cultured

both cell types together in transwells and for a longer time period, which may have resulted in a sustained increase in gene expression as opposed to an immediate protein secretion response. Additionally, in each case only one cell line was used, for which metastatic status information was not available, so a direct comparison cannot be made.

As reported for CCL2, increased IL-6 secretion has also been reported to be elevated following senescence induction in NOF and to be higher in CAF from genetically unstable tumours (Kabir, 2015; Kabir *et al.*, 2016). This was confirmed by a further study that found IL-6 to be expressed more highly in CAF than NOF, or tumour cells, from the same patient (Qin *et al.*, 2018). A comparison of primary tumour and lymph node tumour-derived CAF has not been carried out but would provide a valuable extension to this current work.

Other interleukins

The pro-inflammatory chemokine IL-8 (also known as CXCL8) is a key recruiter and activator of neutrophil and through its downstream signalling pathways has been shown to stimulate cancer cell survival and migration and induce angiogenesis (Waugh and Wilson, 2008). Elevated IL-8 expression has been previously linked to poor prognosis in OSCC (Fujita *et al.*, 2014) and salivary IL-8 has been suggested as a potential biomarker for OSCC (Punyani and Sathawane, 2013). Although IL-8 is known to be expressed by fibroblasts (Turley, Cremasco and Astarita, 2015), the role and importance of fibroblast IL-8 production has not been widely reported. As seen for IL-6 and CCL2, NOF incubated with TR146 conditioned media expressed high levels of IL-8 mRNA (section 4.2.6.). The exact reason for the strong reaction of NOF to TR146 conditioned media is unknown. IL-8 expression by TR146 and in untreated NOF has been previously shown (Khurram *et al.*, 2014) but the influence of TR146 conditioned media on NOF IL-8 expression is a novel extension to this. TR146 are derived from a lymph node metastasis of a well-differentiated OSCC originating in the buccal mucosa but the nature of the immune response of this tumour is not known. It may be that a strong neutrophil and macrophage infiltrate was present at the tumour site, which would match to the

ability of TR146 to induce the high CCL2 and IL-8 expression levels seen in this study.

mRNA expression of IL-1 α was also assessed given its central role in immune response coordination but expression could not be detected in any of the NOF samples in this study. The same lack of response was found for IL-1 β , a potent pro-angiogenic cytokine (section 4.2.6.) whereas expression of both of these cytokines was detected in HMEC and HLEC using the same experimental protocol (section 5.2.3-4). This lack of expression could be explained by the use of NOF rather than CAF, suggesting that OCCL conditioned media is not sufficient to induce expression of these molecules in healthy fibroblasts in the time period used. However, previous work in OSCC has shown that co-culture of OCCL and NOF could induce an increase in IL-1 β mRNA expression (Dudás, Bitsche, *et al.*, 2011) but this was carried out over 7 days with both cell types present in a transwell system and used periodontal ligament fibroblasts which may explain the difference in results. Extending this work to include protein expression analysis may help determine the full expression pattern. Additionally, there is evidence that IL-1 α and IL-1 β secretion by tumour cells can alter CAF behaviour (Dudás, Fullár, *et al.*, 2011; Bae *et al.*, 2014), which suggests that investigation into IL-1 receptor expression in CAF or NOF may be a more interesting avenue of research.

To fully assess the contribution of fibroblasts to immune signalling in lymph node tumours a microarray of common immune signalling molecules could be investigated to identify further targets for study. This could be done using either the same experimental design as used here to compare the effect of different OCCL conditioned media on NOF secretion, or compare CAF from multiple sites including lymph node metastases. Alternatively, the effect of CAF conditioned media on OCCL cytokine and chemokine secretion could be investigated.

6.5.2. OCCL and CAF effect on immune signalling in endothelial cells

The study of endothelial cells in the context of cancer has mainly focused on vessel formation and the link of this to metastasis. However, it is now becoming clear that endothelial cells contribute to the immune response to

cancer, are capable of interacting with both innate and adaptive immune cells, and can produce a large range of immune signalling molecules (Young, 2012). Endothelial cells have been shown to mount an inflammatory response to stimuli such as bacterial or viral infection and in the presence of cancer cells. In the context of cancer, they have also been implicated in the induction of immune tolerance through the secretion of immune inhibitory molecules and antigen presentation to T lymphocytes (Young, 2012). This is a potentially important, but understudied, area of tumour immunobiology as endothelial cells form a barrier both to immune cells infiltrating into the tumour microenvironment and to metastasising tumour cells.

OCCL induced cytokine/chemokine expression in endothelial cells

To investigate chemokine and cytokine secretion in endothelial cells in response to OCCL conditioned media, expression of the cytokines IL-6, IL-1 α , IL-1 β and the chemokines IL-8 and CCL2 was assessed in dermal vascular (HMEC) and lymphatic (HLEC) endothelial cells (section 5.2.3.). Secretion of IL-6 by HMEC and HLEC following incubation with OCCL conditioned media was increased in response to all OCCL although this was significant only in the case of H357 and BICR22-derived conditioned media. However, there was a large amount of variation in response level between experimental repeats. Surprisingly, high levels of the macrophage-attracting chemokine CCL2 were secreted in the media of HMEC and HLEC even under SFM control conditions (section 4.2.6. and 5.2.3.). The reason for this high level of secretion is unknown but suggests that endothelial cells may be important for the recruitment of macrophages. mRNA expression of all five signalling molecules was evident in both HLEC and HMEC including IL-1 α/β , which is in contrast with the lack of expression in NOF (see section 6.5.1.). OCCL conditioned media treatment revealed only small changes in expression levels and these were mostly attributable to cells treated with conditioned media from the lymph node-metastasis-derived OCCL BICR22 and TR146. IL-6 mRNA expression was significantly increased only in HMEC treated with BICR22-derived conditioned media and IL-8 mRNA expression was increased in response to conditioned media from both lymph node-derived OCCL (BICR22

and TR146), but this was significant only for HLEC (section 5.2.3.). This shows that both lymphatic and vascular endothelial cells are capable of secreting a wide range of immune modulating molecules and that OCCL are capable of altering their expression to some extent. Evidence of IL-6 expression and secretion by endothelial cells is particularly interesting as elevated serum IL-6 levels have been proposed as a biomarker for OSCC (Shinriki *et al.*, 2011; Goda *et al.*, 2017; Qin *et al.*, 2018). A significant response of HLEC and HMEC to some of the OCCL observed here supports the idea that endothelial cells may be one of the cell sources contributing to this specific inflammatory response. However, a large inter-experimental variation was observed so further repeats are needed to clarify and establish this relationship.

There are limited published data available for direct comparison but elevation of IL-6 and IL-8 mRNA expression in dermal HMEC as a result of co-culture with an OSCC cell line has been previously reported (Neiva *et al.*, 2009). This expression change was detected in a microarray but the effect was not validated using PCR or ELISA. Instead, the remaining part of the study focussed on inducing expression using VEGF or BCL-2 over-expression in the endothelial cells, and the effect of these cytokines on the tumour cells themselves. Therefore, it is unclear to what extent this result is reproducible in other OSCC model systems.

Studies in other cancer types, including those analysing multiple markers through a gene microarray, most commonly highlight IL-6 and IL-8 as factors expressed by endothelial cells in response to cancer cell conditioned media or co-culture (Goerge *et al.*, 2006; Mierke *et al.*, 2008; Rhim *et al.*, 2008; Wang *et al.*, 2013; Jin *et al.*, 2016). Some of these studies also reported that the more invasive cell lines could induce IL-8 expression to a greater extent (Goerge *et al.*, 2006; Mierke *et al.*, 2008) which appears to be somewhat similar to our finding that only lymph node metastases-derived OCCL conditioned media significantly increased IL-8 mRNA expression in endothelial cells. However, how the invasive ability was determined was not defined by Goerge *et al.* (2006) and is unclear from available cell line data. Mierke *et al.* (2008) determined invasive ability by

the propensity of cell lines to invade into a collagen gel containing endothelial cells. However, both invasive and non-invasive cell line groups contained cell lines derived from lymph node metastases, which complicates this definition in terms of clinical relevance, and in comparison to this study. In addition, all of these studies used human umbilical vein endothelial cells (HUVEC) as opposed to adult dermal endothelial cells as used in this study. HUVEC are an embryonic cell line so dermal HMEC may provide a more relevant cell lines for adult cancer models.

The extraction of endothelial cells from primary tumour and lymph node-metastases tissue could alternatively be used to screen for OSCC specific markers. Isolation of lymph node endothelial cells from both mouse and human tissue using magnetic bead sorting has been reported (Clasper *et al.*, 2008; Garrafa *et al.*, 2015). Garrafa *et al.* (2015) also reported that secretion of IL-6, IL-8 and CCL2 was significantly higher by lymphatic endothelial cells isolated from lymph nodes proximal to the tumour site compared to cells from distant lymph nodes. However, this methodology still needs optimisation and access to clinically relevant samples is hampered by the difficulty in obtaining patient lymph nodes without hindering diagnostic procedures.

Fibroblast induced cytokine/chemokine expression in endothelial cells

As previously discussed, CAF also play a role in the immune response to tumours and are known to interact with endothelial cells (discussion 6.4.2.). Therefore, the effect of myofibroblast and senescent fibroblast conditioned media on secretion of IL-6 and CCL2, and mRNA expression of IL-6, CCL2, IL-1 α , IL-1 β and IL-8 in HLEC and HMEC was assessed. However, few significant changes were observed following conditioned media treatment (section 5.2.4.). A small but significant increase in IL-6 secretion by HLEC was seen as a result of incubation with myofibroblast conditioned media treatment but no other expression changes were seen observed in either secretion or mRNA expression levels. H₂O₂-senesced fibroblast conditioned media did not alter IL-6 or CCL2 secretion in either HMEC or HLEC. mRNA expression of most of the molecules studied showed an increase in expression as a result of H₂O₂-senescent

fibroblast conditioned media treatment but there was a large variation between experimental repeats and only CCL2 and IL-8 expression in HLEC were significantly increased. As for OCCL, this provides evidence that endothelial cells contribute to the inflammatory milieu of the tumour microenvironment but provides limited evidence that this is significantly altered by the presence of CAF. Further experimental repeats may be needed to clarify this due to the large variation in response between experiments.

There are limited data looking at the effect of CAF on the endothelial immune response in cancer, making it hard to compare these findings to others. However, co-culture incorporating cancer cells, CAF and endothelial cells has been reported (Wang *et al.*, 2017). This previous study reported that inflammatory marker expression was increased in tumour spheroids that contained fibroblasts and endothelial cells compared to tumour cell only spheroids but did not look at any of the markers used in this study. Models such as these or indirect co-culture using successive conditioned media treatments to incorporate all three cell types could be used to extend this work. However, especially given the inter-experiment variation seen already, care must be taken to reduce the variability between conditions and include adequate controls.

6.6. Conclusion and impact

This thesis has described data relating to the role of the tumour microenvironment in the growth and development of lymph node metastases in OSCC. This is the first study to comprehensively examine stromal and EMT markers in OSCC lymph node metastases and their matched primary tumours. It revealed the novel finding that α SMA-expressing myofibroblasts are more abundant in the stroma of ECS+ lymph nodes, as well as their matched primary tumours, and that microvascular vessel density is also elevated in ECS+ nodes. EMT marker expression in OCCL and patient tissues was investigated but more work is needed to determine the prognostic impact in lymph node metastases and the impact of CAF on expression levels *in vitro*. This work also demonstrated the ability of both primary

and lymph node metastases-derived OCCL to induce tubule formation by lymphatic endothelial cells. Furthermore, this report extended on previous findings by showing that OCCL can induce IL-6 and CCL2 secretion in NOF and that lymph node metastases-derived OCCL have a heightened ability to induce this inflammatory signalling response. Finally, inflammatory signalling in endothelial cells was investigated and the novel exposure of these cells to OCCL and fibroblast conditioned media gave some insight into the potentially important role of endothelial cells in the tumour immune response.

This work has the potential to impact clinical outcomes and procedures for OSCC patients. The most immediate potential impact is the development of prognostic and diagnostic biomarkers for OSCC patients. Evidence from this study shows that α SMA positive fibroblast numbers are elevated in the stroma of ECS+ patients both in the primary tumour and in lymph node metastases. This suggests that identification of high α SMA levels either in the primary tumour or lymph node biopsy samples indicates a higher risk of ECS, which advocates for the need for neck dissection. Additionally, the ability of OCCL to induce IL-6 secretion in NOF supports the use of IL-6 as a cancer biomarker in OSCC, as has been previously suggested (Shinriki *et al.*, 2011; Goda *et al.*, 2017; Qin *et al.*, 2018), and warrants more investigation in the context of ECS.

In addition, the targeting of stromal cells as an alternative therapeutic strategy has great potential to improve the treatment options available to OSCC patients, especially those with lymph node metastasis and ECS, which are associated with treatment failure. The tumour microenvironment has been suggested as a source of therapeutic resistance (Sun, 2016), and so may provide an additional avenue of treatment options for patients for whom current therapies are not successful. The greater genetic stability of stromal cells and their influence on the ECM, which is often a barrier for the delivery of drugs to solid tumours, makes them even more attractive. Many of the cell markers and molecules highlighted in this thesis are already being investigated as potential treatment targets in other cancer types. For example, anti-IL6 and anti-IL-6 receptor antibody therapeutics have entered clinical trials in a number of cancer types (Kumari *et al.*, 2016).

Multitudinous mechanisms for targeting CAF and CAF signalling pathways have also been proposed, including targeting fibroblast activation protein (FAP) to kill CAF and administration of thrombospondin-1, which was shown to reduce CAF activation by down-regulating α SMA (Wang *et al.*, 2014). Extending this current body of work, both *in vitro* and using clinical data/samples, may enable these stromal-targeted treatment strategies to be transitioned to OSCC in the clinic.

6.7. Future work

There are several ways by which the work detailed in this thesis could be extended to expand current knowledge of the OSCC lymph node tumour microenvironment.

Firstly, further markers could be investigated by IHC to compare the tumour microenvironments of ECS+ and ECS- lymph node metastases. This could include senescence markers, other ECM components including MMPs, HEV density, proportions of M1 and M2 macrophage and the presence of other innate immune cells, such as neutrophil and mast cells.

Secondly, characterisation of primary lymph-node derived CAF, especially if paired with their corresponding primary tumour CAF would provide a valuable insight into the similarities and differences between these two sites. This characterisation could take the form of whole genome sequencing or use microarrays to assess expression of particular markers, such as cytokines and chemokines. Another important cell type for the study of lymph node CAF development are FRC as they are the predominant fibroblast population in the lymph node and so have been proposed as a major source of lymph node CAF. The effect of TGF- β 1 or OCCL conditioned media on activation marker expression, pro-angiogenic factor secretion and expression of pro-inflammatory molecules could be investigated.

There are many experiments that could be used to directly expand the *in vitro* work described in this thesis. OCCL cytokine and chemokine expression and relative ability to promote monocyte differentiation and macrophage migration

could be investigation using established markers and transwells assays. The effect of CAF on both of these behaviours would also provide a valuable extension to this.

Finally, the development of 3D models incorporating myofibroblasts, senescent fibroblasts or primary CAF as well as OCCL would extend the experiments described here investigating migration and EMT expression in OCCL. Both invasion patterns and EMT marker expression could be assessed in parallel providing a valuable comparison. These could take the form of previously developed oral mucosa models or utilise spheroid culture to form an environment more analogous to that found in the lymph node.

References

- Abbas, A., Lichtman, A. and Pillai, S. (2015) *Cellular and molecular immunology*. 8th edn. Philadelphia, PA: Elsevier Saunders.
- Abdul-Aziz, M. A. *et al.* (2017) 'Lymphangiogenesis in Oral Squamous Cell Carcinoma: Correlation with VEGF-C Expression and Lymph Node Metastasis', *International Journal of Dentistry*, 2017(1), pp. 1–10. doi: 10.1155/2017/7285656.
- Acton, S. E. *et al.* (2014) 'Dendritic cells control fibroblastic reticular network tension and lymph node expansion', *Nature*, 514(7523), pp. 498–502. doi: 10.1038/nature13814.
- Adel, M. *et al.* (2015) 'Evaluation of Lymphatic and Vascular Invasion in Relation to Clinicopathological Factors and Treatment Outcome in Oral Cavity Squamous Cell Carcinoma', *Medicine*, 94(43), p. e1510. doi: 10.1097/MD.0000000000001510.
- Aiken, A. H. *et al.* (2015) 'Accuracy of Preoperative Imaging in Detecting Nodal Extracapsular Spread in Oral Cavity Squamous Cell Carcinoma', *American Journal of Neuroradiology*, 36(9), pp. 1776–81. doi: 10.3174/ajnr.A4372.
- Allen, C. D. C. and Cyster, J. G. (2008) 'Follicular dendritic cell networks of primary follicles and germinal centers: phenotype and function', *Seminars in Immunology*, 20(1), pp. 14–25. doi: 10.1016/j.smim.2007.12.001.
- Arnaoutova, I. and Kleinman, H. K. (2010) 'In vitro angiogenesis: Endothelial cell tube formation on gelled basement membrane extract', *Nature Protocols*, 5(4), pp. 628–635. doi: 10.1038/nprot.2010.6.
- Ataie-Kachoei, P., Pourgholami, M. H. and Morris, D. L. (2013) 'Inhibition of the IL-6 signaling pathway: A strategy to combat chronic inflammatory diseases and cancer', *Cytokine & Growth Factor Reviews*, 24(2), pp. 163–173. doi: 10.1016/j.cytogfr.2012.09.001.
- Bae, J. Y. *et al.* (2014) 'Reciprocal Interaction between Carcinoma-Associated Fibroblasts and Squamous Carcinoma Cells through Interleukin-1 α Induces Cancer Progression', *Neoplasia*, 16(11), pp. 928–938. doi: 10.1016/j.neo.2014.09.003.
- Baker, E. A. *et al.* (2006) 'The matrix metalloproteinase system in oral squamous cell carcinoma', *British Journal of Oral and Maxillofacial Surgery*, 44(6), pp. 482–486. doi: 10.1016/j.bjoms.2005.10.005.
- Bello, I. O. *et al.* (2011) 'Cancer-associated fibroblasts, a parameter of the tumor microenvironment, overcomes carcinoma-associated parameters in the prognosis of patients with mobile tongue cancer.', *Oral Oncology*, 47(1), pp. 33–8. doi: 10.1016/j.oraloncology.2010.10.013.
- Berdiel-Acer, M. *et al.* (2011) 'Hepatic Carcinoma—Associated Fibroblasts Promote an Adaptive Response in Colorectal Cancer Cells That Inhibit Proliferation and Apoptosis: Nonresistant Cells Die by Nonapoptotic Cell Death', *Neoplasia*, 13(10), pp. 931–946. doi: 10.1593/neo.11706.
- Berndt, A. *et al.* (2014) 'Effects of activated fibroblasts on phenotype modulation, EGFR signalling and cell cycle regulation in OSCC cells.', *Experimental Cell Research*,

322(2), pp. 402–14. doi: 10.1016/j.yexcr.2013.12.024.

Bernier, J. *et al.* (2005) 'Defining risk levels in locally advanced head and neck cancers: a comparative analysis of concurrent postoperative radiation plus chemotherapy trials of the EORTC (#22931) and RTOG (# 9501).', *Head & Neck*, 27(10), pp. 843–50. doi: 10.1002/hed.20279.

Bolzoni Villaret, A. *et al.* (2009) 'Immunostaining patterns of CD31 and podoplanin in previously untreated advanced oral/oropharyngeal cancer: Prognostic implications', *Head & Neck*, 32(10), pp. 786–792. doi: 10.1002/hed.21256.

Cancer Research UK (2011) *Cancer Incidence in the UK in 2011*.

Cancer Research UK (2014) *Oral cancer*.

Chang, J. E. and Turley, S. J. (2015) 'Stromal infrastructure of the lymph node and coordination of immunity', *Trends in Immunology*, 36(1), pp. 30–39. doi: 10.1016/j.it.2014.11.003.

Chen, C. *et al.* (2008) 'Gene expression profiling identifies genes predictive of oral squamous cell carcinoma', *Cancer Epidemiology, Biomarkers & Prevention*, 17(8), pp. 2152–2162. doi: 10.1158/1055-9965.EPI-07-2893.

Chen, H.-F. *et al.* (2014) 'Twist1 induces endothelial differentiation of tumour cells through the Jagged1-KLF4 axis.', *Nature Communications*, 5(1), p. 4697. doi: 10.1038/ncomms5697.

Choe, C. *et al.* (2013) 'Tumor-stromal interactions with direct cell contacts enhance motility of non-small cell lung cancer cells through the hedgehog signaling pathway', *Anticancer Research*, 33(9), pp. 3715–3724. doi: 10.1016/B978-0-12-386469-7.00001-3.

Chung, M. K. *et al.* (2012) 'Lymphatic Vessels and High Endothelial Venules are Increased in the Sentinel Lymph Nodes of Patients with Oral Squamous Cell Carcinoma Before the Arrival of Tumor Cells', *Annals of Surgical Oncology*, 19(5), pp. 1595–1601. doi: 10.1245/s10434-011-2154-9.

Chyou, S. *et al.* (2008) 'Fibroblast-Type Reticular Stromal Cells Regulate the Lymph Node Vasculature', *The Journal of Immunology*, 181(6), pp. 3887–3896. doi: 10.4049/jimmunol.181.6.3887.

Cirri, P. and Chiarugi, P. (2011) 'Cancer associated fibroblasts: the dark side of the coin.', *American Journal of Cancer Research*, 1(4), pp. 482–97.

Cirri, P. and Chiarugi, P. (2012) 'Cancer-associated-fibroblasts and tumour cells: a diabolic liaison driving cancer progression.', *Cancer Metastasis Reviews*, 31(1), pp. 195–208. doi: 10.1007/s10555-011-9340-x.

Clasper, S. *et al.* (2008) 'A Novel Gene Expression Profile in Lymphatics Associated with Tumor Growth and Nodal Metastasis', *Cancer Research*, 68(18), pp. 7293–7303. doi: 10.1158/0008-5472.CAN-07-6506.

Coatesworth, A. P. and MacLennan, K. (2002) 'Squamous cell carcinoma of the upper aerodigestive tract: the prevalence of microscopic extracapsular spread and soft tissue deposits in the clinically N0 neck.', *Head & Neck*, 24(3), pp. 258–61. doi: 10.1002/hed.10020.

- Colley, H. E. *et al.* (2011) 'Development of tissue-engineered models of oral dysplasia and early invasive oral squamous cell carcinoma', *British Journal of Cancer*, 105(10), pp. 1582–1592. doi: 10.1038/bjc.2011.403.
- Cooper, J. S. *et al.* (2012) 'Long-term Follow-up of the RTOG 9501/Intergroup Phase III Trial: Postoperative Concurrent Radiation Therapy and Chemotherapy in High-Risk Squamous Cell Carcinoma of the Head and Neck', *International Journal of Radiation Oncology*Biophysics*, 84(5), pp. 1198–1205. doi: 10.1016/j.ijrobp.2012.05.008.
- Coppe, J.-P. *et al.* (2008) 'A role for fibroblasts in mediating the effects of tobacco-induced epithelial cell growth and invasion.', *Molecular Cancer Research*, 6(7), pp. 1085–98. doi: 10.1158/1541-7786.MCR-08-0062.
- Coppé, J.-P. *et al.* (2006) 'Secretion of vascular endothelial growth factor by primary human fibroblasts at senescence.', *The Journal of Biological Chemistry*, 281(40), pp. 29568–29574. doi: 10.1074/jbc.M603307200.
- Coppé, J.-P. *et al.* (2008) 'Senescence-Associated Secretory Phenotypes Reveal Cell-Nonautonomous Functions of Oncogenic RAS and the p53 Tumor Suppressor', *PLoS Biology*, 6(12), p. e301. doi: 10.1371/journal.pbio.0060301.
- Coppé, J.-P. *et al.* (2010) 'The Senescence-Associated Secretory Phenotype: The Dark Side of Tumor Suppression', *Annual Review of Pathology*, 5(1), pp. 99–118. doi: 10.1146/annurev-pathol-121808-102144.
- Costa, A., Scholer-Dahirel, A. and Mehta-Grigoriou, F. (2014) 'The role of reactive oxygen species and metabolism on cancer cells and their microenvironment', *Seminars in Cancer Biology*, 25(1), pp. 23–32. doi: 10.1016/j.semcancer.2013.12.007.
- Costa, N. L. *et al.* (2013) 'Tumor-associated macrophages and the profile of inflammatory cytokines in oral squamous cell carcinoma', *Oral Oncology*, 49(3), pp. 216–223. doi: 10.1016/j.oraloncology.2012.09.012.
- Costea, D. E. *et al.* (2006) 'Species-specific fibroblasts required for triggering invasiveness of partially transformed oral keratinocytes.', *The American Journal of Pathology*, 168(6), pp. 1889–97. doi: 10.2353/ajpath.2006.050843.
- Costea, D. E. *et al.* (2013) 'Identification of two distinct carcinoma-associated fibroblast subtypes with differential tumor-promoting abilities in oral squamous cell carcinoma.', *Cancer Research*, 73(13), pp. 3888–901. doi: 10.1158/0008-5472.CAN-12-4150.
- D'Cruz, A. K. *et al.* (2015) 'Elective versus Therapeutic Neck Dissection in Node-Negative Oral Cancer', *New England Journal of Medicine*, 373(6), pp. 521–529. doi: 10.1056/NEJMoa1506007.
- Daly, A. J., McIlreavey, L. and Irwin, C. R. (2008) 'Regulation of HGF and SDF-1 expression by oral fibroblasts - Implications for invasion of oral cancer', *Oral Oncology*, 44(7), pp. 646–651. doi: 10.1016/j.oraloncology.2007.08.012.
- Daniele, A. *et al.* (2010) 'Expression of metalloproteinases MMP-2 and MMP-9 in sentinel lymph node and serum of patients with metastatic and non-metastatic breast cancer', *Anticancer Research*, 30(9), pp. 3521–3527.

- Dhanda, J. *et al.* (2014) 'SERPINE1 and SMA expression at the invasive front predict extracapsular spread and survival in oral squamous cell carcinoma.', *British Journal of Cancer*, 111(11), pp. 2114–21. doi: 10.1038/bjc.2014.500.
- Dimri, G. P. *et al.* (1995) 'A biomarker that identifies senescent human cells in culture and in aging skin in vivo.', *Proceedings of the National Academy of Sciences of the United States of America*, 92(20), pp. 9363–7. doi: DOI 10.1073/pnas.92.20.9363.
- Ding, L. *et al.* (2014) 'α-Smooth muscle actin-positive myofibroblasts, in association with epithelial-mesenchymal transition and lymphogenesis, is a critical prognostic parameter in patients with oral tongue squamous cell carcinoma', *Journal of Oral Pathology and Medicine*, 43(5), pp. 335–343. doi: 10.1111/jop.12143.
- Dudás, J., Bitsche, M., *et al.* (2011) 'Fibroblasts produce brain-derived neurotrophic factor and induce mesenchymal transition of oral tumor cells.', *Oral Oncology*, 47(2), pp. 98–103. doi: 10.1016/j.oraloncology.2010.11.002.
- Dudás, J., Fullár, A., *et al.* (2011) 'Tumor-produced, active Interleukin-1 β regulates gene expression in carcinoma-associated fibroblasts', *Experimental Cell Research*, 317(15), pp. 2222–2229. doi: 10.1016/j.yexcr.2011.05.023.
- Edington, K. G. *et al.* (1995) 'Cellular immortality: A late event in the progression of human squamous cell carcinoma of the head and neck associated with p53 alteration and a high frequency of allele loss', *Molecular Carcinogenesis*, 13(4), pp. 254–265. doi: 10.1002/mc.2940130408.
- Egeblad, M., Rasch, M. G. and Weaver, V. M. (2010) 'Dynamic interplay between the collagen scaffold and tumor evolution', *Current Opinion in Cell Biology*, 22(5), pp. 697–706. doi: 10.1016/j.ceb.2010.08.015.
- El-Rouby, D. H. (2010) 'Association of macrophages with angiogenesis in oral verrucous and squamous cell carcinomas', *Journal of Oral Pathology and Medicine*, 39(7), pp. 559–564. doi: 10.1111/j.1600-0714.2010.00879.x.
- Elmusrati, A. A. *et al.* (2017) 'Cancer-associated fibroblasts promote bone invasion in oral squamous cell carcinoma', *British Journal of Cancer*, 117(6), pp. 867–875. doi: 10.1038/bjc.2017.239.
- Essa, A. A. M. *et al.* (2016) 'Tumour-associated macrophages are recruited and differentiated in the neoplastic stroma of oral squamous cell carcinoma', *Pathology*, 48(3), pp. 219–227. doi: 10.1016/j.pathol.2016.02.006.
- Ferlay, J. *et al.* (2013) *GLOBOCAN 2012 v1.0, Cancer Incidence and Mortality Worldwide: IARC CancerBase No. 11*. Lyon, France. Available at: <http://globocan.iarc.fr> (Accessed: 14 April 2015).
- Ferreira, F. O. *et al.* (2008) 'Association of CCL2 with lymph node metastasis and macrophage infiltration in oral cavity and lip squamous cell carcinoma', *Tumor Biology*, 29(2), pp. 114–121. doi: 10.1159/000137669.
- Francí, C. *et al.* (2006) 'Expression of Snail protein in tumor-stroma interface', *Oncogene*, 25(37), pp. 5134–5144. doi: 10.1038/sj.onc.1209519.
- Franz, M. *et al.* (2009) 'Expression of Snail is associated with myofibroblast phenotype development in oral squamous cell carcinoma.', *Histochemistry and Cell*

- Biology*, 131(5), pp. 651–60. doi: 10.1007/s00418-009-0559-3.
- Fujii, N. *et al.* (2012) 'Cancer-associated fibroblasts and CD163-positive macrophages in oral squamous cell carcinoma: Their clinicopathological and prognostic significance', *Journal of Oral Pathology and Medicine*, 41(6), pp. 444–451. doi: 10.1111/j.1600-0714.2012.01127.x.
- Fujinaga, T. *et al.* (2014) 'Biological characterization and analysis of metastasis-related genes in cell lines derived from the primary lesion and lymph node metastasis of a squamous cell carcinoma arising in the mandibular gingiva', *International Journal of Oncology*, 44(5), pp. 1614–1624. doi: 10.3892/ijo.2014.2332.
- Fujita, S. and Ikeda, T. (2017) 'The CCL2-CCR2 Axis in Lymph Node Metastasis From Oral Squamous Cell Carcinoma: An Immunohistochemical Study', *Journal of Oral and Maxillofacial Surgery*, 75(4), pp. 742–749. doi: 10.1016/j.joms.2016.09.052.
- Fujita, Y. *et al.* (2014) 'Prognostic significance of interleukin-8 and CD163-positive cell-infiltration in tumor tissues in patients with oral squamous cell carcinoma', *PLoS ONE*, 9(12), pp. 1–17. doi: 10.1371/journal.pone.0110378.
- Gaggioli, C. *et al.* (2007) 'Fibroblast-led collective invasion of carcinoma cells with differing roles for RhoGTPases in leading and following cells.', *Nature Cell Biology*, 9(12), pp. 1392–400. doi: 10.1038/ncb1658.
- Gao, M.-Q. *et al.* (2010) 'Stromal fibroblasts from the interface zone of human breast carcinomas induce an epithelial-mesenchymal transition-like state in breast cancer cells in vitro.', *Journal of Cell Science*, 123(Pt 20), pp. 3507–14. doi: 10.1242/jcs.072900.
- Garrafa, E. *et al.* (2015) 'Lymphatic endothelial cells derived from metastatic and non-metastatic lymph nodes of human colorectal cancer reveal phenotypic differences in culture.', *Lymphology*, 48(1), pp. 6–14.
- Georgakopoulou, E. A. *et al.* (2013) 'Specific lipofuscin staining as a novel biomarker to detect replicative and stress-induced senescence. A method applicable in cryo-preserved and archival tissues', *Aging*, 5(1), pp. 37–50. doi: 10.18632/aging.100527.
- Gewirtz, D. a., Holt, S. E. and Elmore, L. W. (2008) 'Accelerated senescence: An emerging role in tumor cell response to chemotherapy and radiation', *Biochemical Pharmacology*, 76(8), pp. 947–957. doi: 10.1016/j.bcp.2008.06.024.
- Goda, H. *et al.* (2017) 'Prognostic impact of preoperative serum interleukin-6 levels in patients with early-stage oral squamous cell carcinoma, defined by sentinel node biopsy', *Oncology Letters*, 42(10), pp. 1274–1275. doi: 10.3892/ol.2017.7183.
- Goerge, T. *et al.* (2006) 'Tumor-derived matrix metalloproteinase-1 targets endothelial proteinase-activated receptor 1 promoting endothelial cell activation', *Cancer Research*, 66(15), pp. 7766–7774. doi: 10.1158/0008-5472.CAN-05-3897.
- Govers, T. M. *et al.* (2013) 'Sentinel node biopsy for squamous cell carcinoma of the oral cavity and oropharynx: A diagnostic meta-analysis', *Oral Oncology*, 49(8), pp. 726–732. doi: 10.1016/j.oraloncology.2013.04.006.
- Greenberg, J. S. *et al.* (2003) 'Extent of extracapsular spread: a critical prognosticator in oral tongue cancer.', *Cancer*, 97(6), pp. 1464–70. doi:

10.1002/cncr.11202.

Grille, S. J. *et al.* (2003) 'The Protein Kinase Akt Induces Epithelial Mesenchymal Transition and Promotes Enhanced Motility and Invasiveness of Squamous Cell Carcinoma Lines', *Cancer Research*, 63(9), pp. 2172–2178.

Grivennikov, S. I., Greten, F. R. and Karin, M. (2010) 'Immunity, Inflammation, and Cancer', *Cell*, 140(6), pp. 883–899. doi: 10.1016/j.cell.2010.01.025.

Hanahan, D. and Weinberg, R. A. (2011) 'Hallmarks of cancer: The next generation', *Cell*, 144(5), pp. 646–674. doi: 10.1016/j.cell.2011.02.013.

Harwood, N. E. and Batista, F. D. (2010) 'Antigen presentation to B cells.', *F1000 Biology Reports*, 2(1), p. 87. doi: 10.3410/B2-87.

Hassona, Y. *et al.* (2013) 'Progression of genotype-specific oral cancer leads to senescence of cancer-associated fibroblasts and is mediated by oxidative stress and TGF- β .', *Carcinogenesis*, 34(6), pp. 1286–95. doi: 10.1093/carcin/bgt035.

Hassona, Y. *et al.* (2014) 'Senescent cancer-associated fibroblasts secrete active MMP-2 that promotes keratinocyte dis-cohesion and invasion.', *British Journal of Cancer*, 111(6), pp. 1230–7. doi: 10.1038/bjc.2014.438.

Hayflick, L. and Moorhead, P. S. (1961) 'The serial cultivation of human diploid cell strains.', *Experimental Cell Research*, 25(1), pp. 585–621. doi: 10.1016/0014-4827(61)90192-6.

He, K.-F. *et al.* (2014) 'CD163+ Tumor-Associated Macrophages Correlated with Poor Prognosis and Cancer Stem Cells in Oral Squamous Cell Carcinoma', *BioMed Research International*, 2014(1), pp. 1–9. doi: 10.1155/2014/838632.

Hearnden, V. *et al.* (2009) 'Diffusion Studies of Nanometer Polymersomes Across Tissue Engineered Human Oral Mucosa', *Pharmaceutical Research*, 26(7), pp. 1718–1728. doi: 10.1007/s11095-009-9882-6.

Hu, Y. *et al.* (2016) 'Tumor-associated macrophages correlate with the clinicopathological features and poor outcomes via inducing epithelial to mesenchymal transition in oral squamous cell carcinoma.', *Journal of Experimental & Clinical Cancer Research*, 35(1), p. 12. doi: 10.1186/s13046-015-0281-z.

Hwang, Y. S. *et al.* (2012) 'Functional invadopodia formation through stabilization of the PDPN transcript by IMP-3 and cancer-stromal crosstalk for PDPN expression.', *Carcinogenesis*, 33(11), pp. 2135–46. doi: 10.1093/carcin/bgs258.

Inoue, H. *et al.* (2006) 'Quality of life after neck dissection', *Archives of Otolaryngology - Head and Neck Surgery*, 132(6), pp. 662–666. doi: 10.1001/archotol.132.6.662.

Jin, G. *et al.* (2016) 'Genome-wide analysis of the effect of esophageal squamous cell carcinoma on human umbilical vein endothelial cells', *Oncology Reports*, 36(1), pp. 155–164. doi: 10.3892/or.2016.4816.

Jithesh, P. V. *et al.* (2013) 'The epigenetic landscape of oral squamous cell carcinoma', *British Journal of Cancer*, 108(2), pp. 370–379. doi: 10.1038/bjc.2012.568.

Jones, H. B. *et al.* (2009) 'The impact of lymphovascular invasion on survival in oral

- carcinoma.', *Oral Oncology*, 45(1), pp. 10–5. doi: 10.1016/j.oraloncology.2008.03.009.
- Joo, Y. H. *et al.* (2013) 'Extracapsular spread and FDG PET/CT correlations in oral squamous cell carcinoma', *International Journal of Oral and Maxillofacial Surgery*, 42(2), pp. 158–163. doi: 10.1016/j.ijom.2012.11.006.
- Jung, D. W. *et al.* (2010) 'Tumor-stromal crosstalk in invasion of oral squamous cell carcinoma: A pivotal role of CCL7', *International Journal of Cancer*, 127(2), pp. 332–344. doi: 10.1002/ijc.25060.
- Jung, S. *et al.* (2015) 'Analysis of angiogenic markers in oral squamous cell carcinoma-gene and protein expression.', *Head & Face Medicine*, 11(1), p. 19. doi: 10.1186/s13005-015-0076-7.
- Kabir, T. D. (2015) *Micro-managing fibroblast senescence: The role of small non-coding RNA in senescence-associated secretory phenotype (SASP)*. University of Sheffield.
- Kabir, T. D. *et al.* (2016) 'A miR-335/COX-2/PTEN axis regulates the secretory phenotype of senescent cancer-associated fibroblasts', *Aging*, 8(8), pp. 1608–1635. doi: 10.18632/aging.100987.
- Kazakydasan, S. *et al.* (2017) 'Prognostic significance of VEGF-C in predicting micrometastasis and isolated tumour cells in N0 oral squamous cell carcinoma', *Journal of Oral Pathology and Medicine*, 46(3), pp. 194–200. doi: 10.1111/jop.12476.
- Kellermann, M. G. *et al.* (2007) 'Myofibroblasts in the stroma of oral squamous cell carcinoma are associated with poor prognosis.', *Histopathology*, 51(6), pp. 849–53. doi: 10.1111/j.1365-2559.2007.02873.x.
- Kellermann, M. G. *et al.* (2008) 'Mutual paracrine effects of oral squamous cell carcinoma cells and normal oral fibroblasts: induction of fibroblast to myofibroblast transdifferentiation and modulation of tumor cell proliferation.', *Oral Oncology*, 44(5), pp. 509–17. doi: 10.1016/j.oraloncology.2007.07.001.
- Khurram, S. A. *et al.* (2014) 'The chemokine receptors CXCR1 and CXCR2 regulate oral cancer cell behaviour', *Journal of Oral Pathology and Medicine*, 43(9), pp. 667–674. doi: 10.1111/jop.12191.
- Kokemueller, H. *et al.* (2011) 'The Hannover experience: surgical treatment of tongue cancer--a clinical retrospective evaluation over a 30 years period.', *Head & Neck Oncology*, 3(1), p. 27. doi: 10.1186/1758-3284-3-27.
- Krisanaprakornkit, S. and Iamaron, A. (2012) 'Epithelial-Mesenchymal Transition in Oral Squamous Cell Carcinoma', *ISRN Oncology*, 2012(1), pp. 1–10. doi: 10.5402/2012/681469.
- Kumari, N. *et al.* (2016) 'Role of interleukin-6 in cancer progression and therapeutic resistance', *Tumor Biology*, 37(9), pp. 11553–11572. doi: 10.1007/s13277-016-5098-7.
- Kyzas, P. a *et al.* (2005) 'Evidence for lymphangiogenesis and its prognostic implications in head and neck squamous cell carcinoma.', *The Journal of Pathology*, 206, pp. 170–177. doi: 10.1002/path.1776.

- Larsen, S. R. *et al.* (2009) 'The prognostic significance of histological features in oral squamous cell carcinoma.', *Journal of Oral Pathology and Medicine*, 38(8), pp. 657–62. doi: 10.1111/j.1600-0714.2009.00797.x.
- Lebret, S. C. *et al.* (2007) 'Induction of epithelial to mesenchymal transition in PMC42-LA human breast carcinoma cells by carcinoma-associated fibroblast secreted factors.', *Breast Cancer Research*, 9(1), p. R19. doi: 10.1186/bcr1656.
- Lee, S. Y. *et al.* (2012) 'Changes in specialized blood vessels in lymph nodes and their role in cancer metastasis', *Journal of Translational Medicine*, 10(1), p. 206. doi: 10.1186/1479-5876-10-206.
- Lee, W.-Y. *et al.* (2014) 'Prognostic significance of epithelial-mesenchymal transition of extracapsular spread tumors in lymph node metastases of head and neck cancer.', *Annals of Surgical Oncology*, 21(1), pp. 1904–11. doi: 10.1245/s10434-014-3567-z.
- Levy, L. and Hill, C. S. (2006) 'Alterations in components of the TGF- β superfamily signaling pathways in human cancer', *Cytokine and Growth Factor Reviews*, 17(1), pp. 41–58. doi: 10.1016/j.cytogfr.2005.09.009.
- Lewis, M. P. *et al.* (2004) 'Tumour-derived TGF- β 1 modulates myofibroblast differentiation and promotes HGF/SF-dependent invasion of squamous carcinoma cells.', *British Journal of Cancer*, 90(4), pp. 822–32. doi: 10.1038/sj.bjc.6601611.
- Li, C. *et al.* (2005) 'Microvessel density and expression of vascular endothelial growth factor, basic fibroblast growth factor, and platelet-derived endothelial growth factor in oral squamous cell carcinomas.', *International Journal of Oral and Maxillofacial Surgery*, 34(5), pp. 559–65. doi: 10.1016/j.ijom.2004.10.016.
- Li, H. *et al.* (2015) 'Cancer-associated fibroblasts provide a suitable microenvironment for tumor development and progression in oral tongue squamous cancer', *Journal of Translational Medicine*, 13(1), p. 198. doi: 10.1186/s12967-015-0551-8.
- Li, X. *et al.* (2014) 'A CCL2/ROS autoregulation loop is critical for cancer-associated fibroblasts-enhanced tumor growth of oral squamous cell carcinoma.', *Carcinogenesis*, 35(6), pp. 1362–1370. doi: 10.1093/carcin/bgu046.
- Liao, C.-T. *et al.* (2007) 'Analysis of risk factors for distant metastases in squamous cell carcinoma of the oral cavity', *Cancer*, 110(7), pp. 1501–1508. doi: 10.1002/cncr.22959.
- Lim, K. P. *et al.* (2011) 'Fibroblast gene expression profile reflects the stage of tumour progression in oral squamous cell carcinoma', *Journal of Pathology*, 223(1), pp. 459–469. doi: 10.1002/path.2841.
- Lin, N. N. *et al.* (2017) 'Significance of oral cancer-associated fibroblasts in angiogenesis, lymphangiogenesis, and tumor invasion in oral squamous cell carcinoma', *Journal of Oral Pathology and Medicine*, 46(1), pp. 21–30. doi: 10.1111/jop.12452.
- Livak, K. J. and Schmittgen, T. D. (2001) 'Analysis of relative gene expression data using real-time quantitative PCR and the 2- $\Delta\Delta$ CT method', *Methods*, 25(4), pp. 402–408. doi: 10.1006/meth.2001.1262.

- Lyons, A. J. and Jones, J. (2007) 'Cell adhesion molecules, the extracellular matrix and oral squamous carcinoma', *International Journal of Oral and Maxillofacial Surgery*, 36(8), pp. 671–679. doi: 10.1016/j.ijom.2007.04.002.
- Madar, S., Goldstein, I. and Rotter, V. (2013) "'Cancer associated fibroblasts" - more than meets the eye', *Trends in Molecular Medicine*, 19(8), pp. 447–453. doi: 10.1016/j.molmed.2013.05.004.
- Malaquin, N. *et al.* (2013) 'Senescent fibroblasts enhance early skin carcinogenic events via a paracrine MMP-PAR-1 axis.', *PLoS ONE*, 8(5), p. e63607. doi: 10.1371/journal.pone.0063607.
- Mantovani, A. *et al.* (2008) 'Cancer-related inflammation', *Nature*, 454(7203), pp. 436–444. doi: 10.1038/nature07205.
- Mantovani, A., Barajon, I. and Garlanda, C. (2018) 'IL-1 and IL-1 regulatory pathways in cancer progression and therapy', *Immunological Reviews*, 281(1), pp. 57–61. doi: 10.1111/imr.12614.
- Marsh, D. *et al.* (2011) 'Stromal features are predictive of disease mortality in oral cancer patients', *Journal of Pathology*, 223(4), pp. 470–481. doi: 10.1002/path.2830.
- Matjusaitis, M. *et al.* (2016) 'Biomarkers to identify and isolate senescent cells', *Ageing Research Reviews*, 29(1), pp. 1–12. doi: 10.1016/j.arr.2016.05.003.
- Matsumoto, K. *et al.* (1989) 'A study of an in vitro model for invasion of oral squamous cell carcinoma', *Journal of Oral Pathology & Medicine*, 18(9), pp. 498–501. doi: 10.1111/j.1600-0714.1989.tb01350.x.
- Maxwell, J. H. *et al.* (2013) 'Extracapsular spread in head and neck carcinoma: impact of site and human papillomavirus status.', *Cancer*, 119(18), pp. 3302–8. doi: 10.1002/cncr.28169.
- Mayorca-Guiliani, A. E. *et al.* (2012) 'Premetastatic vasculogenesis in oral squamous cell carcinoma xenograft-draining lymph nodes', *Oral Oncology*, 48(8), pp. 663–670. doi: 10.1016/j.oraloncology.2012.02.007.
- McGurk, M. *et al.* (2005) 'Delay in diagnosis and its effect on outcome in head and neck cancer', *British Journal of Oral and Maxillofacial Surgery*, 43(4), pp. 281–284. doi: 10.1016/j.bjoms.2004.01.016.
- Melling, G. *et al.* (2018) 'A miRNA-145/TGF- β 1 Negative Feedback Loop Regulates the Cancer-Associated Fibroblast Phenotype', *Carcinogenesis*. doi: 10.1093/carcin/bgy032.
- Meng, W. *et al.* (2014) 'A systems biology approach identifies effective tumor-stroma common targets for oral squamous cell carcinoma.', *Cancer research*, 74(8), pp. 2306–15. doi: 10.1158/0008-5472.CAN-13-2275.
- Mermod, M. *et al.* (2016) 'Extracapsular spread in head and neck squamous cell carcinoma: A systematic review and meta-analysis', *Oral Oncology*, 62(1), pp. 60–71. doi: 10.1016/j.oraloncology.2016.10.003.
- Mermod, M. *et al.* (2017) 'Correlation between podoplanin expression and extracapsular spread in squamous cell carcinoma of the oral cavity using subjective immunoreactivity scores and semiquantitative image analysis', *Head & Neck*, 39(1),

pp. 98–108. doi: 10.1002/hed.24537.

Michikawa, C. *et al.* (2011) 'Epidermal growth factor receptor gene copy number aberration at the primary tumour is significantly associated with extracapsular spread in oral cancer.', *British Journal of Cancer*, 104(5), pp. 850–855. doi: 10.1038/bjc.2011.22.

Michikawa, C. *et al.* (2018) 'Small size of metastatic lymph nodes with extracapsular spread greatly impacts treatment outcomes in oral squamous cell carcinoma patients', *International Journal of Oral and Maxillofacial Surgery*. doi: 10.1016/j.ijom.2017.12.007.

Mierke, C. T. *et al.* (2008) 'Breakdown of the endothelial barrier function in tumor cell transmigration', *Biophysical Journal*, 94(7), pp. 2832–2846. doi: 10.1529/biophysj.107.113613.

Mishra, P., Banerjee, D. and Ben-Baruch, A. (2011) 'Chemokines at the crossroads of tumor-fibroblast interactions that promote malignancy', *Journal of Leukocyte Biology*, 89(1), pp. 31–39. doi: 10.1189/jlb.0310182.

Mistry, M. *et al.* (2011) 'Cancer incidence in the United Kingdom: projections to the year 2030', *British Journal of Cancer*, 105(1), pp. 1795–1803. doi: 10.1038/bjc.2011.430.

Miyahara, M. *et al.* (2007) 'Tumor lymphangiogenesis correlates with lymph node metastasis and clinicopathologic parameters in oral squamous cell carcinoma', *Cancer*, 110(6), pp. 1287–1294. doi: 10.1002/cncr.22900.

Moharamzadeh, K. *et al.* (2008) 'Development, optimization and characterization of a full-thickness tissue engineered human oral mucosal model for biological assessment of dental biomaterials', *Journal of Materials Science: Materials in Medicine*, 19(4), pp. 1793–1801. doi: 10.1007/s10856-007-3321-1.

Morita, Y. *et al.* (2015) 'Cellular fibronectin 1 promotes VEGF-C expression, lymphangiogenesis and lymph node metastasis associated with human oral squamous cell carcinoma', *Clinical and Experimental Metastasis*, 32(7), pp. 739–753. doi: 10.1007/s10585-015-9741-2.

Myers, J. N. *et al.* (2001) 'Extracapsular Spread: A Significant Predictor of Treatment Failure in Patients with Squamous Cell Carcinoma of the Tongue', *Cancer*, 92(12), pp. 3030–3036. doi: 10.1002/cncr.10148.

Naresh, K. N., Nerurkar, A. Y. and Borges, A. M. (2001) 'Angiogenesis is redundant for tumour growth in lymph node metastases', *Histopathology*, 38(5), pp. 466–470. doi: 10.1046/j.1365-2559.2001.01061.x.

Nathanson, S. D., Shah, R. and Rosso, K. (2015) 'Sentinel lymph node metastases in cancer: Causes, detection and their role in disease progression', *Seminars in Cell & Developmental Biology*, 38(1), pp. 106–116. doi: 10.1016/j.semcd.2014.10.002.

Neiva, K. G. *et al.* (2009) 'Cross talk Initiated by Endothelial Cells Enhances Migration and Inhibits Anoikis of Squamous Cell Carcinoma Cells through STAT3/Akt/ERK Signaling', *Neoplasia*, 11(6), pp. 583–593. doi: 10.1593/neo.09266.

Ni, Y.-H. *et al.* (2015) 'Microlocalization of CD68+ tumor-associated macrophages in tumor stroma correlated with poor clinical outcomes in oral squamous cell

carcinoma patients.', *Tumour Biology*, 36(7), pp. 5291–8. doi: 10.1007/s13277-015-3189-5.

Nijkamp, M. M. *et al.* (2011) 'Expression of E-cadherin and vimentin correlates with metastasis formation in head and neck squamous cell carcinoma patients.', *Radiotherapy and Oncology*, 99(3), pp. 344–8. doi: 10.1016/j.radonc.2011.05.066.

Olsen, A., Parkin, D. and Saseini, P. (2008) 'Cancer mortality in the United Kingdom: projections to the year 2025', *British Journal of Cancer*, 99(1), pp. 1549–1554. doi: 10.1038/sj.bjc.6604710.

Pal, A. *et al.* (2013) 'Cigarette smoke condensate promotes pro-tumourigenic stromal-epithelial interactions by suppressing miR-145.', *Journal of Oral Pathology & Medicine*, 42(4), pp. 309–14. doi: 10.1111/jop.12017.

Peng, C. H. *et al.* (2011) 'A novel molecular signature identified by systems genetics approach predicts prognosis in oral squamous cell carcinoma', *PLoS ONE*, 6(8). doi: 10.1371/journal.pone.0023452.

Pereira, E. R. *et al.* (2018) 'Lymph node metastases can invade local blood vessels, exit the node, and colonize distant organs in mice', *Science*, 359(6382), pp. 1403–1407. doi: 10.1126/science.aal3622.

Pickup, M. W., Mouw, J. K. and Weaver, V. M. (2014) 'The extracellular matrix modulates the hallmarks of cancer', *EMBO Reports*, 15(12), pp. 1243–1253. doi: 10.15252/embr.201439246.

Pietras, K. and Ostman, A. (2010) 'Hallmarks of cancer: interactions with the tumor stroma.', *Experimental Cell Research*, 316(8), pp. 1324–31. doi: 10.1016/j.yexcr.2010.02.045.

Podgrabinska, S. and Skobe, M. (2014) 'Role of lymphatic vasculature in regional and distant metastases.', *Microvascular Research*, 95(1), pp. 46–52. doi: 10.1016/j.mvr.2014.07.004.

Polette, M. *et al.* (2004) 'Tumour invasion and matrix metalloproteinases', *Critical Reviews in Oncology/Hematology*, 49(3), p. 179. doi: 10.1016/j.critrevonc.2003.10.008.

Prabhu, R. S. *et al.* (2014) 'Extent of pathologic extracapsular extension and outcomes in patients with nonoropharyngeal head and neck cancer treated with initial surgical resection.', *Cancer*, 120(10), pp. 1499–506. doi: 10.1002/cncr.28596.

Prime, S. S. *et al.* (1990) 'The behaviour of human oral squamous cell carcinoma in cell culture.', *The Journal of Pathology*, 160(3), pp. 259–69. doi: 10.1002/path.1711600313.

Prime, S. S., Game, S. M., *et al.* (1994) 'Epidermal growth factor and transforming growth factor alpha characteristics of human oral carcinoma cell lines.', *British Journal of Cancer*, 69(1), pp. 8–15.

Prime, S. S., Matthews, J. B., *et al.* (1994) 'TGF- β receptor regulation mediates the response to exogenous ligand but is independent of the degree of cellular differentiation in human oral keratinocytes', *International Journal of Cancer*, 56(3), pp. 406–412. doi: 10.1002/ijc.2910560320.

Prime, S. S. *et al.* (2016) 'Fibroblast activation and senescence in oral cancer',

- Journal of Oral Pathology & Medicine*, 46(2), pp. 82–88. doi: 10.1111/jop.12456.
- Punyani, S. R. and Sathawane, R. S. (2013) 'Salivary level of interleukin-8 in oral precancer and oral squamous cell carcinoma', *Clinical Oral Investigations*, 17(2), pp. 517–524. doi: 10.1007/s00784-012-0723-3.
- Puram, S. V. *et al.* (2017) 'Single-Cell Transcriptomic Analysis of Primary and Metastatic Tumor Ecosystems in Head and Neck Cancer', *Cell*, 171(7), p. 1611–1624.e24. doi: 10.1016/j.cell.2017.10.044.
- Qiao, B., Johnson, N. W. and Gao, J. (2010) 'Epithelial-mesenchymal transition in oral squamous cell carcinoma triggered by transforming growth factor- β 1 is Snail family-dependent and correlates with matrix metalloproteinase-2 and -9 expressions', *International Journal of Oncology*, 37(1), pp. 663–668. doi: 10.3892/ijo.
- Qin, X. *et al.* (2018) 'Cancer-associated Fibroblast-derived IL-6 Promotes Head and Neck Cancer Progression via the Osteopontin-NF-kappa B Signaling Pathway', *Theranostics*, 8(4), pp. 921–940. doi: 10.7150/thno.22182.
- Randall, D. R. *et al.* (2015) 'Diagnostic utility of central node necrosis in predicting extracapsular spread among oral cavity squamous cell carcinoma', *Head & Neck*, 37(1), pp. 92–96. doi: 10.1002/hed.23562.
- Rema, J. *et al.* (2015) 'Field cancerization of oral cavity - A case series with review of literature', *Journal of Oral and Maxillofacial Surgery, Medicine, and Pathology*, 27(6), pp. 867–875. doi: 10.1016/j.ajoms.2015.05.008.
- Rhim, J. H. *et al.* (2008) 'Cancer cell-derived IL-1 α induces IL-8 release in endothelial cells', *Journal of Cancer Research and Clinical Oncology*, 134(1), pp. 45–50. doi: 10.1007/s00432-007-0243-8.
- Richter, P. *et al.* (2011) 'EGF/TGF β 1 co-stimulation of oral squamous cell carcinoma cells causes an epithelial-mesenchymal transition cell phenotype expressing laminin 332', *Journal of Oral Pathology & Medicine*, 40(1), pp. 46–54. doi: 10.1111/j.1600-0714.2010.00936.x.
- Riedel, A. *et al.* (2016) 'Tumor-induced stromal reprogramming drives lymph node transformation', *Nature Immunology*, 17(9). doi: 10.1038/ni.3492.
- Rizwan, A. *et al.* (2015) 'Metastatic breast cancer cells in lymph nodes increase nodal collagen density', *Scientific Reports*, 5(1), p. 10002. doi: 10.1038/srep10002.
- Rozenendaal, R., Mebius, R. E. and Kraal, G. (2008) 'The conduit system of the lymph node', *International Immunology*, 20(12), pp. 1483–1487. doi: 10.1093/intimm/dxn110.
- Rowe, R. G. and Weiss, S. J. (2008) 'Breaching the basement membrane: who, when and how?', *Trends in Cell Biology*, 18(11), pp. 560–574. doi: 10.1016/j.tcb.2008.08.007.
- Rupniak, H. T. *et al.* (1985) 'Characteristics of Four New Human Cell Lines Derived From Squamous Cell Carcinomas of the Head and Neck', *Journal of the National Cancer Institute*, 75(4), pp. 621–635. doi: 10.1093/jnci/75.4.621.
- Sales, C. B. S. *et al.* (2016) 'Elevated VEGFA mRNA levels in oral squamous cell carcinomas and tumor margins: a preliminary study', *Journal of Oral Pathology and*

Medicine, 45(7), pp. 481–485. doi: 10.1111/jop.12398.

Salo, T. *et al.* (2014) 'Insights into the role of components of the tumor microenvironment in oral carcinoma call for new therapeutic approaches', *Experimental Cell Research*, 325(2), pp. 58–64. doi: 10.1016/j.yexcr.2013.12.029.

Sapp, J. P., Eversole, L. R. and Wysocki, G. P. (2004) *Contemporary Oral and Maxillofacial Pathology*. 2nd Ed. Edited by P. Rudolph and K. Alvis. St. Louis: Elsevier. doi: 10.1016/B978-0-323-01723-7.50010-0.

Schwock, J. *et al.* (2010) 'SNAI1 expression and the mesenchymal phenotype: an immunohistochemical study performed on 46 cases of oral squamous cell carcinoma.', *BMC Clinical Pathology*, 10(1), p. 1. doi: 10.1186/1472-6890-10-1.

Shaw, R. J. *et al.* (2010) 'Extracapsular spread in oral squamous cell carcinoma.', *Head & Neck*, 32(6), pp. 714–722. doi: 10.1002/hed.

Shen, H. *et al.* (2014) 'Alterations of high endothelial venules in primary and metastatic tumors are correlated with lymph node metastasis of oral and pharyngeal carcinoma', *Cancer Biology and Therapy*, 15(3), pp. 342–349. doi: 10.4161/cbt.27328.

Shibuya, Y. *et al.* (2014) 'Oral squamous cell carcinoma with microscopic extracapsular spread in the cervical lymph nodes.', *International Journal of Oral and Maxillofacial Surgery*, 43(4), pp. 387–92. doi: 10.1016/j.ijom.2013.09.015.

Shield, K. D. *et al.* (2017) 'The global incidence of lip, oral cavity, and pharyngeal cancers by subsite in 2012', *CA Cancer Journal for Clinicians*, 67(1), pp. 51–64. doi: 10.3322/caac.21384.

Shinriki, S. *et al.* (2009) 'Humanized anti-interleukin-6 receptor antibody suppresses tumor angiogenesis and in vivo growth of human oral squamous cell carcinoma', *Clinical Cancer Research*, 15(17), pp. 5426–5434. doi: 10.1158/1078-0432.CCR-09-0287.

Shinriki, S. *et al.* (2011) 'Interleukin-6 signalling regulates vascular endothelial growth factor-C synthesis and lymphangiogenesis in human oral squamous cell carcinoma', *Journal of Pathology*, 225(1), pp. 142–150. doi: 10.1002/path.2935.

Shintani, Y. *et al.* (2013) 'Pulmonary Fibroblasts Induce Epithelial Mesenchymal Transition and Some Characteristics of Stem Cells in Non-Small Cell Lung Cancer', *The Annals of Thoracic Surgery*, 96(2), pp. 425–433. doi: 10.1016/j.athoracsur.2013.03.092.

Shivamallappa, S. M. *et al.* (2011) 'Role of angiogenesis in oral squamous cell carcinoma development and metastasis: an immunohistochemical study.', *International Journal of Oral Science*, 3(4), pp. 216–24. doi: 10.4248/IJOS11077.

Sica, A. *et al.* (2008) 'Macrophage polarization in tumour progression', *Seminars in Cancer Biology*, 18(5), pp. 349–355. doi: 10.1016/j.semcan.2008.03.004.

Siriwardena, B. S. M. S. *et al.* (2008) 'VEGF-C is associated with lymphatic status and invasion in oral cancer', *Journal of Clinical Pathology*, 61(1), pp. 103–108. doi: 10.1136/jcp.2007.047662.

Soames, J. V. and Southam, J. C. (2005) *Oral pathology*. Forth. Oxford University Press.

- Sobral, L. M. *et al.* (2011) 'Myofibroblasts in the stroma of oral cancer promote tumorigenesis via secretion of activin A.', *Oral oncology*, 47(9), pp. 840–6. doi: 10.1016/j.oraloncology.2011.06.011.
- Soon, P. S. H. *et al.* (2013) 'Breast cancer-associated fibroblasts induce epithelial-to-mesenchymal transition in breast cancer cells', *Endocrine Related Cancer*, 20(1), pp. 1–12. doi: 10.1530/ERC-12-0227.
- Stadler, M. *et al.* (2015) 'Increased complexity in carcinomas: Analyzing and modeling the interaction of human cancer cells with their microenvironment', *Seminars in Cancer Biology*, 35, pp. 107–124. doi: 10.1016/j.semcan.2015.08.007.
- Su, Z. *et al.* (2016) 'Predicting extracapsular spread of head and neck cancers using different imaging techniques: A systematic review and meta-analysis', *International Journal of Oral and Maxillofacial Surgery*, 45(4), pp. 413–421. doi: 10.1016/j.ijom.2015.11.021.
- Sun, Y. (2016) 'Tumor microenvironment and cancer therapy resistance', *Cancer Letters*, 380(1), pp. 205–215. doi: 10.1016/j.canlet.2015.07.044.
- Sundelin, K. *et al.* (2005) 'Effects of cytokines on matrix metalloproteinase expression in oral squamous cell carcinoma in vitro', *Acta Oto-Laryngologica*, 125(7), pp. 765–773. doi: 10.1080/00016480510027484.
- Suton, P. *et al.* (2017) 'Prognostic significance of extracapsular spread of lymph node metastasis from oral squamous cell carcinoma in the clinically negative neck', *International Journal of Oral and Maxillofacial Surgery*. doi: 10.1016/j.ijom.2017.02.1277.
- Taddei, M. L. *et al.* (2014) 'Senescent stroma promotes prostate cancer progression: The role of miR-210', *Molecular Oncology*, 8(8), pp. 1729–1746. doi: 10.1016/j.molonc.2014.07.009.
- Takeya, M. and Komohara, Y. (2016) 'Role of tumor-associated macrophages in human malignancies: friend or foe?', *Pathology International*, 66(9), pp. 491–505. doi: 10.1111/pin.12440.
- Takkunen, M. *et al.* (2006) 'Snail-dependent and -independent epithelial-mesenchymal transition in oral squamous carcinoma cells.', *The Journal of Histochemistry and Cytochemistry*, 54(11), pp. 1263–1275. doi: 10.1369/jhc.6A6958.2006.
- Takkunen, M. *et al.* (2010) 'Podosome-like structures of non-invasive carcinoma cells are replaced in epithelial-mesenchymal transition by actin comet-embedded invadopodia.', *Journal of Cellular and Molecular Medicine*, 14(6B), pp. 1569–93. doi: 10.1111/j.1582-4934.2009.00868.x.
- Tandon, S. *et al.* (2008) 'Fine-needle aspiration cytology in a regional head and neck cancer center: Comparison with a systematic review and meta-analysis', *Head & Neck*, 30(9), pp. 1246–1252. doi: 10.1002/hed.20849.
- Turley, S. J., Cremasco, V. and Astarita, J. L. (2015) 'Immunological hallmarks of stromal cells in the tumour microenvironment', *Nature Reviews Immunology*, 15(11), pp. 669–682. doi: 10.1038/nri3902.

- Vered, M., Dayan, D., *et al.* (2010) 'Cancer-associated fibroblasts and epithelial-mesenchymal transition in metastatic oral tongue squamous cell carcinoma.', *International Journal of Cancer*, 127(6), pp. 1356–62. doi: 10.1002/ijc.25358.
- Vered, M., Dobriyan, A., *et al.* (2010) 'Tumor-host histopathologic variables, stromal myofibroblasts and risk score, are significantly associated with recurrent disease in tongue cancer.', *Cancer Science*, 101(1), pp. 274–80. doi: 10.1111/j.1349-7006.2009.01357.x.
- Voronov, E. *et al.* (2013) 'Unique versus redundant functions of IL-1 α and IL-1 β in the tumor microenvironment', *Frontiers in Immunology*, 4(1), p. 177. doi: 10.3389/fimmu.2013.00177.
- Voulgari, A. and Pintzas, A. (2009) 'Epithelial-mesenchymal transition in cancer metastasis: mechanisms, markers and strategies to overcome drug resistance in the clinic.', *Biochimica et Biophysica Acta*, 1796(2), pp. 75–90. doi: 10.1016/j.bbcan.2009.03.002.
- Wakisaka, N. *et al.* (2015) 'Primary tumor-secreted lymphangiogenic factors induce pre-metastatic lymphovascular niche formation at sentinel lymph nodes in oral squamous cell carcinoma', *PLoS ONE*, 10(12), pp. 1–14. doi: 10.1371/journal.pone.0144056.
- Wang, C. *et al.* (2012) 'Deregulation of Snai2 is associated with metastasis and poor prognosis in tongue squamous cell carcinoma', *International Journal of Cancer*, 130(10), pp. 2249–2258. doi: 10.1002/ijc.26226.
- Wang, J. *et al.* (2014) 'Genetic regulation and potentially therapeutic application of cancer-associated fibroblasts in oral cancer', *Journal of Oral Pathology and Medicine*, 43(5), pp. 323–334. doi: 10.1111/jop.12098.
- Wang, W. *et al.* (2015) 'An eleven gene molecular signature for extra-capsular spread in oral squamous cell carcinoma serves as a prognosticator of outcome in patients without nodal metastases', *Oral Oncology*, 51(4), pp. 355–362. doi: 10.1016/j.oraloncology.2014.12.012.
- Wang, X. *et al.* (2013) 'Endothelial Cells Enhance Prostate Cancer Metastasis via IL-6 - Androgen Receptor - TGF- β - MMP-9 Signals', *Molecular Cancer Therapeutics*, 12(6), pp. 1026–1037. doi: 10.1158/1535-7163.MCT-12-0895.
- Wang, Y. *et al.* (2017) 'Microenvironment of a tumor-organoid system enhances hepatocellular carcinoma malignancy-related hallmarks', *Organogenesis*, 13(3), pp. 83–94. doi: 10.1080/15476278.2017.1322243.
- Warnakulasuriya, S. (2009) 'Global epidemiology of oral and oropharyngeal cancer', *Oral Oncology*, 45(4–5), pp. 309–316. doi: 10.1016/j.oraloncology.2008.06.002.
- Waugh, D. J. J. and Wilson, C. (2008) 'The interleukin-8 pathway in cancer', *Clinical Cancer Research*, 14(21), pp. 6735–6741. doi: 10.1158/1078-0432.CCR-07-4843.
- Weber, M. *et al.* (2014) 'Small oral squamous cell carcinomas with nodal lymphogenic metastasis show increased infiltration of M2 polarized macrophages - An immunohistochemical analysis', *Journal of Cranio-Maxillofacial Surgery*, 42(7), pp. 1087–1094. doi: 10.1016/j.jcms.2014.01.035.
- Weber, M. *et al.* (2016) 'Prognostic significance of macrophage polarization in early

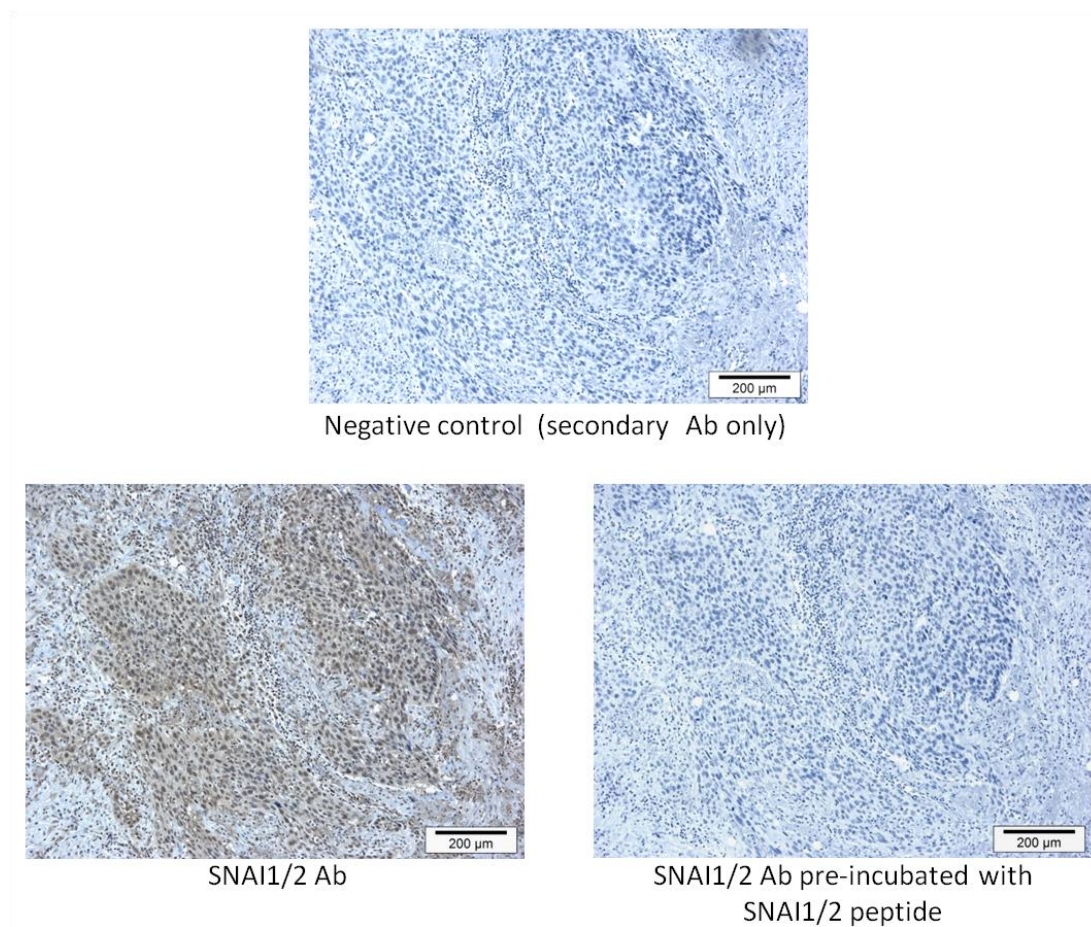
- stage oral squamous cell carcinomas', *Oral Oncology*, 52, pp. 75–84. doi: 10.1016/j.oraloncology.2015.11.001.
- Wehrhan, F. *et al.* (2014) 'Increased malignancy of oral squamous cell carcinomas (oscc) is associated with macrophage polarization in regional lymph nodes – an immunohistochemical study', *BMC Cancer*, 14(1), p. 522. doi: 10.1186/1471-2407-14-522.
- Welch-Reardon, K. M., Wu, N. and Hughes, C. C. W. (2014) 'A Role for Partial Endothelial-Mesenchymal Transitions in Angiogenesis?', *Arteriosclerosis, Thrombosis, and Vascular Biology*, 35(2), pp. 303–308. doi: 10.1161/ATVBAHA.114.303220.
- Wenzel, S. *et al.* (2004) 'The prognostic impact of metastatic pattern of lymph nodes in patients with oral and oropharyngeal squamous cell carcinomas', *European Archives of Oto-Rhino-Laryngology*, 261(5), pp. 270–275. doi: 10.1007/s00405-003-0678-8.
- Wheelock, M. J. *et al.* (2008) 'Cadherin switching.', *Journal of Cell Science*, 121(6), pp. 727–735. doi: 10.1242/jcs.000455.
- Woolgar, J. a. *et al.* (2003) 'Cervical lymph node metastasis in oral cancer: The importance of even microscopic extracapsular spread', *Oral Oncology*, 39(2), pp. 130–137.
- Wu, T. *et al.* (2016) 'Modulation of IL-1 β reprogrammes the tumor microenvironment to interrupt oral carcinogenesis', *Scientific Reports*, 6(1), p. 20208. doi: 10.1038/srep20208.
- Yamada, S. *et al.* (2016) 'Evaluation of the level of progression of extracapsular spread for cervical lymph node metastasis in oral squamous cell carcinoma', *International Journal of Oral and Maxillofacial Surgery*, 45(2), pp. 141–146. doi: 10.1016/j.ijom.2015.09.005.
- Yamagata, Y. *et al.* (2017) 'CD163-Positive Macrophages Within the Tumor Stroma Are Associated With Lymphangiogenesis and Lymph Node Metastasis in Oral Squamous Cell Carcinoma', *Journal of Oral and Maxillofacial Surgery*, 75(10), pp. 2144–2153. doi: 10.1016/j.joms.2017.03.009.
- Yanase, M. *et al.* (2014) 'Prognostic value of vascular endothelial growth factors A and C in oral squamous cell carcinoma', *Journal of Oral Pathology and Medicine*, 43(7), pp. 514–520. doi: 10.1111/jop.12167.
- Yang, N. C. and Hu, M. L. (2005) 'The limitations and validities of senescence associated- β -galactosidase activity as an aging marker for human foreskin fibroblast Hs68 cells', *Experimental Gerontology*, 40(10), pp. 813–819. doi: 10.1016/j.exger.2005.07.011.
- Yao, X. and Sun, S. (2017) 'Clinicopathological significance of ZEB-1 and E-cadherin proteins in patients with oral cavity squamous cell carcinoma', *OncoTargets and Therapy*, 10(1), pp. 781–790. doi: 10.2147/OTT.S111920.
- Yokoyama, K. *et al.* (2001) 'Reverse correlation of E-cadherin and snail expression in oral squamous cell carcinoma cells in vitro', *Oral Oncology*, 37(1), pp. 65–71. doi: 10.1016/S1368-8375(00)00059-2.

- Young, M. R. (2012) 'Endothelial cells in the eyes of an immunologist', *Cancer Immunology, Immunotherapy*, 61(10), pp. 1609–1616. doi: 10.1007/s00262-012-1335-0.
- Yu, C. *et al.* (2011) 'TGF- β 1 mediates epithelial to mesenchymal transition via the TGF- β /Smad pathway in squamous cell carcinoma of the head and neck.', *Oncology Reports*, 25(6), pp. 1581–7. doi: 10.3892/or.2011.1251.
- Yu, Y. *et al.* (2014) 'Cancer-associated fibroblasts induce epithelial–mesenchymal transition of breast cancer cells through paracrine TGF- β signalling', *British Journal of Cancer*, 110(3), pp. 724–732. doi: 10.1038/bjc.2013.768.
- Zeisberg, E. M. *et al.* (2007) 'Discovery of Endothelial to Mesenchymal Transition as a Source for Carcinoma-Associated Fibroblasts', *Cancer Research*, 67(21), pp. 10123–10128. doi: 10.1158/0008-5472.CAN-07-3127.
- Zhao, D. *et al.* (2008) 'Intratumoral lymphangiogenesis in oral squamous cell carcinoma and its clinicopathological significance.', *Journal of Oral Pathology & Medicine*, 37(10), pp. 616–25. doi: 10.1111/j.1600-0714.2008.00707.x.
- Zhao, D. *et al.* (2012) 'Over-expression of integrin-linked kinase correlates with aberrant expression of Snail, E-cadherin and N-cadherin in oral squamous cell carcinoma: Implications in tumor progression and metastasis', *Clinical and Experimental Metastasis*, 29(8), pp. 957–969. doi: 10.1007/s10585-012-9485-1.
- Zhou, B. *et al.* (2014) 'A role for cancer-associated fibroblasts in inducing the epithelial-to-mesenchymal transition in human tongue squamous cell carcinoma', *Journal of Oral Pathology & Medicine*, 43(8), pp. 585–592. doi: 10.1111/jop.12172.
- Zhou, B. *et al.* (2015) 'Tumor necrosis factor α induces myofibroblast differentiation in human tongue cancer and promotes invasiveness and angiogenesis via secretion of stromal cell-derived factor-1', *Oral Oncology*, 51(12), pp. 1095–1102. doi: 10.1016/j.oraloncology.2015.08.017.
- Zhou, C. X. *et al.* (2010) 'Immunoexpression of matrix metalloproteinase-2 and matrix metalloproteinase-9 in the metastasis of squamous cell carcinoma of the human tongue', *Australian Dental Journal*, 55(4), pp. 385–389. doi: 10.1111/j.1834-7819.2010.01258.x.
- Zhou, X. *et al.* (2006) 'Global expression-based classification of lymph node metastasis and extracapsular spread of oral tongue squamous cell carcinoma.', *Neoplasia*, 8(11), pp. 925–32. doi: 10.1593/neo.06430.
- Zhou, Y. *et al.* (2015) 'Over-expression of TWIST, an epithelial-mesenchymal transition inducer, predicts poor survival in patients with oral carcinoma', *International Journal of Clinical and Experimental Medicine*, 8(6), pp. 9239–9247.
- Zhuang, Z. *et al.* (2010) 'Altered phenotype of lymphatic endothelial cells induced by highly metastatic OTSCC cells contributed to the lymphatic metastasis of OTSCC cells.', *Cancer Science*, 101(3), pp. 686–92. doi: 10.1111/j.1349-7006.2009.01444.x.
- Ziober, A. F. *et al.* (2006) 'Identification of a gene signature for rapid screening of oral squamous cell carcinoma', *Clinical Cancer Research*, 12(20), pp. 5960–5971. doi: 10.1158/1078-0432.CCR-06-0535.
- Ziober, A. F., Falls, E. M. and Ziober, B. L. (2006) 'The extracellular matrix in oral

squamous cell carcinoma: friend or foe?', *Head & Neck*, 28(8), pp. 740–749. doi: 10.1002/hed.

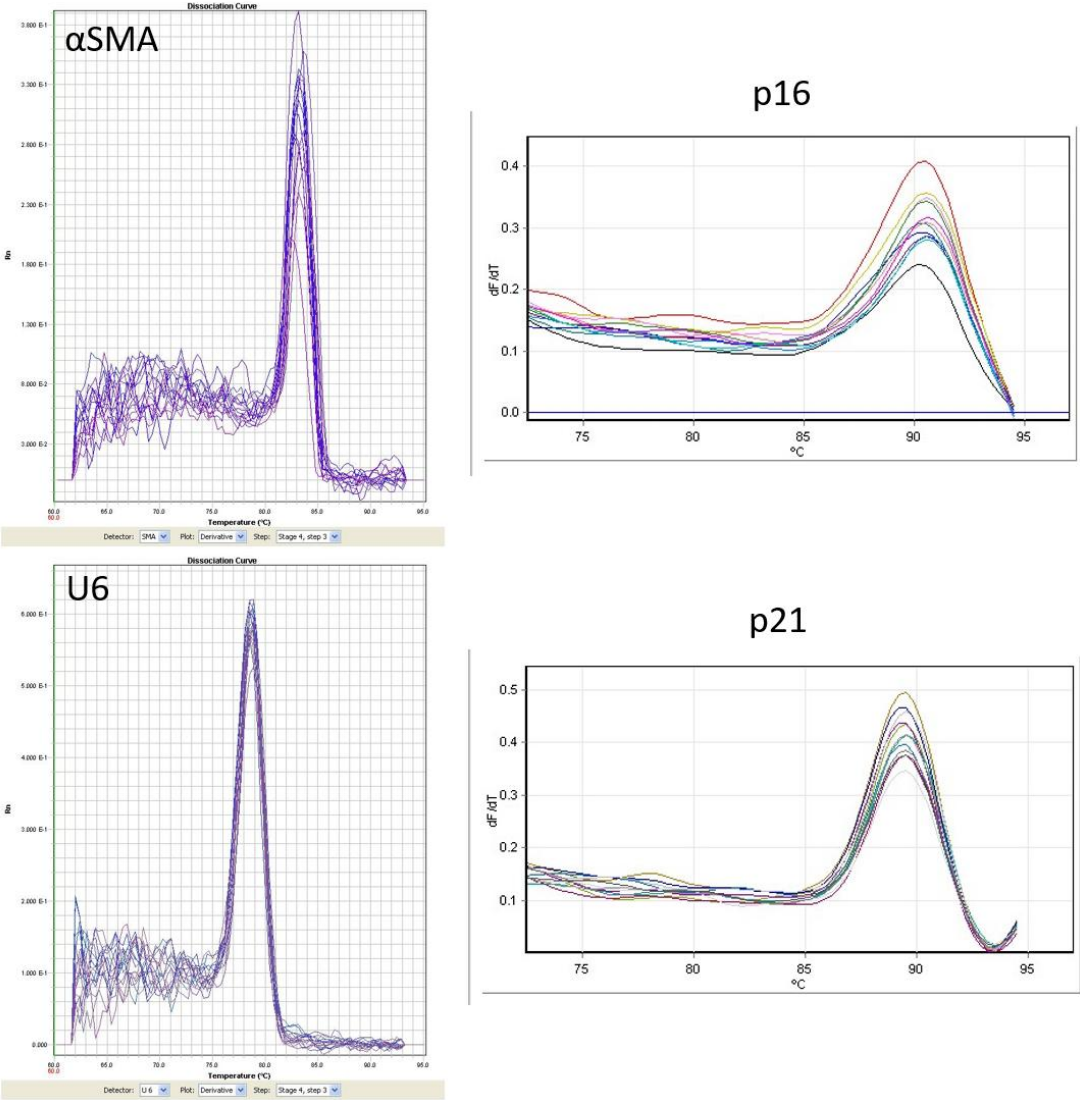
Appendices

Appendix A: IHC blocking experiments



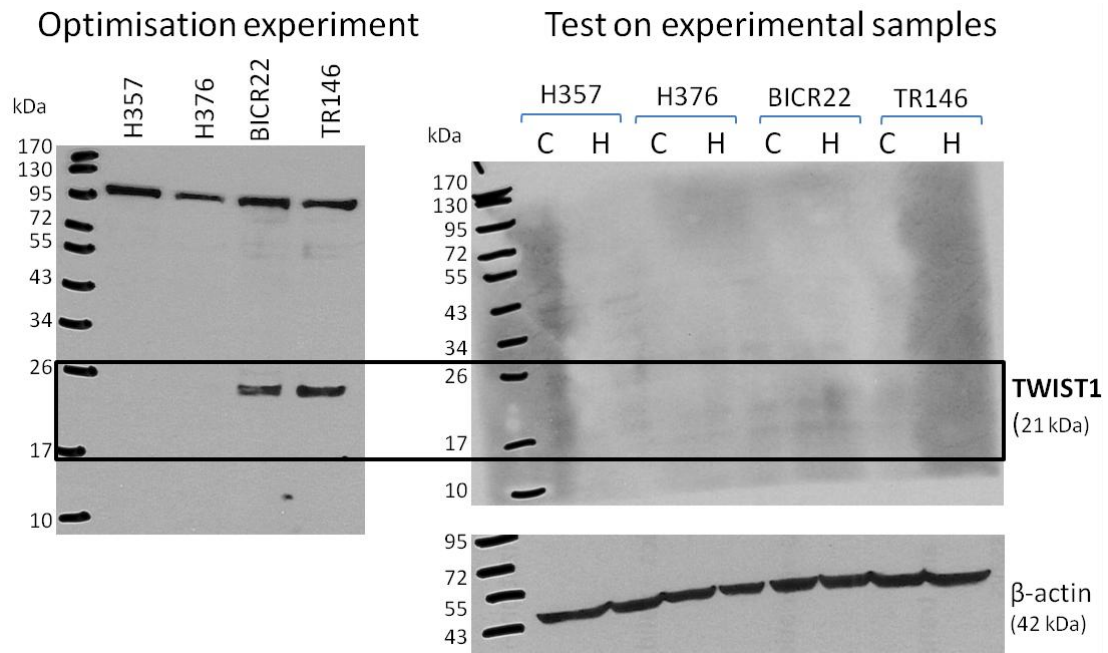
Appendix Figure A.1. SNAI1/2 antibody immunohistochemical (IHC) blocking control experiment. Representative images of IHC staining taken from the same slide location from either the negative control (anti-rabbit secondary antibody (Ab) only), SNAI1/2 primary Ab (Abcam ab85936) plus anti-rabbit secondary antibody, or SNAI1/2 Ab pre-incubated with the peptide from which it was raised (ab19126) plus anti-rabbit secondary antibody. Both primary Ab only and the peptide-blocked primary Ab mix were incubated overnight at 4°C before use. x 10 magnification, scale bars 200 μm.

Appendix B: SYBR green primer melt curves



Appendix Figure B.1. SYBR green primer melt curves. Melt curves generated during qRT-PCR analysis using SYBR green primers for α -smooth muscle actin (α SMA), p16^{INK4a} (p16), p21/cip-1 (p21) and U6 endogenous control reference gene. Primer sequences and protocol can be found in section 2.8.3.

Appendix C: TWIST1 antibody optimisation (Abcam ab50887)



Appendix Figure C.1. Optimisation and use of TWIST1 antibody (Abcam ab50887) for western blot. Western blot (left) shows results of optimisation experiment using untreated cell lysates (20 µg/lane) and antibody diluted 1/50 and blocked with 5% (w/v) BSA (as recommended by manufacturer). A specific band at 21 kDa was observed in BICR22 and TR146 cell lines alongside a non-specific 100 kDa band for all cell lines. Western blots using experimental samples (example on right) did not show any specific bands despite prolonged exposure time. Protein presence was confirmed using Ponceau staining and by labelling for β-actin expression (lower blot). Experimental sample blots used the same western blot conditions and were loaded with 20 µg/lane of cell lysate (treated with either normal oral fibroblast (C) or H₂O₂-treated fibroblast (H) conditioned media). All blots developed using ECL and x-ray.